A DUAL HOLLOW FIBRE BIOREACTOR FOR THE GROWTH OF HYBRIDOMAS.

A thesis presented by
Kevin Ian Trevor Wright
to the University of Edinburgh
in application for the
Degree of Doctor of Philosophy.

1996

In loving memory of my Father,

Ian Edward Wright,

You worked too hard,
and died too soon.

ABSTRACT

The use of hollow fibre bioreactors in mammalian cell culture has provided a means by which large populations of viable cells can be grown continuously, for extended periods, in a relatively small volume of vessel. Bioreactors in which one set of fibres are used for nutrient and metabolite exchange from the cell mass are limited by their reliance on an axial flow regime. This pressure mediated flow pattern leads to the formation of nutrient gradients within the cell mass, which occur due to the large diffusional distances present in the growth space, resulting in cell death within the bioreactor.

The Edinburgh Dual Hollow Fibre Bioreactor solves this diffusional problem by using two sets of fibres to mimic the arterio-venous flow found in the body. In this instance the diffusional distances are reduced due to the close proximity of the two sets of fibres. Using this design, and a murine hybridoma (ES4) which produces an IgM blood typing antibody, cells were grown to a maximum density of 1.2×10^7 viable cells ml^{-1} of reactor growth volume, with a maximum antibody production rate of 0.16 mgh^{-1}. This was a 10 fold improvement in the viable cell number obtained using an airlift fermenter.

The successful operation of this design was found to be dependent upon the pressure profiles developed within the bioreactor, with a number of extended culture experiments having been carried out. The influence of bioreactor design, fibre selection and the methods by which these bioreactors should be operated are discussed in this work.

ACKNOWLEDGEMENTS

First, and foremost, thanks go to my wife who kept me in the style to which I was accustomed during the writing of this thesis. All my thanks for the love and support you've given me through the years.

To my parents, I've just realised that the past few years research have been totally fruitless. On that fateful night in 1966 my parents produced, as other parents do, the ultimate in temperature controlled, high density, tissue culture devices (i.e. me). Unfortunately, the process times are somewhat uneconomical and there appears to be a profusion of similar devices on the planet. Love and thanks for totally scuppering my research before I could even write.

Thanks also go to those people in the Department who have helped me to complete this work. Of particular note are Don Glass, John C., John B., Jonathan D., Cui, Colm, the workshop (Kenny, Rab, Bobby and Tommy) and Matthew and Neil for their technical and computing assistance. Thanks to JSC for putting up with the ravings of a biologist, I hope that the sedatives have helped over the years.

Finally, many thanks to those at Bioscot Ltd., without whom none of this work could have been carried out. To Jim, Keith, Nicole and the others, many thanks for all of your help through the years.

Thanks also to William, Fiona and family, who supported Liz, supporting me.

Table of Contents

Chapter 5

Small scale, high density culture

Chapter 6

Materials and Methods

Chapter 7

Bioreactor design and construction

Chapter 8

Mass transport within the bioreactor

Chapter 9

Growth and metabolism of ES4

Chapter 10

Bioreactor culture experiments

List of Figures

List of Tables

List of Photographs

Chapter 1

Background, Aims and Objectives

1.0 Introduction

Developments in molecular biology, immunology and genetics have considerably improved our understanding of the function and behaviour of mammalian proteins within their host systems. This knowledge has been applied to developing a number of analytical techniques, which have been used in a wide range of applications including clinical medicine and industrial processing. As a direct consequence there has been an increase in the requirement for either the original or modified versions of these proteins. These compounds are usually high molecular weight proteins which are either impossible, or impractical for economic reasons, to produce synthetically and so command a high monetary value. Figures from Belfort (1989) suggested that there would be a $4 billion market for mammalian proteins in 1990, with the overall projection for the biotechnology industry, including DNA manipulation and mammalian proteins, accounting for $50 billion per annum by the mid 1990's (Spier, 1990). Mammalian cells are used to produce a wide variety of pharmaceutical and diagnostic products including viral vaccines, interleukins and, of particular relevance to this study, monoclonal antibodies.

In order to maximise the high earning potentials from mammalian cells, intensified production and recovery systems have been developed which are capable of delivering high yields of the end product. These processes have usually aimed to culture the cells at their maximum production rate in an environment which does not nutritionally or physically limit cell viability. Ideally, the higher the viable producing population, the greater the yield of product. Unfortunately, under conditions of high biomass, the cells can become limited by the diffusion of nutrients to and the removal of potentially toxic waste metabolites (and product) from the concentrated biomass. This can result in either cell death, due to starvation, or an alteration in the metabolism of the cells due to nutrient limitation (Levesque *et al.*,1989, Michaels *et al.*,1991).

A range of techniques have been developed for the culture of mammalian cells, either as adaptations of technology developed for the culture of bacteria and fungi, e.g. stirred tank and airlift fermenters, or novel designs such as packed bed and hollow fibre bioreactors. Two approaches have been used to reduce the effects of diffusion on intensified culture techniques. The first method involves increasing the degree of gas or mechanically mediated mixing to improve the supply of fresh nutrients to the cells within the vessel. This method is usually employed in suspension growth systems (e.g. air lift fermenters or stirred tank vessels) where the cells grow individually, as aggregates, or on buoyant support matrices of a defined size (e.g. agarose/alginate beads, Wilson, 1992) . Unfortunately this approach can be limited due to the damage caused to the cells by the attritional or bubble mediated shear forces associated with increased mixing (Mijnbeek, 1991) and the maximum level to which the vessel can be seeded with beads.

The second approach involves the continuous flow of nutrient rich medium through static biomass of defined size. The physical dimensions of the cell mass are maintained at a level where diffusion is non-limiting to the growth of the cells. Such systems include packed beds of glass beads (Spier and Whiteside, 1976) and hollow fibre bioreactors (Knazek *et al.*, 1972). In the latter system a single set of filters is used to supply nutrients to and remove waste metabolites from the cellular growth space (CGS). The flow regimes in these types of bioreactor have been observed to be limiting to cell viability through the formation of cell and nutrient gradients within the growth space (Piret and Cooney, 1990). Designs of hollow fibre bioreactor which counter these factors have either been limited in volume (e.g. SETEC's Tricentric bioreactor) or the circulatory flow to and from the bioreactor has required a higher degree of complexity (Endotronic's ACUCYST system)

This study investigates a particular design of perfusion bioreactor, the Edinburgh Dual Hollow Fibre Bioreactor (Burns, 1991). This system mimics the arterio-venous flow of blood in the body using two sets of hollow fibre membranes, the upstream, supply fibres provide nutrients to a geometrically defined growth space, and the downstream, sink fibres remove the spent medium and product from the growth space (Figure 1.1).

Figure 1.1:- Outline of bioreactor operation

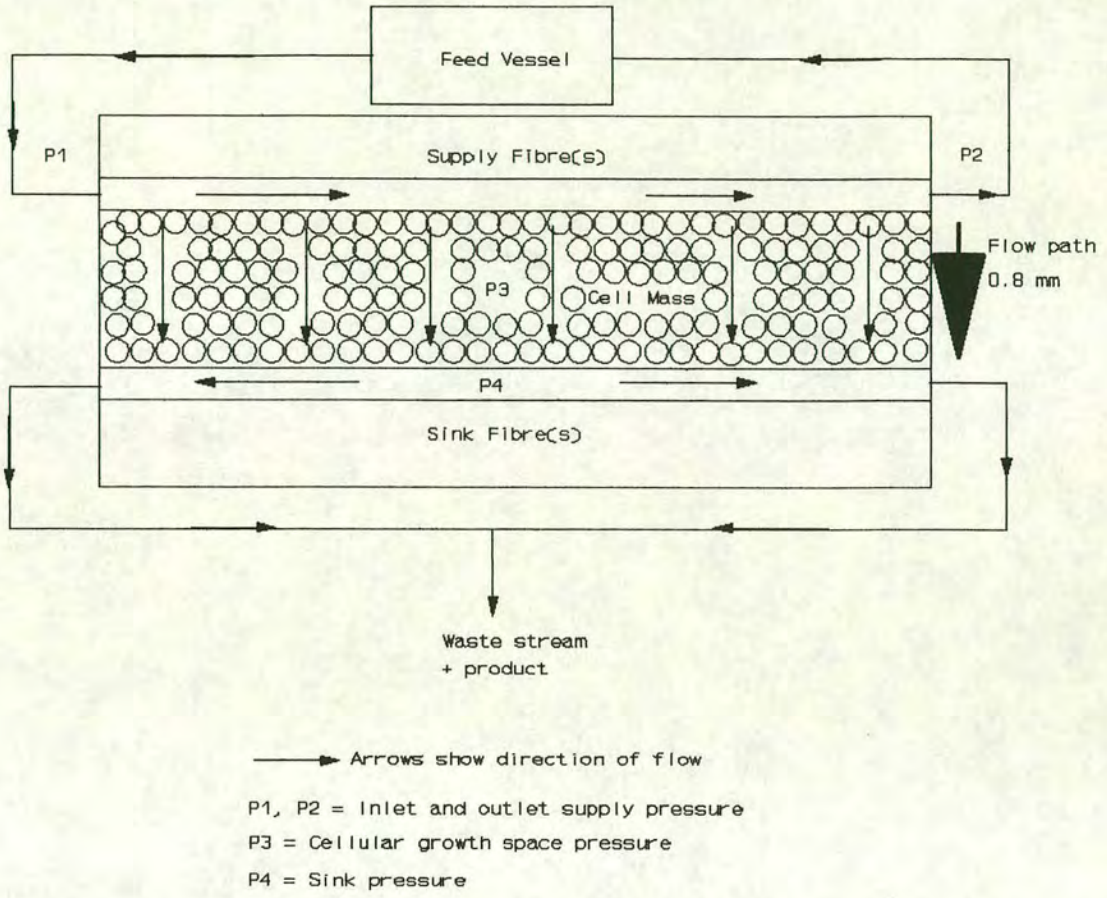

A pressure gradient maintained between the two sets of fibres, where the pressures P1 and P2 are higher than P3, which is greater than P4, enables a radial flow of nutrients from the supply to the sink fibres. The sink fibres outnumber the supply fibres by at least 2:1, with specially designed templates used to ensure an even distribution of the two sets of fibres throughout the bioreactor. The arrangement of fibres within the bioreactor limits the flow path for nutrients between the two circuits to less than 0.8 mm. While it was recognised that this length of flow path was potentially limiting (it has been calculated that cells in a biomass become starved of oxygen at a distance of 256 μm [M^{c}Cullough and Spier, 1990]) it was decided that this aspect of the design would be addressed at a later stage of the project. In theory, under the previously outlined pressure conditions, a non-limiting radial flow of nutrients through the biomass was expected to be developed.

1.1 Aims and Objectives

The work outlined in this thesis describes the developments in the design and operation of the prototype bioreactor produced by Burns (1991, described in Chapter 6). All of the work described in subsequent Chapters was initiated and carried out by the author, unless otherwise stated.

While other designs of hollow fibre bioreactor were available for the culture of mammalian cells e.g. SETEC's Tricentric (Cima *et al.*, 1990) and Endotronic's ACUCYST system (Hirschel and Gruenberg, 1987), the aim of this work was to develop and characterise a novel, patentable high density culture system which was superior to existing technology. The initial idea for this project came from discussions between the Department of Chemical Engineering (Edinburgh), Bioscot Ltd, a local biotechnology company and Professor J. Howell (Bath). Based on the diffusional limitations associated with the designs utilising a single set of fibres (Piret and Cooney, 1990), the limited volume of more complex designs (e.g.the SETEC system), and the non-steady state nature of the ACUCYST system, it was believed that a device with controlled radial convection could be developed which allowed a steady state to be achieved. The authors' initial project objectives were as follows:-

(1) To grow cells within the bioreactor designed by Burns (1991).

(2) To enhance the performance of the bioreactor, with respect to viable cell numbers and antibody production, by identifying the physical limitations to its operation and improving the control and design of the unit.

(3) Having achieved cell growth, to examine the growth characteristics and metabolism of the cells within the bioreactor.

By understanding these factors it was hoped that a commercially viable design could be developed. No successful cell culture experiments had been carried out using Burns' design, with the method used for the bioreactor construction resulting in high failure rates due to leaks within the hollow fibre module. The author extended the first of these aims to include the redesign of the bioreactor in order to solve these constructional problems and provide a suitable bioreactor for cell growth.

Having improved the design of the bioreactor, a series of cell culture experiments highlighted a range of previously unforeseen problems with its operation. The metabolic information obtained from these experiments proved difficult to interpret due to a mixture of sampling and control related problems. As a result the aims were further expanded to examine the way in which filtration and alterations in the pressure profile influenced the performance of the system and the growth of cells within the bioreactor.

1.2 Outline and scope of thesis

The following introductory chapters provide a general introduction into the field of a mammalian cell culture (Chapter 2), the metabolism and growth of hybridomas (Chapter 3), an overview of conventional culture techniques and the process related limitations to their culture (Chapter 4), an introduction to basic filtration theory (Chapter 5) and finally an overview of a number of hollow fibre bioreactors and the predicted advantages of the Edinburgh design over these systems.

Chapter 6 describes the materials, biochemical analysis methods and the construction protocol used for the first prototype bioreactor. Chapters 7-10 highlight a number of areas important to the maintenance of a viable population within bioreactor systems. These include the cells basic metabolic requirements and the positive and negative aspects of the culture environment which the cells are maintained and, with particular relevance to this study, the effects of filtration and mass transfer limitations on the supply of nutrients and the removal of waste metabolites from the cells.

The operation of the Edinburgh dual hollow fibre bioreactor enabled the culture of up to 1.2×10^7 viable cells ml^{-1} of growth space volume. The maximum viability of the cells within the bioreactor was measured at 30% of the total biomass. While the viable population was a 10 fold increase on the numbers realised in conventional culture techniques, it was less than that observed with other similar devices (e.g. $1\text{-}5 \times 10^8$ viable cells ml^{-1}, Hirschel and Gruenberg, 1987). Hence, it was concluded that the improved design of the Edinburgh bioreactor was not commercially viable.

Chapter 2

Advances in mammalian cell culture

2.0 Introduction

The use of products derived from mammalian cells has been introduced in Chapter 1. This chapter provides a general overview of this field of research, including a description of the characteristics of hybridomas, of their products, monoclonal antibodies, and a basic introduction to current bulk culture techniques. The latter topics are examined to a greater depth in Chapters 3 to 5.

There are several areas in which mammalian culture systems can be improved, increasing their productivity on a per unit volume basis. These include:-

(1) Metabolic enhancement of cell growth, to favour product formation, through formulation of the culture medium, examined further in Chapter 3.

(2) The use of genetic engineering for maximising product formation on a per cell basis (discussed breifly in Chapter 3).

(3) Improving the culture environment for the cell, e.g. nutrient supply and minimised cell damage (Chapter 4), through either the modification of existing vessels or their operation, or alternatively the design of novel bioreactors (Chapter 5).

The advantages and disadvantages of such approaches will be discussed in the relevant introductory chapters.

2.1 General characteristics of hybridomas

Hybridomas are a fusion between two types of cell, a B lymphocyte producing the antibody of choice and a myeloma cell, both derived from the immune system of

mammals. They are grown in a complex medium formulation containing glucose, buffering agents, amino acids, organic acids, metal salts and a range of protein supplements.

These hybrid cells can either be derived from one species, for example mice, or from different species such as a human-mouse fusion. Division times can range from 11 h (Seaver *et al.*,1984, for a murine hybridoma) up to about 30 h (Thompson *et al.*,1986, for a human/mouse heterohybridoma) and cell diameters of 8-15 μm.

Their principal products, monoclonal antibodies, are a population of identical proteins which recognise a specific determinant on a simple or complex antigen, e.g. a protein on the surface of blood cells during blood typing. This feature of monoclonal antibodies is used for diagnostic assays in both molecular research and clinical medicine.

2.1.1 The creation of hybridomas

The first hybridomas were produced by the laboratory of Kohler and Milstein (1975). They were created from the fusion of a B lymphoblastoid cell to a malignant B lymphoblast, generally called a myeloma. This is a fusion in which each partner is selected for certain desired characteristics to be expressed in the resultant cell. For example the myeloma provides the fusion with 'immortality' in the sense that the cells will continue to divide for extended periods without the ageing process normally associated with mammalian cells. The untransformed B lymphoblast contributes the expression of the monoclonal antibodies.

The fusion protocols are usually dependent upon the partial disruption of the cell membrane, enabling the two cells to form a single fusion product (the hybrid). This fusion is usually facilitated through the use of a detergent-like compound, such as Polyethylene glycol, abbreviated to PEG (M^{c}Cullough and Spier, 1990, Catty, 1988, Butler 1991), or the use an electric current in a process called electrofusion (Neil and Urnovitz, 1988, Butler, 1991).

The key features of these procedures can be defined as follows:-

(1) Selection of the appropriate cells required for the fusion.
(2) Fusion of the cells using a membrane disruption technique (PEG or electrofusion/electroporation).
(3) Selection, cloning and expansion of the required, high productivity fusion.
(4) Production and storage of a stock of these cells for general use.

The selection of the correct cells for the formation of a hybridoma is especially important. The myeloma must be deficient in the production of its own antibodies so that only one type of antibody is produced (eg. murine Balb/c, murine NS 1, murine X63-Ag8-653, murine SP2/0). Ideally the fusion partners should be actively dividing with the cells entering mitosis at the same time. A comprehensive summary of these features and the techniques required for the formation of hybridomas can be found in Catty (1988) and McCullough and Spier (1990) and the reader is referred to these texts for further details.

2.1.2 Monoclonal antibodies

A brief summary of the production, structure and function of antibodies within the immune system is provided below but for further details the reader is referred to Paul (1989) and M^{c}Cullough and Spier (1990).

The antibody response

Antibodies are secreted into the blood stream and saliva as part of the body's immune response, which combats infection. In the initial (primary) response to an infection, small sections of the foreign molecule or cell, called antigens, are bound by the surface antibodies of an immature form of B lymphocytes (B cell). The antigen can either bind directly to the B cell or be processed via phagocytosis and representation of a section of the foreign molecule on the surface of another type of immune cell called an antigen presenting cell (APC). Each B lymphocyte will bind to a specific site

on the foreign molecule, with more than one antigenic site possible per antigen molecule. Each site has a specific three-dimensional structure, consisting of between 4-6 amino acid or sugar residues (Catty, 1988). Once the B lymphocyte has been stimulated by the binding process, a maturation and expansion of the number of B lymphocytes secreting this configuration of antibody occurs with the help of another immune cell, the T_{Helper} lymphocytes (T_H cell). These cells are responsible for the initiation and amplification of an immune response, often interacting with B lymphocytes and other immune cells. Antibodies generated in this response can show a degree of cross reactivity, where antibodies can be bound to alternative antigenic sites which show a degree of stereochemical homology with the site to which the antibodies were raised. However, the strength of binding and affinity of the antibody for this site is usually weaker.

Various forms of B lymphocyte exist in the body and are associated with the infecting agent at different stages of infection. The primary form, the resting B lymphocyte is a cell which does not secrete antibody and is derived directly from bone marrow. On binding the antigen, this type of cell can proliferate to form either memory or antibody producing plasma cells. In the primary response plasma cells usually produce IgM. The memory cells, remember the different forms of infection previously encountered by the body. On reinfection memory cells are activated by APC's eliciting a more efficient secondary (or anamnestic) response to the antigen consisting mainly of IgG. T_H cells then recognise the activated B cells which then divide increasing the population of antibody producing plasma cells.

Antibody structure

Antibodies, or immunoglobulins (Ig), are large glycoproteins which have a molecular weight (MW) ranging from 150,000 to 900,000 Daltons. Their basic structural form consists of a Y-shaped unit composed of two identical 'heavy chain' polypeptides and two identical 'light chain' polypeptides. Figure 2.1 outlines the basic structure of the antibody, with the paired heavy chains (MW approx. 50,000) forming the stem and arms of the Y, with the light chains covalently bound to the arms of the Y.

The complete structure is joined together through a series of disulphide bonds formed between interacting cystine residues. Similar bonds also form intrachain loops which allow the following classification of constant (C) and variable (V) domains, subscripted with an 'L' or 'H' based on their position on the heavy or light chain. A C_{H4} region exists on monomeric and pentameric IgM and IgE. The variable domains are found at the ends of the arms of the Y shape, on both the heavy and light chains. It is these variable domains that determine the immunoglobulins specificity for the antigenic site.

There are two different types of light chain, termed *kappa* (κ) and *lambda* (λ). The differences between the amino acid sequences of these two types are found within the C_L region, with further subtypes found within the λ light chains. The antibody can have either one or other of the light chain types, but never both.

The heavy chains determine the class of the immunoglobulin, with the constant domains containing sites for interacting with other branches of the immune response. There are five classes of immunoglobulin, IgM (μ), IgG (γ), IgA (α), IgD (δ) and IgE (ϵ), all of which differ in structure and function. The basic structure of the immunoglobulin classes are outlined in Figure 2.2, with their function outlined in Table 2.1.

Antibody function

Antibodies are primarily involved in recognising and marking foreign molecules as 'non-self', enabling other branches of the immune system to respond to infection. The response invoked on the creation of antibody-antigen complexes can be varied. When IgG and IgM form a complex with the antigen, conformational changes occur in the structure of the antibody, exposing receptor sites for the C1 protein of the complement pathway. The complement pathway involves a series of nine blood borne proteins which are involved in killing certain types of foreign cells. After the formation of the C1-antibody complex, a series of interactions follows leading to the formation of a complex aggregate of complement proteins which kill the cell by 'punching' holes in the cell membrane.

Figure 2.1:- Basic unit structure of antibody

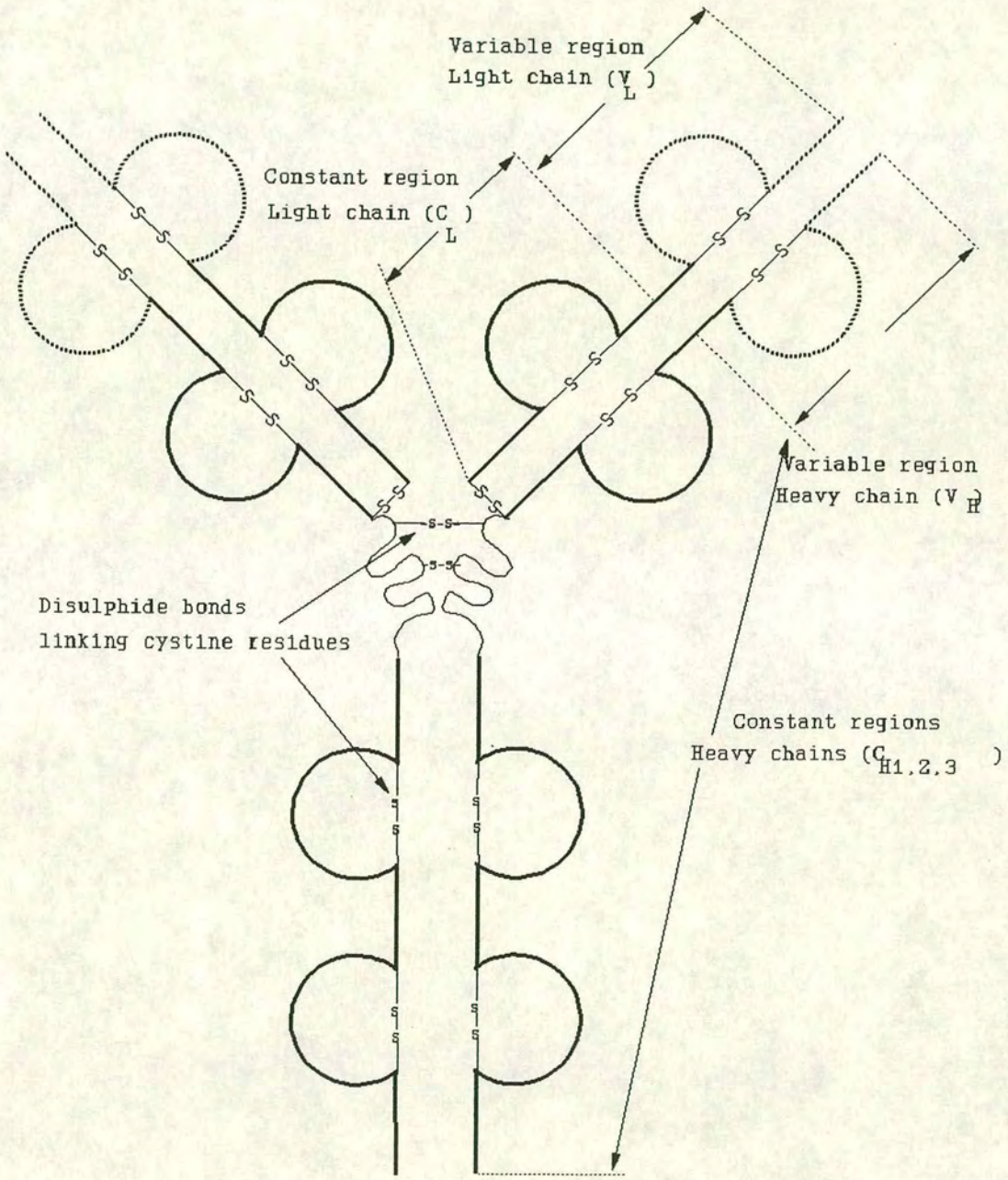

Figure 2.2:- Common blood borne antibody structures

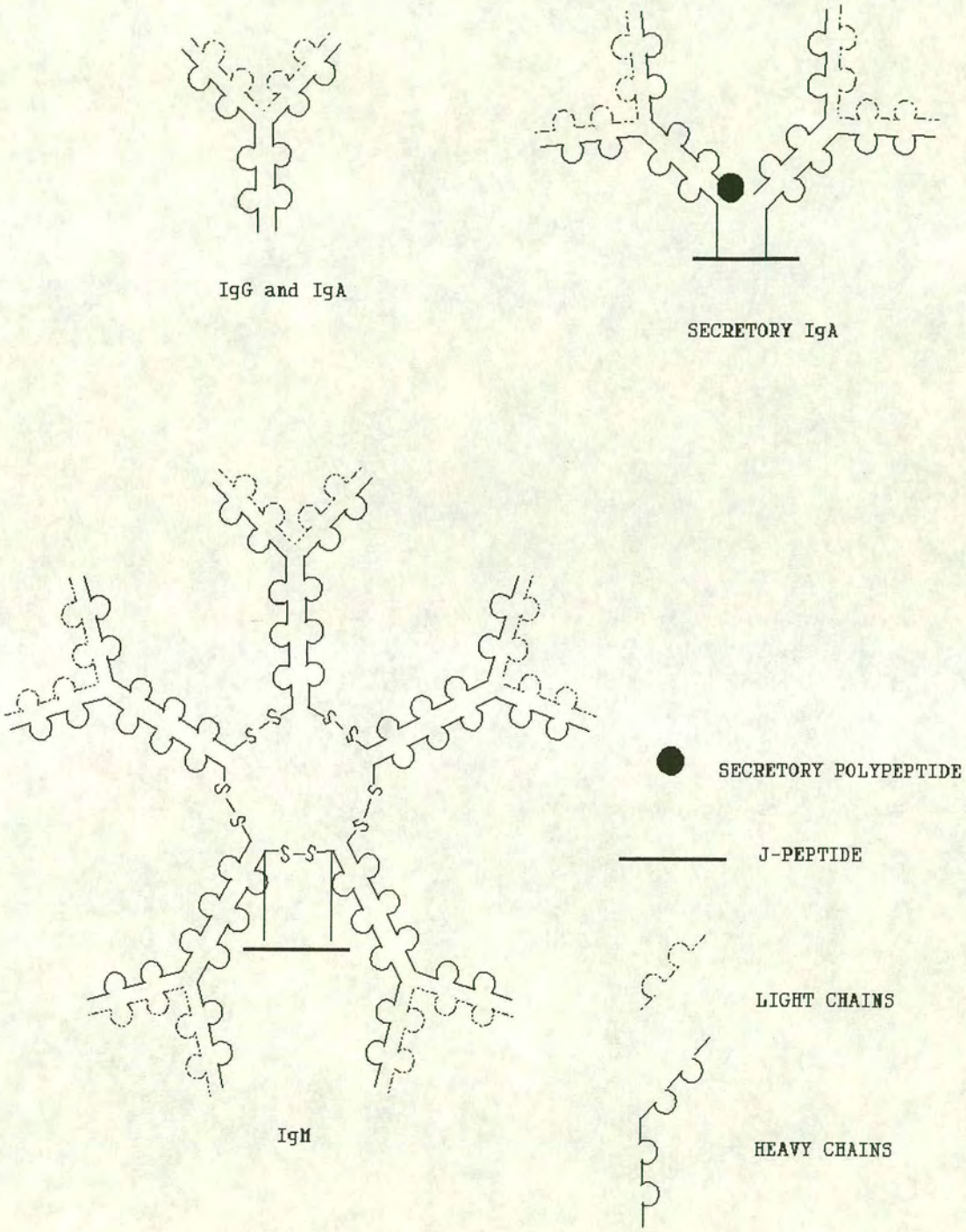

Table 2.1:- General features of antibody classes (from M'Cullough and Spier 1990).

Antibody Class	Molecular weight (Daltons) and shape	Primary Area of activity	Activation of complement pathway
IgG	150,000 to 180,000, monomer	Recirculated in the blood stream	Classic or alternate pathways
IgA	160,000, monomer in blood or 400,000 in dimeric secretory form	Tears, saliva respiratory and gastro-intestinal tract, some blood borne	Alternate complement pathway
IgM	900,000 pentamer	Mainly confined inside blood vessels	Classic pathway
IgD	180,000 monomer	Mainly bound to mature B-cells, small amount blood borne	none activated
IgE	200,000 monomer	Bound to the membrane of basophils and mast cells, small amount blood borne	none activated

There are two complement pathways, the Classical pathway and the Alternate pathway. The complement pathway relies on the presence of the antibody-antigen complex for the formation of the final complex. The alternate pathway can act with or without the presence of the antibody complex, specifically in the presence of Gram-negative bacteria. The pathway is basically a truncated form of the full classical pathway, with the response from this process being less efficient.

The complement pathway and certain IgG subclasses also stimulate opsonization, with the antigen-immune complex binding to a macrophage for ingestion via phagocytosis. As each immunoglobulin has at least two binding sites, it enables the formation of larger antibody-antigen complexes, which enhance the action of phagocytic cells. The

interaction between basophil and mast cell bound IgE antibodies (other cells responsive to infection) and the antigen aids the inflammatory response, releasing histamine.

2.1.3 Commercial and research use of antibodies

The body's usual antibody response is polyclonal, that is more than one antibody is raised against more than one site on the infecting agent. This is advantageous for the treatment of the infection by the body, however, this sort of response is not easily, or reproducibly created *in vitro* (Catty, 1988). The multispecific response attained is of little use for fine structural analysis, although a wide range of laboratory tests using polyclonal antisera have been developed. Such tests include radial immunodiffusion (RID), immunoelectrophoresis (IED) and many more (Catty, 1988, 1989).

Hybridomas enable the production of a source of antibody, which recognises one type of antigenic site. Assuming a low level of cross reactivity between sites, this enables the identification of specific antigens by procedures including enzyme linked immunosorbent assay (ELISA) and fluorescence activated cell sorting (FACS).

Two features of monoclonal antibody technology have led to an increase in the range of applications and subsequent commercial demand. The first is the limitless range of antigens to which antibodies can be raised. According to Catty(1988), a mouse injected with a compound with a molecular weight of greater than 5000 Daltons can elicit a response specific to this antigen. The B lymphocytes can then be used to form a fusion product. Antibodies can also be produced for lower molecular weight compounds through the use of carrier molecules. The target molecule, termed the hapten, is chemically linked to the carrier. Any immune response elicited to this hybrid molecule will generally include hapten specific antibodies. By careful selection, the lymphocytes producing these antibodies can be identified and used in a fusion.

Reporter molecules such as Fluorescein and Horse Radish Peroxidase can also be tagged to antibodies. These hybrid molecules enable the development of analytical

assays in which a colour indicates the presence of the test compound. These colorimetric assays further enhance the sensitivity of techniques such as ELISA and FACS.

2.2 Bulk culture techniques

The designs of fermenters used in the bulk culture of mammalian cells are based on those developed for the culture of bacterial cells. A range of different designs are available (Figure 2.3) although stirred tank and airlift fermenters are the most common. A comparison of the different culture techniques, based on the paper of Knight (1990), can be found in Table 2.2.

2.2.1 Fermenter design and operation

There are different types of stirred fermenter which can range in size from 0.02 litres to 30 litres, for glass vessels, and from 1 litre to 50,000 litres for stainless steel vessels (Knight,1990). These vessels are mixed using impellers, with gas being supplied to the medium through a sparge tube. There are several modes in which these vessels can be operated including batch, fed-batch, semicontinuous and continuous, described in Section 2.2. With minor modifications most reactors can be operated in a mode called continuous perfusion.

Airlift fermenters differ from the previous vessels in that they rely on aeration for mixing the medium instead of an impeller (Bliem and Katinger, 1988 a,b). They are operated in a similar way to stirred vessels, with operational procedures ranging from batch to continuous. The advantages of this type of fermenter include the simplicity of its construction, the provision of a low shear, well mixed environment for cell culture and ease of operation. These fermenters range in size from 0.5-10,000 litres (Knight,1990).

There are two basic designs of airlift fermenter, the concentric tube and the side arm airlift fermenter with both designs utilising the same mixing principle. Gas is sparged

Figure 2.3:- Simplified diagrams of bioreactor types

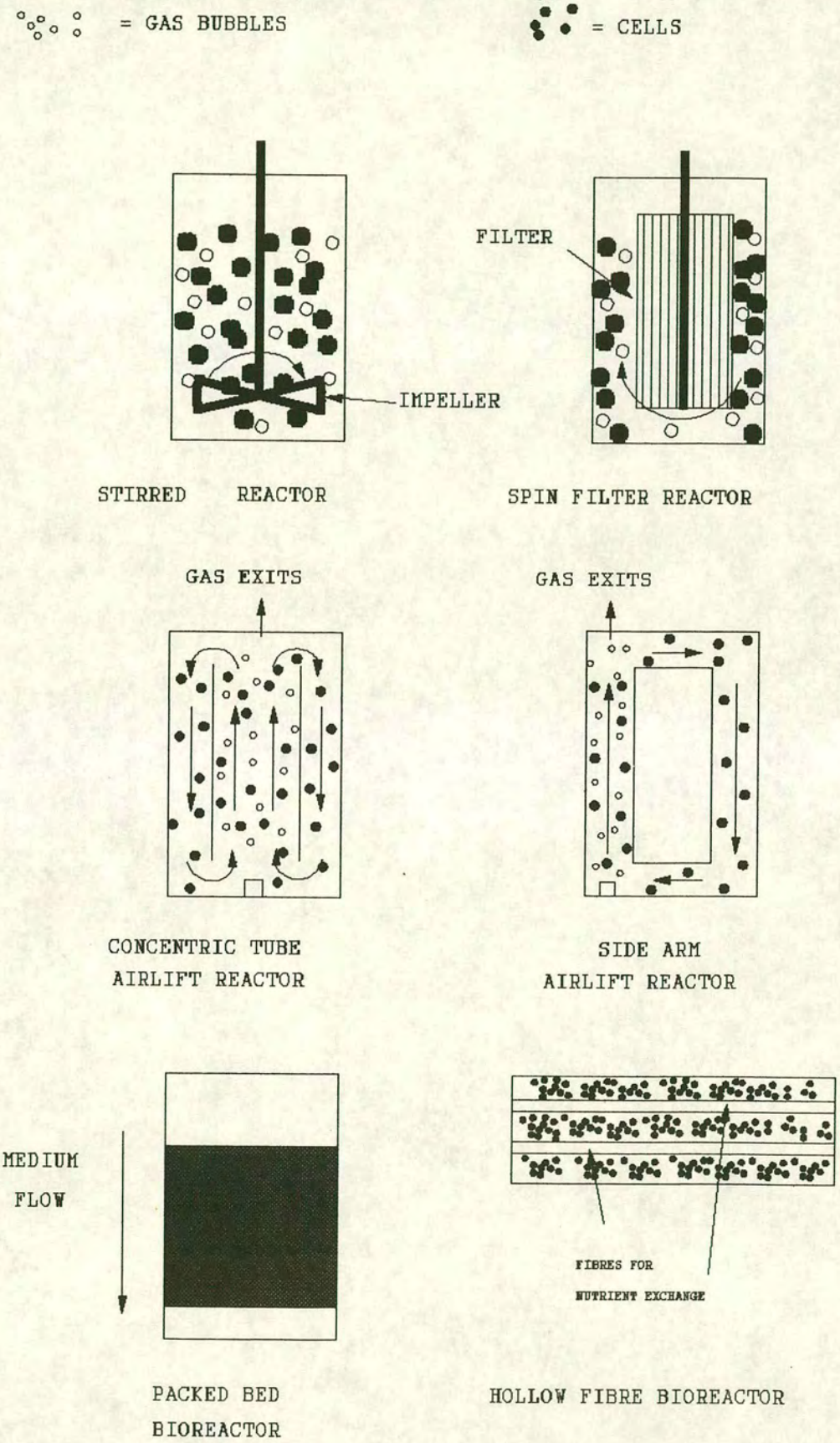

through the riser tube causing an alteration in the bulk density of the medium allowing a net flow up the riser tube. At the top of the vessel the gas is released and the bulk density of the accompanying medium increases. The welling at the top of the vessel causes the medium to be forced into the downcomer tube, which reintroduces the medium to the sparge at the base of the vessel.

Certain problems arise in mammalian cell culture which are not encountered with bacterial or fungal culture. Mammalian cells are more sensitive to shear forces present in their environment, with difficulties in ensuring an adequate supply of nutrients to the cells because of the size and hardiness of the cell wall (Croughan *et al.*, 1989). While the cells are relatively shear insensitive in a liquid only environment (Kunas and Papoutsakis,1990), the cells requirement for oxygen in stirred vessels can lead to mixing and sparging regimes which can lead to a significant level of cell damage. Under these conditions cell damage occurs at the air-liquid interface, primarily due to bubble rupture and foaming. Similar bubble related problems also occur in airlift fermenters. Hence, the effects that the culture environment has upon the cells must be taken into account in the design of both standard and novel fermentation systems.

2.2.2 Enhancing conventional fermentation technology

Conventional fermentation systems are primarily designed for the growth of cells in suspension, rather than anchorage dependent cultures, hence the surface area available for the attachment of these cells is limited. The mode in which these bioreactors are operated, either to harvest the cells and product together or to expect the presence of a low level of cells in the product stream is important. In the latter continuous systems where producing cells are lost with the waste stream, the cell numbers present in the fermenter are dictated by the dilution rate. Modifications to existing fermenters have been developed, accommodating anchorage dependent cells and retaining cells within the vessel. Improving cell retention maintains a larger proportion of viable, secreting cells within the bioreactor, increasing the per unit volume productivity of the system. This assumes that the cells are maintained in a state with a similar per cell production rate.

Table 2.2:- General overview of culture techniques.

Fermenter system	Cell Density ($x10^6$cells ml^{-1})	Antibody Production ($\mu g ml^{-1}$)	Cell Type	Operation
Airlift (Batch)	0.5 - 3.0	500	Anchorage/ suspension	Simple
Stirred tank (Batch)	0.5 - 3.0	500	Anchorage/ suspension	Simple
Stirred tank/ Hollow Fibre	10	600	Anchorage/ suspension	Complex
Spin filter	10	600	Anchorage/ suspension	Complex
Hollow fibre bioreactor	100	1000	Anchorage/ suspension	Complex
Ceramic matrix	100	1000	Anchorage/ suspension	Complex
Flat membrane bioreactor	100	1000	Anchorage/ suspension	Complex
Attachment/ adsorption systems	100	1000	Anchorage/ suspension	Complex
Entrapment	100	1000	Anchorage/ suspension	Complex
Encapsulation	100	1000	Anchorage/ suspension	Complex

Note:- Unless otherwise stated all systems were operated continuously.

Anchorage-dependant cells

One approach to growing anchorage dependent cells is to provide an immobilisation matrix, increasing the surface area on which the cells can be grown, removing the cell losses associated with the dilution rate. Nilsson (1987) and Belfort (1989) identify two different immobilisation techniques for these cells.

(1) Attachment/adsorption on to the surface of a carrier bead. Examples of such microcarriers include Pharmacia's Cytodex 1 beads and glass beads (Spier and Whiteside, 1976) with others listed in Butler (1991) and Griffiths (in Spier and Griffiths, 1990).

(2) Entrapment of the cells within a porous matrix, although this technique is not restricted to anchorage-dependent cells. Commercial systems include the gelatin Cultispher-G microcarriers and Verax Corporations Microspheres (Griffiths in Spier and Griffiths, 1990). Other systems have been developed where the gel beads are formed around the cells enabling them to grow in pockets within the beads (Nilsson, 1987). Wilson (1992) examined alginate and agarose based bead systems.

Beads can either be maintained in suspension (Wilson, 1992), or alternatively by using the beads in a packed bed (Spier and Whiteside, 1976). One of the primary differences between these two systems is the way in which the medium is supplied to the cells, with the former supplied by the mixing associated with suspension culture and a continuous flow of medium through the beads for the latter. The two systems also differ in the quantity of beads used in the bioreactor, with larger number of beads used in the packed bed system. While the latter system provides large areas for cell attachment, it tends to be limited in scale by the effects of concentration gradients and the maldistribution of the perfused flow through the packed bed due to channelling (M^{c}Cullough and Spier,1990).

Bead systems have an added advantage in allowing the separation of cells from the product, due to the greater density of the beads and the use of sedimentation techniques. The improved separation characteristics can be of further advantage in cultivation systems where the cells are to be retained within the culture vessel.

Cell retention systems based on conventional fermenters

A number of cell retention systems have been developed allowing the continuous culture of mammalian cells. These involve the incorporation of one or more permiselective barriers in the culture vessel. The barriers, or membranes, retain the cells within the vessel, while allowing the continuous perfusion of the cells.

One system involves the encapsulation of the cells within a hollow sphere. In this system, cells are entrapped in a gel matrix, which is then coated with a permiselective

barrier. The gel is then dissolved, retaining the cells within the bead while allowing the exchange of nutrients across the permiselective barrier. An example of this system has been commercialised by Damon Biotech (Nilsson, 1987) and was based on a poly-L-lysine coated alginate bead.

Modifications to existing apparatus include the use of spin filters (Himmelfarb *et al.*, 1969, Van Wezel *et al.*,1985), where a tubular mesh was fitted around the impeller shaft of a stirred vessel, with the culture mixed by the rotation of the filter. The spent medium was removed from the cell-free side of the filter, while the cells were retained on the other side of the filter. Reuveny *et al.*(1986a), in a comparative study of culture techniques, used a 5 μm pore sized filter retaining all of the cells. Avgerinos *et al.*(1990) found that this method could be further improved by increasing the pore size of the filter to 127 μm, and growing the cells in aggregates.

A more conventional approach, using standard filtration devices such as flat membrane and hollow fibre cartridges in parallel with a fermenter has also been used (De La Broise *et al.*, 1992). The filtration cartridge is operated as a crossflow filter allowing the separation of cells from the product. The cells are retained and recirculated back to the fermenter, with the product and spent medium collected as permeate. The fouling of the membranes often limits these systems, requiring the replacement or cleaning of the unit on a regular basis (Zhang *et al.*, 1993).

Other systems allowing cell retention through sedimentation, while separating medium and product from the fermenter, have been developed without the use of membrane cartridges. Hülscher *et al.* (1992) have reported a device which can separate viable and non viable cells through the use of cell size and low temperature. A device along similar lines has recently been developed by Bioscot Plc. (Thomson and Wilson, 1993). Hamamoto *et al.*(1989) have successfully used a continuous centrifuge in parallel with a fermenter, allowing cell recycle back to the main vessel.

Novel perfusion reactors

A range of hollow fibre bioreactors have been developed for the growth of

mammalian cells, first described by Knazek *et al.* (1972) with further designs described in Knight (1989). The cells are generally grown on the outside of the fibres, with the medium being provided from the inside of the fibre. These systems employ pressure gradients within the cartridge for the supply of nutrients and the removal of waste metabolites from the cells. There have been a range of designs suggested for this genre of bioreactor (Knazek *et al.*, 1980, Patankar and Oolman, 1990a+b, Tharakan and Chau, 1986, Brotherton and Chau, 1990, Cima *et al.*, 1990), with the principal limitation to their wider adoption associated with the fouling of the membranes and a lack of scale-up potential. A full examination is given to this subject in Chapter 5.

2.3 Hybridoma culture environment

Given the need for optimising the number of viable, antibody producing cells in a fermentation vessel, it becomes necessary to consider the environmental factors constraining their growth. Two approaches for improving the yield of product from the cells can be used:-

(1) The metabolic management of cells.
(2) The nurturing and maintenance of the cells in a maximal production state.

Metabolic management entails the cells being surrounded with a constant supply of fresh nutrients to enable their continued growth, while the concentration of potential metabolic inhibitors is minimised. This involves both the medium supply regime to the cell and the optimal formulation of the medium. If the cells are grown in suspension in a well mixed system, then medium should be readily available to the cells. However, if the cells are grown in layers, then zones of nutrient depletion are likely to occur, lowering cell viability (Stoker, 1973).

The nurturing of cells in a productive state aims to arrest the cells in the phase between cell divisions most conducive to product formation (Figure 2.4). There are

various identifiable phases during this period. The mitotic phase covers the time where the parental cell divides into two daughter cells. The G1 (gap) phase is a period just after cell division and just before the DNA replication in the S phase (stationary). Then a second gap phase (G2) occurs prior to mitosis and cell division. A further gap phase (G0) has been identified, where cells are no longer committed to entering the S phase (Ramirez and Mutharasan,1990). For hybridomas the maximal antibody production period has been reported to be in the G1 stage of the cell cycle (Hayter *et al.*,1992, Ramirez and Mutharasan,1990, Al Rubeai and Emery,1990). By adopting the strategy of maintaining cells at their maximum cell density in this state it should be possible to attain the highest possible production rate for the system.

A different approach involves the use of genetic engineering techniques increasing the production of existing cell lines. By introducing extra copies of genes coding for product, or alternatively, enhancing the control mechanism for existing genes, mammalian protein production can be increased. Engineered retroviruses and other such techniques have been used to amplify gene expression (Sanders,1990). Although promising, this topic is beyond the scope of this thesis.

Figure 2.4:- Outline of cell cycle

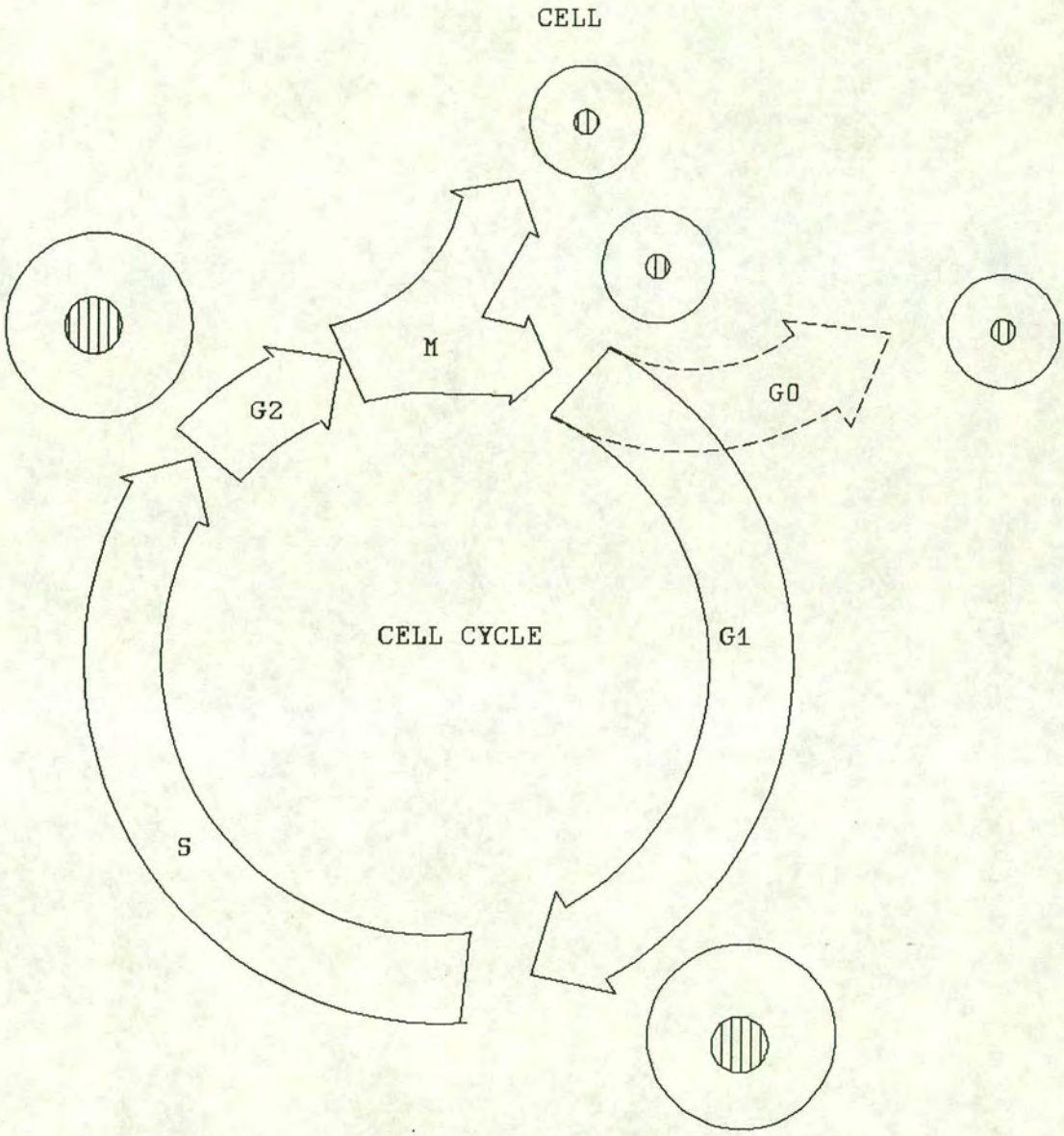

M = MITOTIC PHASE, CYTOPLASMIC AND NUCLEAR DIVISION OCCUR LEADING TO THE FORMATION OF TWO DAUGHTER CELLS

G1= GAP PHASE, BIOSYNTHESIS AND CELL SIZE INCREASE

S = DNA SYNTHESIS PHASE, WHERE CHROMOSOMES ARE DOUBLED

G2= GAP PHASE PRIOR TO MITOSIS

G0= CELL NO LONGER COMMITED TO DIVISION, LEADS TO CELLULAR SENESCENCE (NOT PRESENT IN HYBRIDOMAS)

Chapter 3

Metabolic management of hybridomas

3.0 Introduction

Before considering the methods by which a non-limiting supply of nutrients is provided to cells grown in an intensified culture system, via the design of the bioreactor, the nature and composition of basal medium formulations has to be considered. In Chapter 2, several methods of improving product yield were introduced including metabolic management, nurturing the cells in their maximal productive state and productivity enhancement via genetic engineering. This chapter will expand on these topics further.

3.1 Metabolic control through medium modification

The simplest method of controlling cell number and productivity involves modifying the composition of basal medium formulations through the gross addition of key nutrients such as glucose and glutamine. This approach is limited in that it does not take into account the effects that enhanced levels of these nutrients have on the metabolic state of the cell. A more practical approach takes into account these effects, considering their implications on the metabolism of the cell. Using such information, feeding regimes can be based on matching the supply of these key nutrients to the requirements of the cell.

Mammalian cells are similar to microorganisms in their basic nutritional requirements for carbon, nitrogen and oxygen, however, given their specialised function within the body they often lack biosynthetic pathways for all of the species required for their growth and maintenance. As a result the formulation of the medium used in their culture is often complex, with a further requirement for macromolecular growth factors and vitamins. A range of basal medium formulations are commonly used for the culture of hybridomas containing glucose, buffering agents, amino acids, vitamins, fatty acids and metal salts (Shacter,1989). M°Cullough and Spier (1990) identify and

summarise the culture characteristics of five different types of medium including DMEM, RPMI 1640, Iscoves modifications of DMEM (Dulbecco's Modified Eagle Medium) and RPMI 1640 (Roswell Park Memorial Institute) and Eagle's (Glasgow modification) medium. These formulations normally require further supplementation with foetal calf serum (FCS) in order to provide essential growth factors. Differences between the performance of these medium formulations included alterations in the mean generation time, maximum cell densities achieved and the duration of the death phase of the batch growth curve.

Various improvements have been made to these individual formulations via the gross addition of amino acid and glucose supplements (Glacken *et al.*, 1986, Miller *et al.*, 1989a+b, Jo *et al.*, 1990, Wohlpart *et al.*, 1990) or additions based on more accurate metabolic information (Duval *et al.*, 1991). Using the latter approach, Duval *et al.* (1991) determined the amino acid consumption patterns of two murine hybridomas during batch culture. This information was then used to improve the performance of a basal medium formulation (RPMI 1640), raising the maximum viable cell count achieved from 1.5 to $3x10^6$ cells per ml. However, while this approach shows obvious promise, Duval *et al.* suggest that its application is limited due to metabolic differences between cell lines requiring the individual optimisation of each medium formulation.

Serum, from either cattle or horses, at levels of between 5 and 20 % is used as the final medium component. These quantities have been reported to be maximal for both product and cell yield (Velez *et al.*, 1986, Dalili *et al.*, 1989). The effects of growing cells in serum below these levels have been reported to either match or lower (Low and Harbour, 1985a) the growth rate and antibody yields (Shacter, 1989). Ozturk and Palsson (1991), while comparing the growth of two murine hybridomas in a low serum formulation, found that one maintained its growth and antibody production rates, while both of these parameters decreased for the other cell line. They suggest that the serum acts as a source of growth factors and other essential proteins required for growth, although the emergence of a subpopulation capable of growing at low serum levels in the first culture was not ruled out. Other advantages of using FCS

include the mechanical protection of cells during stirred culture and the maintenance of relatively higher cell numbers than those observed when serum free formulations are used (Shacter, 1989, Dalili *et al.*, 1989).

However, commercial concerns are aiming to develop formulations which either use very low levels of the FCS, or that negate the need for FCS altogether. This area of research is fuelled, in part, by the following reasons:-

(1) FCS is expensive (about £65 for 500 ml), due to the costs of harvesting and the processing of the product, although these costs are often recouped by the relatively high value of the product.

(2) It is a highly complex, poorly defined additive, with only a small portion of the components identified, some of which may be inhibitory to growth (Shacter, 1989, M^{c}Cullough and Spier, 1990).

(3) FCS is also a source of ammonia, identified as a potential metabolic growth inhibitor, which is produced during its storage over a range of temperatures (M^{c}Limans *et al.*, 1981).

In an attempt to produce medium which can be licensed for use in the production of therapeutic product, a range of 'serum-free' and 'low serum' formulations have been made (McCullough and Spier,1990, Shacter,1989). Principal components of these formulations usually include transferrin, insulin, albumin, and a range of compounds including sub-toxic levels of ß-mercaptoethanol. These formulations have shown variable success in replacing serum (Shacter, 1990), with a sacrifice usually being made in the mean cell division time and final cell densities. Alternatively the formulations, requiring quantities of rare compounds, have proven uneconomical to produce on a bulk scale.

The use of cheaper sources of serum, for example new born calf serum, extracted from calves ranging from 0 to 10 days old, tends to be excluded due to the presence of contaminating proteins (e.g.antibodies) and iron deficiencies in the serum.

Wagner and Lehmann (1988) have noted a 20% reduction in antibody production using recombinant Baby Hamster Kidney cells grown in a serum free formulation. The

cells often have to be 'conditioned' to grow in serum free formulations. Even after conditioning the cell numbers supported by these formulations tend to be a fraction of those present in serum supplemented medium (Shacter, 1989). However, Shacter reports that an ERDF supplemented media, based on a supplemented mixture of RPMI 1640 and DMEM/Ham's F12, has outperformed serum supplemented medium, proving that the goal is attainable.

3.2 Metabolic Management

The number of viable, antibody producing cells per unit volume of medium is central to maximising product yields in hybridoma culture. By manipulating the metabolic pathways within the cell, the factors leading to cell death can be minimised. Methods for maintaining the cells in their maximal producing state will be examined in the next section.

3.2.1 Hybridoma catabolism and anabolism

The biosynthetic and metabolic pathways used by mammalian cells are highly complex, consequently the information presented in this chapter has been simplified, being based on a number of studies covering a range of different cell lines. Hence, given the reported variance between cell lines, this chapter should be considered as a general overview.

Transformed cells, including hybridomas, are locked into a continuous cycle of cell division, which can only be stopped by nutrient exhaustion, or the build up or addition of toxic metabolites or compounds. In order to facilitate this "grow or die" model, the biochemical machinery of the cell has to provide energy and raw materials for the synthesis of new cells and product. There are two classes of biochemical pathway
designated to these aims, catabolic, producing energy and raw materials for biosynthesis and anabolic, requiring energy and raw materials for biosynthesis. These pathways are under tight internal control by the cell so that potentially toxic over

production of any one component does not readily occur. This section will concern itself with the primary catabolic pathways of the cell, Glycolysis, Glutaminolysis and the Tricarboxylic Acid cycle (TCA cycle), outlined briefly in Figure 3.1 (adapted from Miller *et al.*, 1988).

Mammalian cells usually obtain energy from the oxidation of organic molecules, e.g. glucose and glutamine, using the energy associated with these reactions to produce Adenosine Tri-Phosphate (ATP) from Adenosine Di-Phosphate (ADP). These high energy phosphate bonds can then be used in subsequent energy requiring reactions. These reactions are usually carried out in the presence of oxygen, allowing the complete oxidation of the organic molecules to carbon dioxide and water, in a process called Oxidative Phosphorylation. However, under oxygen limited conditions, the cell cannot use oxygen as the terminal proton acceptor, forcing the cell to generate its own source of these molecules in order to continue ATP production. This latter process is termed Substrate Level Phosphorylation, with lactate acting as the terminal proton acceptor, Figure 3.2.

In hybridoma culture, glutaminolysis and the TCA cycle are dominant during Oxidative Phosphorylation, while glycolysis is dominant during substrate level phosphorylation.

3.2.2 Glycolysis

Glucose has two possible fates on entering the cell, being converted to a five carbon sugar to be used for biosynthesis via the Pentose Phosphate Pathway (PPP), or alternatively, conversion to pyruvate via glycolysis (Figure 3.2). This latter conversion can lead to the nett production of two moles of Adenosine Triphosphate (ATP) per mole of glucose converted, with ATP providing energy to power further chemical reactions. Pyruvate can then be converted to either lactate or to an intermediary of the TCA cycle, Acetyl Coenzyme A (AcCoA). By entering the TCA cycle, a maximum of 36 moles of ATP can be produced per mole of glucose, when

Figure 3.1:- Key catabolic pathways of the mammalian cell

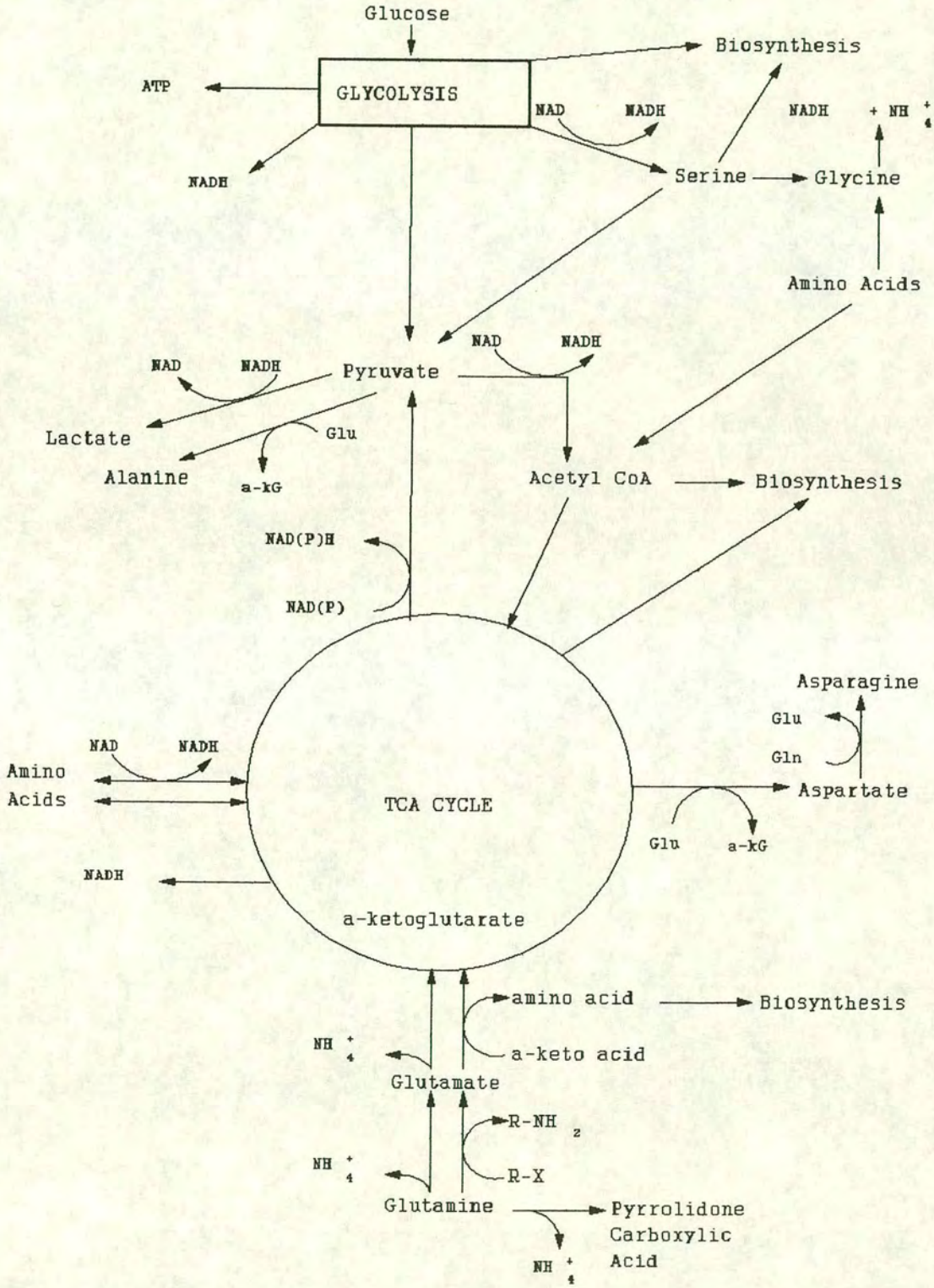

full oxidation occurs to carbon dioxide and water (Glacken et al, 1986).

Under normal conditions, the conversion of pyruvate to lactate only occurs in an anaerobic or oxygen limited environment, with the conversion of pyruvate to AcCoA occurring in the presence of oxygen. However, hybridomas have been reported as having dramatically accelerated glycolytic activity when compared with normal respiring cells (Luan *et al.*, 1987a, Sianno and Mutharasan, 1991) leading to an abnormally high rate of lactate production. Hybridomas also have a low rate of pyruvate transfer into the TCA cycle (Low and Harbour, 1985b). The primary significance of this conversion to lactate is the regeneration of the proton accepting cofactors (reduced NAD) required for the further ATP generation.

The contribution of glycolysis to the cells' energy requirements is primarily dependant on two factors, the level of oxygen, as previously discussed, and the initial level of glucose in the medium. The transport of glucose across the membrane when its extracellular levels are low (below 50 μM) is predominantly carrier mediated, with the cell controlling its transport (Luan *et al.*, 1987a). This controlled intake allows the cell to channel glucose through glycolysis, the pentose phosphate pathway and the TCA cycle. At this level glucose is primarily used for macromolecular synthesis.

As extracellular levels of glucose increase from 50 μM to 2 mM, there is a gradual shift from carrier mediated transport across the membrane towards a higher rate of facilitated diffusion, which is dominant at higher concentrations (Renner *et al.*, 1972). Luan *et al.* (1987a) suggest that as the cells shift towards passive diffusion, the levels of glucose within the cell become potentially toxic. The cell then increases glycolytic activity as a form of cellular detoxification, reducing these levels through the production of and secretion of lactate into the medium (Hatanaka, 1970). Several studies support this hypothesis, with Reitzer *et al.* (1979) observing a 50% increase in carbohydrate flux towards glycolysis and lactate production when glucose levels were increased from 0.2 to 10 mM. Groups exploring the effects of glucose pulsing upon continuous culture have noted that as glucose levels increase, glycolysis and lactate production increase, while oxygen and glutamine consumption rates are rapidly

Figure 3.2:- Glycolysis and substrate level phosphorylation

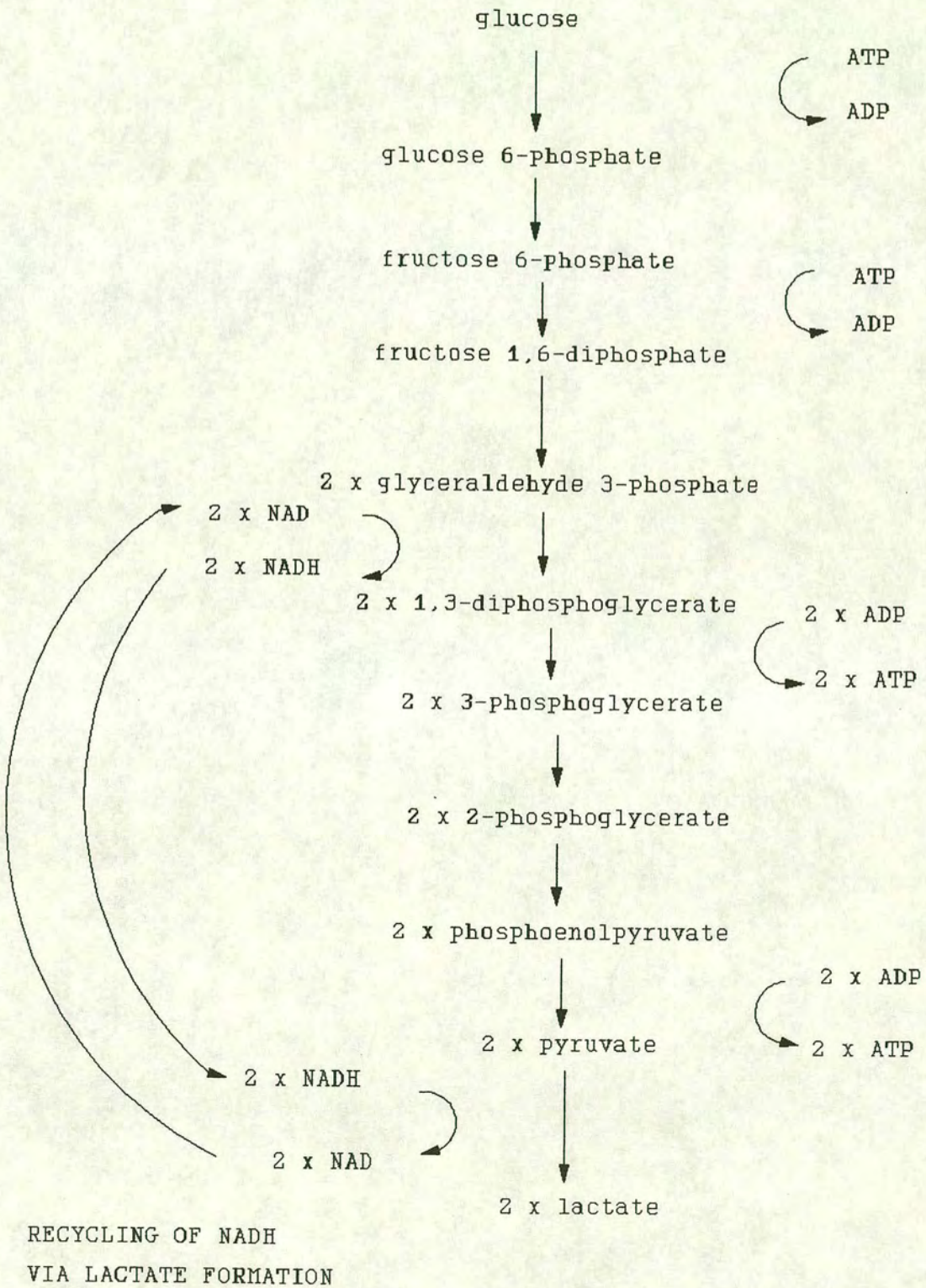

suppressed, with all of these parameters returning to normal as the concentration of extracellular glucose decreases (Miller *et al.*, 1989a, Wohlpart *et al.*, 1990). M^{c}Queen and Bailey (1990a) suggest that this is indicative of a switch in metabolism from oxidative phosphorylation to substrate level phosphorylation, a view supported by the work of Sianno and Mutharasan (1991).

Oxygen levels also have an important role to play in determining the method by which the cell carries out energy production. Miller *et al.* (1987) and Reuveny *et al.* (1985) found that as dissolved oxygen levels decrease, lactate production increases and antibody production decreases. Miller *et al.* concluded that cell growth was optimal at low levels of dissolved oxygen (0.5%), while antibody production was optimal at higher levels (50%) of saturation.

3.2.3 Glutaminolysis and the TCA cycle

Glutamine also has a primary role in catabolism and anabolism, with its complete oxidation through the TCA cycle providing up to 21 moles of ATP per mole of completely oxidised glutamine (Glacken *et al.*, 1986). Glutamine exhaustion has also been correlated with the cessation of antibody synthesis (Dalili *et al.*, 1990b), suggesting a central role in cellular synthesis. Glucose and glutamine have been shown to be interchangeable as energy sources, with glutamine providing between 33 and 65% of the cells energy (Wohlpart *et al.*, 1990, M^{c}Queen and Bailey, 1990a). Glutamine pulse experiments, unlike the parallel glucose pulse experiments, lead to a delayed increase in the glutamine and oxygen consumption rates, with an associated decline in the relative amounts of lactate produced per mole of glucose metabolised (Miller *et al.*, 1989b). At the other extreme, glutamine exhaustion, Sianno and Mutharasan (1991) have shown that there is a decrease in the oxygen consumption rate just after the point of exhaustion. They suggest that at this point the cell switches to substrate level phosphorylation for its energy requirement.

It would appear that, of the two systems, substrate level phosphorylation is more

responsive to extracellular levels of nutrient than oxidative phosphorylation, although the latter system is a more efficient method for providing the energy requirements of hybridomas.

3.2.4 Metabolic inhibition

Two byproducts of glycolysis and glutaminolysis, lactate and ammonia, have been suggested as potentially toxic to cells in batch culture. The formation of lactate in the cell, and subsequently its secretion into the medium, can prove limiting to cell growth and product formation. The effects of lactate appear to be cell line dependent, with both reports of no effect on cultured cells (e.g. Dodge *et al.*, 1987, Dalili *et al.*, 1990b, Wilson, 1992) and reports of decreased growth and antibody production rates (Luan *et al.*, 1987a, Glacken *et al.*, 1986). There are two reported hypotheses as to the action of lactate, firstly through a direct effect on the buffering capabilities of the medium altering the pH of the medium, and secondly through the presence of high levels of intracellular lactate indirectly affecting antibody secretion by chelating calcium ions (Luan *et al.*, 1987a).

In the deamination reactions associated with the conversion of glutamine to α-ketoglutarate, 2 moles of ammonium ions are liberated per mole of glutamine (M^{c}Queen and Bailey, 1990a). Ammonium ions affect the viability and growth of hybridomas by affecting the cells' metabolism (M^{c}Climans *et al.*, 1981, Glacken *et al.*, 1986, Dodge *et al.*, 1987, M^{c}Queen *et al.*, 1990). It is reported that between a 5-10 mM concentration of ammonium ions can inhibit mitochondrial respiration (M^{c}Climans *et al.*, 1981). As the levels of ammonia in spent medium can reach up to 3 mM, this may be a possible explanation for its inhibitory effect. Indeed one study has found that 2 mM ammonia can be severely inhibitory to cell growth (Dalili *et al.*, 1990a). M^{c}Queen and coworkers (1990b) have suggested that an increase in the ammonium ion concentration can lead to the acidification of the cells' cytoplasm, leading to the inactivation of enzymes whose operation at the new pH is inhibited. Intracellular acidification could also explain the inhibitory effects associated with the

presence of lactate in the medium. Georgen *et al.* (1992), have described an increase in cell death and lysis when extracellular pH levels fall below 7, supporting the previously noted effects of intracellular acidification.

3.2.5 Metabolic Management

Several methods of managing the metabolism of hybridomas have been suggested, including the methods by which they are grown (batch, continuous) and the levels of nutrients employed in their culture. Any regime in which the nutrients are repeatedly replenished, while the waste metabolites are continuously diluted to sub-toxic levels, should provide a suitable growth environment for the cells. Continuous, or semi-continuous culture also allows tighter control of the levels of the primary carbon sources, glucose and glutamine. The advantages of this approach include low waste accumulation, encouraging the cells into a more product oriented metabolic state.

In batch culture the control of waste metabolites can be central to the extension of the culture period, and hence productivity. According to Luan *et al.*(1987a) and Seaver *et al.*(1984), lactate production is primarily in the exponential phase of growth, suggesting the use of substrate level phosphorylation by the cells during this phase. Miller *et al.*(1987) confirm this hypothesis further with the observation that by lowering the dissolved oxygen level, the rate of lactate formation can be increased, suggesting the incomplete oxidation of glucose.

The production of lactate can be minimised in several ways. The first of these is the replacement of glucose with another, more slowly metabolised sugar, such as fructose or galactose (Eagle *et al.*,1958). The level of glucose in the extracellular environment is also important, so by decreasing the concentration of glucose in the medium the amount of lactate can also be reduced (Ray *et al.*,1989, Luan *et al.*,1987b).

The levels of ammonia can be controlled in a similar way to those of lactate, by decreasing the extracellular levels of glutamine (Glacken *et al.*, 1986). The effects of enhanced glutamine concentrations are important as they affect the rates at which

carbohydrate and oxygen are transported (Miller *et al.*, 1989b, Glacken *et al.*, 1986, Ramirez and Mutharasan, 1990), altering the respiration rate of the cells, and hence their metabolism. Glacken *et al.*(1986) controlled levels of ammonia produced during hybridoma culture by keeping the levels of glutamine in the medium low. Ramirez and Mutharasan (1990) suggest that the overfeeding of cultures with glutamine results in the toxic levels of ammonia observed, agreeing that a dosing regime was a better alternative for limiting waste metabolites. Schump and Schlaeger (1992) have taken a slightly different approach, selecting for hl-60 cells which are resistant to high levels of ammonia and lactate. Using this method they have been able to culture cells in 4 mM ammonia concentrations and 60 mM lactate, although this may indicate that some other factor (e.g. enhanced alanine levels) may be responsible for limiting cell growth.

3.3 Improving antibody production

There are three main areas in which antibody yield can be improved :-

(1) Increased numbers of viable producing cells in the culture medium.
(2) Maintenance of the cells in their optimal productive state via cell cycle control and enhanced antibody secretion.
(3) Genetically enhanced production of antibody by increasing the copy number of product genes or enhancing their control mechanism.

The first of these has been discussed using metabolic control, with a further discussion of the effects of bioreactor design provided in Chapter 4. This section will briefly discuss the remaining two features.

3.3.1 Cell cycle control

Although the number of viable producing cells present in the culture is of importance in optimising the yield of product from the fermentation, their maintenance in their maximal productive state is also important. Dalili *et al.* (1989) have suggested that

the production of antibody by the cell was 'non-growth' associated, with the specific production of antibody associated with the stage of the cell cycle that the hybridoma was in. Previously the production of antibody had been described as growth associated, being dependent upon cell number rather than the position of the cell in its cycle (Luan *et al.*, 1987b, Long *et al.*, 1988, Shacter, 1989). Leno *et al.*(1992) have suggested that the relationship between production and growth is dependant upon the way in which the cells are grown, with batch growth presenting a growth related model of antibody production, while continuous culture presents a non-growth associated model. The general features of the cell cycle were described in Section 2.3 and Figure 2.4, the following sections describe the effects of the cell cycle upon antibody synthesis, with the metabolic information associated with each phase.

M phase of the growth cycle

During this phase the cells undergo nuclear division (mitosis) and cell division (cytokinesis). Both of these functions require a lot of energy, with the cell switching its resources from macromolecular synthesis, for example antibody production, to cell division. Ramirez and Mutharasan (1990), have noted that small cells, i.e. newly formed cells, have the lowest requirement for oxygen, indicating substrate level phosphorylation. In rapidly growing cultures exhibiting high rates of growth, e.g. cells during exponential growth in batch culture and continuous and semi-continuous cultures with high dilution rates, antibody production is low (Hayter *et al.*, 1987 & 1992, Ramirez and Mutharasan, 1990, Al Rubeai and Emery, 1990). Further indications during this period include high yields of lactate from glucose and low oxygen and glutamine consumption rates. This would suggest a switch from oxidative phosphorylation to substrate level phosphorylation for the rapid supply of energy.

G1 phase of the cell cycle

The G1 phase of growth is associated with the end of the mitotic period just after the cells have divided to form two daughter cells. In this phase the cells increase their biosynthetic activity and size, preparing the cells for DNA synthesis and further cell division. A number of groups have identified the G1/S phase of the growth cycle as maximal for antibody production and secretion (Hayter *et al.*, 1987 & 1992, Ramirez

and Mutharasan, 1990, Al Rubeai and Emery, 1990, Coco-Martin *et al.*, 1992). Ramirez and Mutharasan (1990) have shown that variations in the length of the cell cycle are associated with the G1 phase, with slowly growing cells spending an increased time in this phase. This is supported by the work of Leno *et al.* (1992), who have shown monoclonal antibody production rates are highest in slowly dividing cultures, at low dilution rates in continuous culture.

S phase of growth

The cell, having attained a certain size and prepared all of the proteins required for DNA duplication, undergoes DNA synthesis, doubling the number of chromosomes in the cell. Several groups have reported the cessation of monoclonal antibody production with the commencement of DNA synthesis (Hayter *et al.*, 1987, Ramirez and Mutharasan, 1990). Modha *et al.*(1992), using an inhibitor of DNA synthesis to maintain cells in a non-proliferative state, have noted an increase in antibody production rates of up to 170%. Cells cultured under these conditions, while showing and increase in antibody production per cell, were larger in size than the untreated control. Modha *et al.* conclude that, based on the work of Larry and Studzinski (1969) correlating cell size with protein content, that the production rate per unit volume of biomass was similar. The inhibition of DNA synthesis would be expected to stop the cell cycle at the G1/S interface, where antibody production was maximal.

Metabolic information on this period of the cell cycle includes a decrease in the oxygen consumption rate (Ramirez and Mutharasan, 1990), and increased levels of ATP and the amount of cell associated monoclonal antibody (Modha *et al.*, 1992, Coco-Martin *et al.*, 1992). These features support the use of substrate level phosphorylation by the cell, providing energy for the major events associated with nuclear duplication.

Modha *et al.* (1992) also noted an increase in cell size during the inhibition of DNA synthesis. Kilburn, in a comment after the presentation of the Modha paper, suggested that this increase in size was a method by which the cell could maintain a constant intracellular concentration of ATP. Kilburn, based on work carried out by his group,

added that the absolute concentration of ATP increased up to S phase, decreasing to lower levels after the M phase of the cell cycle.

G2 phase of growth

During this period synthetic activity favours the production of the synthetic proteins required for the division of the nucleus and cells. Teillaud *et al.* (1989) found that by treating hybridomas with 10-40ng of Doxorubicin per millilitre of medium, there was a 3-5 fold increase in the amount of secreted antibody. They found that over 50% of the cells were maintained in the G2/M phase of growth, suggesting a variation in the rate of antibody secretion during the cell cycle.

Hence, it would appear that, by controlling the time during which the cells are in the G1/S phase of growth, antibody levels can be improved. Indeed, Deutschmann *et al.* (1993) have attempted to use cell cycle analysis as a method of control in continuous culture.

3.3.2 Improving the secretion of antibody

Sambinis *et al.* (1990) identify two routes by which antibodies may be secreted. The first of these routes is passive, involving the packaging of antibody into transport vesicles, which then travel to the cell membrane for release. The second route involves the storage of antibodies in vesicles, which are stimulated into release by a specific factor. Sambinis *et al.* suggest that the cell may be stimulated externally by a hormone, leading to an increase in the levels of cAMP/cGMP and calcium. These then act as a signal for the storage vesicles to fuse with the outer membrane, releasing their contents and increasing the amount of antibody secreted.

Dalili *et al.* (1990a) have examined the effects of cAMP and cGMP on the rate of monoclonal antibody secretion, finding that medium supplemented with 1 mM cAMP improves the amount of secreted antibody by 37%. Supplementation of the medium with a similar amount of cGMP lead to a 41% increase in the rate of secretion.

Sambinis *et al.* (1990) found a similar effect on the secretion rate of Human growth factor. Both groups concluded that cAMP and cGMP must be affecting the way in which the antibody is secreted.

3.3.3 Genetic control

Merten *et al.*(1984) recognise two types of cell line, one with a negative feed back control system, where the amount of antibody produced controls the flux of intermediary species through the biosynthetic pathway, and one without any feed back control. Antibody production rates can vary by between 0.1 μg/ml for the former type of cell and up to 100 μg/ml for the latter cell type during batch culture (McCullough and Spier, 1990). Genetic control can therefore have a marked effect on the production rates achieved by hybridomas in cell culture.

Sanders (1990) and MacDonald (1991) provide summaries of the use of genetically engineered vectors and the techniques employed for their introduction into mammalian cells. Generally this technique employs the use of retroviruses which inject their DNA into mammalian cells. Unlike other viruses where the viral infection of the cell usually results in lysis as a means of releasing new viral particles, retroviruses integrate their DNA with the host cells DNA. The viral DNA can then be expressed and passed on to subsequent daughter cells. By using the viral particles to inject genetically engineered DNA into the cell, extra copies of host genes, or alternatively non-host genes can be introduced into the cell.

These viral vectors usually incorporate the required DNA combined with a strong promoter, which ensures the high expression of the introduced gene. These are usually combined with a specific marker gene, conferring the ability of the cell to survive in adverse conditions. For example, glutamine synthetase is a commonly used marker which confers the ability of cells to synthesize glutamine from glutamate. Hence, cells containing the required sequence can be grown in glutamine free medium. Hassell *et al.* (1992) have used this system to enhance antibody production from NS0 and CHO

cell lines, reporting antibody production rates of up to 560 mg/l of medium.

While recognising the power of this technique for improving production, this area of mammalian cell technology will not be explored further as it falls beyond the scope of this thesis.

3.4 Summary

The growth and production of mammalian cells can therefore be controlled by altering the composition of the medium formulation, restricting the cells to a particular phase of the growth cycle or by genetically enhancing their production rate. All of these approaches have a basic requirement that the cells are supplied with the correct levels of nutrient. While the medium may be formulated to fulfil this criterion, cell growth may still be limited by the supply of these nutrients to the cells due to the formation of nutrient gradients within the bioreactor. The influence of these gradients can be reduced by altering the way in which the bioreactor is operated through a combination of medium supply regimes (e.g. Batch or Continuous culture) and the level of mixing within the vessel.

Chapter 4

Limitations to bulk culture

4.0 Introduction

This chapter discusses the principal limitations associated with the design and operation of bioreactors used for the culture of hybridomas. It will be assumed throughout this chapter that the medium used has been formulated to provide the maximum per cell production level and that the cell lines have been adapted for growth in a large scale system. It will also be assumed that, based on current fermentation technology, the culture vessel can be maintained free from contamination.

Several parameters are of importance in the design and operation of a fermentation system:-

(1) The provision of nutrients and oxygen to the cells, which involves the state in which the cells are grown and the supply regime of nutrients to the cells.

(2) The maintenance of the maximum viable cell population within the vessel.

(3) The culture of the cells in a low shear environment, which minimises the damage caused to the cells through mixing and sparging.

The following sections will examine the limitations associated with these criteria, describing the current solutions to these problems.

4.1 Nutrient supply

There are two features of medium supply which should be considered in the design of a fermenter. The first involves the access of cells to a source of nutrient, while the second requires the levels of the supply nutrients to be optimal for growth and product

formation.

4.1.1 Cellular access to nutrients

M°Cullough and Spier (1990), in a discussion on the role of cell derived growth factors, identify the importance of the cells proximity to the source of nutrients. The role of growth factors in hybridoma culture has been discussed in Chapter 3.

Dulbecco and Elkington (1973), showed that fibroblasts and epithelial cells were not subject to growth inhibition when physically touching, suggesting that no contact inhibition was occurring. They suggested that nutrient deprivation was the likely source of observed growth limitation. They also discussed the state of the cells as being of importance, with tissue density cells being more likely to be nutrient limited than dispersed, suspension grown cells. Stoker (1973) described the existence of a diffusionally limited boundary layer around the cell. Based on this information, two models can be proposed for the possible sources of nutrient limitation encountered by the cells.

The single cell model

The first is associated with the interaction an individual cell has with its local environment, as described by Stoker (1973). The zone directly surrounding the cell will be actively depleted of nutrients through metabolism by the cell. Once depleted, cell growth will be limited by the diffusion rate of nutrients down the formed concentration gradient, with the nutrients diffusing from the higher to the lower concentration (Figure 4.1). The converse is also true, that the concentration of potentially toxic metabolites produced by the cell will be highest at the cell surface. In this case, the cell is dependent on diffusion for their removal from its local environment.

The rate of diffusion of a nutrient across a mass transfer boundary layer is dependant upon the concentration gradient. The higher the concentration difference between the bulk nutrient ($[N]_B$) and that found at the cell wall ($[N]_W$), the higher the diffusion

Figure 4.1:- Single cell, boundary layer model

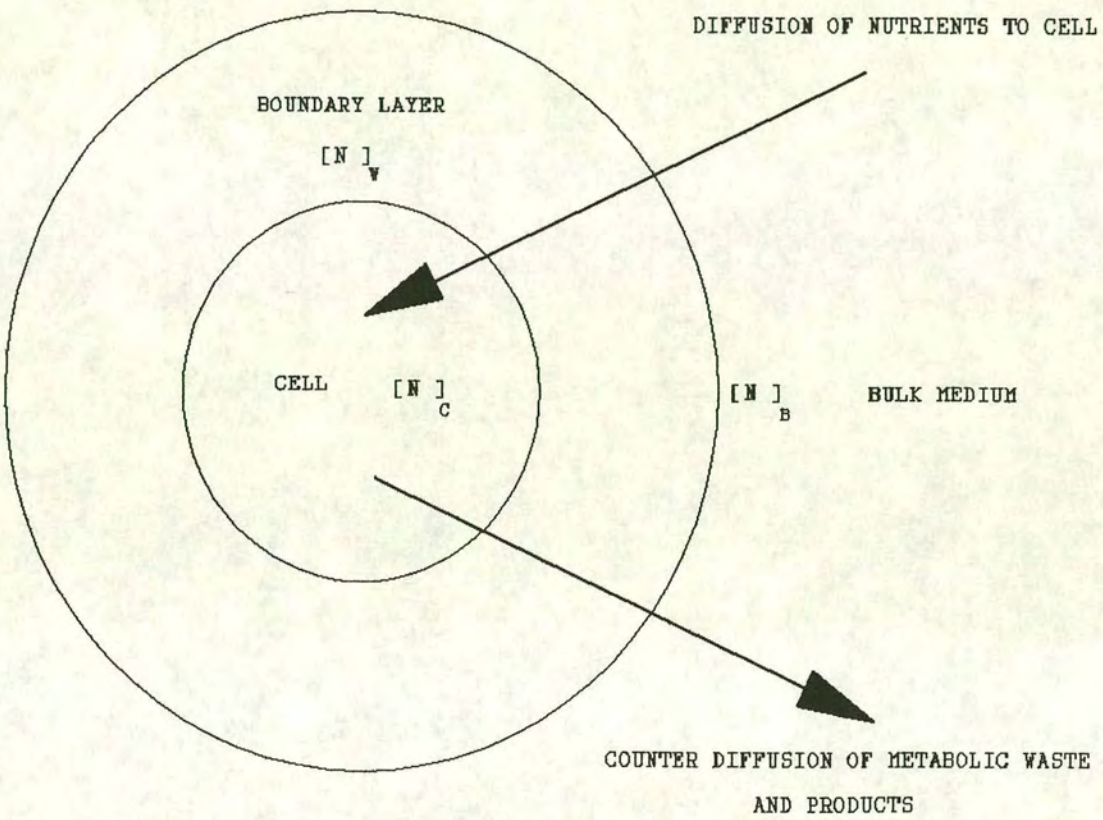

rate, complying with Fick's first law of diffusion. As the difference between the two concentrations approaches zero, the net rate of diffusional transport decreases to zero. For the cell, this latter case becomes limiting where $[N]_w$ is less than that required for the growth and maintenance of the cell ($[N]_c$).

The tissue type model

The second model applies to multilayered systems of cells, equating to tissue, in which there are two nutrient gradients to consider. The first gradient is associated with the individual cell which has been described in the previous paragraphs. This gradient

is further enhanced by a tissue mediated nutrient gradient. The concentration of nutrients will decrease as medium passes through the layers of tissue due to diffusional limitations and metabolism by the cells within the cell mass. The further the cell is from the source of nutrient ($[N]_S$), the lower the pool concentration of nutrients around the cell $[N]_B$ and hence the lower the rate of diffusion (Figure 4.2). Therefore, at a certain depth of tissue the cells will become totally depleted of nutrient where $[N]_W$ is less than $[N]_C$, leading to starvation.

As with the previous model, there is a counter diffusion of waste metabolites, which would be slowed by both the cell mediated, and tissue mediated concentration gradients. It is therefore necessary to maintain $[N]_W$ at a level, sufficient to maintain cellular metabolism. This can be achieved by increasing the flow of nutrients to the cell, ensuring that the concentration of bulk nutrients is high enough to supply the individual cells. It will be assumed that the bulk concentration of the nutrients fulfils this criterion for the remainder of this chapter, with the exception of oxygen, which will be discussed in the following section.

Oxygen limitation

Oxygen is often a potentially limiting nutrient, the supply of which is heavily dependent on mixing, diffusion and its solubility in the medium. The metabolic effects of oxygen concentration has been discussed in Chapter 3, with this section concentrating on the bulk supply of oxygen to the cell.

Oxygen is usually supplied to the fermentation vessel through an air-liquid interface, either directly through gassing the surface of the medium, by using gas bubbles, or indirectly through the use of a gas permeable membrane (Zhang *et al.*, 1993). The transfer of oxygen across the air-liquid/air-membrane-liquid interface is limited by the solubility of the gas in the medium and the volumetric transfer coefficient across the interface, termed K_La. Bleim and Katinger (1988b) describe this coefficient as the volume of gas transferred to the liquid phase per unit time (K_L) per unit surface area of the interface, per unit volume of the vessel (a = area/volume). This coefficient is affected by the degree of mixing within the vessel and the interfacial area associated

Figure 4.2:- Multilayered cell model

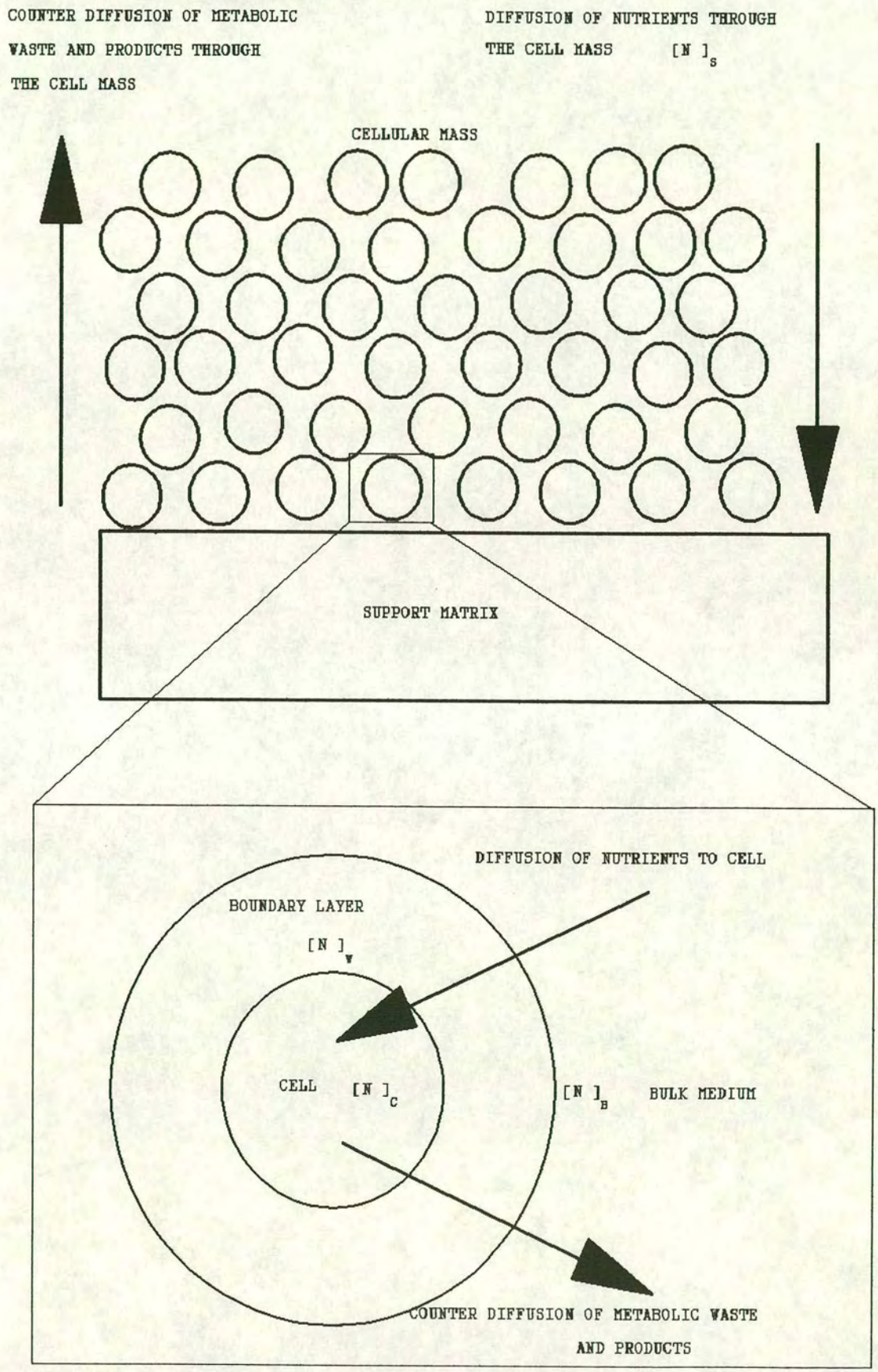

with gassing. In an unmixed, surface aerated vessel it has been shown that oxygen transfer is dependent upon the surface area to volume ratio, with oxygen diffusing 300 to 700 μm in static culture (Miller *et al.*, 1987). Gas bubble aeration has been shown to be maximal for smaller bubbles, which due to their higher surface area to volume ratio, have a greater transfer rate (Zhang *et al.*, 1992a). Silicone tube aeration, according to Zhang *et al.* (1993), has been shown to be a relatively slow and uncontrollable process, with dissolved oxygen levels fluctuating between 25 and 80% of air saturation in a 1l vessel.

However, all of these techniques are limited by the saturation point of oxygen in the culture medium which, according to Merten (1987), is approximately 6 mg/l at 37°C. Given this limitation, it follows that in poorly mixed systems, for example tissue density cell masses, the medium will only support cells until the supply of oxygen is exhausted. M°Cullough and Spier (1990) have calculated that in a diffusionally limited culture a maximum of 21 cell layers, an approximate depth of 256 μm, could be supported at this oxygen concentration.

Wei and Russ (1977) identify that the principal transfer mechanism present in suspension culture was convective flow, whereas a tissue mass would be reliant upon diffusional flow. In suspension culture, convection currents create a flow of 'fresh' medium near the cell wall, maximising both the distribution of nutrient and diffusional transport. For multilayered culture the nutrient supply is diffusionally limited as the tissue is relatively impermeable to the bulk flow, requiring the cells to be close enough to the supply to allow the diffusional supply of nutrients to be non limiting. Wei and Russ (1977) suggest that cells within the human body are usually only 50 μm from a source of nutrient supply and removal, enabling diffusional exchange to be non-limiting.

4.1.2 Model application to existing fermenters

The single and mulitlayered cell models can be applied to current methods of bioreactor operation. Suspension cultures conform to the single cell model, where

convection currents dominate ensuring a homogeneous mixture of cells and medium in both stirred tank and airlift fermenters.

The development of bead systems for the culture of anchorage dependant cells, increasing the surface area available for cell attachment, has led to an increase in the number of multilayered systems. Surface immobilised cells, such as the previously discussed Cytodex bead system, still comply to the single cell model, whereas entrapment and encapsulation techniques increase the cells' reliance upon diffusion for the supply of nutrients. In these systems there are poorly mixed areas containing high cell densities, equating to tissue. In this instance, bead size can be important as the cells have to overcome diffusion through the beads surface as well as tissue and cell mediated gradients. Wilson (1992) observed dead centres within alginate/agarose beads with a mean diameter of 3 mm, where cell growth did not occur. Packed bed bioreactors can also be prone to diffusional limitations due to the preferential channelling of perfusive flows leading to poorly supplied areas of the bed.

Hollow fibre bioreactors can also be considered as multilayered systems, with poor mixing within the cellular growth space. In these reactors, whether the cells are grown in suspension or immobilised in a gel matrix, nutrient gradients will occur due to the maldistribution of nutrients through the cell mass. However, in this instance the cells are not solely dependent upon diffusion for the supply of nutrients to the cells, as medium is perfused through the cell mass leading to an improvement in the flow characteristics through the tissue. The flow limitations associated with hollow fibre systems will be explored further in Chapter 5.

4.2 Modes of operation

There are several ways in which fermenters can be operated in the culture of hybridomas, these include batch, fed-batch, semicontinuous, continuous and continuous perfusion. These methods differ in the duration of the culture period, the supply of medium and the ways in which the cells and medium are harvested.

The mode of operation can be important in determining the overall cost of the fermentation. In the bulk culture of cells, the actual fermentation can be a limited proportion of the total process time. The process time consists of the growth of the inoculum, the preparation and sterilisation of the equipment and medium, and the fermentation, harvesting and purification of the product (Stanbury and Whitaker, 1989). The ideal process tries to balance the labour intensive periods during the initial set-up procedures and product processing against maximising the yield and hence the overall return. The procedures used can range from non steady state to steady state with respect to cells and nutrients, with the degree of control and monitoring required increasing as steady state is approached. Reuveny *et al.* (1986a) and De la Broise *et al.* (1992) provide a good comparison between these different modes of operation, with their results forming the basis of Table 4.1.

4.2.1 Batch growth

In batch growth the cells are grown using a fixed volume of medium until they have reached their maximum density. At the end of the culture period the cells are separated from the medium and the product harvested. This culture regime is limited in its duration, which means that the yield of product has to be as high as possible in order to counteract the costs of preparation and harvesting. This is a non-steady state system, with both the cell number and nutrient concentrations, for example glucose and glutamine, varying throughout the fermentation (Figure 4.3). While this process is short term, the control and monitoring required is relatively simple, requiring minimal maintenance, proving ideal for limited quantities of product.

4.2.2 Fed-batch growth

In the Fed-batch mode of operation, approximately half of the original medium and cells (termed 'flora') are replaced with an equivalent volume of fresh medium every couple of days. This partial replacement of medium aims to keep the nutrients above exhaustion level in order to maintain a viable cell population. This replacement tends to occur just prior to the attainment of the maximum cell density within the vessel.

Table 4.1:- Comparison of modes of fermenter operation.

Mode employed	Reactor type	Maximum viable cell count ($x10^{-5}$cells ml^{-1} of medium)	Reference
Batch	Stirred Tank	12	Reuveny *et al.* (1986a)
Fed-Batch	Stirred Tank	18	Reuveny *et al.* (1986a)
Semi-Continuous	Stirred tank	24	Reuveny *et al.* (1986a)
Perfusion	Stirred tank with spin filter	220	Reuveny *et al.* (1986a)
Perfusion (suspension)	Stirred tank with external tangential flow filter	12	De la Broise *et al.* (1992)
Perfusion (bead + suspension)	Stirred tank with a 20% total volume of beads	177 (bead volume) + 4.6 (suspension)	De la Broise *et al.* (1992)
Perfusion (hollow fibre bioreactor)	Cells grown in hollow fibre cartridge, in parallel with stirred tank	1100 (based on final value)	De la Broise *et al.* (1992)

N.B. The results from these two papers cannot be directly compared due to their use of different cell lines.

The portion of medium removed is then processed, harvesting the product. The original culture is then allowed to grow to near the maximum cell number, where the harvesting process is repeated. This cycle continues indefinitely, until the operator decides to terminate the fermentation.

This method increases the duration of the culture period, lowering the proportion of time allotted to the set up period, while requiring a higher degree of monitoring and maintenance. This system approaches a crude steady state control system, where the level of key nutrients, such as glucose and glutamine, and cells are maintained

Figure 4.3:- Batch and Fed-batch cell and nutrient profiles

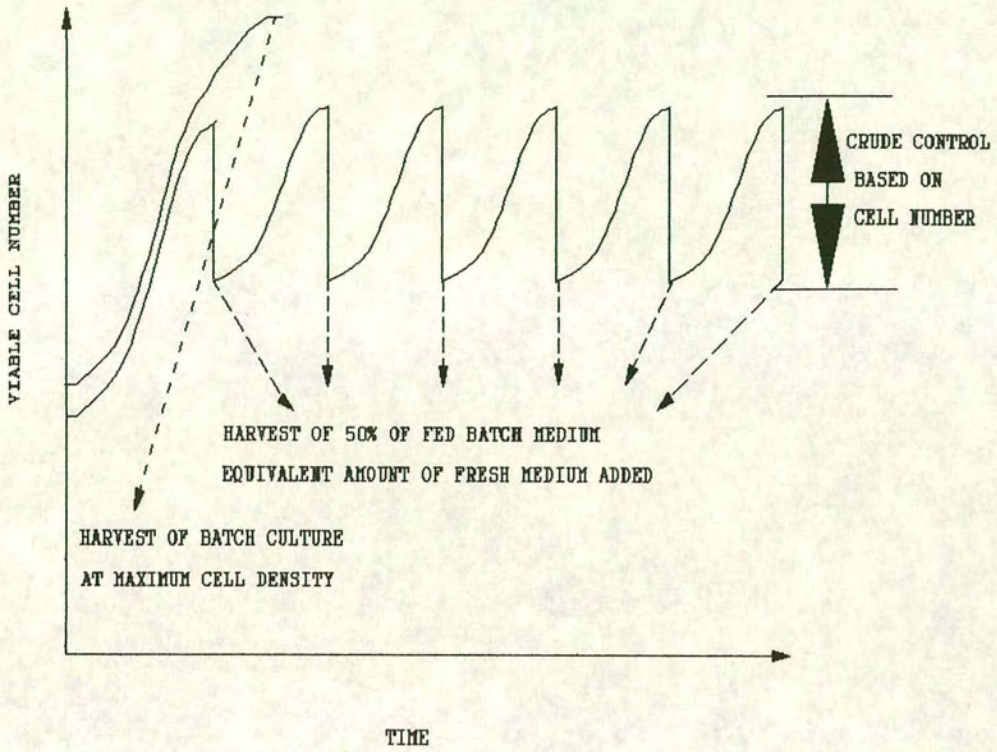

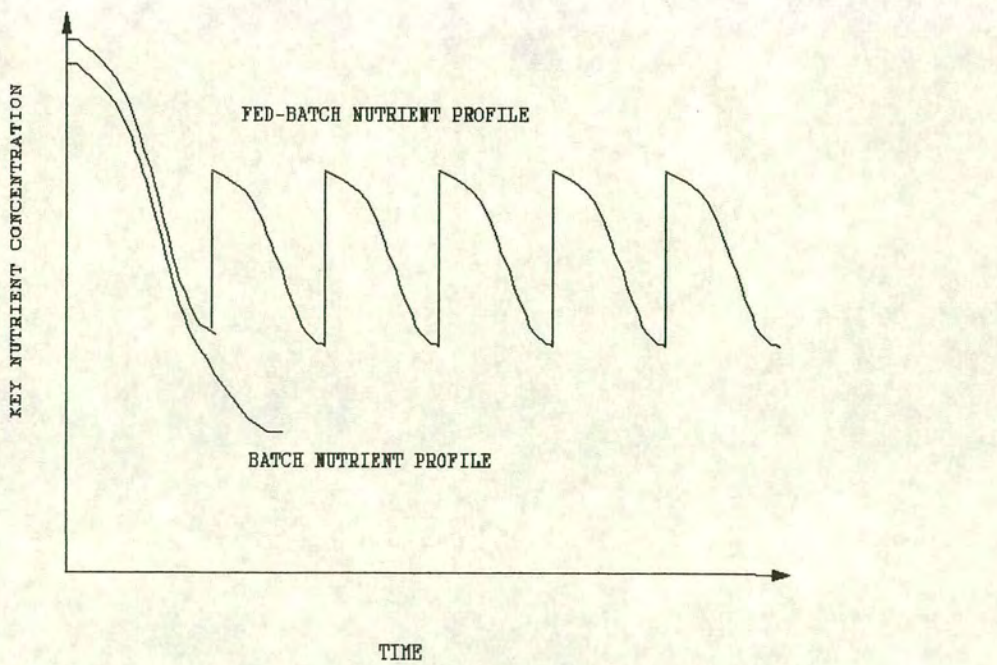

between controlled levels (Figure 4.3). This type of control also allows for the removal of potentially toxic waste products including ammonia and lactic acid.

4.2.3 Continuous culture

Continuous culture involves the constant addition of medium to, and the removal of medium and cells from the bioreactor, with one (or two) medium components acting as a growth-limiting nutrient. The aim of continuously culturing hybridomas is to maintain as high a population of producing cells as possible in the bioreactor. In order to achieve this goal, the dilution rate has to be altered to suit the growth rate of the cells.

The level of limiting nutrient in the vessel can be used to determine the concentration of cells in the vessel, with constant cell numbers being achieved with a constant substrate concentration. The rate at which medium is added to and taken out of the reactor (Dilution rate (D)= Flow/Volume of the reactor) alters the levels of the limiting nutrient and is often expressed as the number of complete replacements of the reactor's volume per day. The rate of increase or decrease of cell concentration can then be calculated from Equation 4.1.

$$dx/dt = (\mu - D)x \qquad \text{(Equation 4.1)}$$

where x= the concentration of cells in the vessel

μ= the specific growth rate of the cells, t= time

D = dilution rate

Under steady state conditions where x is constant and dx/dt=0, the cell growth rate (μ) is determined by the dilution rate, i.e. D = μ. While this condition holds true for a range of dilution rates, deviations from Equation 4.1 occur at high and low values of D. When D exceeds μ_{max} wash out occurs as the concentration of cells within the vessel is no longer determined by the limiting nutrient, but by the maximum growth rate of the cells. Therefore at high values of D ($D > \mu_{max}$) cells are removed from the vessel at a higher rate than they can be replaced by division, leading to non-steady

state conditions. At the other extreme, i.e. low values of D and μ, cell numbers in the vessel decrease as the supply of the limiting nutrient is insufficient to maintain a significant population, leading to cell starvation and death.

This system can be maintained and controlled in a steady state with respect to cells and nutrients, requiring continuous monitoring. However, while this process offers the continuous production and harvesting of product, it is difficult to control and results in the continuous loss of viable cells to the waste stream.

This technique has been improved through the use of cell retention devices in conjunction with the culture vessel. Continuous perfusion, involves the recycling of the cells from the separation device back into the main vessel. This approach maximises the cell numbers within the reactor by removing the constraints of dilution, i.e. wash out, and allowing the bioreactor to be operated at values of D exceeding μ_{max}. Examples of such systems have been described in section 4.3.2 and include the use of spin filters, membrane cartridges, specially designed bioreactors and separation devices. These devices allow the discharge of 'spent' medium which may contain product or cell debris, while retaining the viable cells.

The systems developed by Hülscher *et al.* (1992) and Thompson and Wilson (1993) can separate dead cells and debris from viable cells, ensuring a steady population with a high percentage viability within the reactor. The use of filters can lead to problems due to the fouling of the membrane and the retention of dead cells. The maximum cell population attainable within these systems is usually limited by hydrodynamic and design problems.

4.2.4 Semicontinuous culture

The semicontinuous mode of operation is intermediate between Fed-Batch and continuous operation, with the removal and replacement of a smaller volume of the total medium containing flora in the vessel, at a higher frequency equating to the daily dilution factor used for continuous operation. This method is based on a tighter

Figure 4.4:- Cell and nutrient profiles for bioreactors

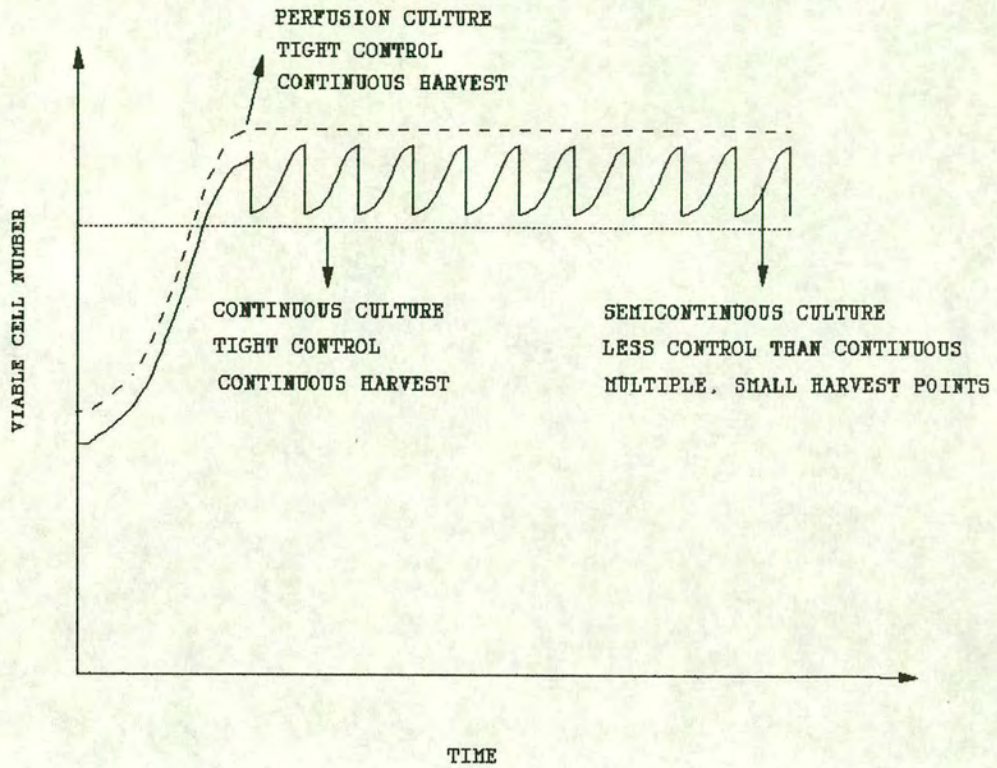

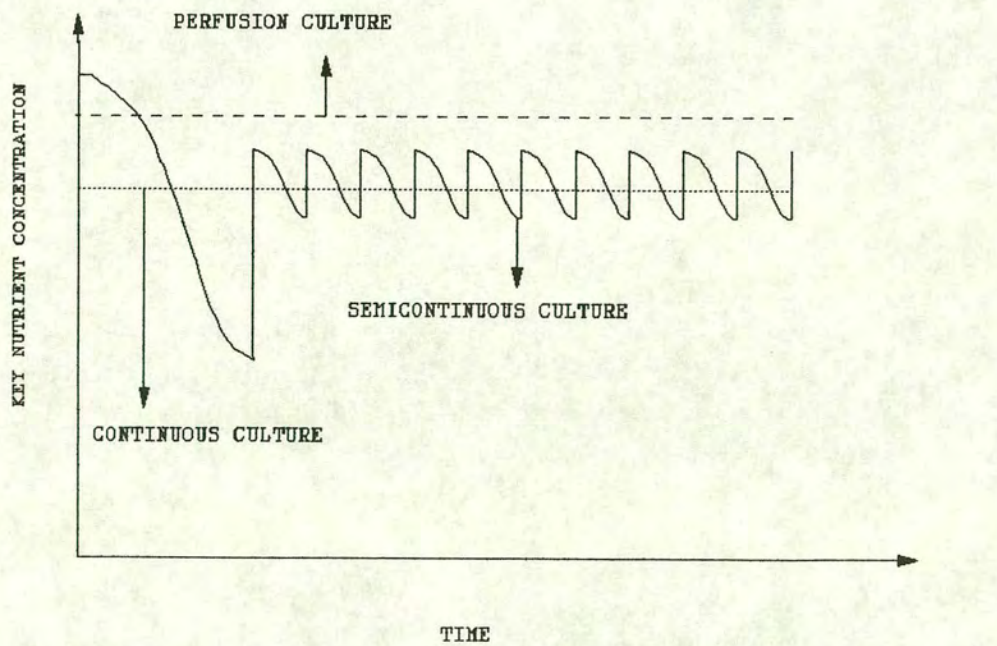

control for maintaining nutrients at a constant level, whereas Fed-batch is a cruder form of control based on extremes of cell density and nutrient levels. With this method the fluctuation in both cell and nutrient levels is less than in the Fed-Batch, but higher than continuous culture.

Reuveny *et al.* (1986a) and Miller *et al.* (1989a, 1989b) found that this technique could be improved by dosing the reactor with presterilised glucose and glutamine at various points in the culture of the cells.

4.3 Metabolism and modes of operation

The information provided in this and the previous chapter can be used to describe the physical and metabolic constraints placed on the culture of mammalian cells in the various forms of bioreactor. This can then be used to further explain the advantages and disadvantages associated with batch and continuous operation and the types of vessel used for the dense culture of mammalian cells.

4.3.1 Batch operation

A typical culture curve for batch operation is outlined in Figure 4.5 consisting of a lag phase, a log/exponential phase, a stationary phase and a decline or death phase.

During the lag phase the newly inoculated cells adjust their metabolism to the local environment. As glucose levels are usually high, a high rate of facilitated diffusion across the cell membrane dictates the formation of lactate via glycolysis as a form of cellular detoxification. During this phase the cells have been reported to be predominantly in the S phase of the growth cycle (Ramirez and Mutharasan,1990).

As the cells enter the exponential phase of growth substrate level phosphorylation dominates, providing energy for high levels of biosynthesis and the resulting high growth rate. A decrease in the levels of S phase cells and an increase in G2/M occurs. Glycolytic activity suppresses the oxygen consumption rate and the levels of

Figure 4.5:- Phases of growth during batch culture.

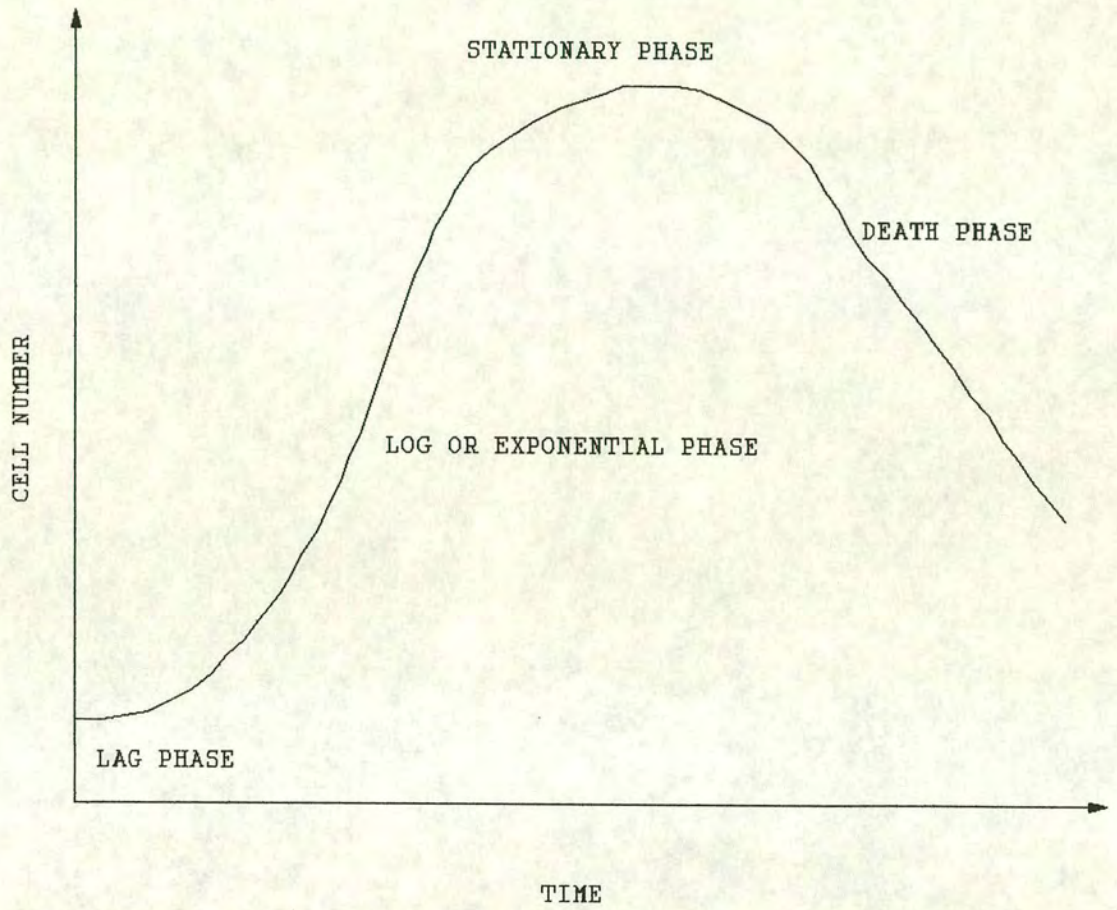

glutaminolysis and TCA activity. As the levels of glucose become sub-toxic, allowing a more controlled level of carrier mediated transport, the fuelling of cellular activity moves from predominantly substrate level phosphorylation to oxidative phosphorylation. This leads to an increase in ammonia and antibody production rates and the glutamine and oxygen consumption rates. As the cells begin to slow their growth rate, an increase in the number of G1 phase cells leads to an increase in antibody production.

Stationary growth indicates the exhaustion of glutamine in the medium, with the cells entering a period of slow growth. At this point the cells, in the absence of glutamine,

attempt to convert to substrate level phosphorylation by lowering their oxygen consumption rate. Under these conditions the cells either lack adequate levels of nutrient or exist in an environment containing toxic levels of waste metabolites, leading to cell death and a subsequent decline in viability. Necrotic and dying cells, according to Al-Rubeai and Emery (1990), can still release significant amounts of antibody, increasing the overall yield of product in batch culture.

While this technique for the bulk culture of mammalian cells remains popular, its crude control limits both cell number, through the exhaustion of nutrients and build up of toxic metabolites, and the maintenance of these cells in the metabolic state most conducive to product formation.

4.3.2 Semi-continuous and continuous culture

These systems allow greater control of the cells environment, enabling the use of lower levels of key nutrients. By continuously adding fresh nutrient and removing waste products, the cell can be nurtured in surroundings which are more conducive to growth. By controlling the rate at which the nutrients are added to the vessel there is also an opportunity of controlling the growth rate of the cells.

Controlling the growth rate of the cells is an important factor in hybridoma culture, with the rate of cell division determining metabolism and consequently the production rate of the cells. At high growth rates it has been shown that the cells tend to use substrate level phosphorylation, metabolising glucose and producing high levels of lactate (Ramirez and Mutharasan, 1990). There is an associated decrease in antibody production rates (Hayter *et al.*, 1987, Ramirez and Mutharasan, 1990) as the cells shift their resources towards supporting cell division, spending less time in the G1/S phase of the cell cycle. The observations of Leno *et al.* (1992), that there is an increase in cell associated antibody during rapid growth, support this switch of resources away from production and/or transport.

At lower dilution rates, and hence specific growth rates, the amount of antibody

produced increases (Hayter *et al.*, 1987). Under these conditions, the cells are able to metabolise glutamine, favouring oxidative phosphorylation and antibody production. Jan *et al.* (1992) note the previously described problems associated with too low a dilution rate, where maintaining cell viability can prove difficult.

In conventional semi-continuous and continuous culture the wash out of cells to the waste stream is accepted as the norm. As previously discussed, the loss of viable, producing cells is an inefficient method of production, while the use of continuous perfusion and other separation devices allows the retention of these cells, improving the yield of product from the bioreactor.

4.4 Problems in hybridoma fermentations

This section will discuss the effects of shear upon the cells caused by the aeration and stirring (or agitation) of the culture vessel. Bleim (1989) suggests that there are three parameters involved in the limitation of cell growth in conventional cultivation systems (i.e. stirred tank reactors and airlift fermenters). These are velocity gradients, turbulence and bubbling, which he suggests affect such cellular processes as DNA synthesis, protein formation, secretion and also result in physical damage and lysis. Mijnbeek (1991) provides a good summary of the general hydrodynamic and bubble mediated shear forces present in bioreactors to which cell damage has been attributed.

4.4.1 Hydrodynamic shear

Mammalian cells have been reported to be particularly sensitive to the effects of shear due to the weakness of the cell membrane (Wagner and Lehmann, 1988). These cells, unlike their simpler prokaryotic and eukaryotic counterparts, do not have a rigid cell wall and are therefore more susceptible to rupture by hydrodynamic shear (Croughan *et al.*, 1989).

Turbulent flows within the vessel, caused by mixing and inserts within the fermenter, can lead to the formation of eddies (Bleim and Katinger, 1988b). The size and energy dissipation associated with eddies were originally described by Kolmogorov (1941) with the size of the eddy being of importance in the amount of damage incurred by the cell. McQueen *et al.* (1987) concluded that small eddies, with a Kolmogorov size of 3.5 μm could lead to the lysis of individual cells. Studies using microcarriers (Croughan *et al.*, 1989), indicate that Kolmogorov eddy sizes of 100 μm caused the most damage to 185 μm beads. Mijnbeek (1991) concludes that eddies which are smaller than the size of the cell or carrier are more likely to cause shear damage than those eddies capable of entraining beads or cells. Croughan *et al.*(1988) describe a secondary hydrodynamic effect for microcarriers, which has been quantified by Cherry and Papoutsakis (1986,1988,1989). This involves the interaction between eddies, leading to microcarriers colliding at speed. The damage caused to the immured cells has been related to the Terminal Collision Severity (TCS) by Cherry and Papoutsakis (1988,1989).

Although eddy formation and TCS have been shown to be involved in suspension and microcarrier related cell damage, there is increasing doubt as to whether hydrodynamic shear is a major cause of cell death in stirred or aerated vessels. Michaels *et al.* (1991) indicate that hydrodynamic shear affects biological effectiveness rather than leading to cell death. Levesque *et al.*(1989) found that the function of endothelial cells cultured in a stirred vessel was altered, suggesting that hydrodynamic shear forces may have been responsible. Kunas and Papoutsakis (1990) have cultured mammalian cells in a 2 l fermenter at a stirrer speed of 700 rpm, in the absence of an air liquid interface. Above this value cell damage was found to correlate with the formation of Kolmolgorov eddies in the size range of the cells. In the presence of this interface, cell viability was severely affected at speeds above 150 rpm, suggesting that the presence of an air-liquid interface led to the damage of the cells. Under these conditions cell damage was related to vortex formation and the associated entrainment and rupture of bubbles.

4.4.2 Bubble shear

Kilburn *et al.* (1968), in reporting the superiority of a sparge technique for the aeration of cultures, suggested that the bursting of bubbles at the medium surface may be a major cause of damage to the cells. Bleim and Katinger (1988a, 1988b) describe two components to bubble shear, the first being the turbulence caused by bubble motion through the media, and the second component being related to the residence time of the cells at the bubbles air/liquid interface. The effects of turbulence have already been discussed in the previous section and will therefore not be discussed further.

Handa(-Corrigan) *et al.* (1987, 1989) found that the maximum cell damage occurred at the region of bubble disengagement, correlating the degree of damage to suspension grown cells with bubble frequency, bubble size, cell type and the exposure time of the cell to the air-liquid interface. Tramper *et al.* (1988) were unable to duplicate these results with respect to bubble size, finding a linear correlation between cell death, gas flow rate and the reciprocal of the vessel diameter. Handa(-Corrigan) *et al.* (1987,1989) have visualised cell-bubble interactions within the head of foam, concluding that surface mediated damage occurs in one of two ways. The first was associated with unstable foams found in serum supplemented medium, where the cells were entrained in the lamellae between the bubbles. The cells were damaged by the bursting of bubbles and the drainage of liquid through the foam layer (Figure 4.6, adapted from Handa-Corrigan *et al.*, 1989). Mathematic modelling of this process (e.g. Boulton-Stone and Blake, 1993) has determined that the energy dissipation associated with the bursting of the bubble (10^4dyn cm^{-2}) is high enough to kill mammalian cells. This value is of a similar order to that recorded by Zhang *et al.* (1991) who have used a micromanipulation technique to estimate the force required to rupture mammalian cells ($5x10^4$dyn cm^{-2}). The second method, found in stable foams containing FCS and antifoam, occurred as a direct result of the bubble oscillations associated with rapidly bursting bubbles.

Figure 4.6:- Bubble damage mechanisms

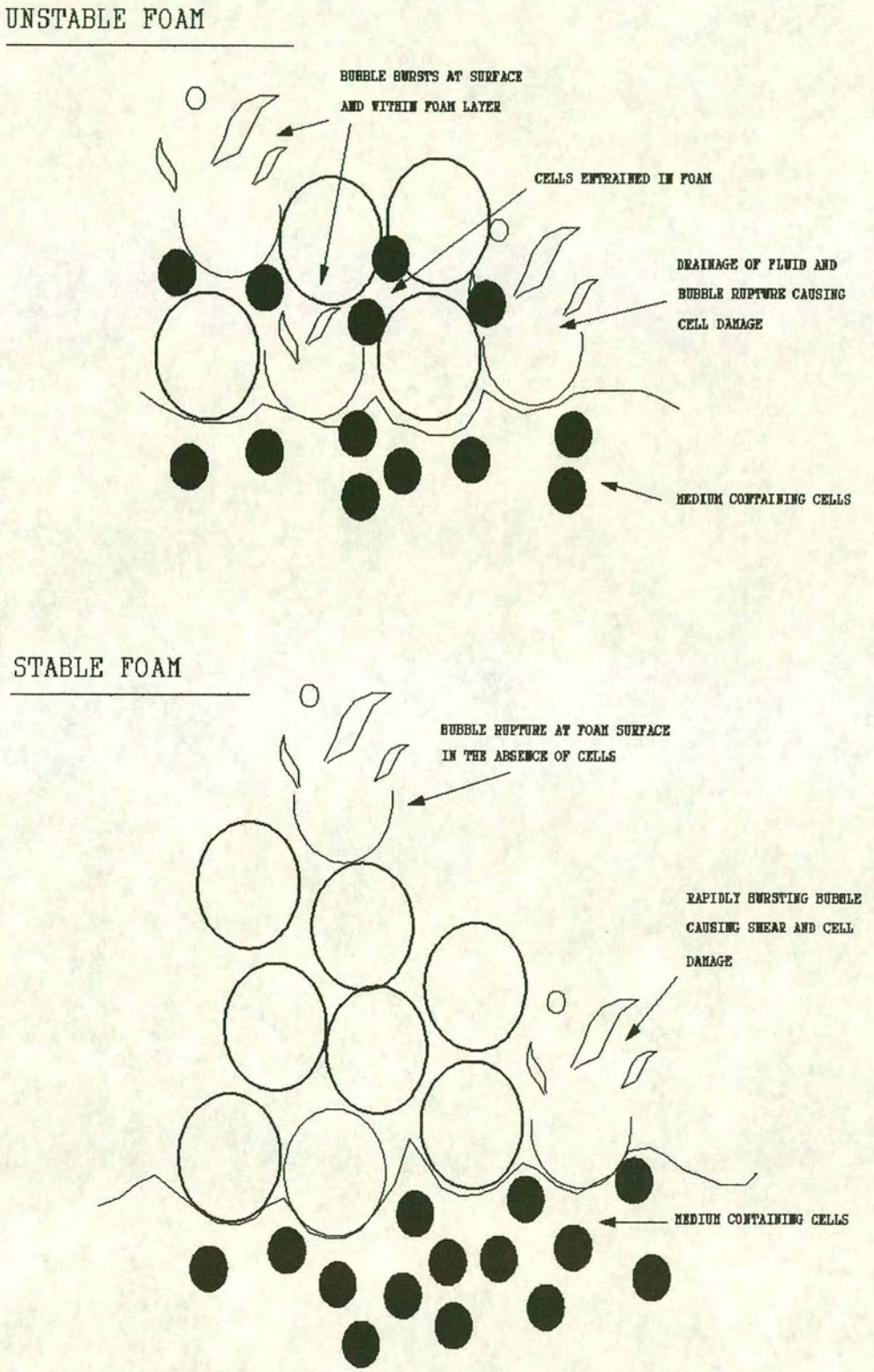

4.4.3 Counteracting shear

There are numerous ways in which these shear forces can be minimised including reactor design, the use of bubble-free aeration, the protection of the cells within a matrix and the addition of antifoam supplements to the medium. The first of these would be to develop a low shear design, minimising the effects of stirring, for example the use of low shear, marine impellers or the development of perfusion type reactors, such as hollow fibre bioreactors. The second involves the utilisation of an external aeration system, such as silicone tubing (Merten, 1987) or hollow fibre aeration units (Wagner and Lehmann, 1988, Setec, 1990, Tharakan and Chau, 1986, Brotherton and Chau, 1990). The third method is based on the previously discussed immobilisation of the cells within a support matrix. Chiou *et al.*(1991) have used an immobilisation technique in an airlift fermenter, providing anchorage dependant cells with mechanical protection while excluding the cells from the air-liquid interface. In this system the cells are attached to glass fibres fixed in the downcomer tube of the airlift, with a reported value of $6.8x10^7$ cells per ml of fibre bed.

The final way in which the effects of shear can be minimised is based on the observation that serum and other protein supplements, can act as a cell protectants by increasing the kinematic viscosity of the medium (Shacter,1989). Michaels *et al.*(1991) report that cell protection occurs at both a physical and biological level, helping to protect the cell prior to injury and aiding the recovery of the cell after injury. Handa-Corrigan *et al.*(1989) have described a relationship between the degree of cell protection and increasing concentrations of serum. Handa-Corrigan (in Spier and Griffiths, 1990) argues that at low serum supplementation levels, i.e. 5%, the kinematic viscosity of the medium is similar to that of water, discounting the effects of viscosity and favouring the active protection of the cell through surface active agents. Using serum as a protectant, Abu-Reesh and Kargi (1991) were able to culture mammalian cells in a surface aerated vessel at a stirrer speed of 300rpm.

Handa-(Corrigan) *et al.* (1987,1989) report that bubbles in the presence of serum can lead to the entrainment of cells within the unstable foam layer, leading to increased

damage. Other chemical additives, including pluronic polyol F68 and silicone based solutions, preferentially adsorb to bubbles limiting the entrainment of cells in the foam layer and hence decrease cell damage.

4.5 Chapter summary

From the previous sections it would appear that the ideal fermentation process should try to incorporate the following features:-

(1) An adequate supply of nutrients should be supplied to the cells, facilitated through mixing in suspension cultures, or perfusion in a multilayered culture.

(2) While hydrodynamic shear can cause cell damage, the culture conditions generally employed in mammalian cell bioreactors are usually limited as a result of bubble mediated damage. Ideally the process should either keep the cells away from the air/liquid interface e.g. in hollow fibre bioreactors, or limit the effects of the bubbles upon the cells by using surface active agents e.g. pluronic polyols.

(3) The process should try to balance the production cost against product value. Generally batch processes are economical for small quantities of product, whereas a continuous process is more suited for bulk quantities of product.

(4) The technique should look to maintain the highest viable producing population, preferably removing cell debris.

The effects of sparging and the associated hydrodynamic shear forces tend to favour the use of an indirect means of oxygenation for cell culture. Membrane bioreactors incorporate this design feature, separating the cells from direct contact with the air-liquid interface.

While membrane bioreactors do allow the culture of higher numbers of cells per unit

volume of vessel, the differences between tissue type and suspension culture cannot be ignored. In suspension culture, mixing ensures that the cells have greater contact with fresh medium, ensuring high cell viability. In dense culture nutrient supply is predominantly via diffusion, which can lead to poor mixing and the formation of large nutrient gradients. Wohlpart *et al.* (1990) have shown a four fold increase in the consumption of oxygen as the cell density increases from $1x10^5$ to $1x10^7$ cells per ml of medium. The formation of gradients within a tissue mass, with this increased requirement for oxygen, would lead to both a switch to substrate level phosphorylation under oxygen limited conditions and cell death.

One reason for the poor mixing within the cell mass in these bioreactors is the flow regimes associated with the use of membranes. The performance characteristics associated with membranes and membrane bioreactors will be discussed in the following chapter.

Chapter 5

Small scale, high density culture techniques

5.0 Introduction

The limitations associated with large scale culture techniques have led to the development of alternative systems for the growth and maintenance of high cell densities, i.e. incorporating hollow fibres or flat sheet membranes (Merten, 1987). The principal advantages of using membrane modules for cell culture have been described as follows (Tharakan and Chau, 1986, Heath *et al.*, 1990, Belfort, 1989):-

(1) The membrane acts as a permiselective barrier between the bulk flow of medium and the cells, decreasing the risk of contamination and reducing the damaging effect of shear forces upon the cells.

(2) Membranes provide a large surface area per unit volume of reactor, furnishing a large surface for cell attachment in close proximity to a source of fresh medium.

(3) Such systems can be operated continuously, for extended periods, at high cell densities.

(4) These designs can also be used as integrated processes, culturing the cells while acting as a primary separation step for the removal of product from the cells.

The bioreactors discussed in this chapter will include only those in which the hollow fibres constitute the main design feature providing a growth environment for the cells. This excludes those reports in which the hollow fibres have been used only for the separation of the product from the cells, enhancing either stirred tank or airlift fermenter operation (Cavegn *et al.*, 1992). As the processes of cell retention by the membranes and nutrient transport across the membranes are analogous to rejection and flux within filtration modules this chapter will consider these systems as both bioreactors and advanced filtration systems. A discussion of basic filtration theory is therefore necessary.

5.1 Basic filtration

Membrane filtration has been widely used for the downstream concentration of proteins or cells from fermentation process streams, usually as a preliminary stage in the harvesting of the cells or product. Filtration is a complex, pressure driven, process dependent upon the mode of filter operation, membrane type and the characteristics of the fluid. This chapter will concentrate on the principles of microfiltration and ultrafiltration as they are directly applicable to the membrane bioreactors describe later on in this chapter.

There are two modes of filter operation, called 'dead-end' filtration and 'crossflow' filtration, schematically represented in Figure 5.1. Dead-end filtration involves the use of pressure to drive small molecules directly through the membrane (permeate) while the larger macromolecules are retained by the pores in the membrane. The primary direction of liquid flow is at right angles to the membrane surface. In crossflow filtration, the bulk of the solution travels parallel to the membrane, with the pressure associated with the bulk medium driving flow across the membrane.

The characteristics of the membrane are only important during the initial stages of the filtration process, with the properties of the fluid dictating the longer term efficiency of the filter. The principal membrane determinants include shape, pore size and number, pore distribution and the charge associated with the surface of the membrane. The fluid properties of importance include the pH, nett charge and concentration of the solutes.

5.1.1 Membrane and fluid characteristics

M^{c}Donogh *et al.*(1992) only consider the characteristics of the membrane to be important during the initial stages of filtration. Electrostatic interactions between the retentate molecules and the membrane surface initially lead to the formation of the adsorbed layer. Thereafter the membrane tends to act as a support matrix for the various dynamic and non-dynamic secondary membranes formed in response to the

Figure 5.1:- Representation of the two modes of filtration

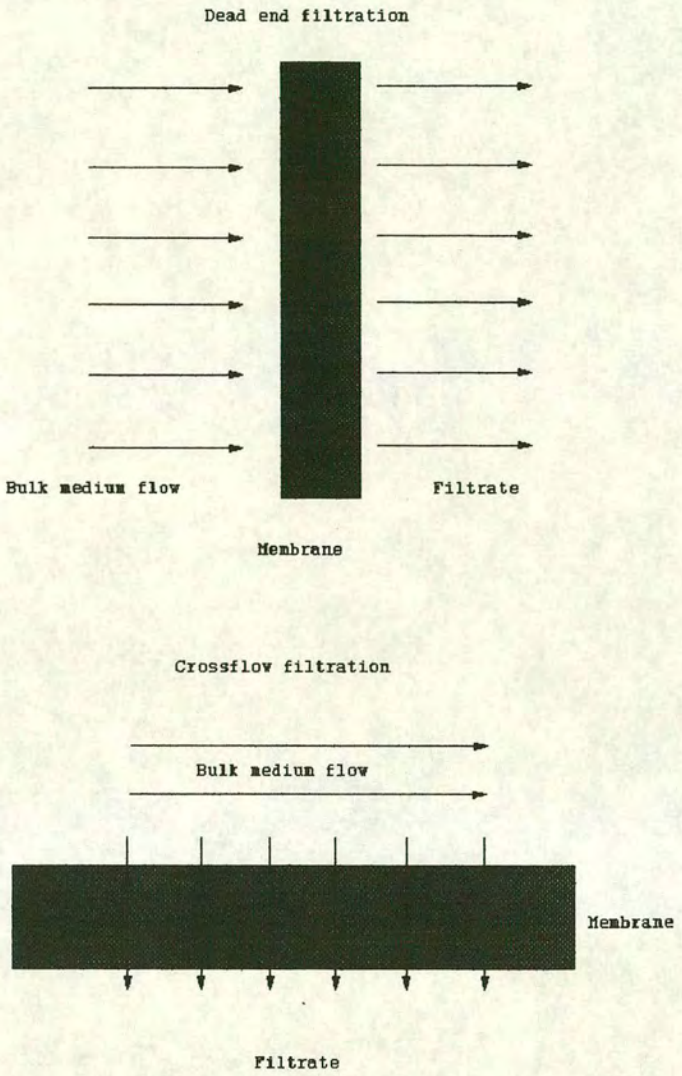

characteristics of the fluid. Models have been developed describing the behaviour of secondary membranes, these will be discussed in the next section.

Membrane charge, porosity and, to a lesser extent, pore shape are the primary determinants involved in influencing the initial behaviour of the filter. The charge associated with the membrane (termed the zeta potential, Jonsson and Tragardh, 1990) determines the type and strength of any electrostatic interactions made with the solution. For example, polysulphone membranes have a net negative charge at a neutral pH (Jonsson and Tragardh, 1990), enhancing any electrostatic interaction with

positively charged moieties in the solution. These interactions lead to the formation of an adsorbed layer at the membrane surface (membrane fouling). The properties of this layer then determine any further interactions made between the bulk medium and the membrane.

Flux during the initial adsorption period, where the membrane is relatively clean, is determined by the operating pressure of the system and membrane permeability. The porosity of the membrane depends on pore size and the number of pores per unit area, which is determined by the manufacturing process for the membrane. Typical values for the pore size of a hollow fibre membrane with a molecular weight cutoff (MWCO) of 100kDa (Fell *et al.*, 1990) range from 10-25 nm and 1.5 - 45.9 nm for a 100kDa MWCO flat membrane (Grund *et al.*, 1992). In the latter study it was found that pore openings constituted about 9.9% of the total surface area for a 30kDa MWCO membrane and 5.5% for the 100kDa MWCO membrane. Grund *et al.* (1992) suggest that the permeability of the membrane was dictated by the larger pores, although these only represented between 15-20% of the total number of pores. The dominant effect of these pores on permeability is relatively short lived, diminishing with the formation of a secondary membrane.

Porous membranes tend to have one of two pore geometries, cylindrical or tortuous (Figure 5.2) with a length to diameter ratio of about 100:1 (Fell *et al.*, 1990). Fell *et al.* further suggest that pore geometry may play a primary role in affecting the level of adsorption at the membrane surface, having a consequent effect on the flux and rejection characteristics of the membrane.

Molecular size has also been shown to be important in determining the filtration behaviour of mixtures, with M°Donogh *et al.*(1992) concluding that the flux of a process containing a number of macromolecular species was controlled by the smaller macromolecules present in the solution. This dominance is thought to be through a combination of electrostatic interactions with the membrane and pore occlusion.

These effects are intensified by the pH and ionic strength of the solution affecting the

Figure 5.2:- Pore geometries found in synthetic membranes

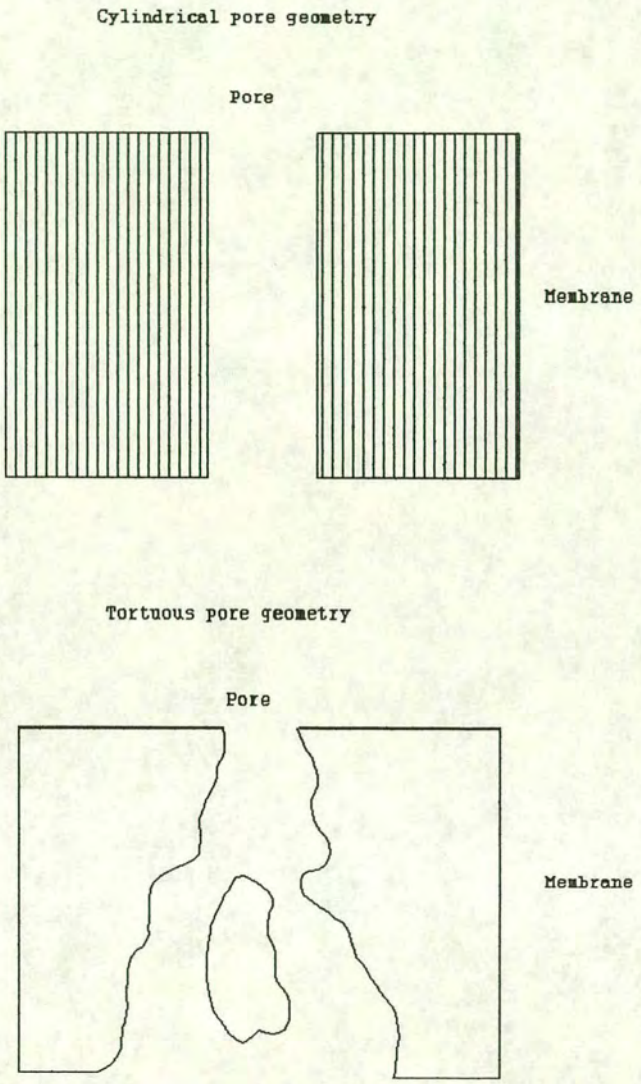

general dimensions and charge of the macromolecule as well as the zeta potential of the membrane. Grund *et al.*(1992) examined the effects of ionic strength on the filtration of a solution of bovine serum albumin (BSA). They found that as the ionic strength of a solution was increased, there was an increase in the rejection and a decrease in flux of the membrane. Grund *et al.* suggest two possible explanations for this effect. The first involves the blanketing of the macromolecule with ions, leading to a reduction in the overall size of the protein. The second involves the effect that the lower molecular weight species may have in strengthening membrane-retentate and retentate-retentate interactions. This effect would be further enhanced by any shear

mediated breakdown in the tertiary structure of the protein, exposing highly charged regions. Chandavarkar *et al.* (1991) have noted the formation of aggregates during the filtration of a solution of BSA ascribing this aggregation to the breakdown of protein structure.

5.1.2 Concentration polarisation and membrane fouling

M^{c}Donogh *et al.* (1992) identify three stages in membrane performance. The first two phases, the characteristics of the membrane and the formation of an adsorption layer at the membrane surface have already been discussed. The third phase involves the formation of the concentration polarisation layer, sometimes referred to as the secondary membrane. The type and resistance associated with the secondary membrane formed depends on the mode of filtration employed during the separation process, i.e. whether the system is operated as a dead end or crossflow filter, the interactions between different species within the solution, i.e. protein-protein interactions and the relative concentration of the macromolecular species in solution.

Similarities exist in both processes with respect to the formation of a secondary membrane. Adsorption and pore occlusion lead to a decrease in the size of the pore (termed fouling). This results in a decrease in flux and an increase in the rejection characteristics of the membrane. As the rate of rejection increases the concentration of retained species on the feed side of the membrane also increases. This concentration effect tends to be localised around the pore, being further enhanced by the relatively small surface area associated with pore openings (Fell *et al.*, 1990, Grund *et al.*, 1992, Shen and Probstein, 1977). This phenomenon, called concentration polarisation, is dependent upon the volume of liquid passing through the pore. If the concentration around the pore continues to increase, for example in dead-end filtration, the resistance to the flow across the membrane will increase, resulting in fouling and a rapid reduction in flux. In crossflow filtration the flow regime tends to aid in maintaining concentration polarisation at a reduced level, reducing fouling and extending effective process time.

Concentration polarisation, while improving the rejection characteristics of the membrane, leads to the development of an osmotic pressure gradient. Probstein *et al.* (1979) have calculated that a 40% solution of BSA (weight per volume) can develop an osmotic pressure equivalent to 40 psi. This pressure acts in direct opposition to the pressure driving the permeate across the membrane, reducing the effective transmembrane pressure (Effective TMP, see Equation 5.1) and flux (where the rejection coefficient indicates the permselectivity of the membrane).The degree to which the secondary membrane limits flux is generally dependent on the mode of filtration employed i.e. dead-end or crossflow filtration.

$$EFFECTIVE\ TMP = \Delta P - \delta\Delta\pi \qquad (5.1)$$

where ΔP = measured TMP (Pa), δ = rejection coefficient, $\Delta\pi$ = osmotic pressure difference across membrane (Pa).

5.1.2 Dead end filtration

Based on the conclusions of Fell *et al.* (1990) and Grund *et al.* (1992) that the efficiency of a filtration process is dependent upon the smallest retained macromolecuar species, the following can be concluded about the development of a secondary membrane in dead end filtration. Once the initial adsorption layer has developed, macromolecules continue to accumulate at the membrane surface forming the secondary membrane. In this instance the secondary membrane continues to grow, forming a filter cake which, if left to build, results in negligible flux across the membrane as the combined resistance to flow balances the driving force. Once again the characteristics of the process fluid will have a major role in determining the type and resistance of the cake formed at the membrane surface.

The theoretical progress of a dead end filtration can be predicted by using Ruth's Law (Murkes and Carlsson, 1990, Equation 5.2). While dead end filtration allows the concentration of the product on the feed side of the membrane, it is heavily limited by the formation of the filter cake. This process may be extended by either the mechanical removal of the filter cake or alternatively by reversing the direction of

flow across the membrane, flushing the system (Murkes and Carlsson,1990). These are, however, only temporary solutions to filter cake formation, with this method being replaced by crossflow filtration.

$$J(t) = \frac{K}{2(V + V_f)} \quad Where\ K = \frac{2\Delta P S^2}{\mu c r} \qquad (5.2)$$

Where J(t) is a flux, in ms^{-1}, at time t

V total filtrate volume at time t (m^3)

V_f volume of filtrate required to produce a cake with the same hydraulic resistance as the membrane support (m^3)

K is the Ruth constant defined by the surface area of the filter (S, m^2), μ is liquid viscosity ($kgm^{-1}s^{-1}$), c is the concentration of the colloid (kgm^{-3}) and r is the specific cake resistance ($m^{-1}s.Pa$) and ΔP is the transmembrane pressure (Pa).

5.1.3 Crossflow filtration

Crossflow filtration utilises the hydrodynamic shear generated at the membrane surface by either the bulk flow of medium or by mechanically induced turbulence to limit the formation of a secondary membrane. In this instance the secondary membrane is considered to be a dynamic membrane, where there is the continuous addition and removal of moieties to and from the formed layer. The technique can be divided into high shear and low shear operations. The high shear system, while maintaining comparatively higher fluxes, is usually too harsh to be considered useful for protein solutions and so this section will concentrate on the low shear technique.

Four theories are used to explain the effects of secondary membrane formation upon the flux and rejection of the crossflow filtration process (Jonsson and Tragardh, 1990,

Murkes and Carlsson, 1990, Probstein *et al.*, 1979, Shen and Probstein, 1977, Grund *et al.*, 1992).

(1) Boundary layer theory
(2) The Osmotic Pressure mode
(3) The Gel Layer model
(4) The Resistance in Series model

These models are discussed in Jonsson and Tragardh (1990), although it appears that different models can apply to the same mode of filtration when different moieties are separated. This differential application seems dependent upon the physical characteristics of the moiety involved in the separation.

In this discussion it will be assumed that pH, temperature and ionic strength are constant so that their effects on the charge of the membrane and solute can be discounted. For all of the situations discussed a general pressure flux curve can be drawn (Figure 5.3). The general features of the crossflow filtration process can be summarised as follows:-

(1) Flux shows a three stage dependency on transmembrane pressure.
(2) High flux membranes show a greater proportional flux decline than low flux membranes.
(3) Flux decreases with decreasing temperature and increasing solute concentration.
(4) Flux increases with increasing crossflow velocity, although the effect diminishes at higher flows.
(5) Flux decreases with time.
(6) Membrane fouling and adsorption are found to be greater with moieties exhibiting a hydrophobic character, than those with a hydrophilic character.

Figure 5.3:- Generalised flux versus pressure graph

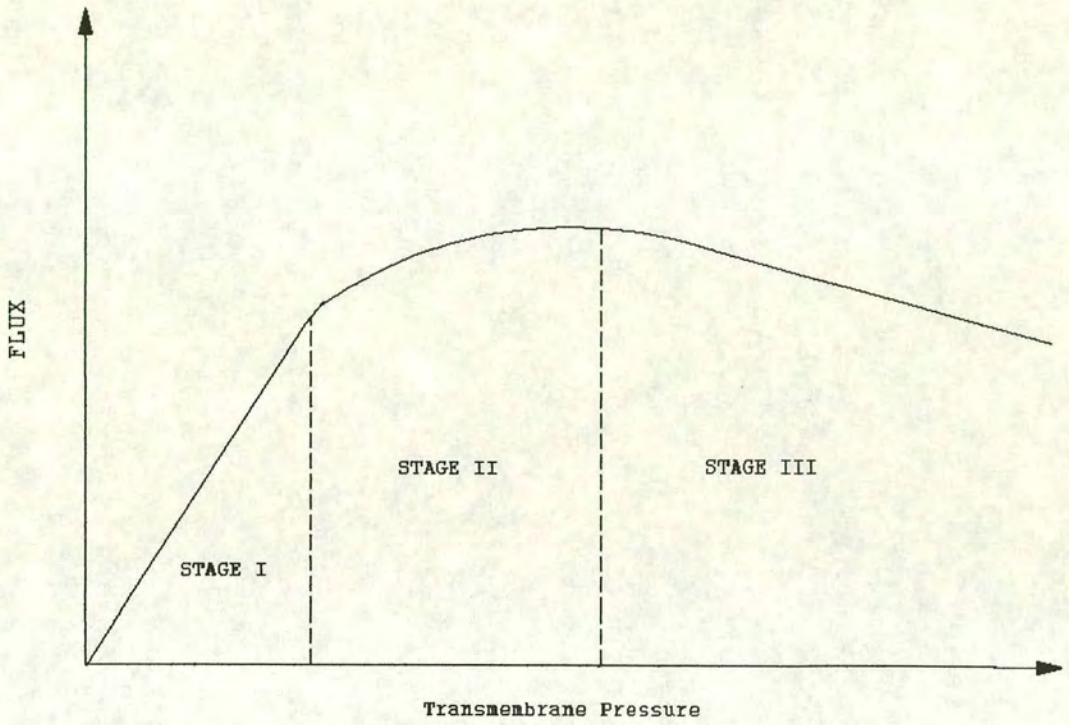

The dependence of flux (J) upon pressure during Stage I of Figure 5.3 can be attributed to the accumulation of the macromolecules at the membrane surface (Boundary layer model). Stage II can be described by concentration polarisation and the Osmotic pressure model, while Stage III is predicted by the Gel layer model. The Resistance in series model excludes the effects of osmotic pressure while attempting to bring together the Boundary and Gel layer models. Each of the models discussed in the following paragraphs considers a different form of resistance acting in opposition to the pressure driving flux across the membrane.

The Boundary layer model

The performance of crossflow filtration during Stage I of Figure 5.3 is dependent upon the relative concentration of macromolecules at the membrane surface. The rate of their accumulation is dictated by the convective flow of molecules and permeate towards the surface of the membrane. This process is countered by the diffusive transfer of these species mediated by the concentration gradient between the membrane surface and the bulk medium.

A steady state boundary layer is achieved when the convective transport of molecules towards the membrane equals the sum of the permeate flow and the diffusive flow. The flux (J, ms^{-1}) can then be estimated by Equation 5.3, where the mass transfer coefficient (k) is determined by the ratio of the diffusion coefficient divided by the thickness of the boundary layer (Mulder, 1991).

$$J = k.\ln\left(\frac{C_w}{C_b}\right) \qquad (5.3)$$

According to this theory, as the value of c_w is increased at higher transmembrane pressures, the flux (J) is also increased with a constant value for the mass transfer coefficient. This theory explains Stage I of Figure 5.3.

The Osmotic pressure model

The osmotic pressure model identifies the concentration difference across the membrane as the primary cause of the resistance to flow (Fell *et al.*,1979, Probstein *et al.*,1990). The following Darcy equation (Equation 5.4), taken from Jonsson and Tragardh (1990), describes the relationship between the various components.

$$Flux\ (J) = \frac{\Delta P - \delta\Delta\pi}{\mu(R_M + R_S)} \qquad (5.4)$$

Where ΔP=TMP (Pa), μ=Viscosity ($kgm^{-1}s^{-1}$),
$\Delta\pi$=Osmotic pressure (Pa), δ=Rejection coefficient,
$R_M + R_S$=membrane + hydraulic resistance, (m^{-1})

Increasing TMP results in higher values of c_w, this leads to a greater concentration difference across the membrane increasing the osmotic pressure. As osmotic pressure acts in direct opposition to the driving force, the flux across the membrane is reduced.

The gel layer model

In the gel layer model it is assumed that the concentration of the retentate at the membrane surface (C_w) will eventually reach a concentration where a gel is formed (C_g), with the bulk concentration described by C_b. In this case the gel layer is thought to be the principal limiting factor to flux, with the effects of osmotic pressure thought to be negligible (Equation 5.5). It is suggested that flux then becomes independent of the pressure as the value of c_g is constant. A slight reduction in flux may be observed at higher pressures due to the compaction of the gel layer.

$$J = \frac{\Delta P}{\mu (R_m + R_g)} = k \ln(\frac{C_g}{C_b}) \qquad (5.5)$$

Wijmans *et al.* (1985) suggest that the osmotic pressure model is favoured for separations involving macromolecules with a size range of between 10-100kDa, whereas the gel layer model applies to a molecular species with a size of greater than 100kDa.

The resistance in series model

The resistance in series model is similar to the gel layer model in that it assumes no osmotic pressure effect, however it considers the solute resistance of the gel layer model to be a multicomponent system with the following composition, Figure 5.4, where the diagram labels refer to the following:-

R_M = resistance of the membrane

R_A = resistance of the adsorbed layer

R_G = resistance of the gel layer

R_{bl} = resistance of the boundary layer, equating to the resistance associated with the increasing concentration of retentate.

Figure 5.4:- Schematic of the resistance in series model

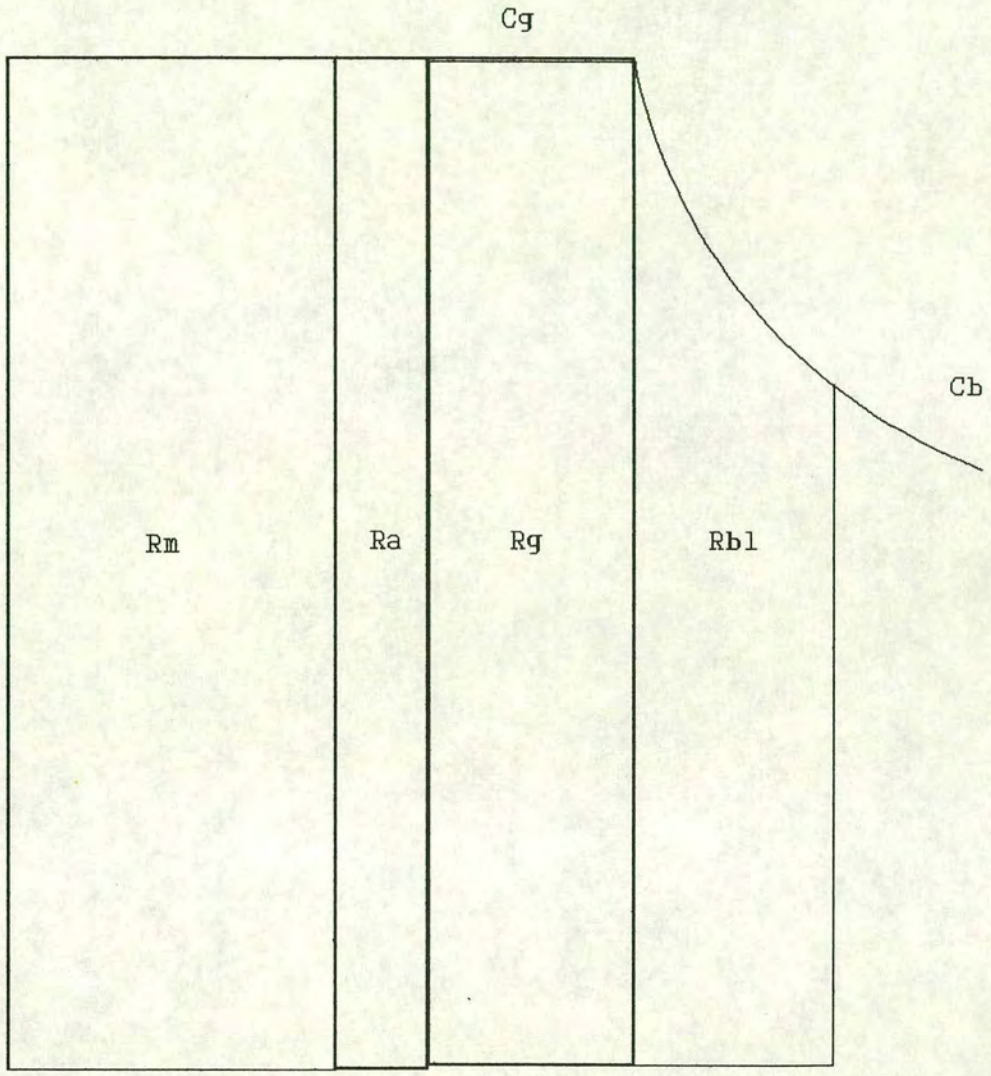

Flux, in this case is determined by Equation 5.6.

$$J = \frac{\Delta P}{\mu (R_m + R_a + R_g + R_{bl})} \qquad (5.6)$$

This relationship has also been shown to be valid for dextran solutions (Jonsson and Tragardh, 1990) and BSA (Grund *et al.*, 1992).

In all of these models, during the first stage of the graph, the mass transfer coefficient depends on the crossflow velocity ($k \propto u^a$), where a is the Reynolds number exponent

in an empirical equation relating the Sherwood, Reynolds, Schmidt numbers, diffusivity and the hydraulic diameter to the flow conditions (Jonsson and Tragardh, 1990).

Hence it can be seen that many factors affect the performance of the filtration process which must be considered in the design of a hollow fibre bioreactor.

5.2 Single Circuit Hollow Fibre Bioreactors

This section will discuss the range of bioreactors which use a single circuit of hollow fibres to maintain a culture environment for mammalian cells.

Bruining (1989) identifies four principal modes of operation for a single circuit of hollow fibres, closed shell, dead end, open shell and suction (outlined in Figure 5.5). Each of these systems will be discussed in turn with relevance to filtration theory and the advantages/disadvantages of the design. Unless otherwise stated it will be assumed that cell growth occurs around the outside of the fibres within the extracapillary space of the bioreactor. It will also be assumed that the growth space volume, and therefore the maximum area available for biomass, does not exceed the volume of the fibres luminal space by more than a factor of four, when, according to Adema and Sinskey (1987), limitations in oxygen diffusion result in cell death.

The closed shell design has been adopted commercially by several manufacturers, for example CD Medical, Amicon and InterSynFibTech. Due to this commercial interest, a number of studies have been published, outlining the optimal operating conditions for such systems (Heifetz *et al.*, 1989, Hopkinson, 1985, Piret and Cooney, 1990, Veeramullu *et al.*, 1991). The flow regimes under these optimised conditions have also been studied with relevance to cell growth and as a general crossflow filtration technique (Hammer *et al.*, 1990, Heath *et al.*, 1990, Piret and Cooney, 1990, Kelsey *et al.*, 1990, Bruining, 1989).

5.2.1 Closed Shell Operation

In closed shell operation the medium is passed through the lumen of the fibre, with the cells and product retained in the shell of the reactor. The feed medium can be either serum or protein supplemented (Heifetz *et al.*, 1989, Piret and Cooney, 1990), protein free, with a shell dosing regime implemented for supplying the cells with the required growth supplements (Veeramullu *et al.*, 1991) or a combination of serum and serum free supplementation (Amicon). The cells can either be grown in a support matrix within the shell, or grown in quasi-suspension, with some of the cells binding to the fibres while the remainder are grown in suspension.

Cell counts of up to 3.6×10^8 viable cells ml^{-1} of growth space have been reported under optimised conditions (Piret and Cooney, 1990). Problems arise in comparing results obtained from single fibre bioreactors due to the marked differences between the cell lines cultured in the studies using these systems. This is further complicated by technical bulletins reporting total cell counts where the proportion of viable cells is not reported.

The diffusional supply and removal of medium to and from the cells is enhanced by using convective currents caused by the axial pressure drop along the fibre. This flow regime is called 'Starling flow' which can be described as follows:

At the feed side of the bioreactor where the medium enters the reactor (proximal), the lumenal pressure exceeds that of the shell, facilitating the flow of medium from the fibre lumen into the shell space. As the pressure of the lumen decreases with axial distance, the pressure of fluid in the lumen at the exit of the reactor (distal end) becomes lower than the shell pressure. Indeed the shell pressure can be predicted as the mean of the proximal and distal pressures. This flow regime has been visualised by using NMR spectroscopy (Heath *et al.*, 1990, Hammer *et al.*, 1990) and modelled (Burns, 1991, Bruining, 1989, Kelsey *et al.*, 1990). The general flows within the reactor and the pressure relationship associated with Starling flow are outlined in Figure 5.6. For ease of description in later bioreactor designs it will be assumed that

Figure 5.5:- Modes of operation for cartridge bioreactors

→ Arrows indicate direction of fluid flow

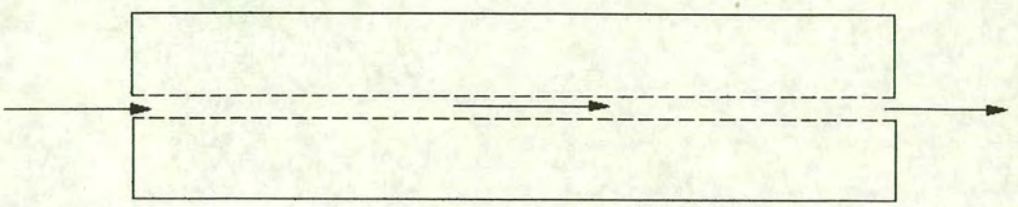

Closed shell mode

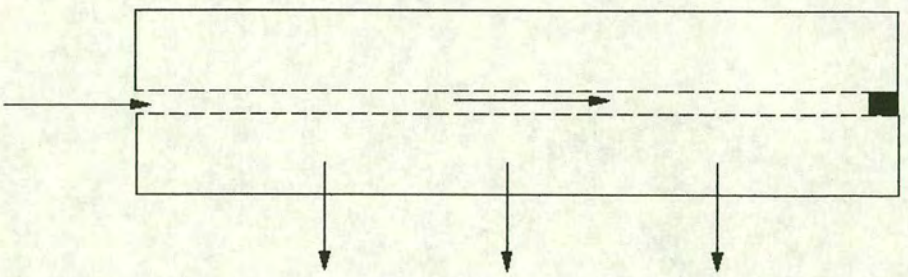

Dead end mode

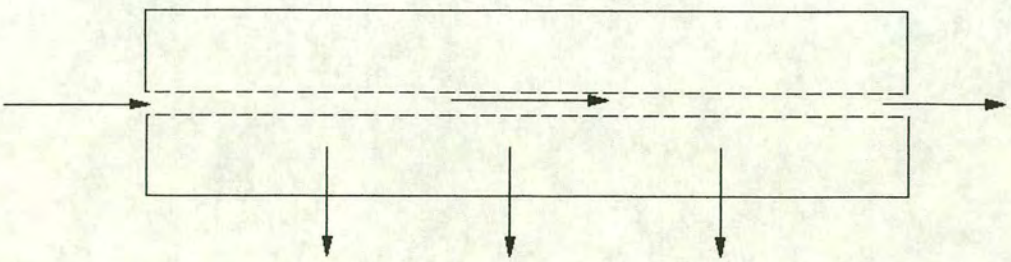

Open shell mode

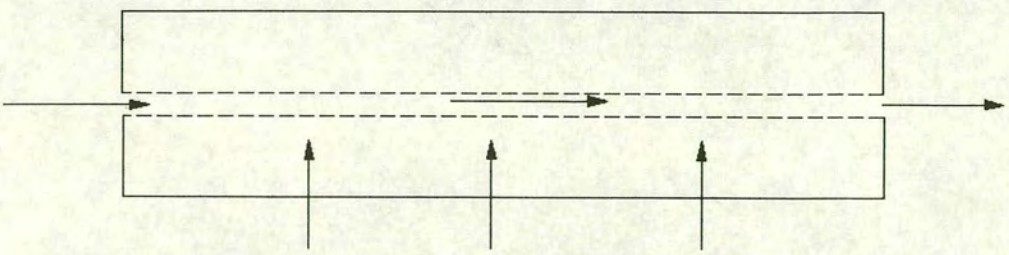

Suction mode

the flows within the shell are dictated by pressure gradients, i.e. flow is predominantly from a high pressure to a low pressure area within the reactor.

The Starling flow regime is the principal limiting factor to this design of single fibre bioreactors. In order to visualise the limitations of closed shell operation, the assumptions of Burns (1991) will be used. Burns considered the growth of the cells in the shell in both free suspension and in the immobilised form of a support matrix. Based on these assumptions and information from other studies the following can be concluded:-

Suspension grown cells

With the Starling flow regime, both cells and product accumulate at the distal end of the reactor. Piret and Cooney (1990) used azoalbumin to show this distal accumulation, also noting the gravitational bias of the build up. This accumulation would mean that nutrients and oxygen would become rapidly depleted from the medium at the distal end of the reactor due to the high localised, cell concentration.

Matrix immobilised cells

For matrix immobilised cells, Burns concluded that there would be a bias of cell growth at the proximal end of the bioreactor, assuming an even flow distribution. The cells would initially be fairly evenly distributed, but as the total number of cells increased, the cells at the proximal end of the reactor would deplete the nutrients from the medium, starving the cells further down the reactor.

Piret and Cooney (1990) showed that the effects of this axial polarisation could be reduced by periodically reversing the direction of medium flow through the fibres, enhancing both the total cell count and the productivity of the bioreactor. This technique could be applied to both suspension grown and matrix immobilised cells.

In these works the effects on the performance of the bioreactor associated with the general filtration theory discussed in Section 5.1 have not been considered. By viewing the hollow fibres as standard crossflow filters as medium leaves the lumen

Figure 5.6:- Starling flow and pressure relationship

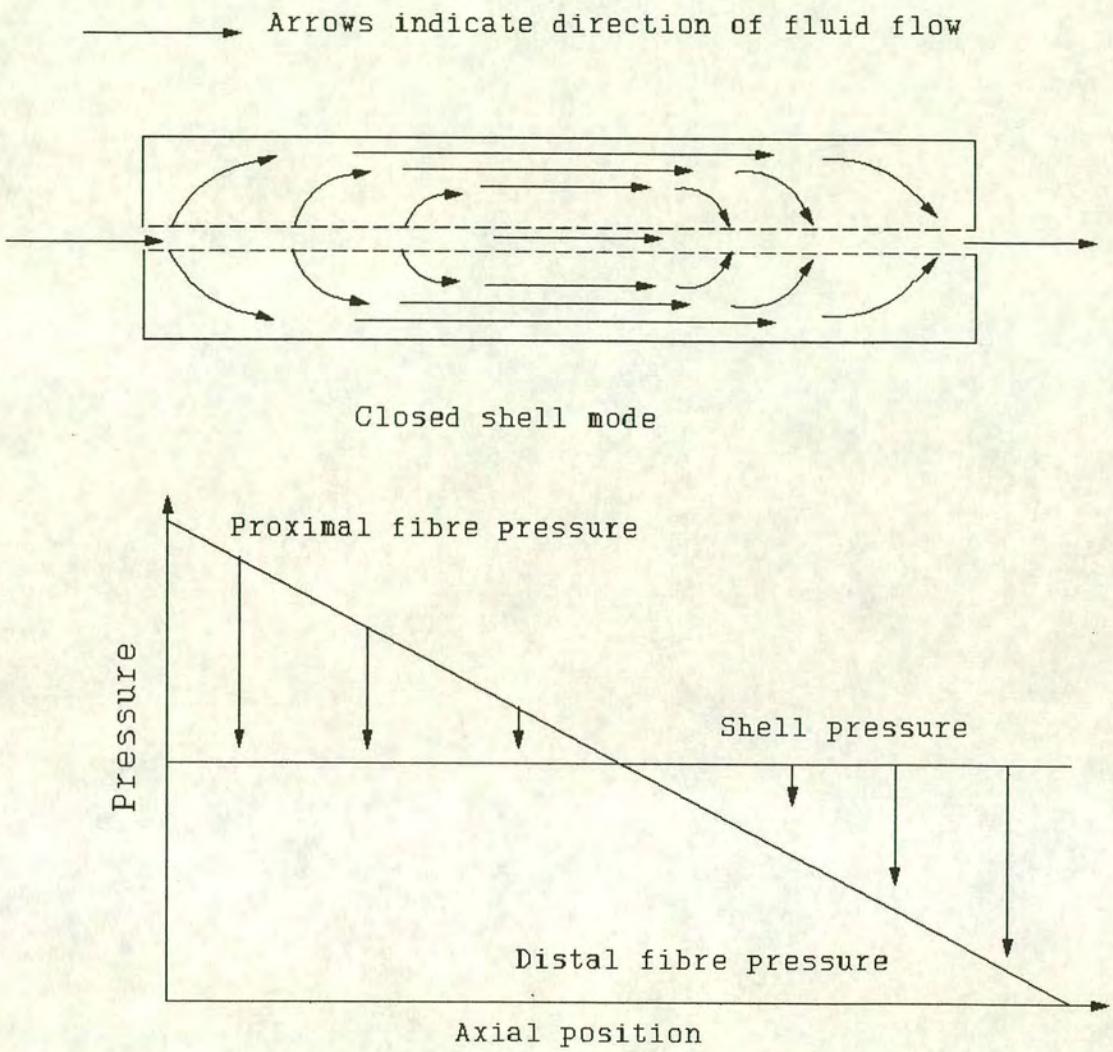

and as dead end filters where the spent medium re-enters the lumen of the fibres, further performance limitations can be suggested.

At the proximal end of the fibre, where the lumen pressure exceeds the shell pressure, the performance of the fibre would be dependent upon the previously discussed characteristics of the medium and the type of secondary membrane allowed to form. The use of proteins in the feed medium would lead to a high rejection ratio and a reduction in flux by either of the previously discussed models. The rate of nutrient transfer to the cells would also be affected by the reduction in flux.

At the distal end of the reactor, the accumulation of product and lower molecular weight proteins would rapidly lead to membrane fouling. The observed effect would be similar to that of filter cake formation in dead end filtration. Under these conditions the size of cake would be related to the volume of filtrate traversing the fibre into the lumen. Cake formation would initially be at its highest at the end of the reactor, where the pressure gradient was at its greatest. As the cake increased the point of highest flux would move back towards the centre of the bioreactor, causing the effective length of the module to decrease. The improvement in performance observed by Piret and Cooney (1990) by the implementation of periodic flow reversal would serve to decrease the limitations associated with this flow pattern by removing external cake formation and reducing the size of the lumenal secondary membrane.

The assumptions made in this section will be applied to a description and a novel re-interpretation (using filtration theory) of the remaining operational models suggested by Bruining (1989), that is dead end, open shell and suction, as follows:-

(1) Different methods of protein supplementation, primarily serum/ protein supplementation of the feed and a shell dosing regime.
(2) Flow will be assumed to be determined by the pressure gradient.
(3) Cells are either fixed in a matrix or suspension grown.
(4) The bioreactor is subject to the previously outlined filtration theory.

5.2.2 Dead end operation

The distribution of flow along the fibre can be assumed to be more even, with the fibre maintained at a higher pressure than the shell. As the shell space is no longer closed the flow would now converge on the point of lowest pressure, i.e. the outlet of the module. The fibres, by being operated as a dead end filter, would foul rapidly in the presence of any protein supplementation of the feed medium according to Ruths law. Indeed, Brotherton and Chau (1990) excluded cake formation from their model of an alternate, dead ended bioreactor. This factor would indicate the use of a protein

free supply medium, with protein supplementation to the shell side of the reactor. Protein addition would require the temporary reversal of flow to distribute the additive adequately amongst the cells. As a direct result of the flushing of the cellular growth space the cells would have to be grown in a matrix to reduce the effects of washout upon reactor productivity.

5.2.3 Open shell operation

The advantages of this system include the limitation of secondary membrane formation within the fibres by using crossflow filtration. This mode of operation, like the closed shell operations, would lead to high membrane rejection if serum were used in the feed stream. This could possibly lead to the cells being starved of essential proteins. With this mode of operation the cells would either have to be retained within the shell space or alternatively the flow regime would have to be optimised to minimise cell loss through wash out.

Kelsey *et al.* (1990) have looked at decreasing the rate of flow from the shell space via the application of a back pressure at the outlet of the module. Their description of this system includes an open shell ultrafiltration factor (f). This factor represents the proportion of the inlet feed volume leaving the module through the outlet, where $f = 0$ indicates no flow through the outlet (closed shell operation) and $f = 1$ the maximum flow from the outlet port.

At $f = 0$, it was found that the flow was symmetrical about the centre point of the reactor, in similarity with closed shell operation. At $f = 0.5$, it was found that the last 20% of the feed fibres were at a negative pressure, leading to flow back into the supply fibre. At $f = 1$ there was no back flow into the fibres, with a predominantly axial flow pattern to the outlet of the reactor. One of the factors that they admit to not taking into consideration was the changing permeability of the fibre associated with axial pressure drop due to fouling. They concluded that this may prove significant for the case of $f = 1$.

5.2.4 Suction operation

This regime can be viewed as the distal end of the closed shell model, where the fibres are operated at a lower pressure than the shell space, with the fibres simulating a dead end filter. Hence, any protein added to, or produced by the cells in the bioreactor would directly foul the membrane, leading to a gradual reduction in flux due to cake formation. Periodic backflushing of the fibres could alleviate this problem, however maldistribution of the flow and the formation of nutrient gradients from the outside of the reactor to the inside would eventually lead to the starvation of the cells.

Patankar and Oolman (1990a+b) developed a system using a single set of fibres (Figure 5.7) in which the cells were grown in the spongy matrix of the fibre wall. To reduce the effects of fouling an axial crossflow current was introduced into the shell of the reactor.

While this flow regime reduces the fouling of the fibres, several other limitations can be foreseen. The cell population within the reactor will be limited by the volume of the support matrix provided by the fibre wall, and any transient population that may be introduced by recycling the washed out cells. Once the crevices in the fibre walls have been filled, a concentration gradient will occur from the outside to the inside. While this may not be limiting during the initial period of operation, fouling of the pores in the membrane will lead to a decline in flux causing a decrease in the rate of nutrient supply to the cells.

Hirschel and Gruenberg (1987) alleviate the fouling of fibres and the formation of nutrient gradients by periodically cycling the flow of medium through the hollow fibre cartridge between an integration and expansion circuit. By changing the pressure differential between the two circuits the flow pattern both cleans the membrane by backflushing and improves the mixing within the cellular growth space. This procedure requires continuous monitoring and control using a computer.

Figure 5.7:- Bioreactor for cell growth in the fibre wall

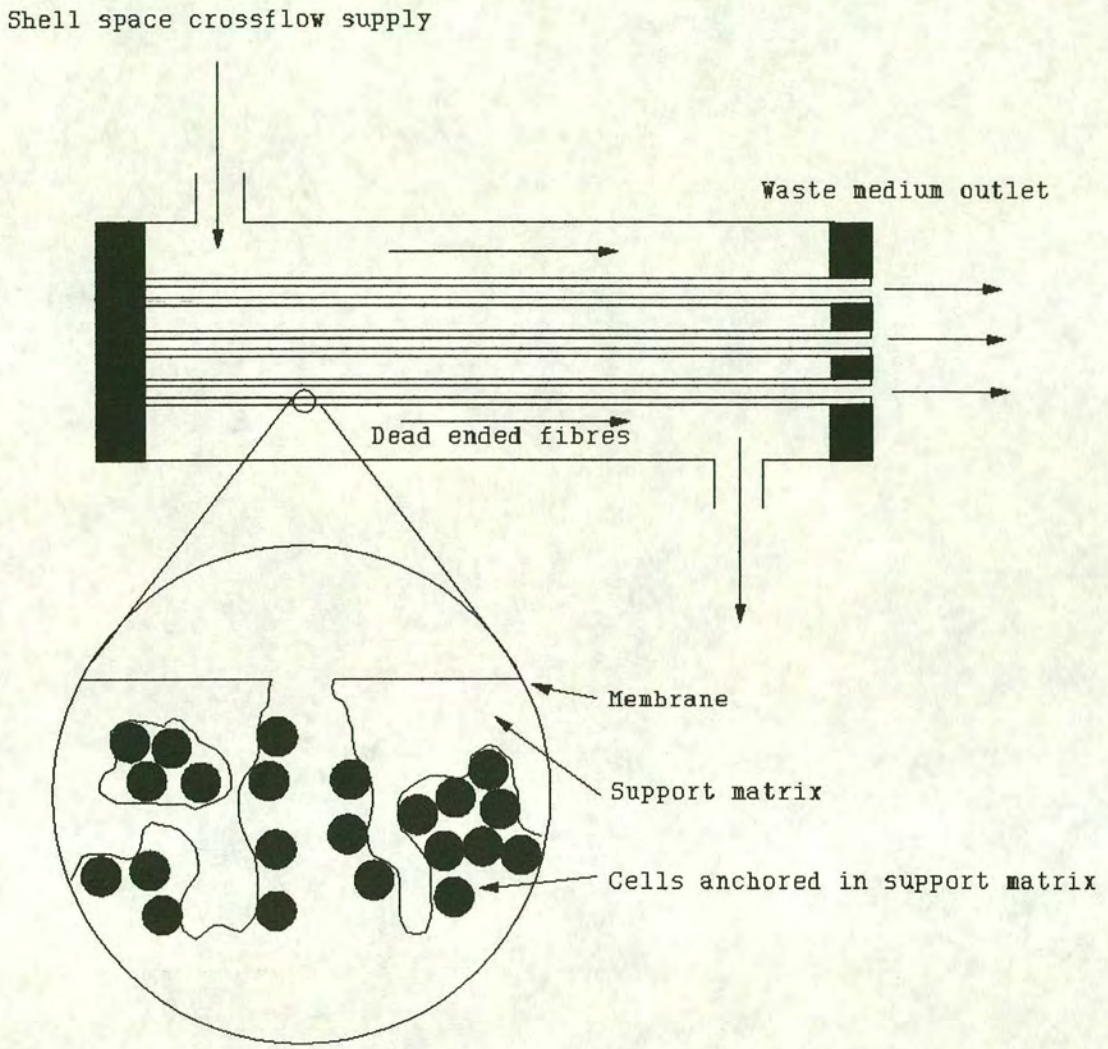

5.2.5 Summary of single circuit hollow fibre bioreactor operation

All of the systems discussed are limited in the long term by either fouling of the fibres described by general filtration theory, or by the development of nutrient and oxygen gradients. In the cases where the fibres are operated as dead end filters, the effectiveness of the reactor is limited by cake formation. In the other systems, the formation of axial flow patterns tends to lead to the creation of nutrient gradients and the maldistribution of product or the cells.

Many of the flow limitations associated with single fibre bioreactors can be avoided by introducing a second set of fibres into the bioreactor, facilitating the removal of waste medium containing product from the growth space (Altshuler *et al.*, 1990). This would shift the emphasis of flow from along the reactor (axial flow) to a pattern where the flow was from one set of fibres to another (a radial flow pattern). Bioreactors using a second set of fibres will be discussed in the following section.

5.3 Dual Hollow Fibre Bioreactors

The introduction of a second set of hollow fibres into a bioreactor is primarily to improve the distribution of nutrients. Dual hollow fibre bioreactors can take two forms. The first of these entails the use of the second circuit for the removal of the spent medium from the cells (Knazek *et al.*, 1980, SETEC, 1990, Brotherton and Chau, 1990, Tharakan and Chau,1986), while the second application involves the use of fibres for improved gas transfer within the reactor (Cousins *et al.*, 1992, Oh and Chang, 1992).

This section will concentrate on the former of these types of bioreactor. While the latter designs do improve viable cell populations, when compared to single fibre bioreactors, they still suffer the same limitations in nutrient distribution imposed through the use of a single set of medium supply fibres. Cousins *et al.*(1992) have designed a system where the second set of fibres are used to enhance gas transfer. However, because of these flow induced limitations, agitation of the bioreactor was required to break up nutrient gradients.

Unfortunately, many of the papers involving dual hollow fibre bioreactors are primarily concerned with the modelling of flow regimes and the putative nutrient profiles attainable for cell culture (Brotherton and Chau,1990, Tharakan and Chau,1986). The results presented are usually derived from the model alone, with little experimental validation. This may be, in part, due to the lack of suitable experimental results, either through difficulties in obtaining representative samples or a lack of actual cell growth. As a direct result of the necessity for model resolution,

the basic assumptions applied are often too crude, leading to flaws in the final model. An analysis of the selection criteria and a comparison of data are presented by Burns (1991). A summary of these findings will be provided in the following discussion where necessary.

Knazek *et al.*(1972) were the first to suggest the use of hollow fibre membranes to mimic the arterio-venous flow of nutrients within the body, as a medium for culturing mammalian cells. The first attempts to copy the nutrient supply system of the body involved the use of two single fibre bioreactors operated in parallel (Belfort and Altshuler, 1986). The circuits were operated at different pressures so that the fibres in the supply cartridge were at a greater pressure than the growth space which, in turn, were maintained at a higher pressure than the lumenal pressure of the second cartridge. By careful selection of the molecular weight cutoffs of the fibres, Belfort and Altshuler were able to keep the supply circuit free of product while recovering product from the second circuit. Cells were continually recirculated, reducing fouling and increasing nutrient distribution within the system.

Knazek *et al.*(1980), in a development from work with single circuit hollow fibre bioreactors, designed and built a dual hollow fibre bioreactor (Figure 5.8). However, the technique employed for its construction was complex and no results were published in conjunction with cell culture. Katinger and Shirrer (1985) have identified scale up as being the main limitation to the development of complex designs.

Tharakan and Chau (1986) designed a dual hollow fibre bioreactor in which a single, porous, stainless steel supply tube was used to supply an annular array of smaller diameter, sink fibres (Figure 5.8). Total cell count of 7.3 x 10^6 cells cm^{-2} of filter surface area were reported for an H1 cell line (1150 cm^2 total surface area). This equates to 1.8 x 10^7 cells ml^{-1} of growth space, in which cell attachment was enhanced by poly-D-lysine. The Central Flow Distributor, while providing a constant axial provision of nutrients, could not overcome the formation of radial nutrient gradients. A secondary problem could be predicted in its operation through the fouling of the fibres due to the use of 6% serum supplemented medium, although this fouling could

Figure 5.8:- Dual hollow fibre bioreactor designs

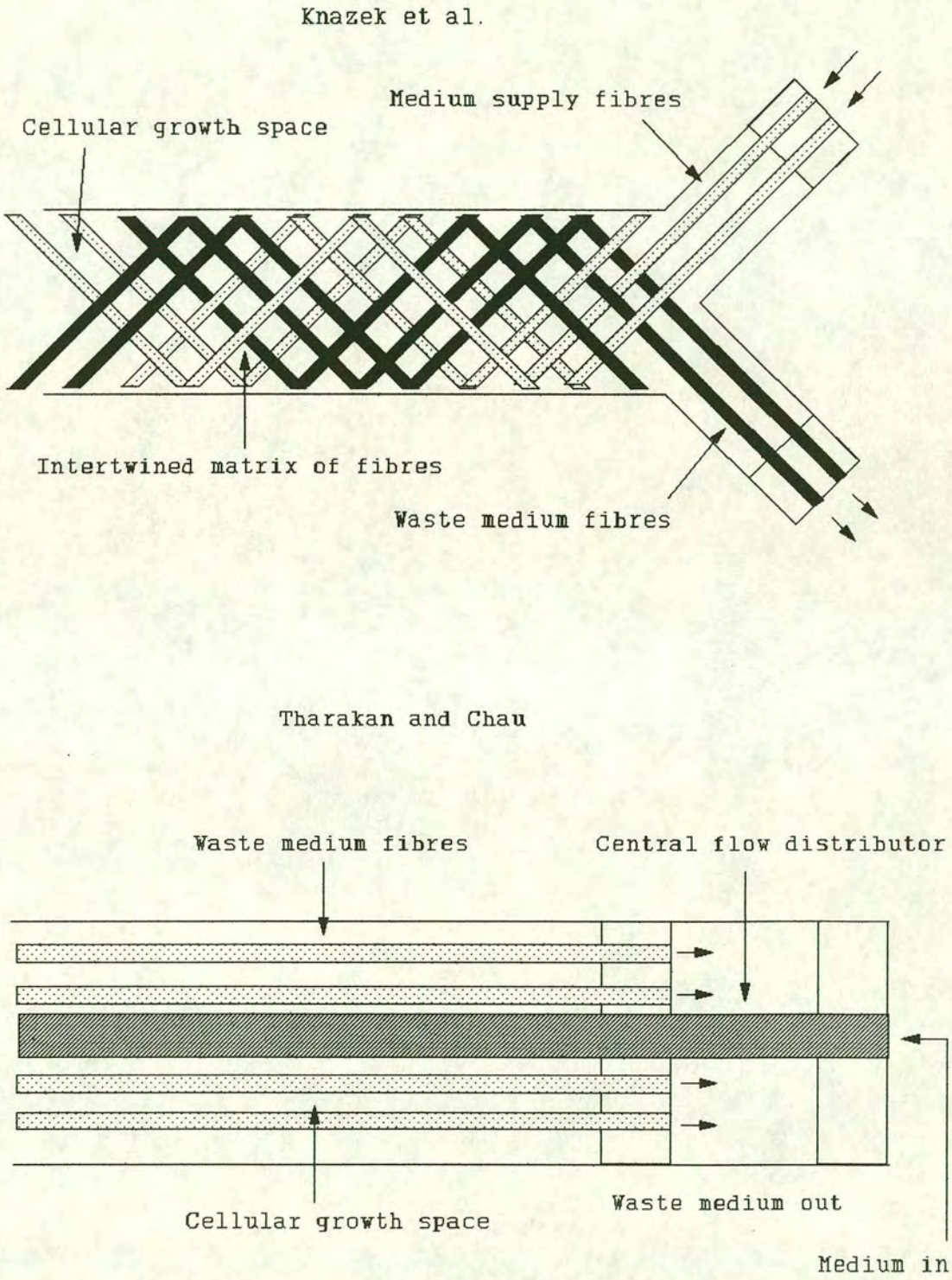

again be reversed by backflushing the system.

Brotherton and Chau (1990) designed a system using intercalated, alternate dead ended hollow fibres (Figure 5.9). While this design once again allowed a more even supply of nutrients to the cells via radial perfusion, it was flawed from a filtration standpoint.The fibres, by being dead ended, would suffer those limitations expected of a dead end filter with respect to a protein supplemented feed. In a protein free supply regime, a similar effect would be observed with the second circuit of fibres, due to protein production by the cells. This could be partially resolved by periodically reversing the flow of medium within the system, however this would only be a short term solution.

One of the primary assumptions on which their associated model was based was that permeability of the fibre to macromolecules was high and that it remained so throughout its operation. While this would be an ideal solution, Murkes and Carlsson (1990) report that highly permeable fibres foul at a higher rate than those of lower permeability. No report was given for the growth of mammalian cells in this system.

The system reported by Cima *et al.*(1990) and developed commercially by SETEC, involves the use of a fibre within a fibre (Figure 5.9). The bioreactor operated by Cima *et al.* consisted of 40 sets of concentric hollow fibres with a 200 μm annular space. Medium is passed through both the lumen of the fibres and the space surrounding the outer fibre, with the lumen of the inner fibre pressurised to force perfusion through the intra-lumenal growth space. The model developed by this group assumes, unlike the other reported models where cell growth is predicted to be in an evenly distributed layer, that the cells are unevenly distributed on the fibre surface, displaying non-uniform growth, an assumption which Burns (1991) has also used. As with the other reported operations, a total of 12.5% serum was used for the culture of a murine tumour cell line Y1. They inoculated the reactor with 2 x 10^8 cells, equivalent to 8 x 10^7 cells/cm^3, and based on data of nutrient consumption, concluded that cell death had occurred reducing the viable cell count within the reactor.

Figure 5.9:- Dual hollow fibre bioreactor designs

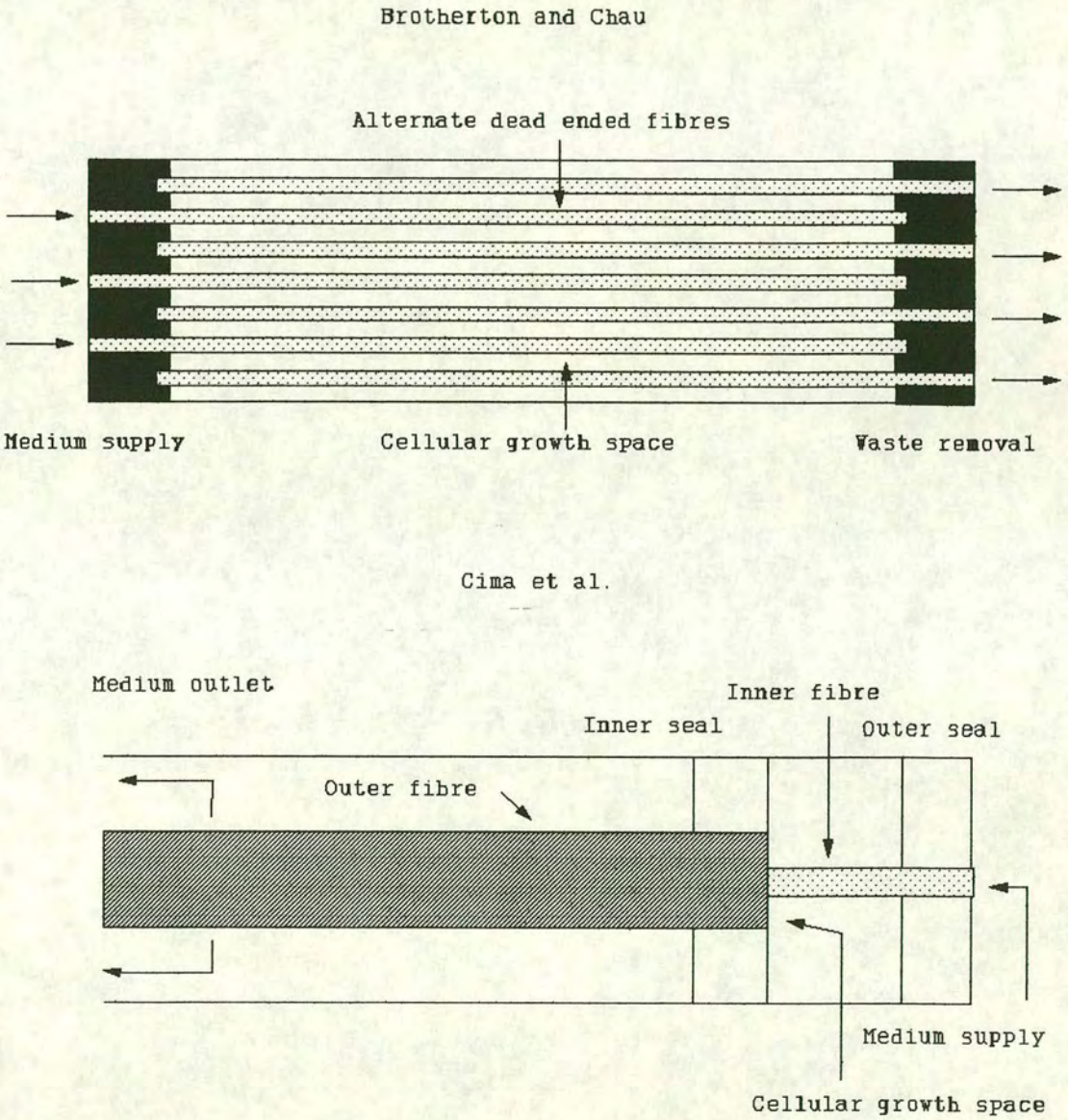

5.3.1 Summary

The high density culture of mammalian cells in hollow fibre bioreactors has not been shown to be as advantageous as expected. The principal limitations for a single fibre bioreactor include the potential for cell starvation and an uneven distribution of cells within the bioreactor, caused mainly by membrane fouling and the flow regimes found in this design of bioreactor.

Dual hollow fibre bioreactors, while potentially overcoming these limitations have been restricted by the sheer complexity of their construction, limited in process time through fibre fouling, or they have been limited in culture volume and hence economic viability.

5.4 The Edinburgh Dual Hollow Fibre Bioreactor

In order to overcome the difficulties in construction and the limitations associated with the previously described single and dual hollow fibre bioreactors, a new type of hollow fibre culture device was developed, the Edinburgh Dual Hollow Fibre Bioreactor (Figure 5.10). The design of this system is similar to that of Knazek *et al.* (1980), using two sets of fibres operated at a pressure differential. The conceptualised design of this bioreactor is described by the author and Burns (1991), who developed a theoretical model of its performance in an associated study on this bioreactor. This work represents a study of the application and further improvement of this design using a murine hybridoma.

The following chapters describe the work carried out during this PhD. project using the Edinburgh Dual Hollow Fibre Bioreactor and a murine hybridoma (ES4). The initial chapters (1-5) have introduced the importance of a controlled, non-damaging culture environment for the cells, where nutrients are supplied in non-limiting quantities and potentially toxic metabolites are removed. The bioreactor described in this study attempts to address these issues, with the methods and results used described in the following Chapters.

Figure 5.10:- The Edinburgh Dual Hollow Fibre Bioreactor

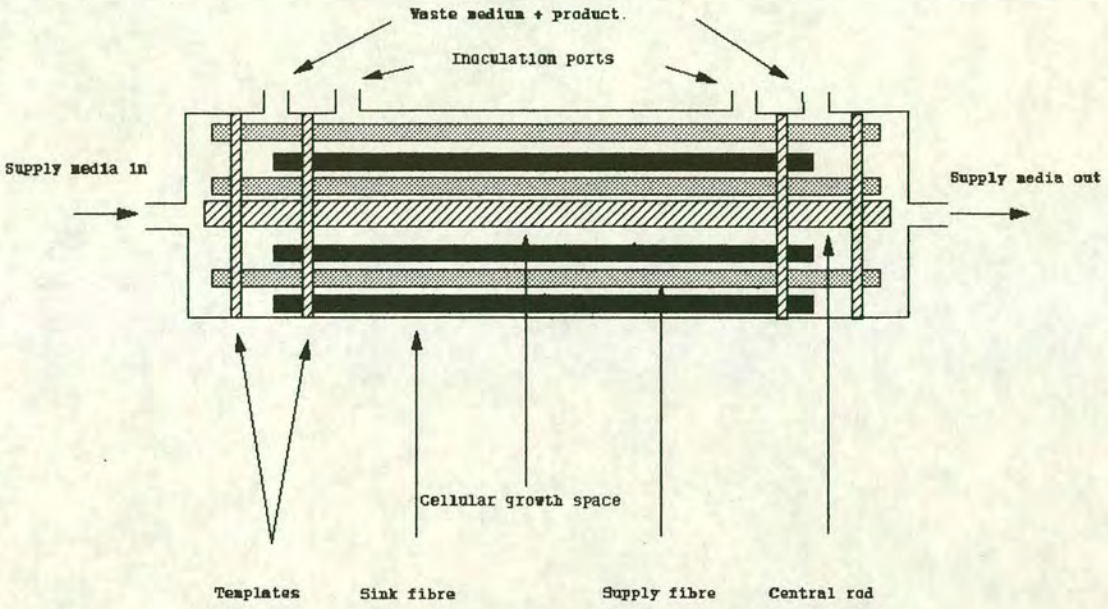

Chapter 6 outlines the analytical and construction methodologies used in the cell culture and bioreactor experiments conducted during this study. Chapter 7 introduces the design basis for the Edinburgh Dual Hollow Fibre Bioreactor, a description of the bioreactor circuits used, and the development of bioreactors design, sampling and control regimes implemented during this work in order to improve the growth environment. Chapter 8 provides a preliminary investigation into the filtration characteristics of the fibres used in the bioreactor, with a view to the provision of nutrients to the cells. Chapter 9 describes a series of growth experiments carried out in culture flasks which investigate the growth characteristics and the effects of glutamine replacement on the experimental cell line, ES4, providing an insight into the cells nutritional requirements. Chapter 10 describes a series of bioreactor experiments in which cells were cultured, highlighting the advantages and disadvantages of the Edinburgh Dual Hollow Fibre Bioreactor. Finally Chapter 11 provides overall conclusions from this work suggesting where the author feels future work would be valuable.

Chapter 6

Materials and Methods

6.0 Hybridoma choice and maintenance

The following criteria were used to select a suitable hybridoma for these studies:-

(1) A cell line which was stable, not readily losing its antibody producing capability.

(2) A hybridoma for which the principle metabolite and product assay procedures were well defined.

(3) A relatively robust, easily grown cell.

The cell line selected was a murine hybridoma called ES4 (produced by Edinburgh Surgeons) supplied by a campus based biotechnology company, Bioscot Plc. The fusion was a mouse-mouse hybridoma, derived from the NS-1 cell line. It secretes an immunoglobulin class M (IgM) antibody which is specific to the human B type blood group.

6.1 General culture techniques

Unless otherwise stated, all cell culture related procedures were carried out in a Type 1 laminar air flow hood (Flow laboratories, Gelaire HF 48) to minimise the risk of contamination.

6.1.1 Media preparation

The cell line was cultured in one of two basic media formulations, powdered RPMI 1640 (Searles modification, Gibco BRL) and glutamine free RPMI 1640 (Gibco BRL Product No. 31870-025) and supplemented as outlined in Table 6.1. The glutamine free RPMI 1640 was supplied filter sterilised in 500 ml bottles, with the addition of supplements occurring just prior to its use. The powdered RPMI 1640 (Searles modification) was prepared in 25 l batches as follows:-

(1) One container (weight ≈ 260.5 g) of the appropriate powdered medium was diluted with distilled water to give 25 l of medium in a 50 l plastic bottle.

(2) Sodium bicarbonate, phenol red and sodium pyruvate were added according to Table 6.1. The pH of the medium was adjusted to 7.5 by means of the drop wise addition of a 1 M solution of either NaOH or HCl.

(3) The medium was filtered using a presterilised 0.2μm Millidisk 10 filter and filter housing (Millipore). After filtration the medium was aliquoted into a number of 2 l, sterile Duran bottles using a filling bell. The bottles were then stored at 4°C.

(4) The medium was prewarmed to 37°C and supplemented with the appropriate amounts of glutamine, antibiotics and serum (Table 6.1) before use.

6.1.2 Cell counts

The technique used for assessing cell viability and cell number was that originally developed by Girardi *et al.*(1956). The trypan blue exclusion method differentiates between viable and non-viable cells by utilising differences in the permeability of their membranes. Viable cells are able to exclude the dye, remaining clear, while the non-viable cells are permeable to the dye leading to an accumulation of the blue stain. By using a haemocytometer, with a predefined sample chamber volume, the relative numbers of each cell type per volume may be calculated. The standardised technique used during this work is outlined below.

(1) Duplicate samples (100 μl) were aseptically removed from a previously mixed test flask and placed into two separate 1.5 ml vials.

(2) To each of the vials, an equal volume (100 μl) of trypan blue solution (0.8% solution of trypan blue dye, Sigma) was added and the contents were mixed thoroughly.

(3) After 2-3 min, a sample (20-50 μl) was removed from the vial and placed under the cover slip of the Haemocytometer.

Table 6.1 :- General culture medium composition.

Final medium concentration (l^{-1})	Method of addition
2 mM Glutamine	10 ml of glutamine (200 mM) from frozen stock (Gibco)
1 mM sodium pyruvate	Powdered supplement added during medium preparation, or 10 ml of a 100 mM refrigerated, sterile stock solution (Gibco).
Penicillin/Streptomycin 25000 i.u./2500 μgml^{-1}	5 ml of stock solution, with 5000 i.u. ml^{-1} of penicillin and 5000 μgml^{-1} streptomycin, stored frozen (Gibco).
Foetal Calf Serum or New born calf serum as 5% (v/v) in medium.	50 ml of serum (Sigma). Each batch was tested for similarity in growth characteristics and stored in a freezer at -20°C.
RPMI 1640 (Searles modification only)	925 ml (as described in text, Gibco)
sodium bicarbonate 2 gl^{-1} (23.8 mM)	added to bulk medium preparation of RPMI 1640 (Searles modification). 5 ml of 100 mM filter sterilised sodium bicarbonate was added to the glutamine free formulation.
Phenol red solution 1 ml (Glutamine free formulation already contained this component)	added to the bulk medium or to the filtered medium (Sigma,0.5% in D-PBS).

(4) The relative numbers of viable and non-viable cells were assessed using a hand counter and binocular microscope (x100 magnification, with a x10 objective). This process was repeated for each of the samples.

(5) Equation 6.1 was used to convert the observed results to the number of cells ml^{-1} of test fluid. This calculation was carried out for each of the four cell counts and the mean of the four values calculated. The critical variance, calculated by the standard deviation divided by the mean. never exceeded 5% .

$$\frac{no.\ of\ cells\ counted}{no.\ of\ squares\ counted} \times dilution\ factor = \times 10^4\ cells\ ml^{-1} \quad (6.1)$$

6.1.3 Long term storage of cells

An ES4 cell bank was created and maintained using the liquid nitrogen storage facilities of Bioscot Plc. The creation of a cell bank was a standard procedure for ensuring the continued integrity of the hybridoma over the duration of this study. Storage of the cells in liquid nitrogen, at -190°C, has been shown to allow the original characteristics of the initial clone to be maintained for several years. The techniques used for the production of the cell bank, the resuscitation and subsequent culture of the cells were as follows :-

Production of the cell bank

(1) A 1 l culture of ES4 cells, derived from the main cell bank of Bioscot PLC, was prepared in a 1 l spinner flask (Bellco). The cells were cultured in fully supplemented RPMI 1640 at 37°C, using a 20 rpm stirrer base and water bath (Techne). The culture vessels were surface aerated using a prefiltered gas supply consisting of 95% air to 5% CO_2.

(2) The cells were harvested when the culture reached between 3-5 x 10^5 viable cells ml^{-1} of medium, with a percentage viability of greater than 80%. The cells were harvested by centrifugation.

(3) The cells were resuspended in the appropriate volume of freezing mix (90% v/v foetal calf serum, 10% v/v dimethyl sulphoxide, DMSO) to give a final viable cell concentration of 1.0 x 10^7 cells ml^{-1}.

(4) Cells were aliquoted in 1 ml volumes into sterile 2 ml freezing vials.

(5) The vials were frozen in two stages to decrease the harmful effects of ice crystal formation on the cells. The vials were frozen over night in a -70°C freezer before being moved to the long term liquid nitrogen storage facility (-190°C).

(6) The cell bank was tested by resuscitating a vial of cells from frozen, ensuring their growth characteristics match those of the original clone.

6.1.4 Resuscitation of the cells from the frozen state

(1) Two 7 ml aliquots of medium (5% serum supplemented RPMI 1640) were transferred aseptically to a 25 cm^2 (surface area of flask base) tissue culture flask (Nunclon) and a sterile 30 ml sample bottle respectively. A further 30 ml aliquot of medium was transferred into an 80 cm^2 tissue culture flask.

(2) A frozen vial from the cell bank was defrosted in a 37°C water bath until almost all of the ice had melted. The contents of the vial were transferred aseptically to the 25 cm^2 flask.

(3) After mixing, the contents of the small flask were transferred aseptically to the 80 cm^2 flask.

(4) The 25 cm^2 flask was then replenished with the 7 ml of fresh medium from the 30 ml sample bottle, forming a back up culture.

(5) Both the 25 cm^2 and 80 cm^2 tissue culture flasks were placed in an incubator at 37°C in an atmosphere consisting of 5% CO_2, 95% air.

(6) The cells were allowed to grow to full confluency (between 3-5 x 10^5 viable cells ml^{-1} after about 1 to 2 days) before being transferred to a larger culture flask (either 80 or 175 cm^2) containing fresh medium.

6.1.5 Maintenance of cultures

A stock culture was maintained for experiments, being allowed to grow to between 3.0-5.0 x 10^5 viable cells ml^{-1} before being used in experiments. Alternatively the cultures were maintained for further experiments by being periodically diluted to 1 x 10^5 viable cells ml^{-1} with fresh medium.

The cells were harvested by centrifugation, 1000 rpm for 10 min in an IEC Central bench top centrifuge, and resuspended in a small volume of medium before being seeded in experimental medium at 1 x 10^5 viable cells ml^{-1}.

6.1.6 Experimental sampling

Samples were taken from each of the experiments and stored for further analysis.

(1) Experimental samples (900 μl) were aseptically removed from the test vessel and transferred to prelabelled Eppendorf vials (1.5 ml).

(2) To each of the vials 100 μl of a 20 % w/v solution of sodium azide, to give a final sample concentration of 2% w/v, were added to kill any viable cells and maintain sample sterility.

(3) The samples were then stored at 4°C until required.

Cells in the stored samples were found to settle out of the stored solution and form a pellet at the bottom of the Eppendorf. The clarity of the supernatant was regularly assessed by microscopy. By carefully removing the upper layers of the sample, cell free samples could be obtained.

6.1.7 Sterility testing

Sampling for sterility tests was carried out after the preparation of medium, prior to and at the end of flask experiments and at various points during the bioreactor experiments. These tests were carried out in triplicate and usually took the form of the addition of test sample (0.1 ml) to 2.0 ml of Peptone broth (Oxoid) and incubation at 37°C for between 3 to 7 days. Settle plates were used in the laminar air flow hood to test for air borne contaminants, primarily during the set up of culture experiments.

The broth was prepared by adding 1g of peptone to 100 ml of distilled water. The broth was then sterilized by autoclaving at 121°C for 15 mins. The sterile broth was then aseptically aliquoted in 2 ml amounts into presterilised bijou bottles (7ml). The bijou bottles were then stored at 37°C. Contamination was determined visually by the cloudiness of the medium after a maximum of 7 days, combined with a microscopic examination of the samples.

Settle plates were prepared by adding 2 g of powdered agar (Oxoid, Product no.

LP013B) to 100 ml of peptone broth prior to autoclaving. After autoclaving the agar supplemented broth was allowed to cool to approximately 50°C and aliquoted into 90 mm petri dishes (Fisons). The agar was then allowed to set and the plates stored at 4°C. Three plates were used per sterility test, one remained unopened during the test (to ensure the plates were not contaminated during preparation), plates 2 and 3 were opened and placed in the hood during the set up of the cell culture experiments. Plate 2 was closed after the work was finished, with plate 3 left open in the hood overnight. Plates were incubated at 37°C for approximately 7 days and inspected visually in order to determine whether air-borne contaminants were present. These were used in conjunction with the liquid medium tests.

The sterility of freshly prepared medium was tested after the initial filtration step, after the addition of supplements (e.g. glutamine) and prior to the start of each bioreactor or flask experiment. The medium used in flask experiments was sterility tested prior to the addition of cells to the flask and then at the end of the experiment (usually on day 7).

Bioreactor experiments were tested immediately after all the apparatus had been connected together, with samples of medium being taken from the bioreactors growth space and the upstream and downstream circuits. Samples were then taken from each of these points every three days, until the end of the experiment.

If any or all of the three replicate samples taken at a specific time point were contaminated, then the experiment was labelled as potentially contaminated. If the following samples taken from the same experiment were contaminated then the results from that experiment were discarded.

6.2 Metabolic assays

A range of off-line, metabolic assays were used for assessing the growth characteristics of the cells. These assays included glucose, lactate, ammonia, glutamine, α-ketoglutarate and an antibody assay.

6.2.1 Glucose assay

The assay used was supplied by Sigma (kit no. 510-A) The kit is based on the simultaneous use of glucose oxidase and peroxidase with a chromogenic acceptor (o-dianisidine). The assay is a derivation of the Raabo and Terkildsen (1978) method. The Sigma kit uses the following coupled reaction:-

$$\text{Glucose} + 2H_2O + O_2 \xrightarrow{\text{Glucose Oxidase}} \text{Gluconic Acid} + 2H_2O_2$$

$$2H_2O_2 + \underset{\text{(colourless)}}{\text{o-Dianisidine}} \xrightarrow{\text{Peroxidase}} \underset{\text{(brown)}}{\text{Oxidised o-Dianisidine}}$$

The net result of this reaction is that the developed brown colour is directly proportional to the original concentration of glucose in the sample. The method used was that suggested by Sigma and summarised in the following paragraph.

Stock solutions, reagents and glucose standard solutions (0-5.0 gl^{-1}, 0-27.8 mM) were prepared according to the manufacturers' instructions. Experimental samples and standard solutions were diluted 20 fold (50 μl of sample/standard: 950 μl of distilled water), with 0.5 ml of each dilution added to separate test tubes containing 4.5ml of the Sigma combined enzyme colour reagent. Distilled water was used for a blank solution. The standards, samples and blank tubes containing the assay mixture were then incubated for 30 min at 37°C. On removal from the incubator the absorbance of each test tube was read at 425 nm using a Unipath visible spectrophotometer.

Standard curves were prepared by plotting absorbance at 425 nm against glucose concentration. Glucose concentrations for the experimental samples could either be determined from the linear portion of the standard curve, or by using Equation 6.2. Each experimental sample, standard and blank was assayed at least in duplicate. Critical variances usually fell within 5% of the mean value for each sample.

$$Glucose\,(mgdl^{-1}) = \frac{Absorbance_{Test}}{Absorbance_{Standard}} x\,conc.\,of\,Standard\,(mgdl^{-1}) \qquad (6.2)$$

6.2.2 Lactate assay

The assay used utilised a Sigma kit (kit no. 735). The mechanism of the reaction involves a coupled reaction with the formation of a chromogen, as shown below:-

$$\text{Lactate} \xrightarrow{\text{Lactate Oxidase}} \text{Pyruvate} + H_2O_2$$

$$H_2O_2 + \text{Precursor Chromogen (Colourless)} \xrightarrow{\text{Peroxidase}} H_2O + \text{Activated Chromogen (Purple)}$$

The procedure used was that suggested by the manufacturer which is summarised in the following paragraph.

The vials supplied with the kit were reconstituted with 10 ml of distilled water and test tubes were labelled for the appropriate number of samples, standards and blanks. A series of standards was prepared from a stock Sigma lactic acid solution (40 $mgdl^{-1}$). To each of the labelled test tubes 1 ml volumes of the lactate reagent and 10 μl of the undiluted test solution (sample, standard or distilled water blank) was added. The contents of the tubes were thoroughly mixed and allowed to react at room temperature for 10 min. The absorbance of each sample at 540nm was read against a distilled water control and the concentration of lactate in each sample determined from either a standard curve or by using Equation 6.3. Samples were assayed in duplicate and means and standard deviations calculated (based on 2 assays per sample, with 2 samples per sample time). As a result of the relatively small volume of sample (10 μl) used in this assay the calculated critical variances fell below 10% .

$$Lactate\,(mg\,dl^{-1}) = \frac{Absorbance_{Test}}{Absorbance_{Standard}} x\,conc.\,of\,Standard\,(mg\,dl^{-1}) \quad (6.3)$$

6.2.3 Ammonia assay

This assay is derived from part of the Sigma assay kit for urea estimation (kit no. 640). The assay is based on the Berthelot reaction, in which free ammonium ions react with phenol nitroprusside and alkaline hypochlorite to form a blue indophenol. By measuring the degree of absorbance of the resulting indophenol an assessment of relative ammonium concentrations can be made, by reference to known standards. The protocol used was as follows:-

Test tubes were labelled for the appropriate number of experimental samples, standards and controls. The standards were prepared using a fresh solution of ammonium chloride to give standards ranging from 1 to 5 mM. The experimental samples and standards were diluted 1:40 by adding 25 μl of the test sample to 975 μl of distilled water. The controls were prepared using 25 μl of distilled water. To each of the test tubes, 500 μl of each dilution, 250 μl of alkaline hypochlorite solution and 250 μl of phenol nitroprusside were added and the contents mixed thoroughly. After incubation at room temperature for 30 min, the absorbance of each sample was read at 525 nm. The readings were then converted to ammonium ion concentrations (mM) using either a standard curve or Equation 6.4. The calculated critical variances for the means fell below 5% .

$$Ammonia\ conc.\ (mM) = \frac{Absorbance_{Test}}{Absorbance_{Standard}} x\ conc.\ of\ Standard\ (mM) \quad (6.4)$$

6.2.4 Glutamine assay

This assay was a two step test for assessing glutamine levels in test samples. The theory behind this assay and its associated calibration curves are described in Section

9.2.1 . The following steps describe the protocol use in this assay.

(1) The glutaminase enzyme was supplied by Sigma (stock no. G-8880) and reconstituted according to instructions with 0.005 M sodium acetate buffer (pH 6.0). The enzyme was stored at -20°C in 200 μl aliquots with 25 units of enzyme ml^{-1} of buffer. Each vial was further diluted with 800 μl of 0.005 M sodium acetate (pH 6.0) before use.

(2) The appropriate number of sample tubes, duplicate distilled water controls, duplicate 'fresh' medium controls and known standards were set up in 1.5 ml Eppendorf tubes.

(3) To each of the tubes, 250 μl of 0.1 M sodium acetate buffer (pH 4.9) and sample were added successively.

(4) A volume of the diluted glutaminase solution (50 μl at 5 units of enzyme ml^{-1}) was added to each of the samples, standards and controls.

(5) The tubes were mixed thoroughly by inversion and incubated at 37°C for 30 min.

(6) Immediately after incubation, a 25 μl aliquot of each sample was added to 975 μl of refrigerated distilled water to slow the glutaminase reaction.

(7) A 500 μl aliquot of each sample was used for the assessment of ammonia levels using the previously described protocol (Section 6.2.3., step 4 onwards).

(8) Using the ammonia data for the glutaminase treated and untreated samples, the amount of enzymatically digested glutamine could be calculated by subtracting the treated sample levels from the untreated.

(9) With each new batch of enzyme, a range of samples was prepared and the validity of the assay assessed by this protocol. In each case the absorbance of the standard gained by measuring ammonia levels was plotted against the initial glutamine concentration of the standard. The degree of linearity of the test graph was used as a measure of the validity of the assay.

6.2.5 α-Ketoglutarate assay

In order to monitor the utilisation of α-ketoglutarate in the medium modification experiments described in Chapter 9 an enzyme based assay was developed for the Dynatech MR5000 microplate reader. The theory of this technique is described in Section 9.2.2 . The following protocol describes the chemicals and procedure used for this assay.

(1) The following stock solutions were prepared using distilled water, 0.1 M sodium phosphate buffer (pH 7.3), 3.2 M ammonium acetate solution, 6 mM ß-NADH solution (Sigma, prepared fresh), a 0.1 M solution of EDTA (courtesy of Bioscot Ltd.). A stock buffer solution containing these components was prepared just prior to the experiment, consisting of 10.8 ml of cold 0.1 M sodium phosphate buffer, 0.2 ml of 3.2 M ammonium acetate, 0.12 ml of 6 mM NADH solution and 0.12 ml of 0.1 M EDTA.

(2) L-Glutamic Dehydrogenase (Sigma, G2626) was supplied in buffer solution which was diluted to 0.5 units ml^{-1} using 0.1 M phosphate buffer(pH 7.3). This preparation was carried out just prior to each assay.

(3) α-ketoglutarate standard solutions were prepared using RPMI 1640 and a 0.1 M stock solution of α-ketoglutaric acid (Sigma K-1750).

(4) The test solution and the α-kg standard solutions were diluted 1:10 with 0.1 M phosphate buffer.

(5) All of the wells in the microtitre plate were seeded with 240 μl of the stock buffer solution prepared in step 1, except the reference blank cells which contained a sample of the stock buffer solution which had the NADH component replaced by water.

(6) The diluted samples and standards (50 μl) were added to the test wells and 50 μl of water to the blank wells.

(7) The microtitre plate was then incubated at 30°C to warm the contents of the wells prior to the addition of 11 μl of the enzyme solution prepared in step 2.

(8) The plate was read at 340 nm in the MR5000 after 30 minutes incubation at 30°C.

(9) The relative amounts of α-ketoglutarate in the test samples were then determined by reference to a standard curve (see Section 9.2.2 for a description).

6.2.6 Antibody assay

The technique used in this study was an indirect sandwich ELISA developed by Bioscot PLC as part of their assessment procedures. The technique involved the binding of a goat anti-mouse antibody (IgM, Sigma) to a microtitre plate. The coating antibody used was species specific, recognising both whole and segments of the murine antibody secreted by ES4. The conjugate antibody used was a goat anti-mouse antibody (IgM) conjugated to horse radish peroxidase. The conjugate antibody was specific for the μ-chain.

The chemicals used in the assay were stock solutions prepared at Bioscot by Miss N. Goulda, with the constituents of the principal solutions described in Table 6.2. The author carried out all of the assays and analysed all of the results reported in this thesis. The following procedure was used for this sandwich technique:-

(1) The 96 well microtitre plates were prepared the day before the assay was carried out. For each plate required, one ampoule (10 μl) of the coating antibody (Calltag M31500, at 0.77 mg ml^{-1}) was added to 10 ml of P.B.S.

(2) Each well was coated using 100 μl of the coating mix and the plate was refrigerated overnight.

(3) The plate was washed and drained several times using washing buffer (1x) and then dried.

(4) Each of the wells of the plate was seeded with either 100 μl of diluent buffer, 200 μl of standard antibody (ICN R0055B, diluted to a standard solution of 500 $\mu g ml^{-1}$ from a stock solution) or 200 μl of

sample as outlined in Figure 6.1.

(5) The standards, in wells A2 and A3 (Figure 6.1), were doubly diluted down the plate via the transfer of 100 μl of sample into the 100 μl of diluent in the well below using a multiple pipette. For example, 100 μl of A2 was transferred into B2, the contents were mixed using the pipette, then 100 μl of B2 were transferred to C2. This process was repeated down to row H. This process gave antibody concentrations of 500, 250, 125, 62.5, 31.25, 15.63, 7.82 and 3.91 μgml^{-1} for a standard curve.

(6) The samples were doubly diluted in a similar way, but only to a 1 in 8 dilution of the first well.

(7) The plate was incubated at room temperature for 30 min, before being washed several times in washing buffer (1x) and allowed to drain.

(8) The conjugate solution, consisting of 2 μl of goat anti-mouse IgM solution conjugated with Horseradish peroxidase (Sigma, A-8786) in 10 ml of diluent buffer, was added in 100 μl aliquots to each well.

(9) The plates were incubated for another 30 min at room temperature, washed and drained.

(10) Substrate solution was added as 100 μl aliquots to each well and the plates allowed to develop for up to 10 min.

(11) The reaction was stopped using 25 μl of 5 M sulphuric acid per well.

(12) The plates were read at 540 nm in a Dynatech MR700 microplate reader.

(13) The results from the plate reader were analyzed using the RIACalc program on an IBM compatible computer. This program calculated a fitting algorithm for the standard curve, plotted as the logarithm of the antibody concentration versus the absorbance of the samples. The algorithm was used to calculate the concentration of the unknown samples in μgml^{-1}.

(14) The sample concentrations were compared in duplicate, down the dilution series, and the values for each dilution averaged with a percentage critical variance, which evaluates the

Table 6.2:- Solutions used in the sandwich ELISA.

	Buffer Solutions (l^{-1})	Constituents
(A)	Phosphate Buffered Saline (PBS) (10x concentrate)	2.97 g $NaH_2PO_4.2H_2O$ 11.5 g Na_2HPO_4 85 g sodium chloride made up to 1l, pH 6.6
(B)	Wash Buffer (10x Concentrate)	400 ml of 10x PBS 2 ml Tween 20
(C)	Diluent Buffer	100 mg Bovine Serum Albumin (BSA) 100 ml 1x Wash buffer
(D)	TMB/DMSO	100 mg TMB** 10 ml DMSO***
(E)	Substrate Buffer (10x Concentrate)	1 M sodium acetate (41 g in 500 ml RO water*) 1 M Citric acid (21 g in 100 ml RO water) Titrate sodium acetate with citric acid to pH 6.0
(F)	Hydrogen peroxide solution	128 μl of 30 % H_2O_2 9.87 ml 1xSubstrate buffer
(G)	Substrate solution	100 μl TMB/DMSO 100 μl Hydrogen peroxide solution
(H)	Stop Solution (5 M Sulphuric acid)	Sulphuric acid (98%) (Approx. 18.3 M, spec. gravity 1.835) 272.5 ml H_2SO_4 to 727.5 ml RO water.

* All solutions were made up and diluted using reverse osmosis (RO) prepared water.
TMB = 3,3',5,5'-Tetramethylbenzidine * DMSO = Dimethyl sulphoxide

total error and counting error.

(15) The program then calculated a precision profile of concentration of standards (log) against percentage critical variance to evaluate the range over which the assay was accurate.

Figure 6.1:- Seeding of diluent, standards and samples on the microtitre plate.

Row												
A	+	S	S	1	1	3	3	5	5	7	7	0
B	+	+	+	+	+	+	+	+	+	+	+	+
C	+	+	+	+	+	+	+	+	+	+	+	+
D	+	+	+	+	+	+	+	+	+	+	+	+
E	+	+	+	2	2	4	4	6	6	8	8	0
F	+	+	+	+	+	+	+	+	+	+	+	+
G	+	+	+	+	+	+	+	+	+	+	+	+
H	+	+	+	+	+	+	+	+	+	+	+	+
Column	1	2	3	4	5	6	7	8	9	10	11	12

(+) denotes addition of 100 μl of diluent,numeric denotes the number of test sample added to well (200 μl),(S) denotes standard solution (200μl).

6.3 Edinburgh Bioreactor construction

This section outlines the construction techniques used for the initial range of bioreactors produced. Later modifications to design and construction are described in Chapter 7.

6.3.1 Selection of materials

The materials used in the construction of the bioreactor and ancillary equipment were selected by Dr. J. Burns and Dr. J. Wilson, as part of their Ph.D. projects (Burns, 1991, Wilson, 1992). A brief outline of the criteria used to select the materials are given in Table 6.3.

6.3.2 Initial construction technique

This section describes the original construction regime used for the dual hollow fibre bioreactor. The polycarbonate components used were designed by Dr J. Burns as part of his PhD. thesis and adopted in the initial stages of this study.

(1) The polycarbonate tube (200 mm long, 26 mm internal diameter, 30 mm external diameter) and four of the desired polycarbonate templates (from 3 mm sheet) were prepared, according to Figures 6.2 and 6.3.

(2) The templates were aligned so that their holes matched and they were then glued to the central glass rod (4 mm diameter, 200 mm long) as per Figure 6.4.

(3) Fibres (1 mm internal diameter, 2 mm outer diameter) of the required pore size were cut according to the following length: supply fibres to 199 mm, sink fibres to 155 mm.

(4) The fibres were threaded through the templates according to Figure 6.3. The fibres were threaded from the centre of the templates to the outside.

(5) The completed template structure was placed inside the machined polycarbonate tube and the tube was stood upright in a shallow glass beaker.

(6) The beaker was filled with saturated sodium chloride to the just below the level of the first template disc (Figure 6.5).

(7) Silastic 3110 was mixed with the Silicone fluid in the ratio of 10:1 by weight. The mix was then stored in a syringe for use during later steps.

(8) The silicone setting catalyst (catalyst 4: Tin (II) octanoate) was diluted 1:1 with 50 μl of the silicone fluid. The diluted catalyst increased the curing time of the rubber solution enabling greater penetration of the mixture between the fibres.

(9) For each template potted, 3 ml of the silastic/ silicone mix (from step 7) was aliquoted into a 50 ml sample bottle and 10 μl of the diluted catalyst was added.

Table 6.3:- Selection criteria for bioreactor construction materials.

Material and Use	Selection criteria
Bioreactor components:-	
Polycarbonate plastic, (used for reactor tube, templates, reactor end caps and oxygen probe housings).	Autoclavable, Clear plastic for visual assessment, machinable, non toxic to cells.
316 Stainless steel, (used for reactor end caps and pressure transducers housings.)	Autoclavable, Durable, Machinable, Non toxic to cells.
Polyethersulphone hollow fibres (Grace Co. Ltd., USA) (used within the reactor)	A range of different molecular weight cutoffs, e.g. 0.1 μm, 100 kDa and 50 kDa. Autoclavable and non toxic to cells.
Rubber potting compounds:-	
(a)Silastic 3110 RTV Silicone rubber (Dow Corning) (b)Silicone fluid, Dow Corning 200/50 cs (diluent to rubber solution) (c)Silicone Rubber catalyst- Catalyst 4 (Tin (II) Octanoate), acts as curing agent (B.D.H.)	Easy use, autoclavable, Non toxic to cells when cured. However, the individual components may be harmful.

(10) After mixing the contents of the bottle were decanted into a 10 ml syringe, which had previously been modified by the addition of a truncated Gilson tip or a blunt 18 gauge syringe needle.

(11) The syringe was used to apply the unpolymerised silicone rubber mix to the template disc through the ports at either side of the bioreactor, closest to the required template. The density of the silicone rubber mix was less than that of the saturated sodium chloride, causing the rubber to float. The floating rubber formed and sealed around the template.

Figure 6.2:- Specifications of the bioreactor tube.

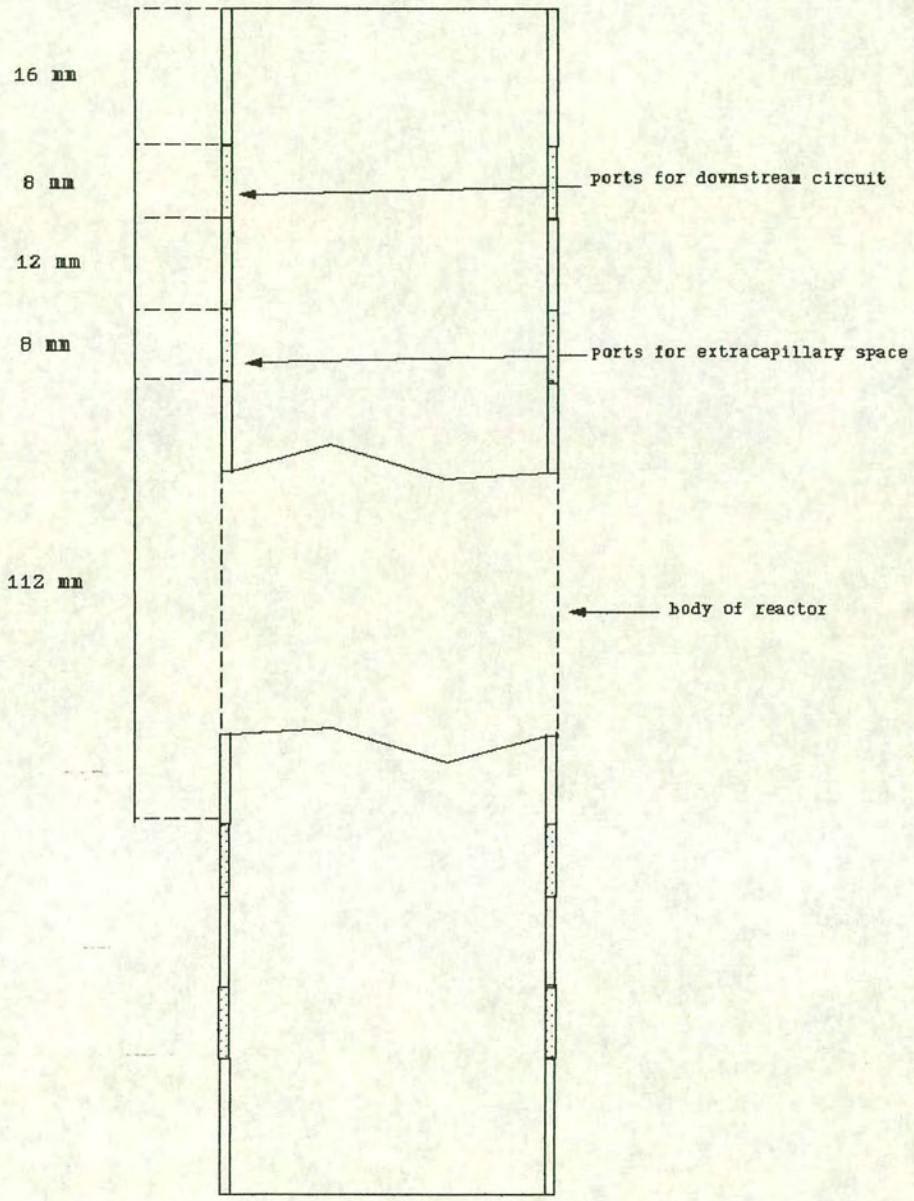

Figure 6.3:- Template layout and threading plan.

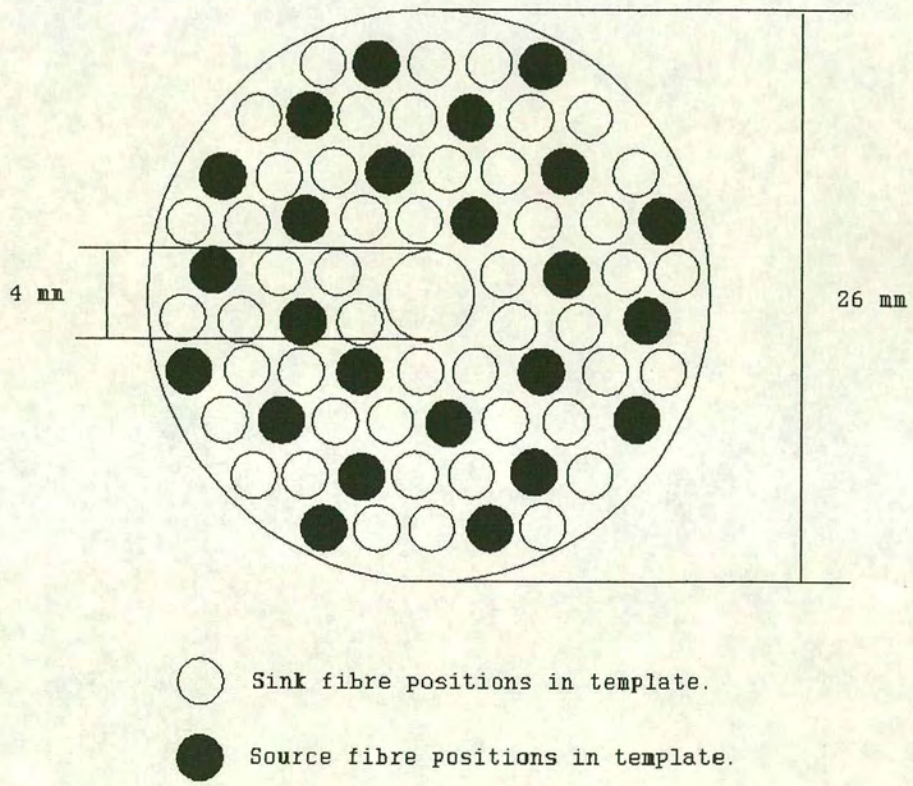

(12) At least 3 h were allowed for the rubber to cure. The potting process was repeated for each of the remaining templates.

(13) On completion the reactor was thoroughly rinsed in distilled water to remove any accumulated catalyst or NaCl.

6.3.3 Dyed dextran preparation

Using a range of Procion dyes, supplied by I.C.I, and dextrans of a predefined molecular weight (Sigma) a range of test solutions was prepared. The procedure outlined below is a derivation of a suggested cotton dyeing protocol used by I.C.I.

(1) For each of the solutions required, 1 g of the Procion dye (Procion Red P-4BN, Procion Blue SP-3R or Procion Yellow H-4G) and 10 g of the dextran (average molecular weights of 19.5, 63.5 or 138.5 kDa) were carefully weighed into a 1 l conical flask.

(2) Sodium chloride solution was prepared (40 gl^{-1}) and 150 ml were added to the flask and stirred for at least 1 h at room temperature.

(3) After mixing, 300 ml of sodium carbonate solution (20 gl^{-1}) were added to the flask and the mixture was heated to about 95°C. The mixture was maintained and stirred at this temperature for approximately 1 h on a stirrer hotplate.

(4) A 10 kDa cutoff capillary flow dialyzer (Travenol, Deerfield, USA, cat. no. 12.11L) was used to separate the unbound dye and inorganic salts from the dyed dextran. The dye mixture was passed through the lumen of the fibre bundle with a counter current flow of distilled water outside the fibres being used to remove the unbound dye from the fibre bundle.

(5) The dyed solution was filtered until no discernable colour could be seen in the dialysate.

(6) The dyed dextran solution was then stored at room temperature and was agitated before use.

(7) For each colour of solution used in the test experiments, a scanning

Figure 6.4:- Threaded bioreactor unit.

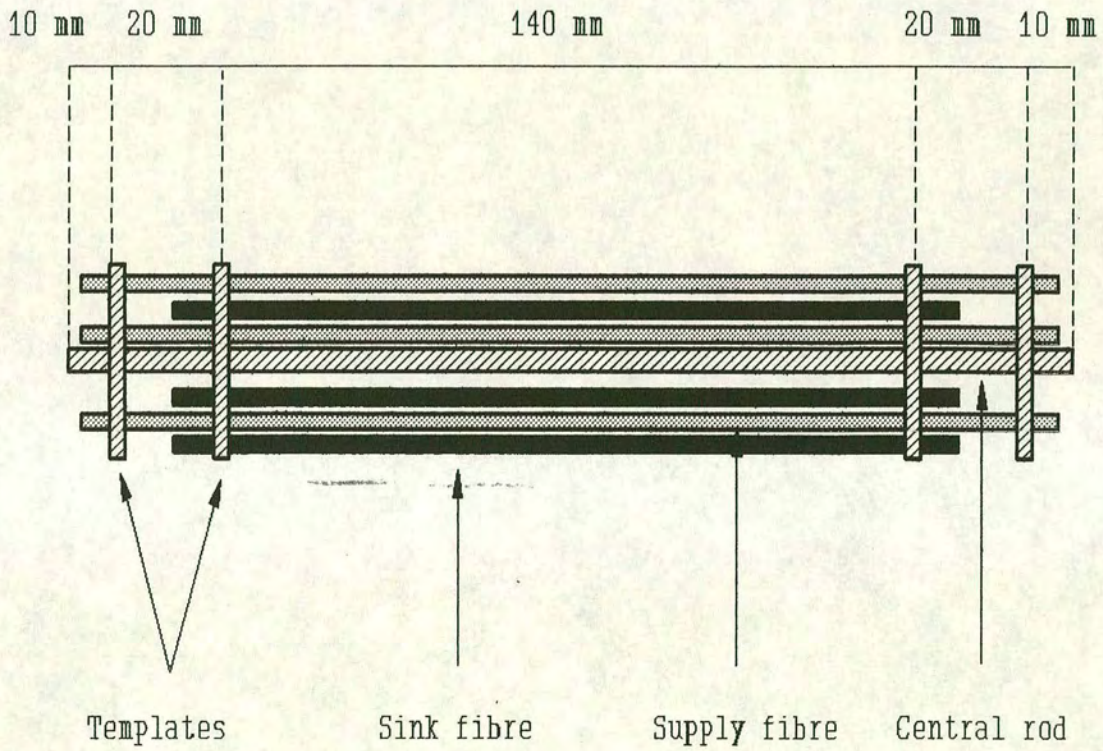

Figure 6.5:- Bioreactor potting technique.

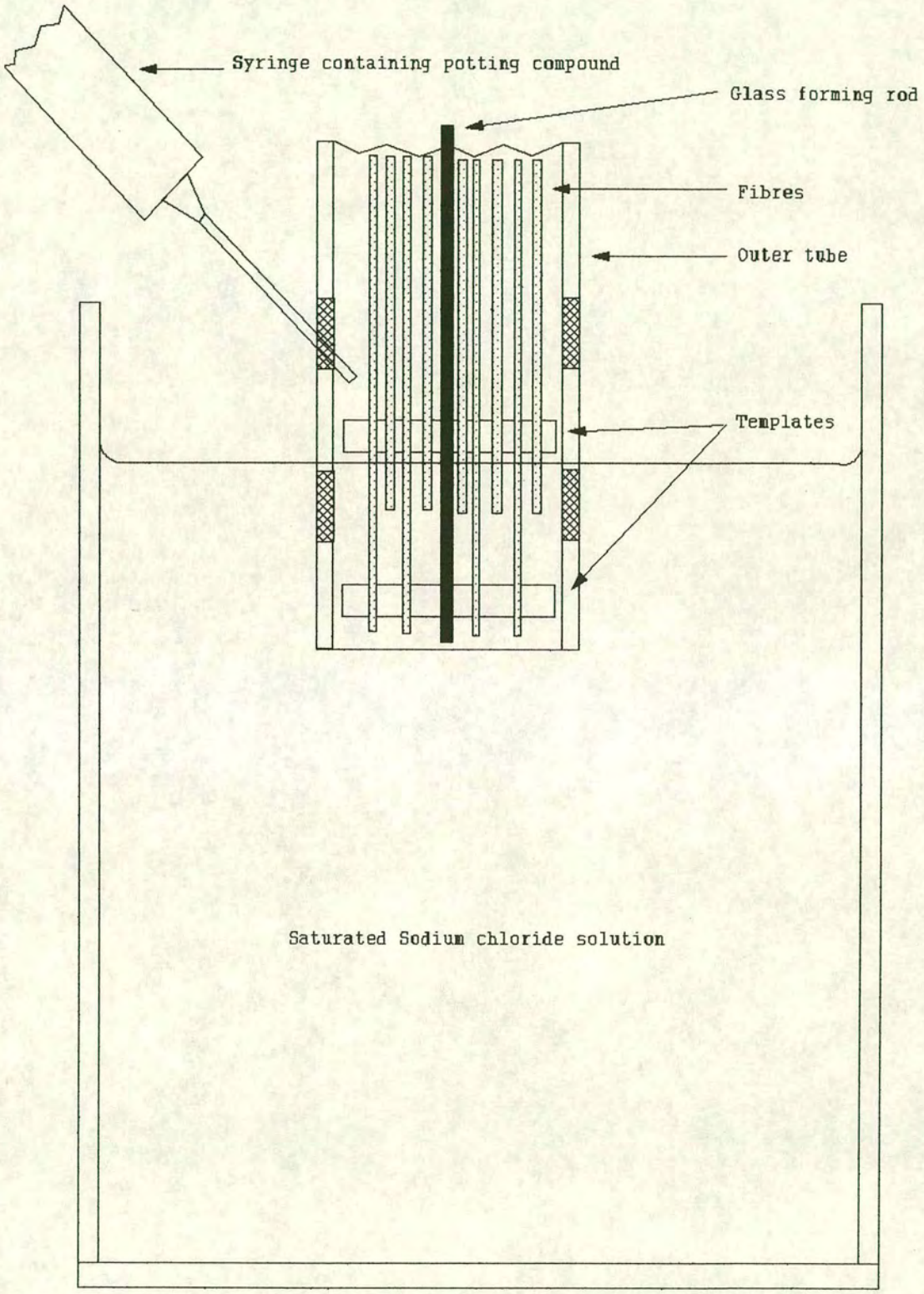

spectrophotometer was used to determine the maximum absorption peaks.

(8) A range of solutions of known absorption at the test wavelength were prepared and known volumes of each solution dried in an oven to determine dry weights. A standard graph of absorption versus dry weight was plotted for future reference.

Procion dyes are reactive chemicals which are known to be skin irritants and cause respiratory allergies. In accordance with the safety notice supplied with the Procion Red P-4BN care was taken to limit skin contact (by wearing a Laboratory coat and gloves) and inhalation (by wearing a mask while the dyes were in a powdered form).

6.3.4 Circuit design for bioreactor operation

There were basically two types of circuit design used throughout this study. The first, and earliest, of the circuits used one medium vessel for the supply of medium to the reactor. The 'spent' medium, having been passed through the cellular growth space, was then recirculated directly into the medium supply vessel for re-use (Figure 6.6). The second circuit design did not incorporate a recirculation loop for the re-use of 'spent' media, with the medium being transferred to the waste bottle after a 'single pass' through the growth space (Figure 6.7).

The demerits and failings of each circuit design will be discussed in the results section.

6.4 On-line monitoring equipment

This section outlines the monitoring equipment used for assessing the behaviour of the bioreactor. The equipment was selected, and where appropriate interfaced with a computer, by Dr. J. Burns as part of his PhD. thesis (Burns,1991). Developments to

Figure 6.6:- Bioreactor circuit for recirculation.

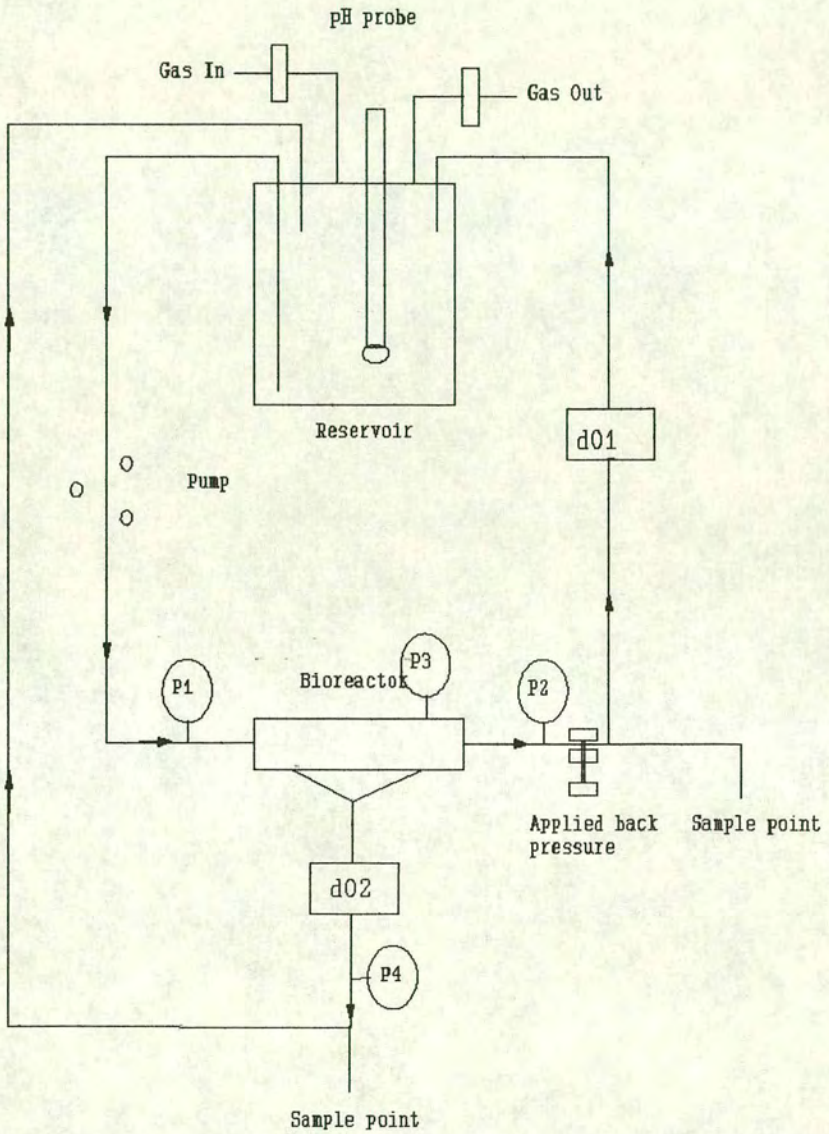

dO1 and dO2 = Oxygen electrodes

P1,P2,P3,P4 = Pressure transducers

Figure 6.7:- Circuit for 'single pass' of medium.

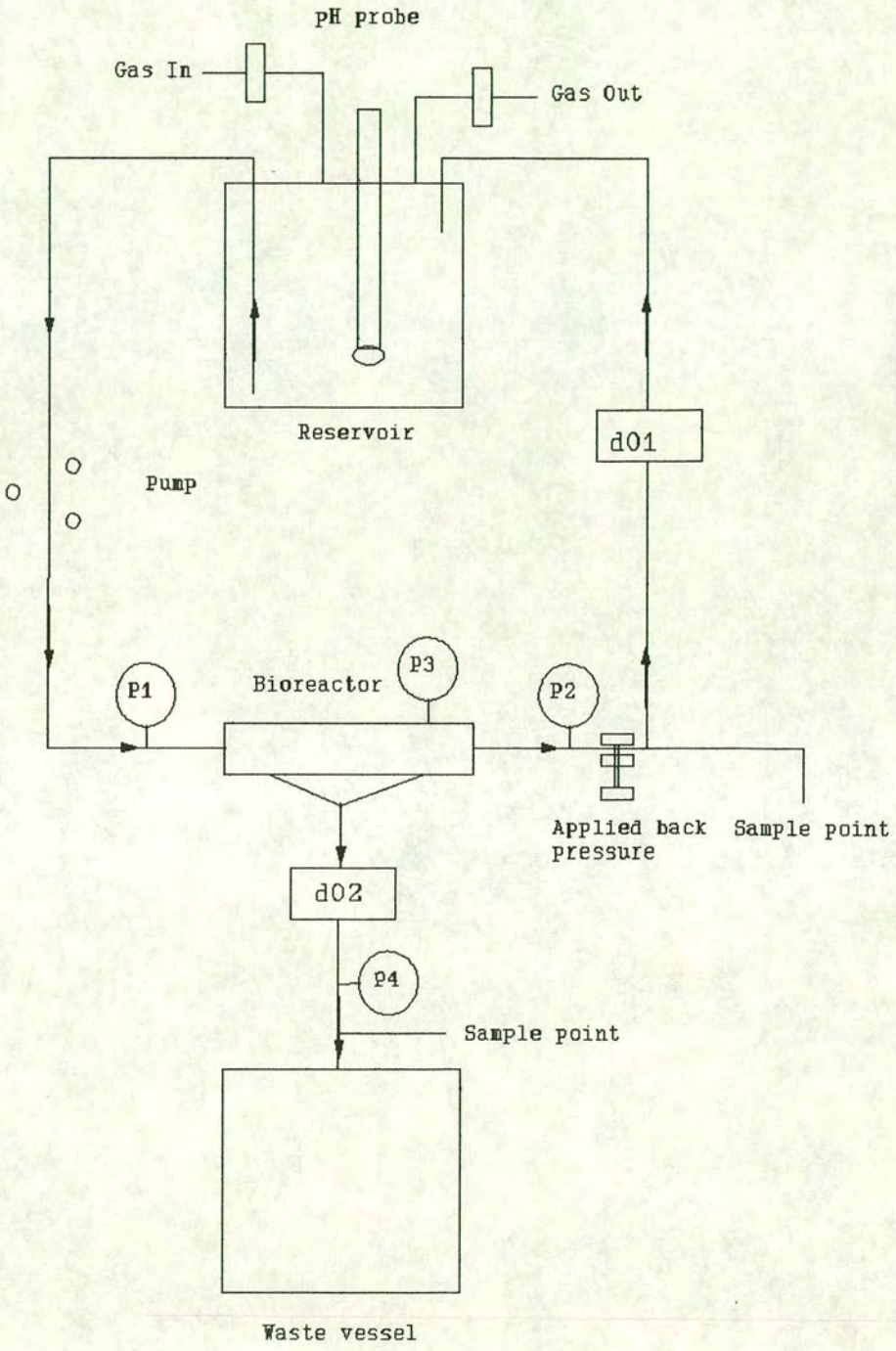

dO1 and dO2 = Oxygen electrodes

P1,P2,P3,P4 = Pressure transducers

the transducer and thermistor housings and the sample ports were carried out as part of this study (Chapter 7)

6.4.1 Computer

The computer used for the on-line monitoring of the bioreactor was an IBM PS/2-30 PC, with a 80286 processor and a 20 MByte hard disc. The computer was fitted with a National Instruments AT-MIO-16 interface card which could input and output both analogue and digital signals, for the control and interfacing of equipment.

The National Instruments card was accessed by using the National Instruments Labwindows Software package, as described by Burns (1991).

6.4.2 Pressure transducers

The pressure transducers used during this work were supplied by Sensortechnics (Cat. No. PS15GA). The transducers chosen operated between 0-15 pounds per square inch (psi) and they could be autoclaved. The values could be converted to Pascal (Pa) by multiplying the psi value by 6894.8 (1 psi = 6894.8 Pa, Perry 1985). The redesign of the pressure transducer housings, constructed from 316 stainless steel, was investigated in this study (Chapter 7).

The pressure transducer produced a signal which was linearly responsive to pressure. On calibration, using a Druck calibration meter, the exact relationship between pressure and the response signal could be ascertained for each transducer by Equation 6.5:-

$$Pressure\ (p.s.i.g) = b^{*}signal + a \qquad (6.5)$$

Variables a and b could be found by plotting the signal response versus pressure. Variable a was the value at which the line of best fit cut the Y-axis and variable b was the gradient of the line. Unfortunately, these values were found to alter between experiments due to the wear on the transducers associated with autoclaving. These problems will be discussed in Chapter 7.

Using this relationship, the signals were converted to pressure readings by the monitoring software for presentation and storage.

6.4.3 pH probe

The probes used were pH Fermprobe combination electrodes (Cat. No. F-610-B130-H, Broadley James). These electrodes were easily maintained, incorporating a pressure compensating device to enable the autoclaving of the probe containing the electrolyte solutions as part of the feed vessel.

The pH probes were used in conjunction with a standard pH meter. The probes were situated in the stirred supply vessel and calibration was carried out by using a sample line to take snatch samples. The pH of the snatch sample was measured by using a secondary, temperature compensated, pH meter. This pH value was then used as the calibration point for the pH probe used in the bioreactor circuit.

The pH of the in situ probe was regularly checked, using the snatch sample technique, to enable one point calibrations when necessary.

6.4.4 Oxygen probes

Polarographic oxygen electrodes were supplied by Uniprobe (Cat. No. ES-19-220-C04). The probes used a 600-750 mv polarising voltage to enable the following redox reactions to occur at the silver anode and platinum cathode:-

Cathode reaction $O_2 + 2H_2O + 4e$ ------> $4OH^-$

Anode reaction $4Ag^+ + 4Cl^-$ ------> $4AgCl + 4e$

The current produced during this reaction is directly proportional to the amount of oxygen diffusing across the probes membrane, exhibiting a similar relationship to the pressure transducers. The current is then amplified and the amplified current used to determine the percentage saturation of oxygen in the solution via the monitoring program.

The probes were primarily calibrated outwith the test apparatus using a 6% (w/v) sodium sulphite solution and fully aerated water to determine the 0% aeration and 100% aeration points. The probes were calibrated as part of the bioreactor circuit by passing fully aerated medium through the probe housing.

In theory, the oxygen uptake rate of the cells could be calculated by determining the difference between the upstream oxygen reading and the downstream oxygen reading over a defined time period. This utilisation is flow dependant as shown by Equation 6.6:-

$$Oxygen\ uptake\ rate = Flow\ x\ (Oxygen_{upstream} - Oxygen_{downstream}) \quad (6.6)$$

The problems encountered in using the polarographic oxygen probes and the calculations of the oxygen uptake rate will be described in the Results section.

6.4.5 Temperature probes

Temperature in the bioreactor circuit was monitored using NTC thermistors which were supplied by RS Electronics. Using a linear relationship between the response current and temperature, the monitoring program could relate the relative temperatures in the circuit. These thermistors were housed in specially designed thermowells described in Chapter 7 (Section 7.2).

6.4.6 Incubator

In order to maintain a constant temperature for cell culture in the bioreactor and ancillary equipment an incubator was constructed. The incubator consisted of a modified printer hood which was heated internally by two 150 watt light bulbs. The temperature of the equipment was maintained at 37°C by using a proportional, integral and derivative (PID) temperature controller (Eurotherm) and a thermocouple placed in contact with the medium in the bioreactor circuit.

6.4.7 Data logging

The sensor signals measured and converted by the computer were stored on floppy disc for analysis at a future date. Analysis of the data was carried out by programs written in Turbo C (Borland International). The programs averaged the data over a 1 h period and stored the data as a file for direct transfer into other analysis and graphics packages.

6.4.8 Gear pump

The pump used in this study was supplied by Flowgen, the UK agent for Verder pumps. This pump was a variable flow gear pump (model no. 2030) used in conjunction with a V 096.07 pump head.

The pump could be controlled by the computer interface to maintain a constant, controlled pressure in the test circuit. The pump could also be made to respond to sudden pressure changes in the circuit by using a proportional and integral control algorithm incorporated in the monitoring program. The pressure readings from one of the in-line pressure transducers was used to supply data to the control algorithm, which then altered the output signal to the pump, maintaining a preset control pressure. The stainless steel pump head was detachable allowing it to be autoclaved as part of the completed circuit.

Chapter 7

Bioreactor design and construction

7.0 Introduction

This chapter outlines the design concept behind the Edinburgh Dual Hollow Fibre bioreactor, summarising the problems encountered in its construction and operation and their subsequent resolution via the modification of the apparatus. The results in this section will be presented as a composite of the overall findings of this work and will be divided into the following three sections:-

(1) The design concept behind the Edinburgh dual hollow fibre bioreactor.

(2) Design of the associated bioreactor circuit.

(3) The design and modification of associated instrument and sample ports.

(4) Improvements in the design and construction of the main bioreactor module.

This chapter will only discuss the modifications made by the author to the design of the bioreactor module described in Chapter 6, based on the initial bioreactor design reported by Burns (1991). The bioreactor presented in the previous chapter was the first to be tested with mammalian cells, with the author being partly involved with its initial construction and responsible for its subsequent priming with cells and operation.

7.1 The Edinburgh Dual Hollow Fibre Bioreactor:- Concept of design.

The Edinburgh dual hollow fibre bioreactor was designed to operate with a radial flow of nutrients through the cell mass between two sets of closely spaced fibres. Figure 7.1 shows a simple schematic of the desired pressure mediated flow pattern within the bioreactor, where the full length of the supply fibres are maintained at a higher pressure (P1,P2) than the cellular growth space (P3), which is, in turn, held at a higher pressure than the sink fibres (P4). The cells are retained within the growth space, between the supply and sink fibres, with a continuous, perfused supply of

Figure 7.1:- Conceptualised operation of bioreactor.

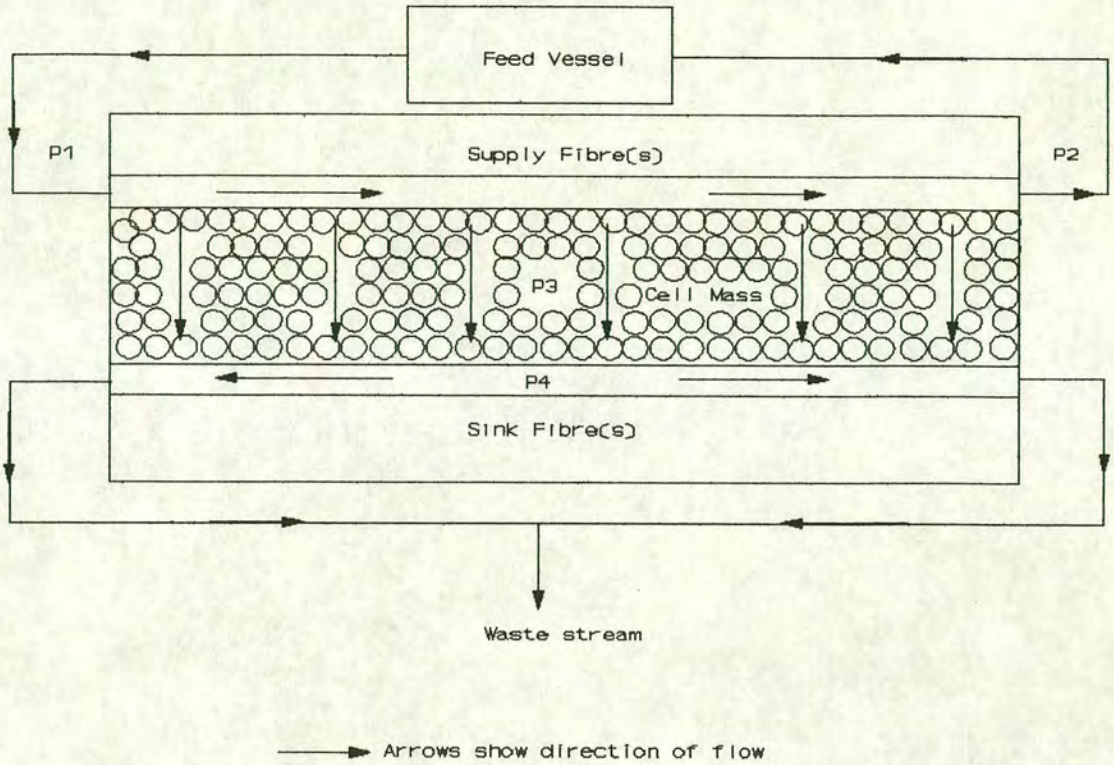

medium removing waste metabolites and product (i.e. monoclonal antibody) from the growth space via the sink fibres.

By switching the predominant flow path within the cell mass from the full length of the bioreactor (axial), to a shorter distance between the two sets of fibres (radial), the problems associated with axial nutrient gradients and the maldistribution of cells within the cellular growth space could be solved (Figure 7.2). In order to achieve radial flow within the bioreactor, it was necessary to operate the supply fibres at a higher pressure than the growth space, which in turn was at a higher pressure than the sink fibres.

The design developed at Edinburgh, being a prototype, was intended to have a degree of flexibility so that modifications could be easily made. With this in mind, the materials (primarily polycarbonate) and individual components used (templates, bioreactor tubes) were recyclable.

Figure 7.2 :- Comparison of axial and radial flows

(A) Flow Profile in a Cartridge Reactor.

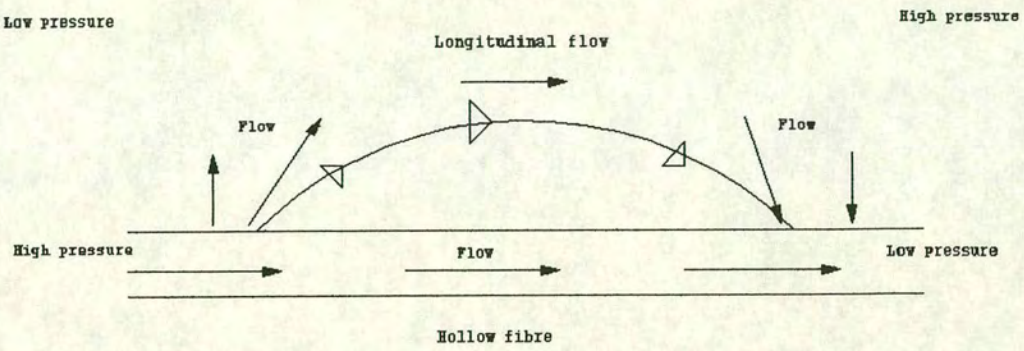

The flow of medium is from the high pressure zone to the low pressure zone.

(B) Flow Profile in a Dual Hollow Fibre Bioreactor.

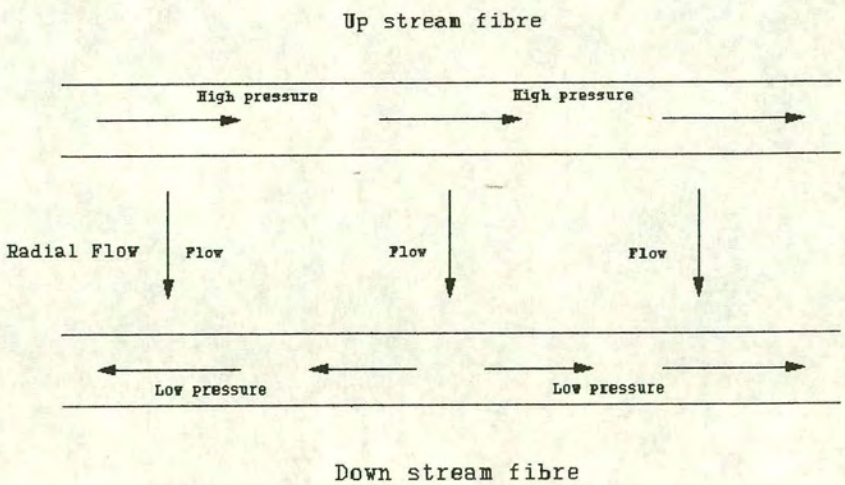

7.2 Circuit design considerations

The apparatus used in these experiments is described in Chapter 6 (Sections 6.3 to 6.4), along with the basic circuit designs used during this work. The basic requirements for each component of the circuit included the following:-

(1) Maintenance of a sterile, closed environment in which the cells could be nurtured, with the apparatus operated in a clean room.
(2) Ease of construction, allowing versatility and the sterile replacement of non-functioning equipment.
(3) Suitable access ports for sampling, inoculation, medium priming and gas recirculation to maintain the sterility of the system during its operation.
(4) An environment in which a constant culture temperature could be maintained.

These points will be discussed in the following sections.

7.2.1 Circuit sterility and construction

Modular design

Given the quantity of monitoring equipment and the size of the respective components involved, a modular system was selected. This system involved the use of Swageloks, constructed from 316 stainless steel, to separate each module of the circuit. For example the apparatus presented in Photograph 1 (Figure 7.3) was split into the following sections:-

A Feed vessel with attached pH and oxygen probes, with the associated medium reservoir.
B Bioreactor with temperature probes and attached pressure transducers.
C The downstream section of the bioreactor, complete with waste medium bottle, downstream sampling device and oxygen probe.

Photograph 1:- Apparatus used in bioreactor culture experiments, showing the feed vessel (left hand side), the bioreactor with stainless steel end caps (right hand side) mounted at a 30° angle with pressure transducers mounted above and below the bioreactor unit.

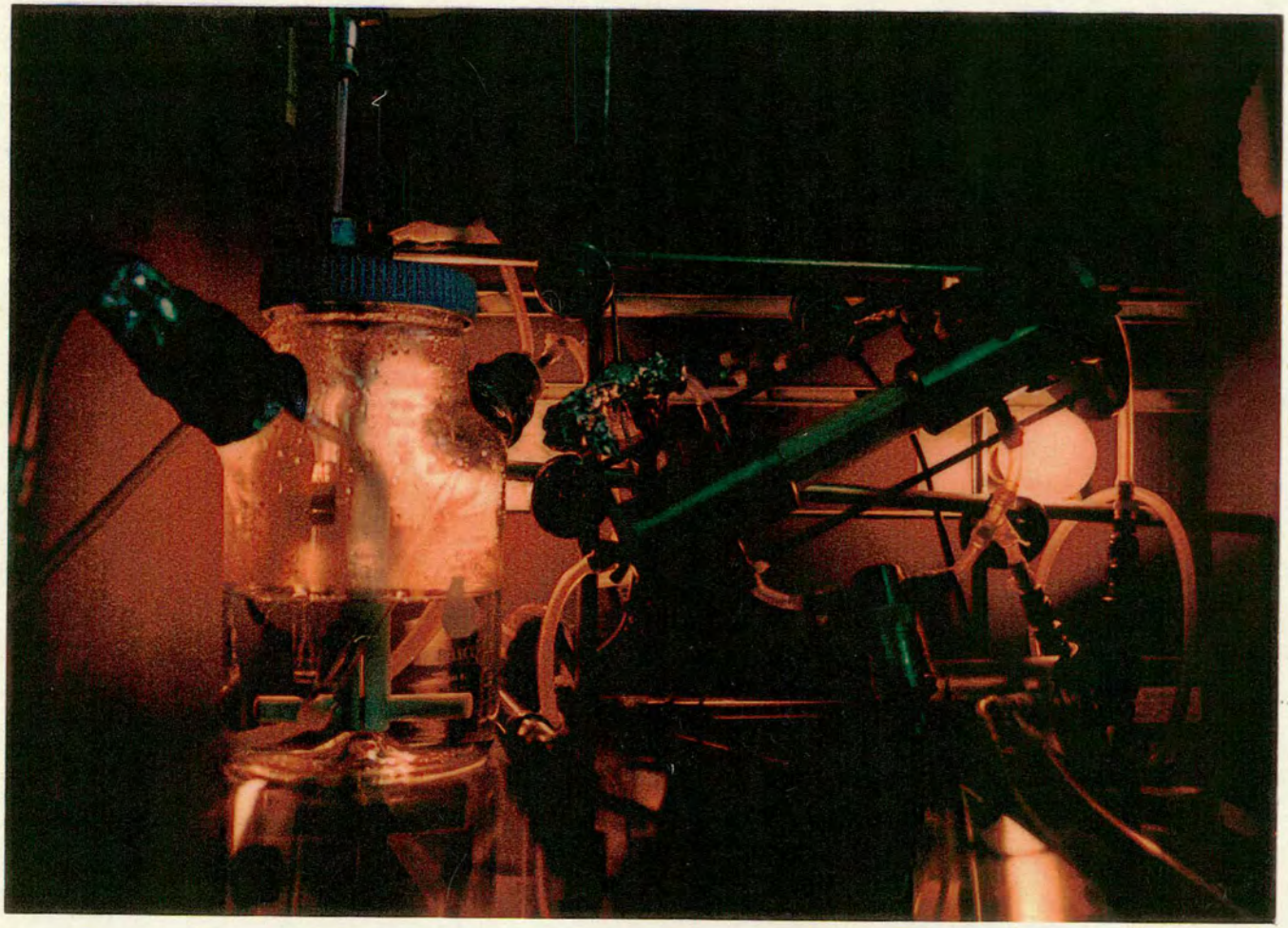

Figure 7.3:- Modular bioreactor circuit

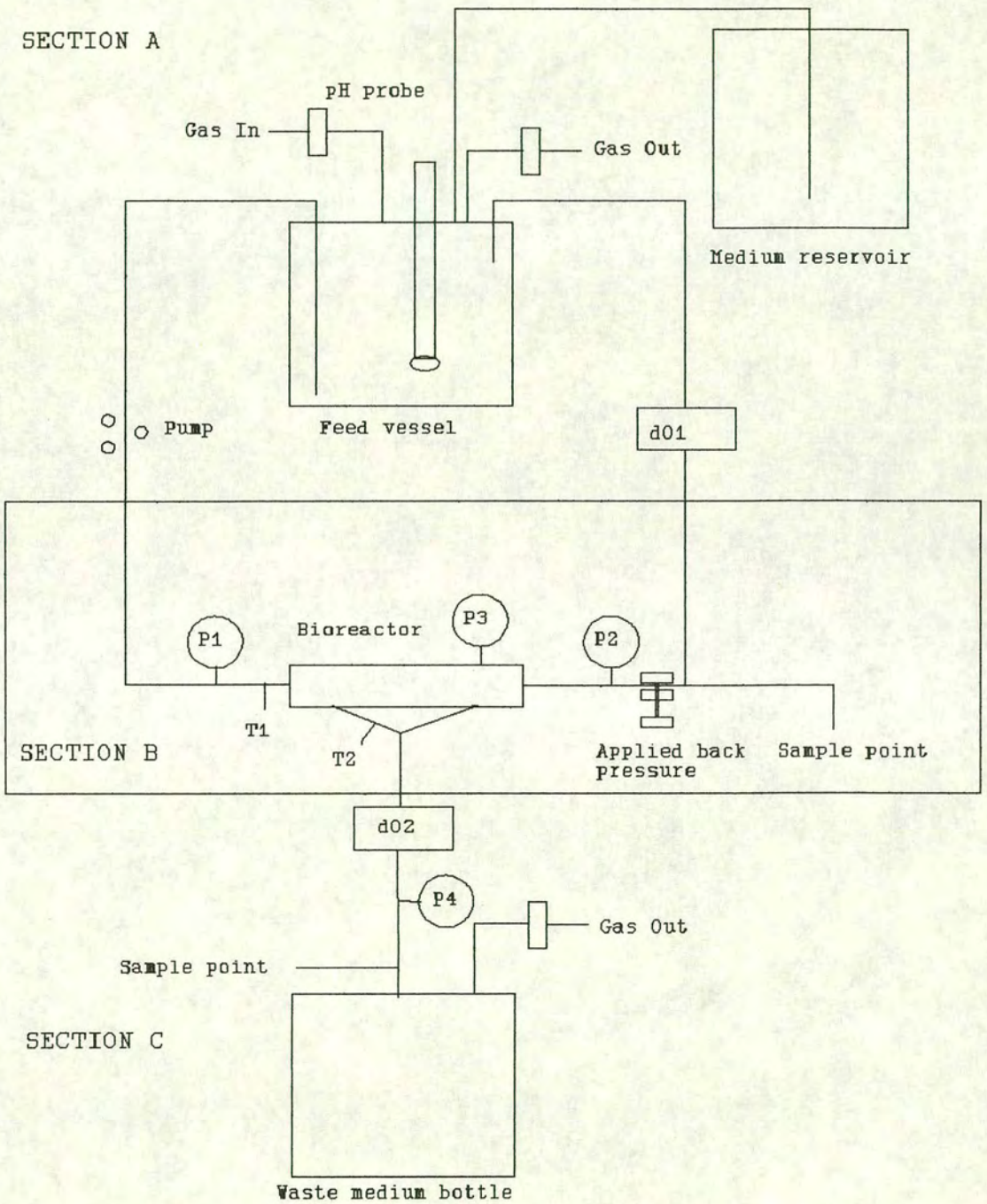

d01 and d02 = Oxygen electrodes
P1,P2,P3,P4 = Pressure transducers
T1,T2 = Temperature probes

The apparatus would be autoclaved in these sections, with the male/female swagelok connectors and other sensitive areas wrapped in aluminium foil. Each section included at least one vent, usually through air filters or open, aluminium foil covered sample ports, allowing for the exchange of gases during the sterilisation process. The apparatus would then be allowed to cool and reassembled in the laminar air flow hood before being transferred to the incubator.

The modular design allowed the replacement of any sections which failed during autoclaving. This usually entailed the reconstruction and resterilisation of sections in which tubes had become disconnected compromising the sterility of the system.

7.2.2 Steam sterilisation

The use of steam sterilisation was preferred over chemical methods for the following reasons. Chemical methods require rigorous cleaning for the removal of potentially toxic species from the circuit, leading to further design requirements and increasing the possibility of contamination. As discussed in Chapter 5, the chemical treatment of the membranes may alter their physical or surface properties, altering the filtration characteristics of the system.

The apparatus was usually autoclaved for 20 minutes at 121°C at a pressure of 20 psig. Due to the age of the autoclave used (J.S.Thackery and Sons, commissioned 1974), this sterilisation cycle took about 3 hours, with the temperature remaining greater than 100°C for approximately 2 hours. This was believed to be more than adequate for the penetration of both heat and steam throughout the bioreactor circuit. This conclusion was supported by operating the apparatus with RPMI 1640 for a minimum of three days prior to inoculation and sterility testing the medium using the method described in Section 6.1.7.

While the duration of this cycle proved suitable for sterilisation of the equipment, several problems were encountered. These were mainly attributable to the effects of the temperature/steam environment causing deterioration of the equipment and

construction materials. These features will be discussed in Section 7.3.

Another practical problem was the repeated breakdown of the autoclave. This was wholly due to its age, with approximately six to eight months of down time occurring in the 3 year period. During this period work either concentrated on cell culture experiments or alternative arrangements were made to use autoclaves in other buildings.

7.2.3 Access, exit and sample ports

These ports could be separated into three different areas: those required for nutrient and gas supply, those involved with the addition and removal of medium samples and cells from the bioreactor circuit and those involved in the direct measurement of pH, temperature, dissolved oxygen and pressure.

Nutrient supply

Nutrient supply concerns the provision of bulk quantities of medium to the bioreactor circuit. Medium was supplied to the system through the connection of 2 litre bottles containing fresh medium via a length of tubing to the feed tank of the system. The connecting tubing, used between the feed vessel and the medium reservoir, was long enough to enable the replacement of empty bottles within the laminar air flow hood, maintaining the sterility of the system. The laminar air flow hood was serviced regularly, with settle plates used at regular intervals to check for air borne contaminants (Section 6.1.7).

Medium was transferred between the feed vessel and medium reservoir using a peristaltic pump. The cap of the medium reservoir bottle was replaced by a silicone rubber bung containing two stainless steel tubes. The first tube extended the full depth of the bottle and was used for removal of the medium. The second tube cleared the bung by about 2 cm either side. This tube was used for a filter (0.2 μm pore size, MILLIPORE), enabling sterile air to displace the medium removed from the bottle

during transfer.

Removal of medium from the circuit could take place by several different routes. The first involved a reversal of the process described in the previous paragraphs. As both the medium reservoir and the feed vessel were vented through air filters, medium could be removed by pumping medium from the feed vessel to the medium reservoir.

The second method involved the use of one of the in-line sampling ports, dispensing medium to a waste bottle. In this instance, a presterilised extension tube had to be connected to the sample port. This was usually carried out *in situ*, that is while the equipment was outside of the laminar air flow hood. This method compromised the sterility of the system and it was only used as a final resort for draining the circuit.

Gas supply

Compressed air and carbon dioxide were supplied to the feed vessel after being passed through a series of two 0.2 μm air filters. The relative supply rates were adjusted using rotameters to give a 20:1 air:carbon dioxide mixture. The mixture of gases was important as the medium used a bicarbonate buffering system.

Initially, the removal of gas from the system was through a 0.2 μm venting filter at the top of the feed vessel. This proved to be inadequate for the following reason. The humidity of the exit gas stream differed from that of the supply stream due to evaporation within the feed vessel. It was found that liquid condensed on the surface of the exit filter, causing a decrease in the flux across its membrane, which led to two associated problems. As the exit filter 'fouled' it created an increased back pressure within the system, increasing pressure throughout the system and causing the gas to exploit any weak seals. A secondary problem related to the pressure increase involves the carbon dioxide/air mixture. While the system was at equilibrium with the filters operating at 100% efficiency, the buffer in the medium maintained a constant pH as carbon dioxide and air transferred into the medium. As the exit filter 'fouled' with condensate, the gas pressure increased causing the solubility of the component gases to increase disproportionately. As carbon dioxide is about twenty times more soluble

than air, the amount dissolved in the medium would increase more rapidly than the air under pressure, leading to an alteration in the dissolved gas composition of the medium and decreasing the pH of the buffer solution.

This problem was initially solved by periodically reversing the gas flow, i.e. by changing the gas supply tube from the input filter to the exit filter. This back flushed the system and dried the filter. However, this solution was inefficient and required constant monitoring to ensure a constant pressure within the feed vessel.

A better solution involved the use of an aspirator bottle to remove liquid from the gas stream before it reached the exit filter. The glass aspirator bottle provided a larger surface area on which the liquid could condense, thus decreasing the fouling effect upon the vent filter. This proved to be the most successful technique, with no significant fouling of the exit filter observed in later experiments.

Sample ports

A number of different sampling techniques were tried (Figure 7.4) for the three principal sites of interest, i.e. in the supply circuit, in the cellular growth space and in the sink circuit. At all of the ports, except the sink port, the medium was held at a positive pressure, minimising the risk of contamination entering the main circuit. The primary requirement of the sample port was that it minimised the risk of contamination to the main circuit. This requirement can be further divided into three components, that of time to take the sample, minimal hold up volume in any sample line and maintenance of the sterility of the port between samples.

The first design was constructed from a small, autoclavable glass bottle with a volume of 10 ml, which used the positive pressure within the bioreactor circuit to provide the sample. The principle of operation was that one bottle could be autoclaved in place with the rest of the circuit and used for the first sample. This bottle would then be replaced aseptically with a presterilised bottle of the same size. This technique, while protecting the port between samples, proved awkward in its operation, extending the risk of contamination. Another problem was that of not being able to flush the

Figure 7.4:- Sampling ports and protocols

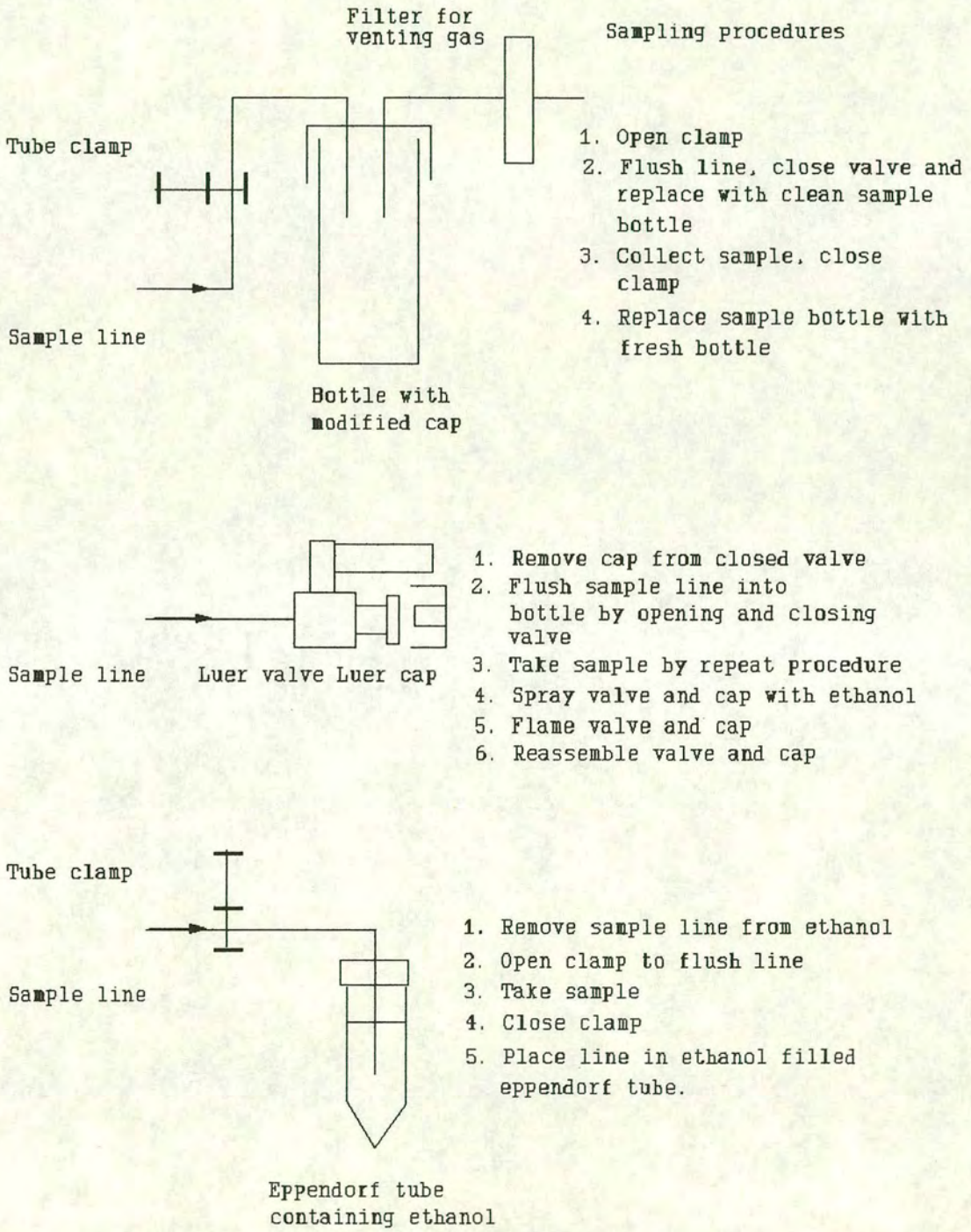

sample line before taking the sample. This led to the problem that any sample consisted of a mixture of the previous and the fresh sample, or alternatively an extended sample period involving the use of a wash bottle, for the removal of the hold-up volume, followed by the actual sample bottle.

The second design incorporated the use of stainless steel luer valves and stopcocks. These valves could be easily opened and closed for sample collection with the exposed opening closed off with the stopcock between samples. These were more easily operated than the above design, reducing the sampling period to a minimum, while allowing the removal of any residual sample from the port. They were also amenable to ethanol treatment and flaming with a bunsen burner. This port design was especially useful for the cellular growth space of the bioreactor, allowing rapid sampling as well as compatibility with different syringe sizes. Syringes were used for the inoculation of cells into the growth space and latterly for the addition of new born calf serum to the growth space. While these ports were suitable for the sampling of the cellular growth space, the frequency of samples taken from these ports was restricted, reducing the risks of contamination.

The final design was the simplest, consisting of a small internal diameter tube, a hose clip and an ethanol (70%) filled sample vial (Eppendorf). The hose clip was used to control the flow from the port, with the small internal diameter of the tube limiting the hold up volume of the sample. The small vial was used to immerse the end of the tube in ethanol between samples, reducing the risk of contamination significantly. The flexibility of the sample tube and vial allowed the tube to be completely closed after sampling.

Of all the described methods, the latter proved to be the most suitable for frequently sampled ports, for example the supply and sink circuits, with the luer valves being used for the less frequently accessed cellular growth space.

7.3 Equipment ports

A range of electrical probes were used for the continuous monitoring of temperature, pH, dissolved oxygen and the pressure of the medium within the system. A description of these probes can be found in Section 6.4.

pH probes

The pH probe was autoclaved, in situ, in the medium supply vessel using a standard 'O' ring seal and a retaining bolt.

Thermistors

The temperature probes were non-autoclavable, requiring the development of an indirect sample port, that is one which could measure the temperature of the medium without compromising the sterility of the system. These ports were constructed from a sealed metal tube incorporated in a plastic T piece forming a thermowell (Figure 7.5). The dimensions of the tube allowed the thermistor to be passed down the inside of the tube enabling the measurement of the temperature of the medium via the conduction of heat through the tube wall.

Oxygen electrodes

The oxygen electrodes were integrated into the circuits using polycarbonate sample ports designed by Dr J Burns as part of his work. These were autoclavable polycarbonate housings, machined to enable direct contact between the medium and the oxygen probe. It was found that the housings tended not to be a problem provided any entrapped air was removed from the system. The first set of probes tended to fail a short period after autoclaving, this was found to be a general manufacturing fault. Replacement of these probes with an updated model alleviated these problems.

Pressure transducers

The pressure transducers were integrated into the circuit using stainless steel housings. The performance of the transducers was found to deteriorate on repeated autoclaving, requiring the regular re-calibration of the transducers. A secondary problem involved

Figure 7.5:- Thermistor housing

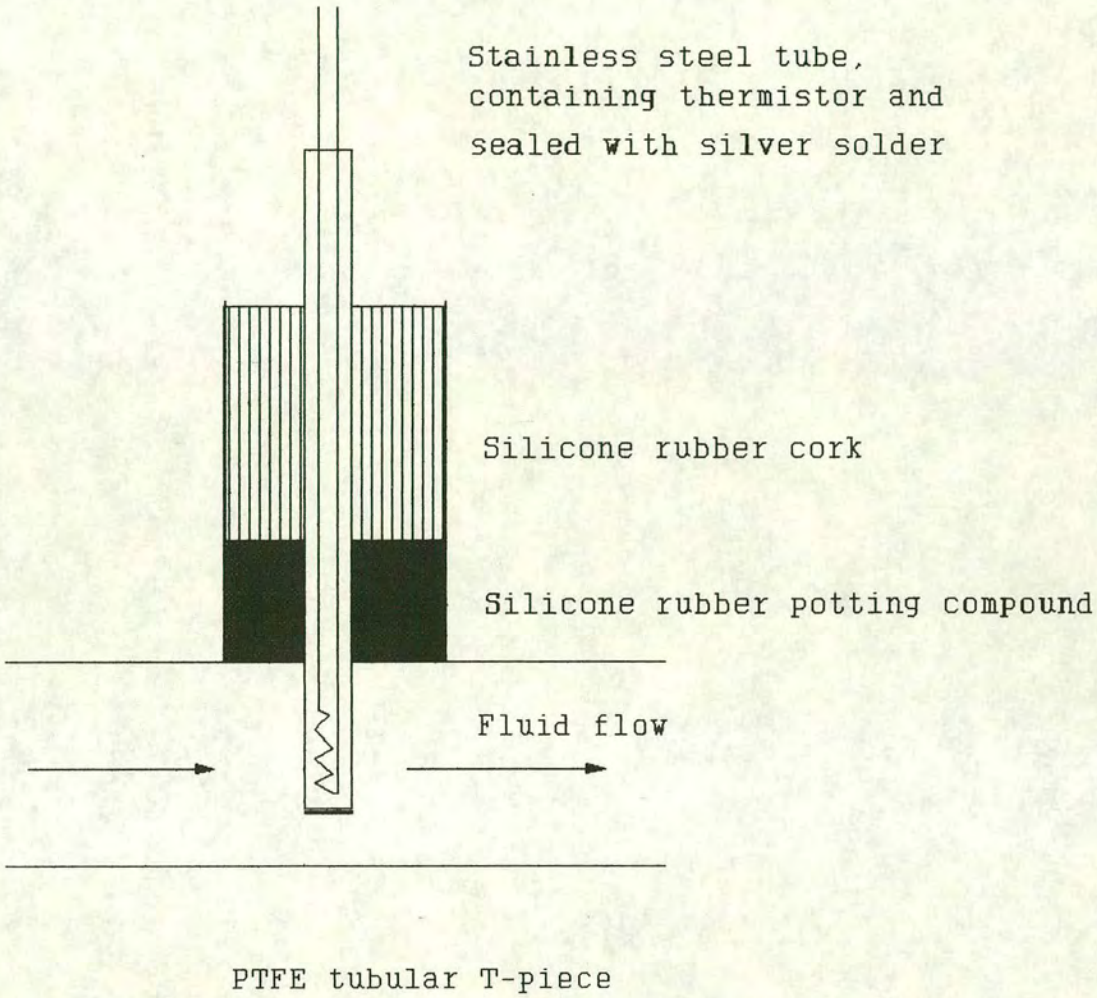

the materials used for the manufacture of the housing. The stainless steel used was not of a suitable grade for tissue culture, leading to the corrosion and pitting of the metal due to the highly ionic nature of the medium (Photograph 2). A form of corrosion was also observed which could, in extreme cases, lead to the partial or total blockage of the port by rust shed from the housing.

In order to minimise steam mediated damage to the original transducer housings (Figure 7.6), adaptations were made and the new design tested. This involved the use

Photograph 2:- Stainless steel pressure transducer housings, transducer housing A shows an unpitted upper surface while housing B has multiple pits as a result of corrosion.

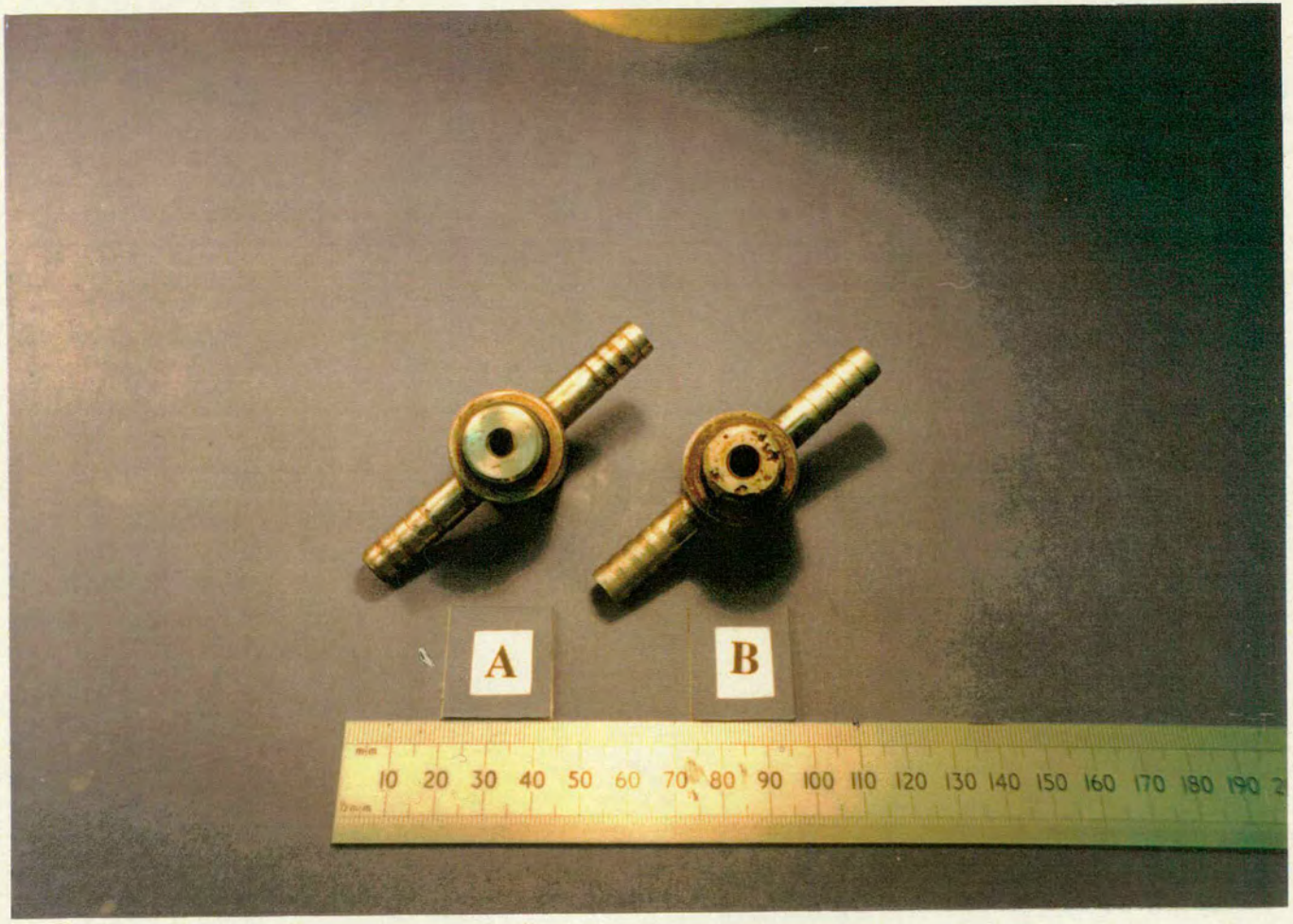

Figure 7.6:- Original design of pressure transducer housing

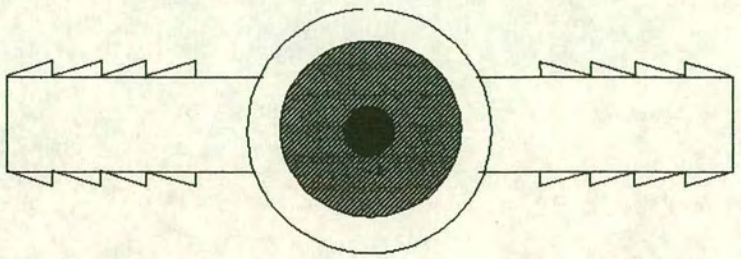

TOP VIEW

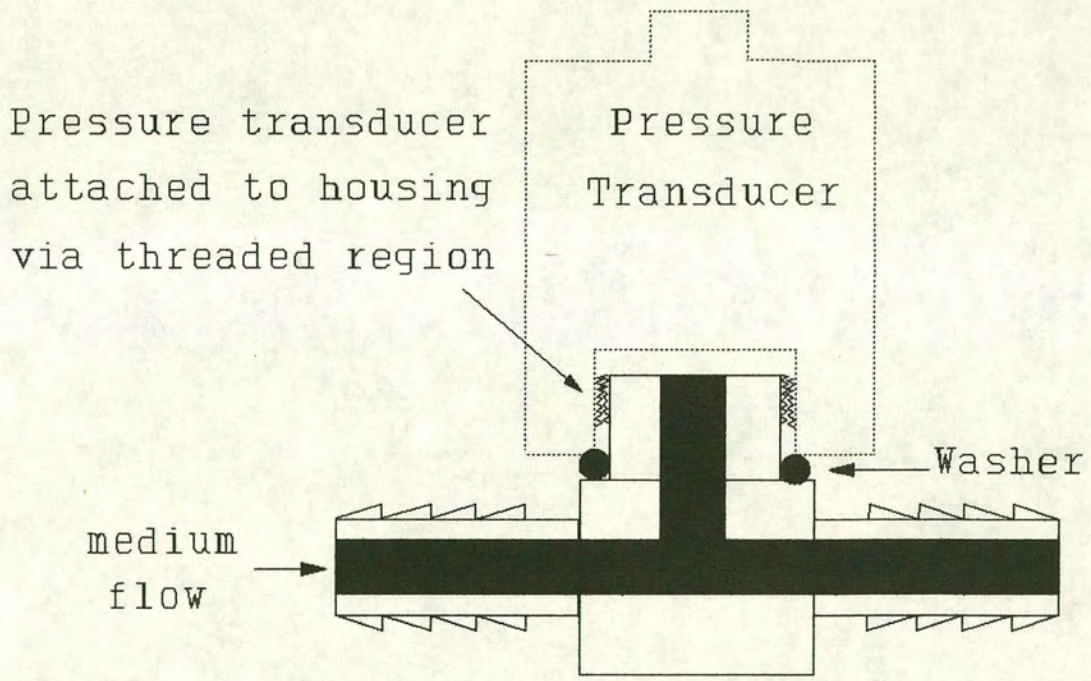

SECTIONAL SIDE VIEW

Figure 7.7:- Adaptation of pressure transducer housing

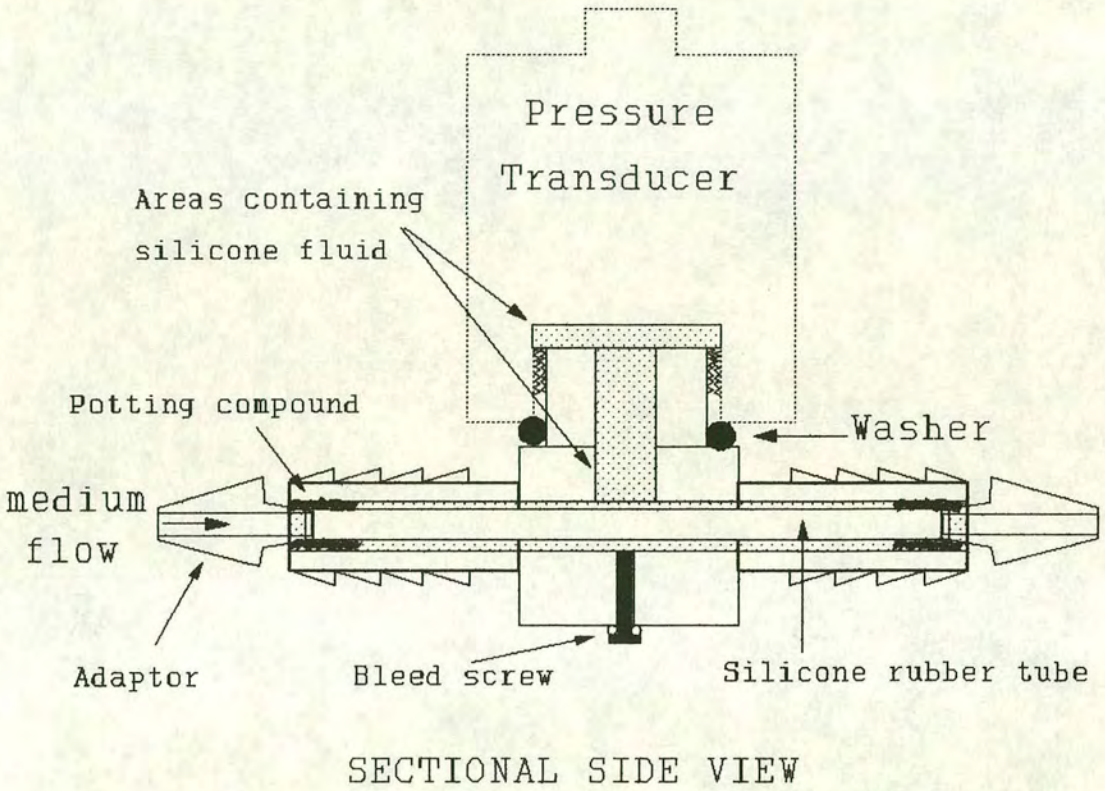

of an internal, thin walled rubber tube and silicone fluid between the transducer and the tube wall (Figure 7.7).

The housing was autoclaved, in situ, with the non-compressible silicone fluid and the transducer added after autoclaving. These transducers were calibrated in line using the apparatus outlined in Figure 7.8. Although these housings could be calibrated to give a direct assessment of pressure, the original design was not adaptable enough to cure the problem of the leakage of silicone fluid from the housing. The loss of silicone

Figure 7.8:- On-line calibration of pressure transducers.

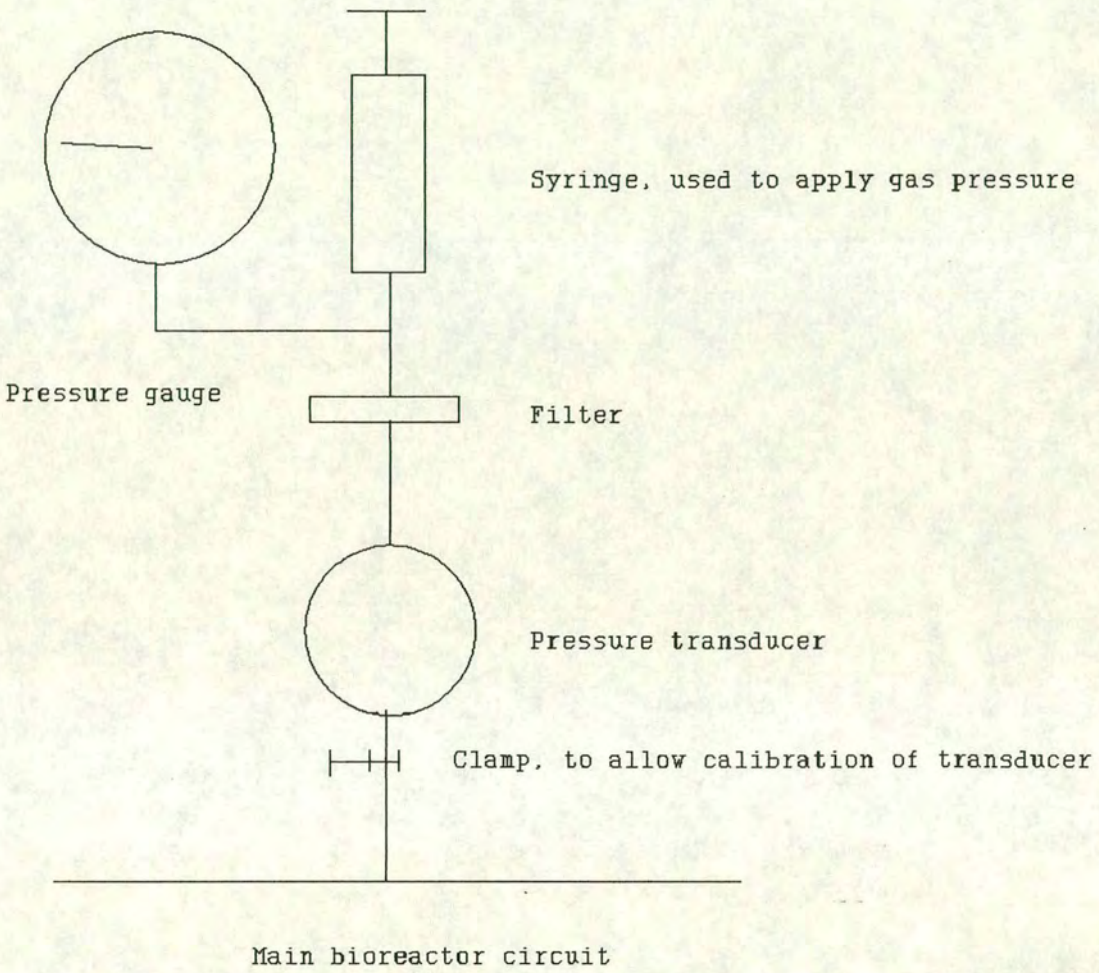

fluid from the housing led to a decline in the response obtained from the transducer at a given pressure. This decline in response altered the slope of the calibration graph, described in Section 6.4.2, which then required the constant re-evaluation of program parameters which could not be altered during the run. As a direct result these transducer housings could not be relied upon during experimental runs.

The deterioration and degradation of the transducer assembly was finally solved by coating the inside of the housing with a layer of silicone rubber, thus preventing

Figure 7.9:- Suggested redesign of pressure transducer housing

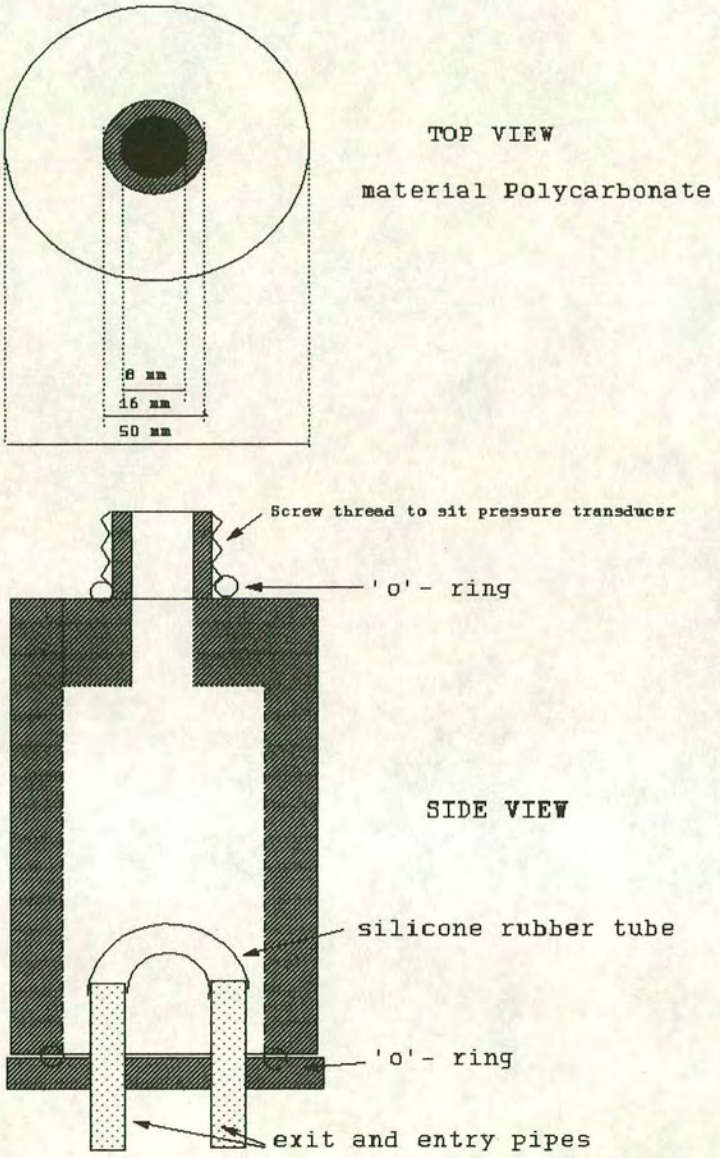

further interactions between the medium and the housing wall. The pressure transducers were sterilised by repeated partial immersion in boiling water. The boiling and reassembly of the transducer housings were carried out in the laminar air flow hood, with the *in situ* calibration of transducers carried out using the apparatus outlined in Figure 7.8. This regime was found to be suitable for sterilising the transducers, minimising the time at which the transducer remained at high temperature and pressure, which was believed to be the main factor involved their damage.

However, the risk of contamination to the circuit was increased.

Figure 7.9 outlines a suggested redesign of the pressure transducer housing, adapted from Figure 7.7, which would be expected to solve the previously described problems. The use of polycarbonate as the primary construction material allows the apparatus to be autoclaved as part of the bioreactor circuit, while its transparency ensures that any air present in the housing after the reattachment of the pressure transducer, is removed prior to calibration.

7.4 Bioreactor Design Considerations

Several construction and operational problems were noted in the initial design described in Section 6.3 (Photograph 3). The design also required further modifications for increasing the fibre packing within the cartridges. The principal areas in which this work progressed can be described as follows:-

(1) Access to and the integrity of the potting of the fibres within the reactor tube.
(2) Leakage from fibres outside the cellular growth space.
(3) Redesign of the templates for increased fibre packing.
(4) Design of a large scale bioreactor.

These points will be described in the following sections.

7.4.1 Fibre potting

The construction technique described in Chapter 6 relied upon the potting of fibres within the polycarbonate tube. Several different problems were associated with this technique.

The access to the inner two templates of the bioreactor was limited to the holes in the outer tube. This led to difficulties in ensuring the full dispersion of the potting

Photograph 3:- Old style bioreactor units, Units A and B are two examples of the 'Old Style' bioreactor and C (Inner, growth space seal) and D (outer seal) are the silicone rubber seals retreived from dismantled bioreactor units

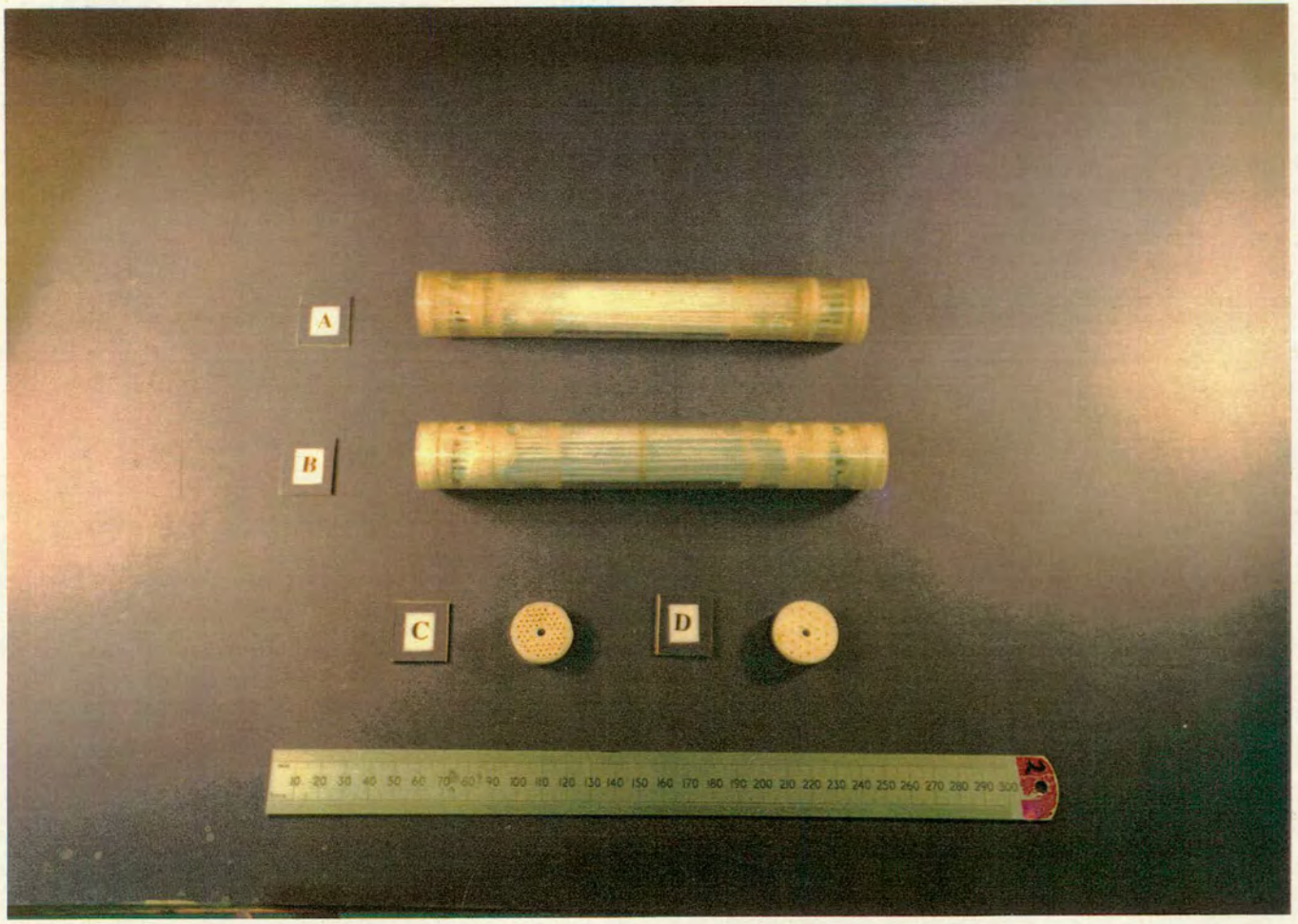

Figure 7.10:- **Leakage associated with potting regime**

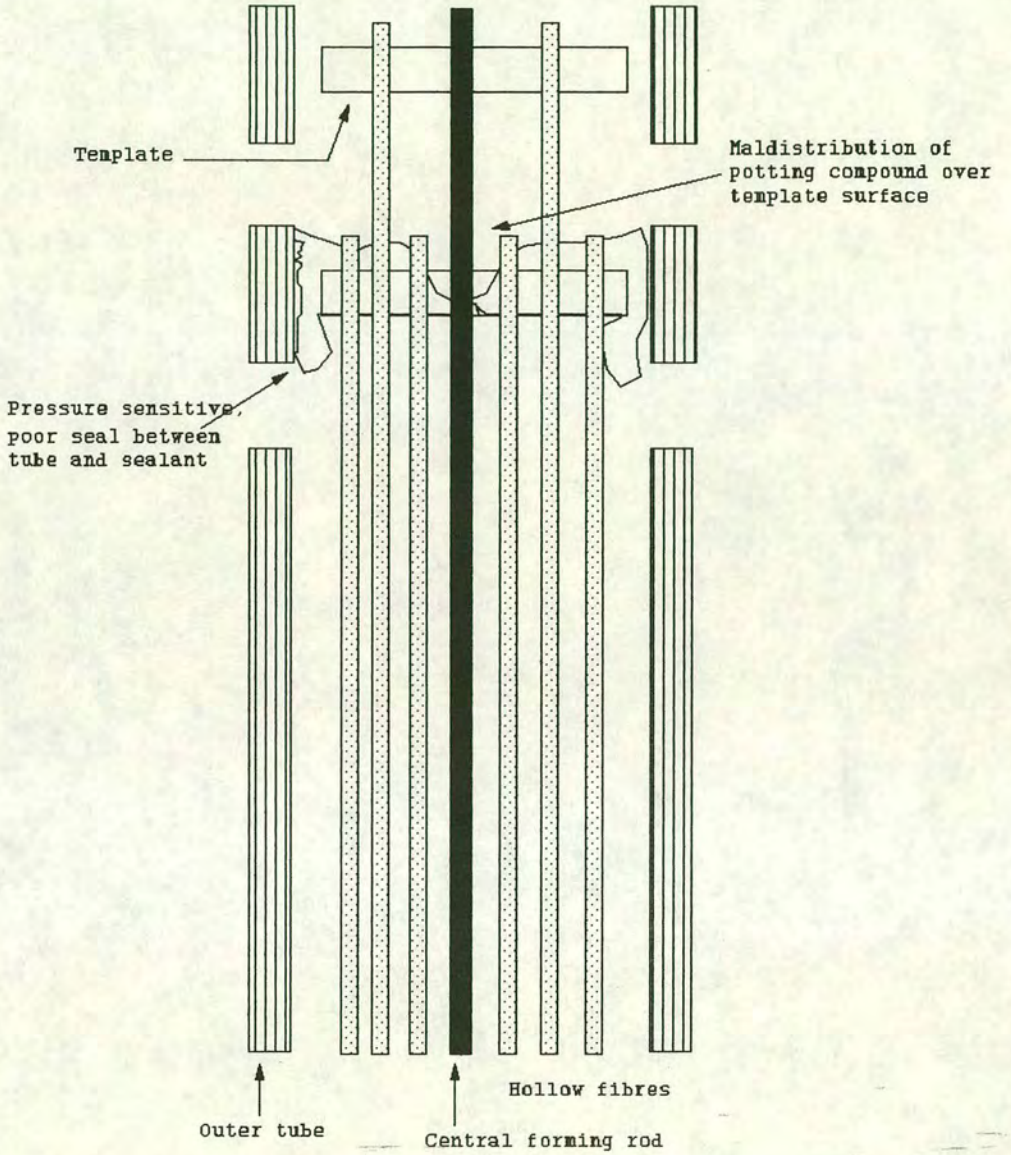

compound between the fibres, resulting in the possibility of leakage through poor seals (Figure 7.10). In several of these bioreactor units the inner silicone rubber seals were demonstrated to leak. A secondary problem associated with the potting was the lack of bonding between the polycarbonate tube and the potting compound. Under pressure these bonds failed, allowing the free passage of medium from the inlet and cellular growth space to the outlet of the bioreactor. This effectively led to the starvation or wash out of cells from the growth space.

Although an accurate method of determining the leakage of these seals was not

developed, the seepage of test fluid between the potting and the polycarbonate shell did allow a visual assessment to be made. By inspecting the cartridge after its operation, the formation of a fine liquid layer between the polycarbonate and potting compound gave the appearance of a silvery sheen when compared with a good seal.

These problems were solved by removing the potting process from the confines of the bioreactor tube. Instead of having flat templates for threading the fibres, the templates were redesigned to form 'buckets', Figure 7.11. These buckets would emulate the tube in restricting the flow of potting compound. The use of buckets enabled easier access to all of the fibres, ensuring a higher success rate in sealing around the tubes. The values of A and B (Figure 7.11) were later altered to 5 mm and 3 mm respectively, this alteration was made after fears about the physical strength of the template base were shown to be unfounded. The different components of the 'New Style' bioreactor are presented in Photograph 4.

This design also allowed a further improvement in the potting technique by removing the use of a saturated salt solution. The salt solution, being more dense than the potting compound, was used to restrict the flow of the fluid in a vertical plane. This lead to salt crystal formation at the air/liquid interface and the maldistribution of potting compound around the template. The potting compound generally took the path of least resistance, travelling between the template and tube wall rather than flowing between and sealing the fibres. The bucket template restricted the leakage of the potting compound to the template surface improving the efficiency of sealing. The use of buckets also enabled easier visual inspection of the seal.

The problem of leakage through the failure of the bonding between the polycarbonate tube and the potting compound was solved by using inset 'O' ring seals within the polycarbonate tube. Once all of the templates had been potted, the completed inner module could then be inserted into the outer tube, a schematic of which can be found in Figure 7.12. The 'O' rings provided compression seals around the polycarbonate bucket, reducing the risk of leaks. It was at this stage that the length of the growth space was increased to 15 cm, compared to the 13 cm used in previous experiments

Figure 7.11:- Bucket design for fibre templates

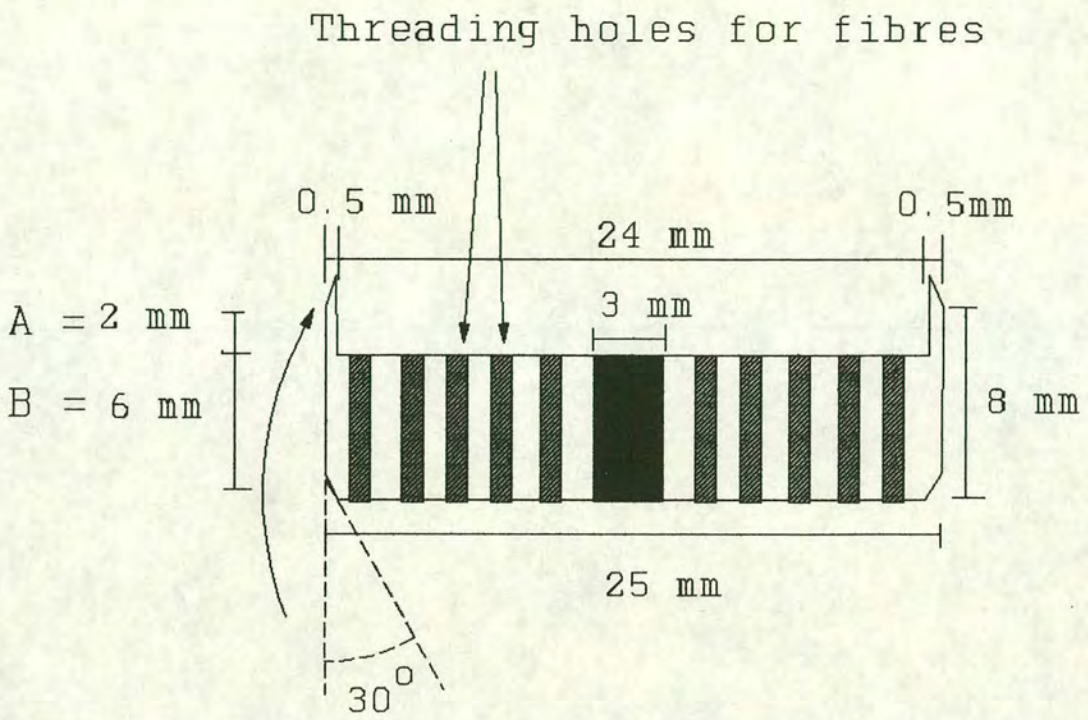

where the potting was carried out in the reactor tube. In view of the pressure required for inserting the fibre assembly into the outer tube, the central glass rod was replaced with 4 mm stainless steel rod (316 grade). The rod was cut into 3 sections, 2 with a length of 1.5 cm for the spacer in the end sections, and a central rod with a length of 15 cm. The three sections could be screwed together, trapping the template securely between the two rods.

Potting compound

The Dow Corning silicone rubber potting compound used in these experiments required the addition of a setting catalyst to the bulk silicone fluid. Several alternatives exist where the hardening procedure occurs via the evaporation of a solvent from the silicone fluid. One such system was selected that could withstand autoclaving (Silastic 734 R.T.V). Unfortunately, this potting expanded during steam sterilisation, leading to the stressing of the outer tube at its weakest point, the 'O' ring grooves. This led

Photograph 4:- Components of the 'New Style' bioreactor showing the polycarbonate end caps (A), the outer body of the bioreactor (B), the sectional stainless steel centre rod (C) with examples of two bucket templates (normal packing density on the right hand side, high packing density (Section 7.3.3) on the left hand side) and a potted fibre unit ready for insertion into the outer body (D).

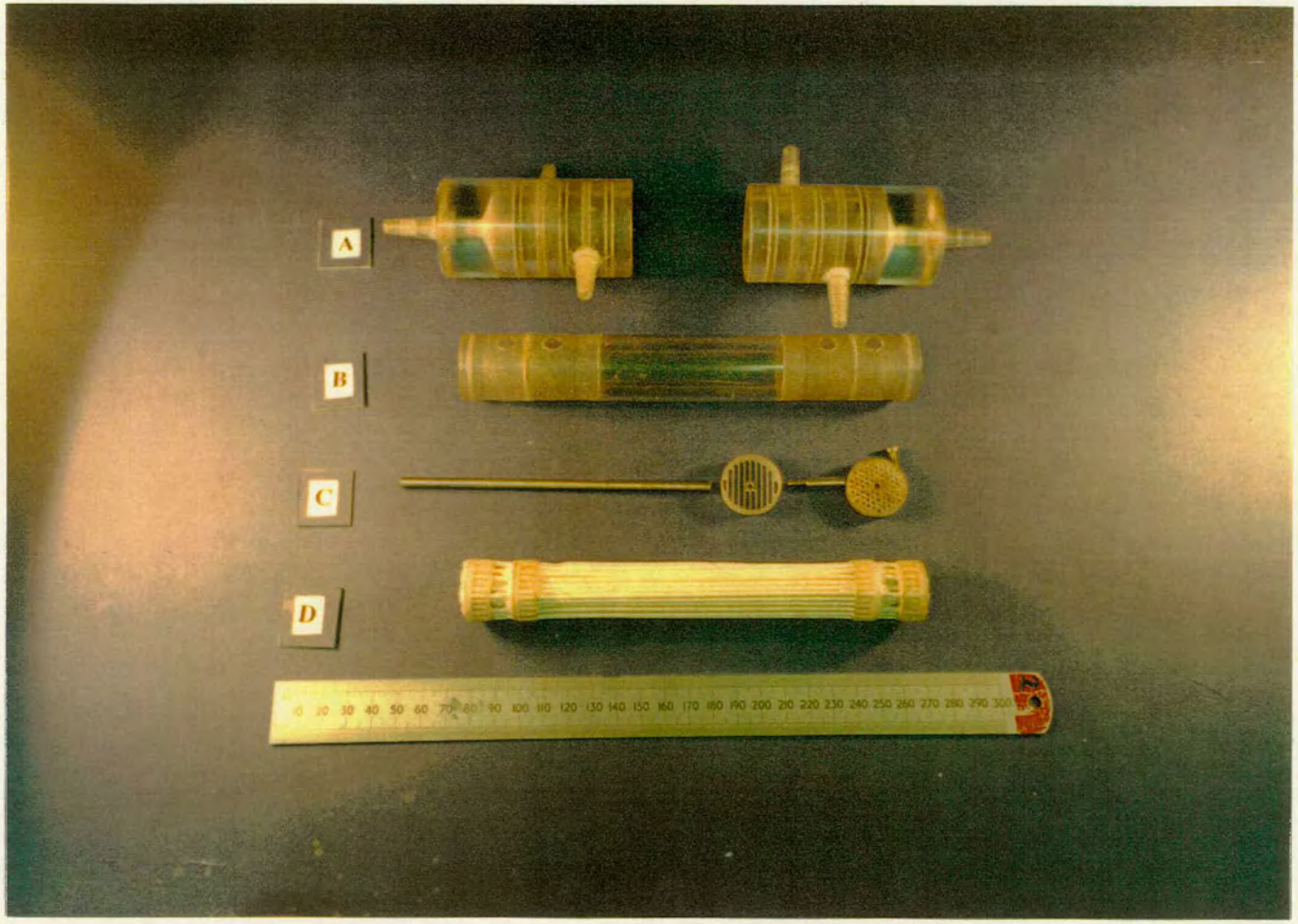

Figure 7.12:- New design of bioreactor construction

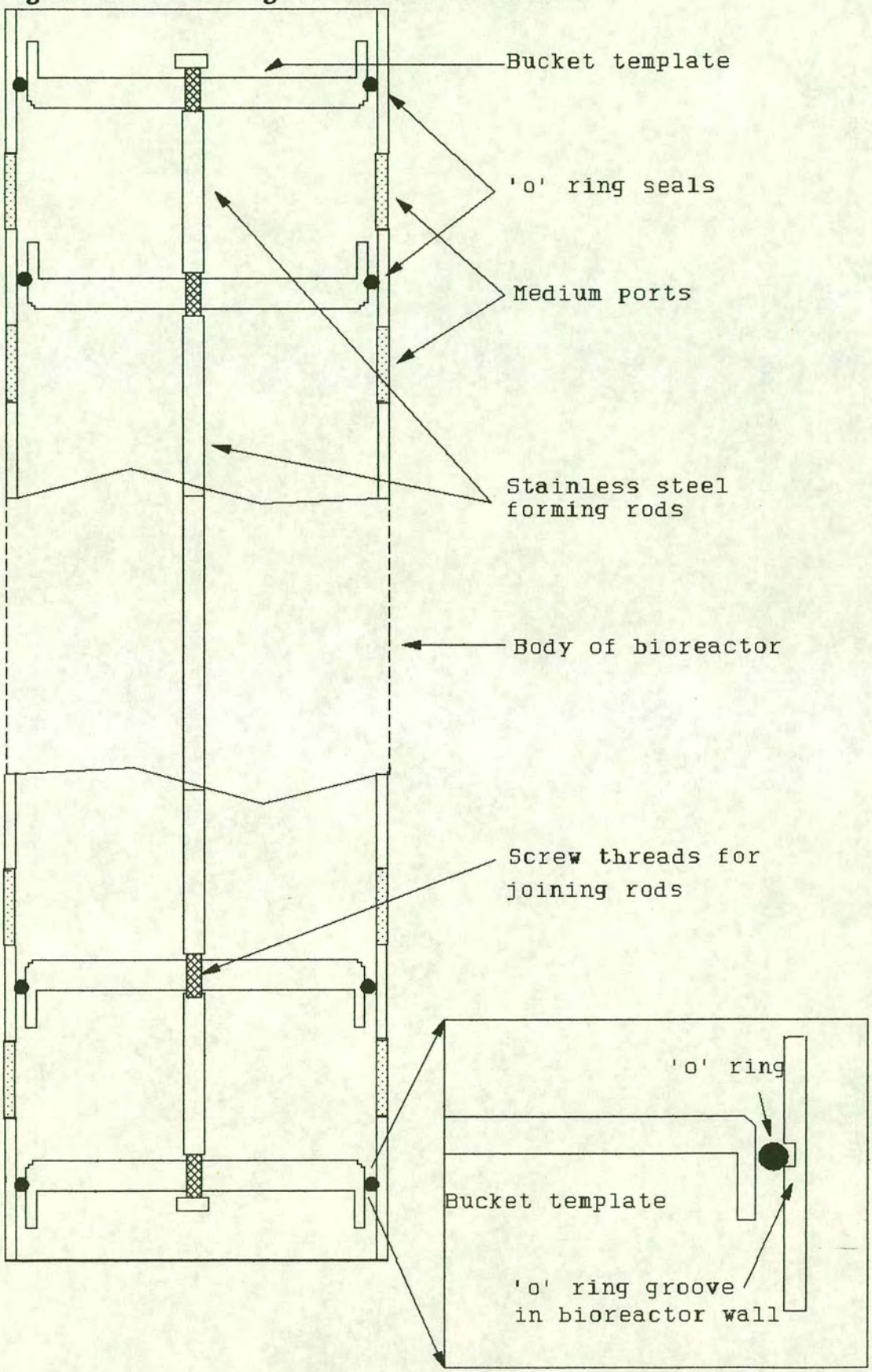

to the deformation and the cracking of the tube at this point, which caused the failure of the bioreactor.

7.4.2 Flow promotion within the cellular growth space

In the original design there were two ways in which medium could pass into the downstream of the reactor. The first is the intended route, via the upstream fibres, through the cellular growth space and then to the down stream fibres. The second is a direct transfer of medium from the supply fibres to the downstream in the proximal and distal gaps between the end templates (Figure 7.13).

The distribution of flow can be quantified theoretically for the hollow fibre bioreactor. The following calculation shows the volume of medium passed by each section of the bioreactor using the following assumptions:-

(1) For simplicity, the pressure of the upstream circuit was represented by the mean pressure of supply fibres, calculated by Equation 7.1:-

$$Upstream\ pressure = \frac{(P_{inlet} + P_{outlet})}{2} \qquad (7.1)$$

$$P_{inlet,outlet} = inlet,\ outlet\ pressures\ for\ the\ upstream\ fibres$$

This value, while not fully representing the pressure drop across the supply fibres, allows a crude estimate of the flux to be made.

(2) The viscosity (μ) of the medium was unitary (ie 1.0 centipoise or 10^{-3} Pa s).

(3) A single 18 cm long supply fibre in the bioreactor has 2 cm of its length associated with the gap region, 13 cm with the growth space, and the remaining 3 cm attributed to potting.

Figure 7.13:- Flow patterns in the bioreactor

Intended flow path for nutrients (solid line):

Supply fibres -> Cellular growth space -> Sink fibres -> Waste

Unintentional flow path (broken line):

Supply fibres -> Proximal/distal gaps -> Waste

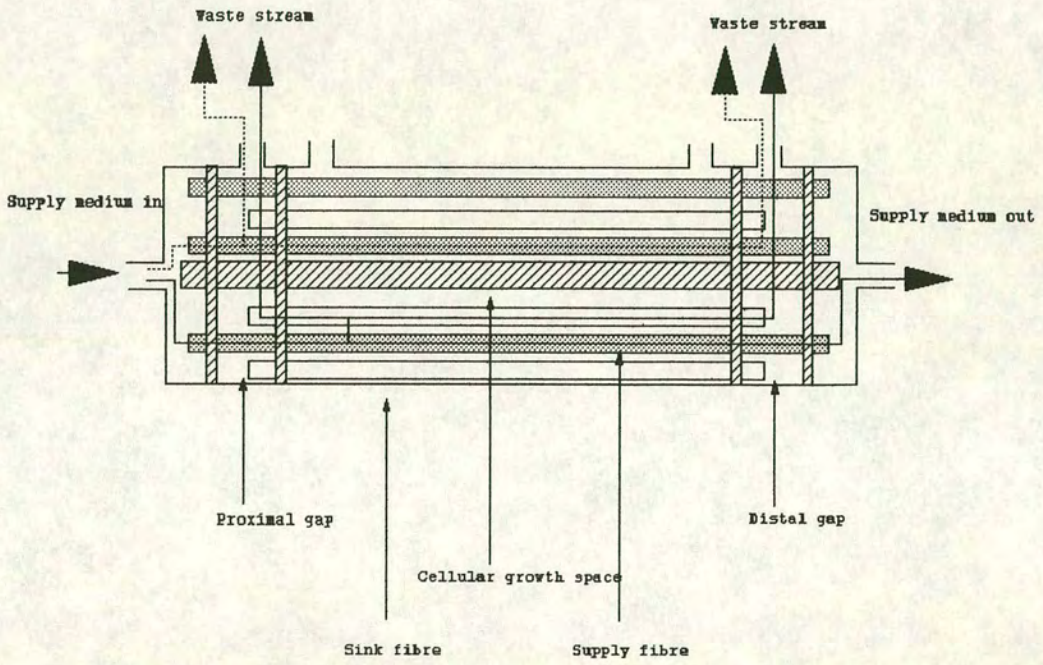

(4) The total resistance (R) to flow across the membrane, attributable to the membrane and any boundary layer, is constant along the membrane at a steady supply pressure.

(5) The flux within the bioreactor is limited by the resistance to flow from the supply fibres and not the sink fibres.

A simplification of the equations predicting flux in a crossflow filtration system can be described by Equation 7.2.

$$Flux\ (J) = \frac{\Delta P}{\mu R} \qquad (7.2)$$

Under steady state conditions, where μ = 1 centipoise and R = constant, it can be seen that flux would be dependent on the transmembrane pressure (ΔP). The experimental determination of flux can be made by measuring the volume of filtrate per unit time, using a given surface area of filter. The correlation between Equation 7.2 and the calculation of the experimental value (Right hand side of equation) is given in Equation 7.3:-

$$\frac{\Delta P}{\mu R} = \frac{V}{S.A.t} \qquad (7.3)$$

which, when reworked for evaluating V gives Equation 7.4:-

$$V = \frac{\Delta P(S.A.t)}{\mu R} \qquad (7.4)$$

where V is the volume of filtrate collected, S.A. is the total surface of the membrane and t is the time of the filtration process.

Using Equation 7.4, and considering the two end regions separately from the supply

fibres in the cellular growth space, the volume transferred by each region can be calculated according to Equations 7.5 and 7.6.

$$V_{cgs} = \frac{\Delta P_1 . SA_{cgs} . t}{\mu R} \quad (7.5)$$

$$V_{endspaces} = \frac{\Delta P_2 . SA_{end} . t}{\mu R} \quad (7.6)$$

Where ΔP_1 = *growth space transmembrane pressure,*

ΔP_2 = *end space transmembrane pressure,*

$SA_{end,cgs}$ = *surface area of the end regions, growth space*

Using the criteria explained in points 1-5, with R a constant for both regions (for ease, a value of 1 m^{-1}), the use of the mean supply pressure (psig converted to Pa), a constant viscosity of 1 centipoise for the fluid ($x10^{-3}$ Pa s) and the values described below, the volume (m^3) transferred across each membrane section in a unit time can be calculated as the product of the transmembrane pressure and the surface area of the membrane associated with each region. The proportion of the total flow associated with the end spaces per unit time can then be calculated using Equation 7.7.

$$\frac{V_{endspaces}}{V_{cgs}+V_{endspaces}} = \frac{\Delta P_2 . SA_{end}}{\Delta P_1 . SA_{cgs} + \Delta P_2 . SA_{end}} \quad (7.7)$$

Sample calculation

Mean pressure of supply circuit (P1)	-	3.0 psig (20.684 kPa)
Cellular growth space pressure (P2)	-	1.5 psig (10.342 kPa)
Sink circuit pressure (P3)	-	1.0 psig (6.895 kPa)
S.A. end spaces (SA_{end})	-	1.508×10^{-3} m^2
S.A. growth space (SA_{cgs})	-	9.816×10^{-3} m^2

$$\Delta P_1 = (P1\text{-}P2) = 20.684 - 10.342 = 10.342 \text{ kPa}$$
$$\Delta P_2 = (P1\text{-}P3) = 20.684 - 6.895 = 13.789 \text{ kPa}$$

Substituting these values into Equation 7.7

$$\frac{V_{endspaces}}{V_{cgs}+V_{endspaces}} = \frac{13.789x1.508x10^{-3}}{10.342x9.816x10^{-3}+13.789x1.508x10^{-3}}$$

$$= \underline{0.170}$$

In this case the end gaps contribute to about 17%, that is (0.17*100)%, of the flow from the supply fibres under these conditions. This is assuming no fouling of the sink membranes, which would increase the flow across the end regions as the transmembrane pressure decreased across the supply fibre.

With increased fouling of the upstream fibres with time, the resistance to flow, as well as the transmembrane pressure would be expected to increase throughout the bioreactor. The flow attributable to the cellular growth space could be expected to decrease at a greater rate than that of the end spaces due to the fouling of the downstream fibres. The fouling of the down stream fibres would increase the value of R in Equation 7.2, with the total resistance to flow being calculated as the sum of two membrane resistances.

Several strategies were adopted for resolving this problem, all of which involved the modification of the end region of the reactor. Stainless steel tubular covers were used to surround the membranes (Figures 7.14 and 7.15). This technique was assessed by injecting fluid into a dead ended fibre with a metal jacket potted directly on to the fibre and a zone where no jacket was present. Using this technique it was observed that liquid only passed through the unjacketed zone. Unfortunately, the increased complexity involved in threading the fibres through the inner templates, then the stainless steel tubes, followed by alignment and threading of the supply fibres through the outer template proved to be too time consuming as a construction technique.

Figure 7.14:- Original end region design

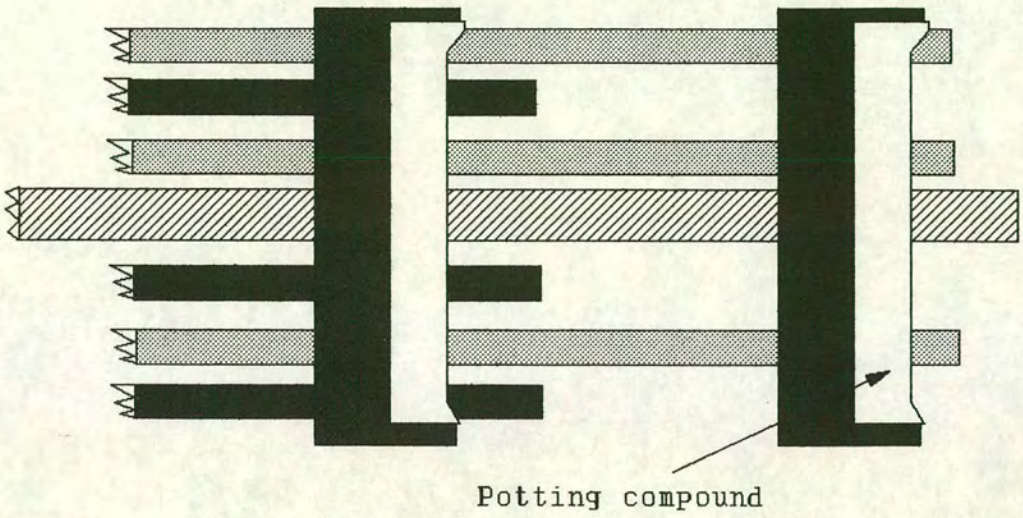

Original end region design

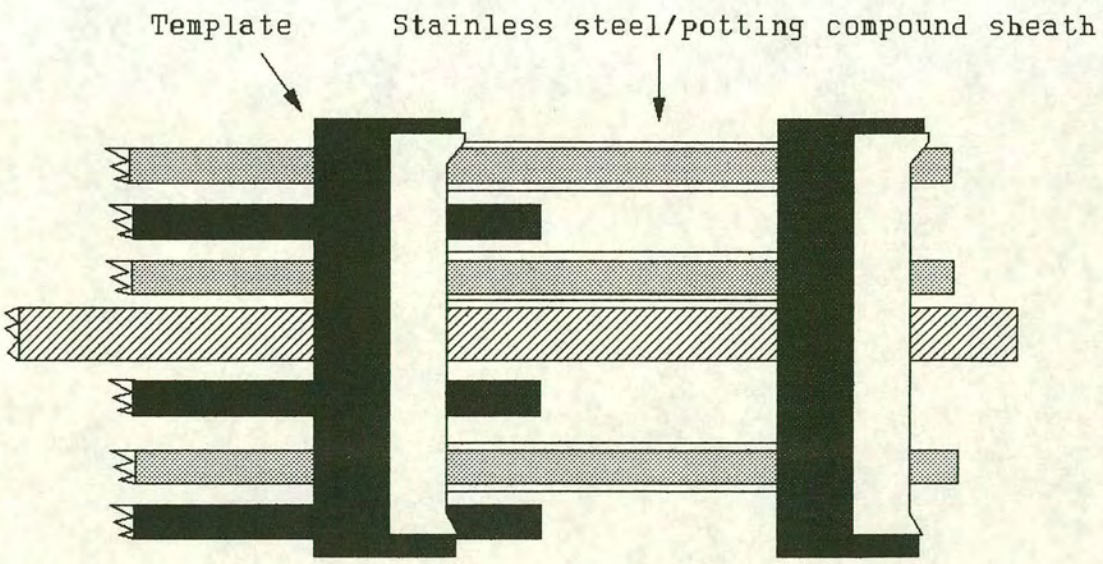

End region with stainless steel covers,
replaced with a layer of potting compound

Observations made during the dismantling of these test fibres led to the development of the final solution to the end zone leakage problem. The potting compound used to seal the tubes in place on the fibre had formed a cylindrical shell around the hollow fibre. Tests on these constructs determined that the potting compound was equally efficient at redirecting flow to the unsheathed zone. Subsequent reactors were constructed using the direct manual application of potting compound to the end zones using a modified syringe. This technique allowed a non-permeable protective sheath to formed around the fibres in the end region.

7.4.3 Templates for increased fibre packing

The original templates and the initial bucket templates were designed with one hole per fibre used in the bioreactor. This led to major limitations in the design and operation of the bioreactor. The requirements of hole integrity and the spacing limitations associated with the lathe meant that there was a relatively small proportion of the templates' surface area associated with fibres. Consequently, the number of fibres used in the bioreactor was limited to 72 in total (24 supply fibres: 48 sink fibres). This limited the surface area of filter available for nutrient transfer to 588 cm^2 for a growth space of 13 cm, with fibres accounting for 29.4 cm^3 of the total tube volume of 69.02 cm^3. This will be presented as a filter packing ratio in the remainder of this thesis, calculated according to Equation 7.8.

$$Packing\ ratio = \frac{Growth\ space\ volume\ of\ fibres}{Total\ growth\ space\ volume\ available} \qquad (7.8)$$

which gives a ratio of 0.43 for a 72 fibre bioreactor. This is the same value obtained for the bioreactor with a 15 cm long growth space.

The number of fibres, and hence the packing ratio, was increased by threading the fibres into slots milled into the template rather than individual holes (Figure 7.16).

Figure 7.16:- High density packing template

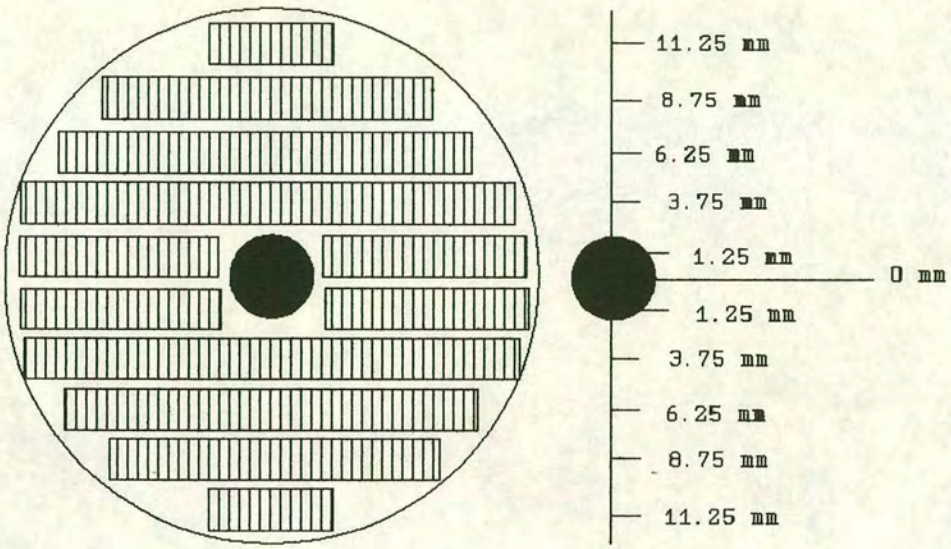

This enabled the addition of a further 18 fibres, 6 supply and 12 sink fibres, increasing the packing ratio to 0.532.

A ratio of 0.532 was found to be the maximum value achievable using the bucket style template, due to the physical limitations associated with the milling machine and the strength of the material used for the templates. In theory the maximum achievable packing ratio is limited by the total volume of the growth space. Practically, this would require the redesign of the dual hollow fibre bioreactor, in which it could be

anticipated that the efficient potting of the bioreactor would be the main construction problem.

7.4.4 Large scale bioreactor

Using the design improvements developed during this work, a large scale bioreactor was constructed from 60 mm polycarbonate tube (internal diameter 52 mm). A schematic of this bioreactor is presented in Figure 7.17, with more detailed diagrams of the individual components used in its construction can be obtained from the author. The three main components have been pictured in Photograph 5. Several modification were made to the design of this bioreactor with the key alterations listed below.

(1) The end caps used in the 30 mm bioreactors were replaced by end plates in the larger reactor. These end plates were sealed by 'O' rings on the inside of the reactor tube, being held in place by metal bolts travelling the full length of the bioreactor.

(2) The 4 mm walls of the 60 mm tube used for the large scale bioreactor were thick enough to allow the direct addition of tubing ports. These were made from 10 mm polycarbonate rod and bonded into place using chloroform.

(3) The increased internal diameter of the tube meant that the central rod holding the templates in place was now subject to bending under the stress applied to the fibre assembly during construction. The template was therefore redesigned to incorporate three support rods situated around the circumference of the template (Figure 7.18).

(4) The fibres were threaded into slots as opposed to individual holes in order to increase the packing ratio.

This design consisted of a total of 306 fibres (106 supply fibres:200 sink fibres), with fibre surface area of 2883.5 cm^2 in the cellular growth space. The packing ratio for this bioreactor was 0.453 . This value is lower than that of the high density, small scale reactor due to the increased area required for the template support rods.

Figure 7.17:- Schematic of large scale bioreactor

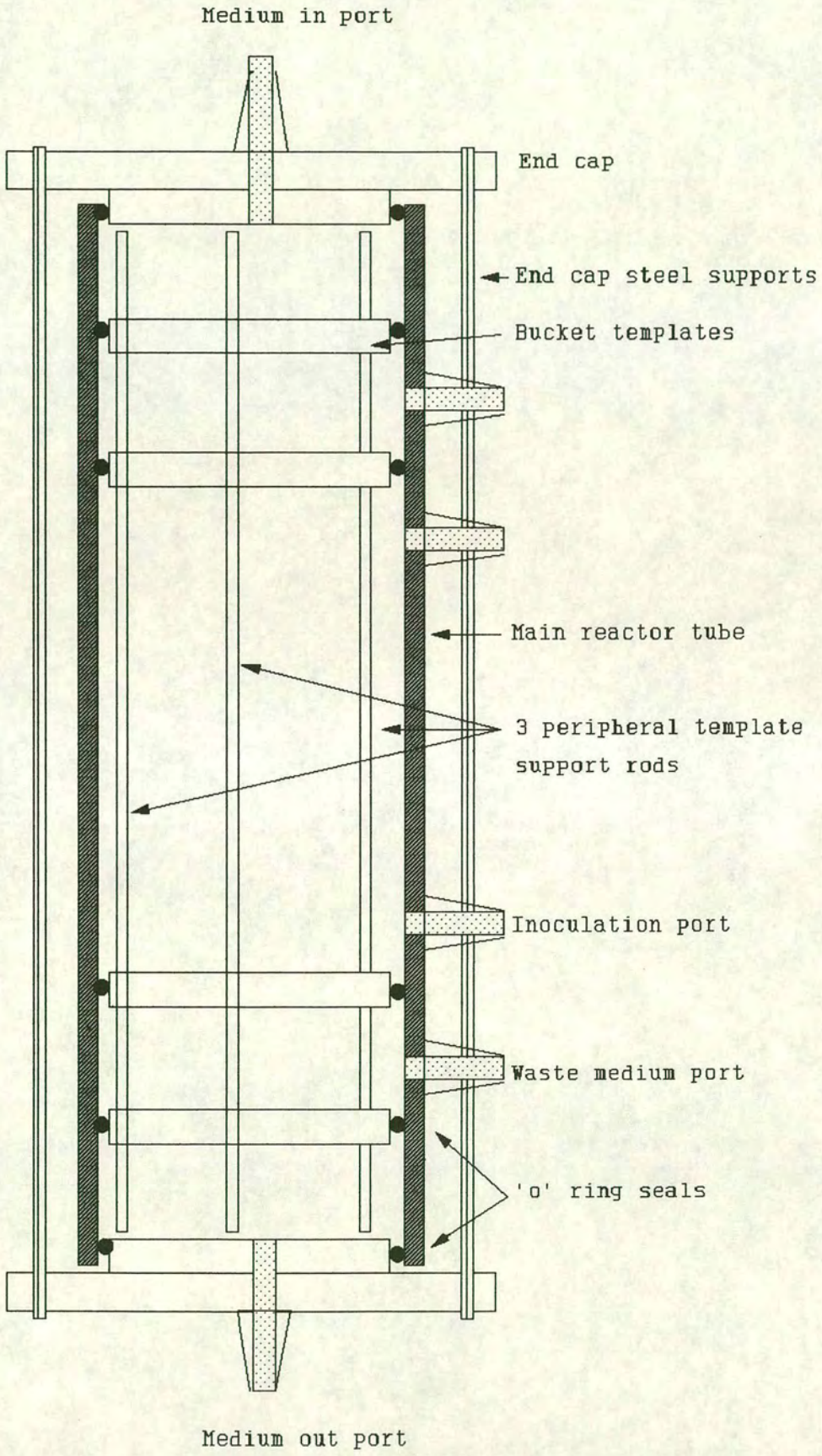

Photograph 5:- The three main components of the 'large scale' bioreactor showing the end caps with the full length supports (A), the outer tube (B) and the threaded bioreactor insert with 'o' rings on each of the potted fibre templates (C).

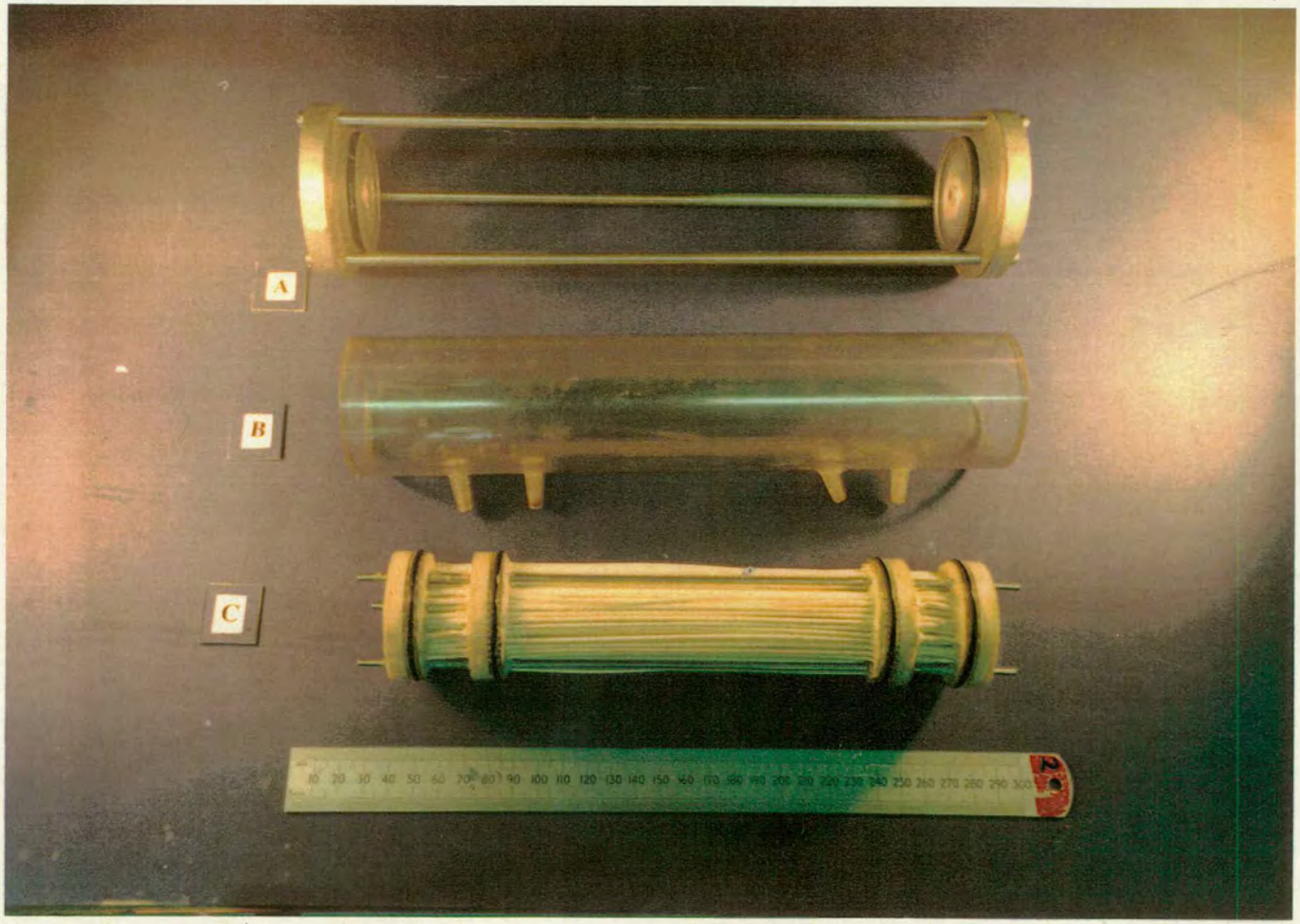

Figure 7.18:- Template design for large bioreactor (Figure drawn by Mr. M.Rea, dimensions in mm)

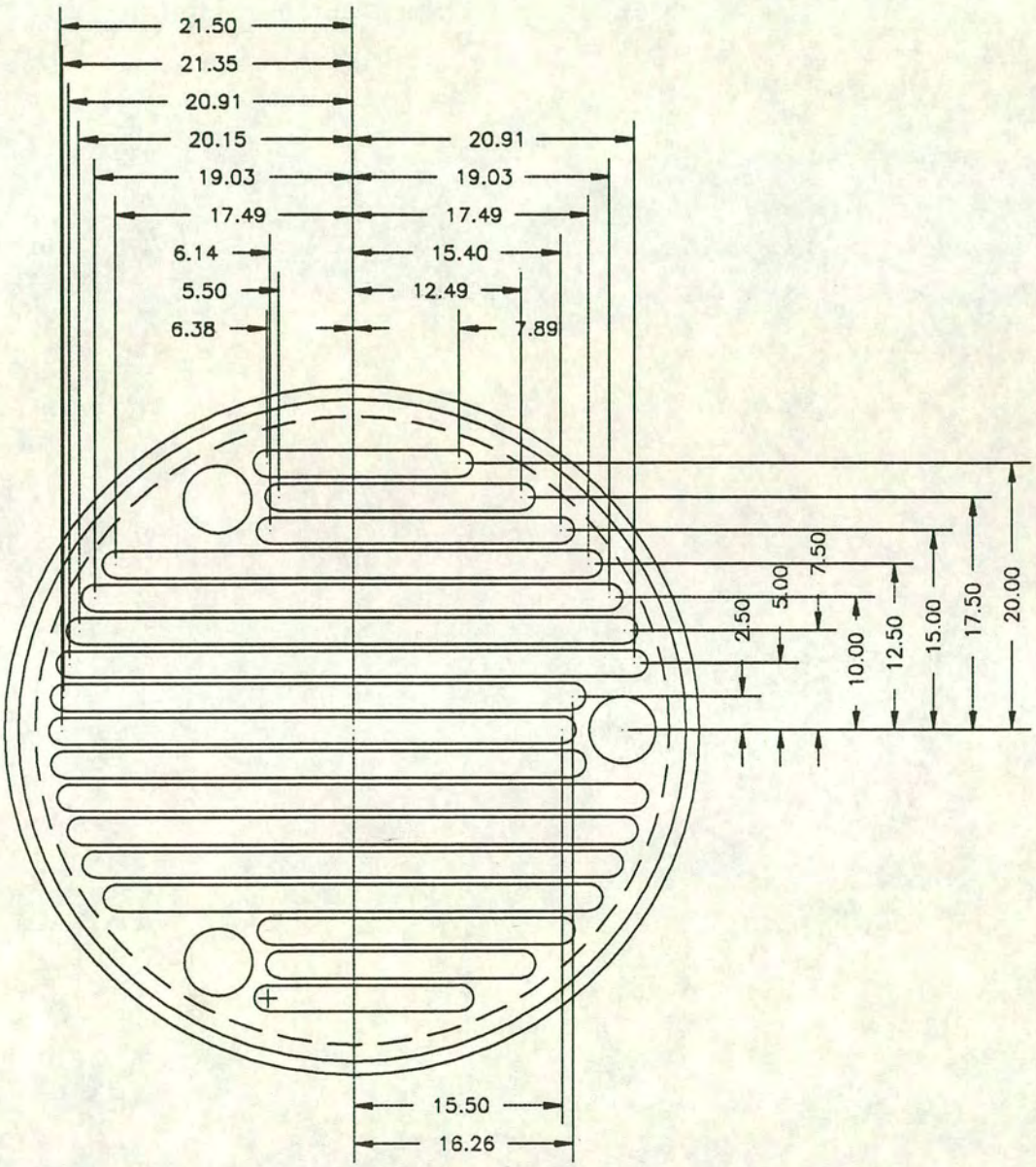

7.5 Summary of chapter

This chapter examined the influence of circuit and component design on the operation of the Edinburgh dual hollow fibre bioreactor. Photograph 6 shows three of the four different types of bioreactor (excluding the high density packing unit) used in this work. The modular design of the circuit was found to be especially useful, given the developmental nature of the project. By being able to isolate individual parts of the circuit, through the use of Swageloks, components could easily be replaced and autoclaved in sections. While it would have been a neater solution to develop an integrated design for the bioreactor, e.g. Serotec's Harvest Mouse (1993) and Setec's Tricentric bioreactor (Cima *et al.*, 1990), the required level of performance and control required for such a stage of the project was never achieved.

The development of housings for the ancillary monitoring equipment used in this work, e.g. pressure transducers and oxygen probes, was based on well established design principles such as the use of 'O' ring seals and thermowells. The further development of the pressure transducer housings, removing the transducers from the need for steam sterilisation and direct contact with the process fluid, did appear to be promising despite the leakage problems encountered. Further design modifications, based on the use of a non-compressible fluid, were required in order to get a fully responsive transducer housing.

By far the greatest bulk of work reported in this chapter involved the further development of the bioreactor. As the number of distinct sets of fibres in a bioreactor circuit is increased, the complexity of the construction technique required for ensuring the integrity of the potting also increased.

For bioreactors in which one set of fibres is used for the transfer and retrieval of medium to and from the cellular growth space, the successful potting of either end of the bioreactor is relatively easy (e.g. Amicons Vitafiber systems). The main problem associated with this technique is ensuring that the potting compound used for the end seals is fully dispersed between the fibres. A number of novel bioreactors reported in

the literature employ one set of potting seals in their design, e.g. Patankar and Oolman (1990) and Brotherton and Chau (1990) (Figures 5.7 and 5.9). Tharakan and Chau (1986) also used a single set of seals for the fibres in their radial flow bioreactor (Figure 5.8), using conventional 'O' ring seals for the stainless steel distributor used for the supply of nutrients at the centre of the bioreactor.

Where two sets of fibres were sealed in place using two potting procedures, two approaches have been used. The first, used by Knazek *et al.* (1980), involved the segregation of the two sets of fibres at either end of the bioreactor into the arms of a terminal Y section (Figure 5.8). The fibres were then sealed in their individual sets using procedures similar to those used in cartridge bioreactor construction.

Setecs' Tricentric bioreactor (Cima *et al.*, 1990) and the Edinburgh dual hollow fibre bioreactor employ two sets of serial potting seals at either end of the bioreactor. While the outer seals can be checked for their integrity after potting, the inner seals are a greater problem. Efforts made to find the methods used by Setec in the construction of their bioreactor proved unsuccessful although, based on the work carried out in the construction of the Edinburgh design, it was thought likely that the following approach was used. The first stage would involve the sealing of the inner seals, containing the outer fibres only (see Figure 5.9). The seals for this section of the bioreactor could then be checked. The second stage of the potting procedure would then involve the threading and subsequent potting of the inner fibres, stretching the full length of the bioreactor. These seals could then be checked.

In the old design of the Edinburgh dual hollow fibre bioreactor, the inspection of the inner seals of the bioreactor proved to be more difficult, given the restrictive presence of the outer fibres, which also had to be sealed during this potting procedure. The problems encountered were related to the maldistribution of the potting compound throughout the fibre bundle, which often resulted in the leakage of the seal.

By removing the potting procedure from the limited access afforded by the outer tube of the bioreactor, these problems were largely solved. The use of bucket templates

further enhanced this technique by restricting the flow of potting compound to around the fibre bundle and allowing the direct inspection of each seal. The use of 'O' ring seals at the interface of the bucket template and the outer tube also enabled the reuse of all of the machined components in the bioreactor.

One of the main limitations of the Knazek *et al.* (1980) design, according to Tharakan and Chau (1986), was the lack of a 'guaranteed perfect distribution between the supply and sink fibres'. This implied that there was no control over the relative positions of the supply and sink fibres and that this disorganised structure would result in unpredictable flow regimes within the bioreactor. The Edinburgh design attempted to address this criticism through the use of templates in which the relative position of supply and sink fibres could be permanently fixed. Two limitations were associated with the use of templates. The first was related to the total number of fibres that could be packed into the available space, due to constraints imposed by the milling machine. The adoption of a slotted template, as opposed to holes for each of the individual fibres, allowed a higher number of fibres to be used in the bioreactor, although it was still limited by the specifications of the milling machine.

The second limitation was associated with not being able to show that the flow regime was improved by the organised packing of the supply and sink fibres. Hammer *et al.* (1990) used an NMR imaging technique to visualise Starling flow in cartridge bioreactors. Similar facilities for examining the flow profile in the Edinburgh design were not readily available.

The following chapters will provide further information into the rationale behind these design changes, while summarising the results obtained with the different designs of bioreactor.

Photograph 6:- **Three of the four bioreactors used in this work showing the 'Large scale' bioreactor (A), the new style bioreactor with polycarbonate end caps (B) and the 'old style' bioreactor with the stainless steel end caps.**

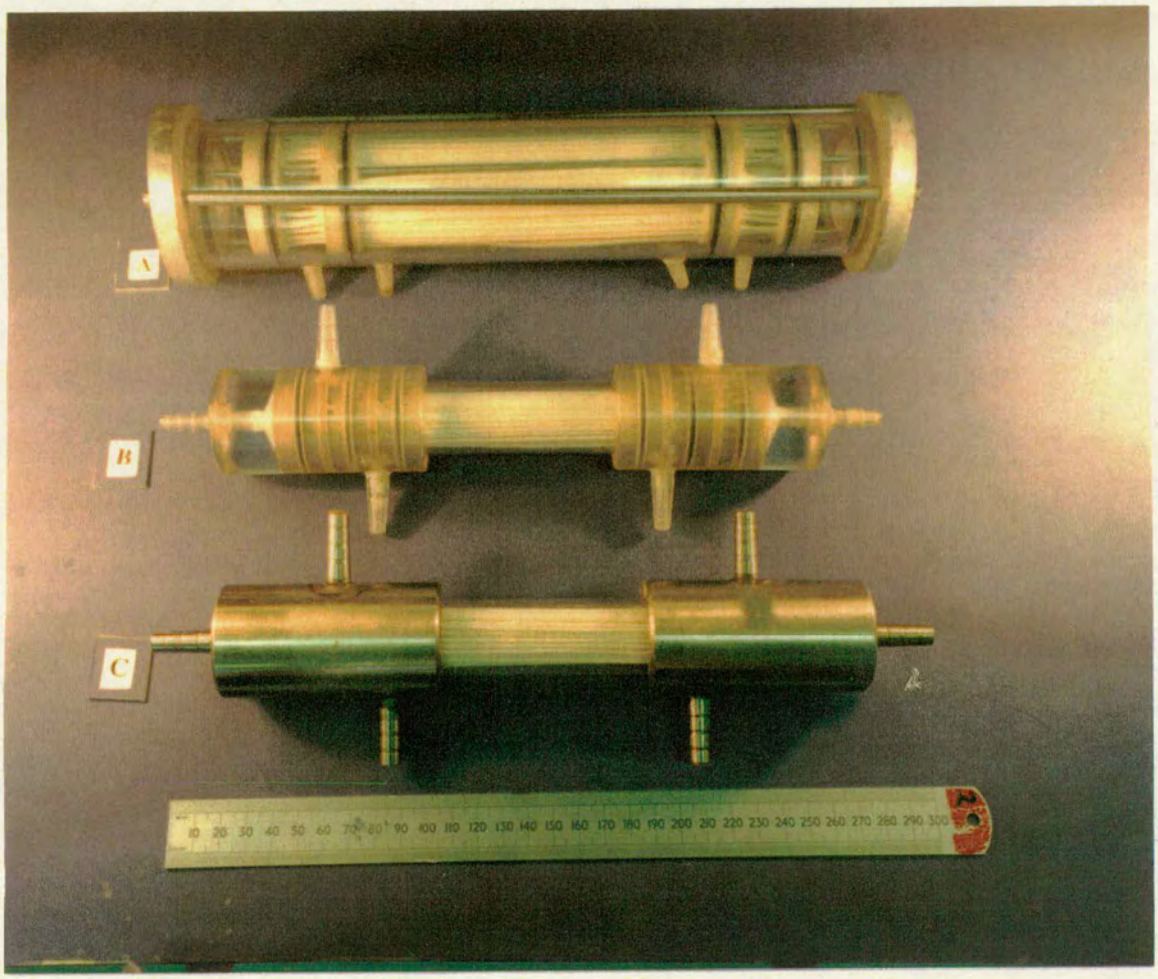

Chapter 8

Mass transport within the bioreactor

8.0 Introduction

Having described the design problems associated with the Edinburgh dual hollow fibre the bioreactor, this chapter reports a series of experiments investigating the effects of membrane selection and fouling on the mass transport within the bioreactor. This prototype was designed to ensure an even distribution of fibres within the bioreactor with a view to ensuring that all of the growth space was supplied with nutrient. However, based on the described effects of filtration on conventional membrane modules (membrane polarisation and fouling) and an extension of these phenomena to other designs of hollow fibre bioreactor (Chapter 5), it was predicted that the performance of this bioreactor system would also be affected.

The filtration characteristics and the way in which the bioreactor is operated are of prime importance to the success of this design. The Edinburgh design can be considered as a composite of two filtration devices. The supply fibres are operated as crossflow filters (Figure 7.2), while the sink fibres can be considered as a dead end filtration device. This chapter describes the use of both a small rig (Figure 8.1) designed to simulate the full sized apparatus and fluid tests on the actual bioreactors. Section 8.1 describes the authors reanalyses of the results of Burns (1991) who used a membrane unit and distilled water to examine the filtration behaviour of individual and mixtures of polysulphone fibres. Section 8.2 describes the fluid characteristics of different solutions used in tests carried out by the author using serum and dyed dextrans. The dyed dextrans were developed for examining the filtration characteristics of macromolecular species of defined molecular weight. Section 8.3 reports the results from a series of experiments carried out using these test solutions and a selection of hollow fibres. Section 8.4 summarises these results and provides a discussion of their implications on the performance of the Edinburgh design and other hollow fibre bioreactors.

8.1 Small rig filtration experiments

This section describes a reanalyses of the work carried out by Burns (1991) investigating the effects of changing the molecular weight cutoff (MWCO) of the hollow fibres on transmembrane pressure and distilled water fluxes. Burns also examined how the filtration characteristics of a dual hollow fibre bioreactor were influenced by using different MWCO for the supply (upstream) and sink (downstream) fibres.

8.1.1 Distilled water filtration experiments.

Distilled water is commonly used for testing the filtration characteristics of hollow fibre membranes (Amicon catalogue, 1993), with values for the permeability of the fibres being determined by this method. This technique allows a broad comparison of the different types of filter material, based on the assumption that most test facilities have a readily available source of this medium. The departmental distilled water supply had a measured conductivity of 32.1 MΩ.cm (σ=3.5, based on 6 water samples), which is approximately twice the maximum value required for its qualification as ultrapure water (18.0 MΩ.cm, Mulder, 1991) suggesting that the purity of the water was suspect.

8.1.2 Fibre characteristics

A range of different hollow fibres were used during this work. These included 0.2 μm polypropylene fibres, supplied by Enka (1987), and a range of polysulphone fibres with different molecular weight cutoffs supplied by Grace & Co. (0.1 μm (MP01.43), 100 kDa (P100.43) and 30 kDa (P30.43)). The reported distilled water fluxes of the fibres are presented in Table 8.1.

The polysulphone hollow fibres were anisotropic, inert and non-ionic in nature, with their selection for use in the Edinburgh bioreactor system being based on their use in other such systems e.g. Amicons Vitafiber or Flo-Path bioreactors. The fibre consists

Table 8.1:- Specifications for hollow fibres

Manufacturer	Fibre type and pore size	Average water flux ($l/min.cm^2$)
W.R. Grace	30 kDa MWCO, polysulphone	$0.5x10^{-3}$ *
	100 kDa MWCO, polysulphone	$1.5x10^{-3}$ *
	0.1 μm pore size, polysulphone	$3.1x10^{-3}$ *
Enka (Akzo)	0.2 μm pore size, polypropylene (type Q 3/2)	$14x10^{-3}$ **

** Based on a transmembrane pressure of 20 psig, assuming the outside of the fibre to be at atmospheric pressure (Amicon, 1993). ** Based on a transmembrane pressure of 14.7 psig, assuming full hydrophilicity via ethanol treatment, and the pressure outside the fibre to be atmospheric (Enka, 1987).*

of the selective membrane on the annulus of the fibre, with a tortuous conical membrane support leading to an external skin covering the outside of the fibre.

Initial experiments using the 0.2 μm fibres provided by Enka showed a negligible flux (practically zero) when compared with the other fibres, under the same conditions. Wagner and Lehmann (1988) have reported that polypropylene fibres are hydrophobic in nature, leading to low permeabilities. It should be noted that the permeability values of the fibres quoted in the Enka data sheet are based on the fibres being "sufficiently hydrophilic". The 'Wetting' of fibres using ethanol was found to improve flux significantly. While this treatment led to higher fluxes from the Enka fibres, the use of these fibres in the bioreactor was excluded for the following reasons:-

(1) These fibres, while apparently giving a higher flux when compared to the polysulphone fibres, required pretreatment with ethanol, the loss of which led to the fibre adopting its original low level of flux.

(2) On autoclaving, these fibres lost the high fluxes associated with the ethanol treatment, causing a major reduction in flux.

(3) Low levels of ethanol were shown to be toxic to an actively dividing culture of ES4 (J.Wilson, personal communication).

Based on these observations, the 0.2 μm fibres were excluded from further consideration.

The polysulphone fibres were used in two different experimental rigs. The first of these, designed as part of Dr J. Burns' PhD work, incorporates a maximum of four fibres (Figure 8.1). This rig was used in conjunction with a gear pump for a number of distilled water experiments, the results from which will be discussed in a later section.

8.1.3 Burns' small rig experiments

Experimental approach

A range of different fibre configurations and modes of operation were tested using the small rig. These experiments were based on the different operational regimes outlined in Chapter 5 :-

(1) Dead end operation, with the permeate flow from the inside to the outside of the fibre.

(2) Dead end operation, with the flow from the outside to the inside of the fibre.

(3) Crossflow operation, with flow internal to the fibres.

(4) One supply fibre to one sink fibre.

It was assumed that testing a crossflow of medium on the outside of the fibres was inappropriate since such flows would not be encountered in the bioreactor. The basic circuit design used for these experiments is outlined in Figure 8.1. A series of distilled water permeability experiments was carried out as part of the modelling work reported by Burns (1991).

Results

Several useful conclusions were made by Burns based on these experiments.

(1) The liquid flux across the fibres operated as a conventional crossflow filter initially declines, then settles to a steady state (Figure 8.2). The

filtration rate is linearly dependent upon pressure up to the maximum supply pressure tested, i.e. 5 psig. These observations agree with conventional crossflow filtration theory, as described in section 4.1.3.

(2) The liquid flux through fibres operated as dead end filters, whether its operation is conventional, i.e. flow from the inside of the fibre to the outside, or unconventional, from the outside of the fibre into the lumen, declines with time (Figure 8.2). The suggestion by Burns, that the observed flux decline is associated with the volume of medium crossing the membrane is also consistent with Ruths Law for dead end filtration (Section 5.1.2). In this case the flux did not decline to zero as the distilled water supply used in these experiments was recirculated reducing the bulk concentration of the foulant species with each pass of the medium across the membrane. Ruths Law assumes a constant bulk concentration in the feed stream which would eventually result in no flux across the membrane. Under conditions where the medium is recycled a reduction in the concentration of the foulant species would lead to a reduction in the rate of fouling. In these experiments the concentration of the foulant species reduced to zero resulting in no further fouling.

(3) The permeability of the fibre is dependent upon the direction in which the fluid crosses the membrane. For example, a fibre with a 0.1 μm pore size has an initial flux of 0.45 $cm^3cm^{-2}min^{-1}$ when operated as a dead end filter with the flow from the inside of the fibre to the outside and a supply pressure of 5 psig. When the fibre is operated at the same supply pressure, with flow from the outside of the fibre to the inside of the fibre, the initial flux drops to 0.1 $cm^3cm^{-2}min^{-1}$. This has obvious design implications for dual-fibre bioreactors where the permeability of the sink fibres should always be greater than that of the supply fibres.

Figure 8.1:- Design of small rig developed by Burns

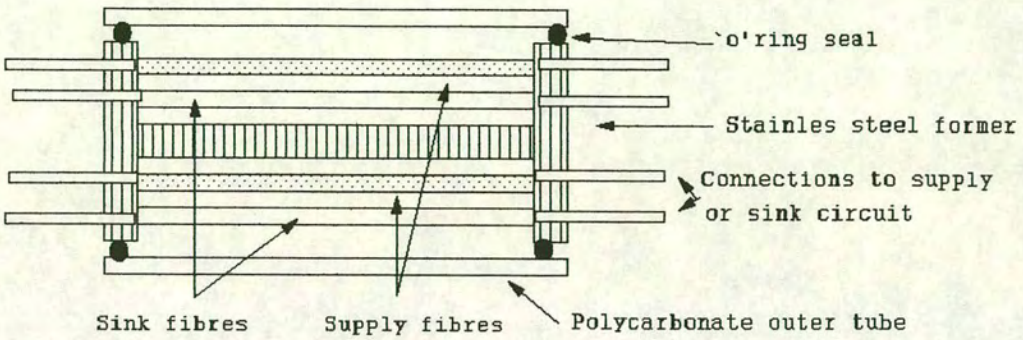

Sectional side view

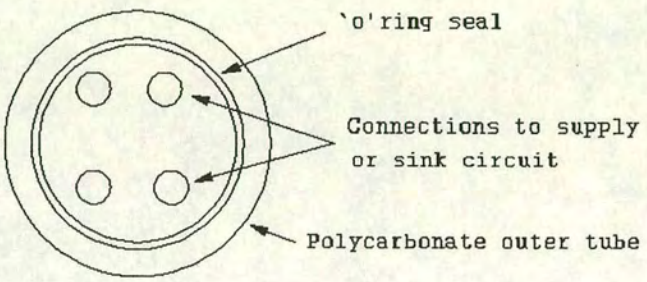

End view

Operation of small rig

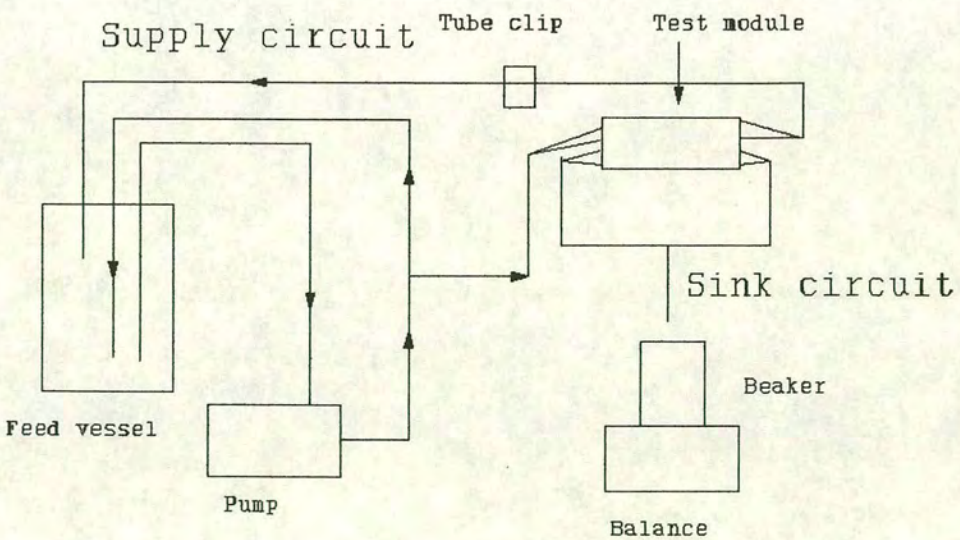

Figure 8.2:- Flux during dead end and crossflow filtration

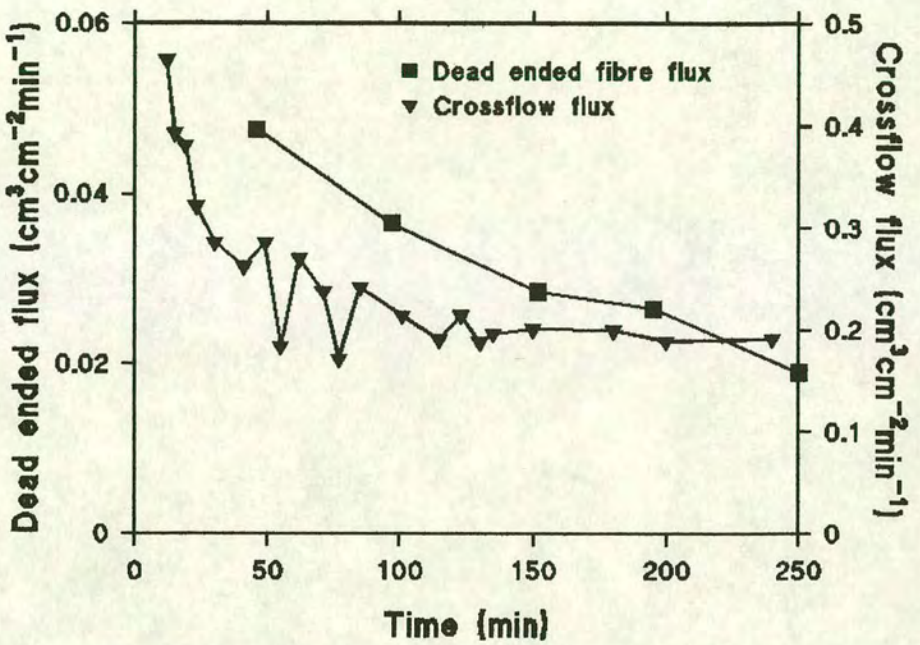

Test conditions:– small rig, 5 psig supply pressure, 0.1 μm fibres, crossflow TMP=3.4 psig, dead end TMP=4.8 psig.

8.1.4 Burns' small rig bioreactor experiments

Burns carried out a series of experiments using the small rig and different configurations of hollow fibres i.e. 100 kDa MWCO supply fibres to supply fibres with a pore size of 0.1 μm, operated in different filtration modes, i.e. dead ended and crossflow. The following section analyses these results with respect to transmembrane pressures and the flux across the bioreactor, based on observations made in the previous section.

Transmembrane pressure

Two methods of calculating transmembrane pressure have been used in the reanalysis of Burns work. Transmembrane pressures can be calculated as the difference of the pressures before and after the membrane, according to Equation 8.1.

$$Transmembrane\ Pressure\ (TMP) = P1 - P2 \quad (8.1)$$

Where P1 = Pressure before membrane,
P2 = Pressure after membrane

For dead end filtration, P1 (pounds per square inch gauge, psig) is simply the pressure exerted on the supply side of the membrane. For crossflow filtration the pressure drop along the fibre means that there may be a pressure difference between the inlet and outlet of the fibre. In this case P1 is expressed as the mean of these two values, as calculated by Equation 8.2.

$$P1 = \frac{(Pressure_{inlet} + Pressure_{outlet})}{2} \quad (8.2)$$

In the dual hollow fibre bioreactor, transmembrane pressures can be calculated for both the supply and sink fibres, using equations 8.3 and 8.4, where P1 is the mean supply pressure, P2 is the pressure found in the cellular growth space, and P3 is the pressure found at the outlet of the sink fibres.

$$TMP\ (Supply\ fibres) = P1 - P2 \quad (8.3)$$

$$TMP\ (Sink\ fibres) = P2 - P3 \quad (8.4)$$

The fibre configurations examined by Burns are summarised in Table 8.2. All of the experiments reported presented were carried out at a supply pressure of 5 psig. The graphs plotted for these experiments are expressed using the transmembrane pressures for the supply and sink fibres, and the flux across the bioreactor expressed in units of

$cm^3cm^{-2}min^{-1}$ and based on the surface area of the supply fibre.

Results from test rigs 1 and 3 (Figures 8.3 and 8.4)

In these experiments the supply and sink fibres were of the same pore size. From the experiments carried out by Burns using single fibres it could be predicted that flux would be limited by the lower permeability of the sink fibres, where the flow of water is from the outside to the inside of the fibre. In Figures 8.3 and 8.4 it can be seen that there are two stages to the graph, stage 1, where bioreactor flux decreases fairly rapidly, while the transmembrane pressures of the supply fibres and sink fibres increase and decrease respectively and stage 2, where the decline in flux and alterations in the respective transmembrane pressures are more gradual.

The first stage would appear to be associated with the fouling of the dead ended fibres. Burns' single fibre experiments suggest that flux would be limited by the sink fibres and that the reduction in flux would be dictated by the fouling of these fibres, leading to an increase in the value of P2. Consequently the transmembrane pressure of the sink fibres would be expected to increase, and that of the supply fibres to decrease. The transmembrane pressures obtained from these experiments during stage 1 are in fact the reverse, i.e. the transmembrane pressure of the supply fibres increases while that of the sink fibre decreases.

The transmembrane pressures suggest that the supply fibres are fouling and hence flux is dictated by these fibres. This conclusion is based on the following reasoning:-

(1) The supply pressure (P1) and sink outlet pressure fibre (P3) do not alter because P1 is controlled and P3 is atmospheric.

(2) As these pressures remain constant, the cellular growth space pressure (P2) must be changing.

(3) The only solution that satisfies an increasing supply TMP and a decreasing sink TMP is a reduction in P2.

(4) P2 would only be reduced if there was an increase in the resistance to flow in the upstream fibres, i.e. the supply fibres were fouling.

Stage 2 would appear to be an artefact of the way in which the experiment was operated. The water used in these experiments was recycled, with the flow from the feed reservoir, through the experimental apparatus and back to the feed reservoir. As a result of this operation any impurities causing the fouling of the supply fibres, would gradually be removed from the feed vessel, improving the purity of the water. In the second stage observed in Figure 8.3 , the water crossing the membranes is effectively clean, causing no more fouling of the supply fibres, and consequently a reduction in the alterations observed in the transmembrane pressures of the fibres. This would also explain the differences observed in the flux of reverse flow, dead ended fibres in the single fibre and small rig bioreactor experiments.

In Figure 8.4, where the 0.1 μm fibres were used, a similar pattern of an increase in the transmembrane pressure of the supply fibres and a decrease in the transmembrane pressure of the sink fibres can be seen. This supports the observations made from the experiment carried out using the 100 kDa fibres, although the decline in flux for the 0.1 μm fibres is not as obvious.

Results from test rigs 2 and 4 (Figures 8.5 and 8.6)

In these experiments, the supply fibres were operated as crossflow filters, whereas the sink fibres were operated as reverse flow, dead ended filters. In these cases the flux remained fairly constant, as opposed to the results observed using test rig 1. In Figure 8.5, the supply transmembrane pressure was found to decrease slightly during the experiment, while that of the sink fibre was found to slowly increase. While this is a less clear cut case than the previous experiment where the changes in the respective transmembrane pressures were more extreme, it can be proposed that the downstream fibres are responsible for these alterations, based on the following reasoning:-

(1) The supply pressure (P1) and the sink outlet pressure (P3) are controlled to 5 psig and atmospheric pressure respectively.

(2) In order for the transmembrane pressure of the supply fibres to decrease, either P1 has to decrease or P2 has to increase.

Table 8.2:- Summary of Burns experiments

Test rig	Supply Fibre	Mode of Operation	Sink Fibre	Mode of Operation
1	100 kDa	Dead end	100 kDa	Dead end
2	100 kDa	Crossflow	100 kDa	Dead end
3	0.1 μm	Dead end	0.1 μm	Dead end
4	0.1 μm	Crossflow	0.1 μm	Dead end
5	0.1 μm	Dead end	100 kDa	Dead end
6	0.1 μm	Crossflow	100 kDa	Dead end

(3) In order for the transmembrane pressure of the sink fibre to increase, either P2 has to increase or P3 has to decrease.

(4) As P1 and P3 are constant, this suggests that P2 is the pressure that is increasing. This is consistent with the gradual fouling of the sink fibres, where an increase to the resistance of flow would increase the pressure drop across the membrane.

These results are consistent with the gradual fouling of the sink fibres. As with the previous experiments, rigs 1 and 3, the rate of fouling of the sink fibres is significantly less than that illustrated by the single fibre experiments. A similar explanation is proposed, where the sink fibres are never exposed to the water borne contaminants responsible for the degree of fouling observed in the single fibre experiments due to the pre-filtration effects associated with the supply fibres.

In Figure 8.6, the results support the fouling of the sink fibre, based on the increase in the transmembrane pressure of the sink fibre, however, there is no appreciable decline in the transmembrane pressure of the source fibre to support this hypothesis. In both of the experiments employing the 0.1 μm fibres, the results are less clear than those of the 100 kDa test rigs, this was most likely due to the differences in pore size. The flux in these experiments remained fairly constant as the supply fibres were operated as crossflow filters, where a steady state flux would be expected. The low fouling rate experienced by the sink fibres, as determined by an increase in TMP,

Figure 8.3:- Supply and sink fibres dead ended (100 kDa)

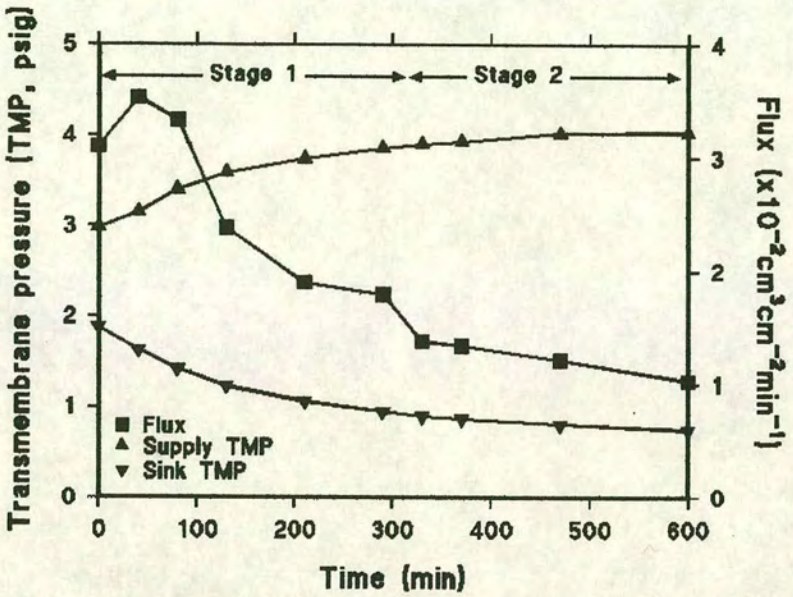

Test conditions:- small rig, 5 psig supply pressure, 100 kDa supply and sink fibres (dead ended).

Figure 8.4:- Supply and sink fibres dead ended (0.1 μm)

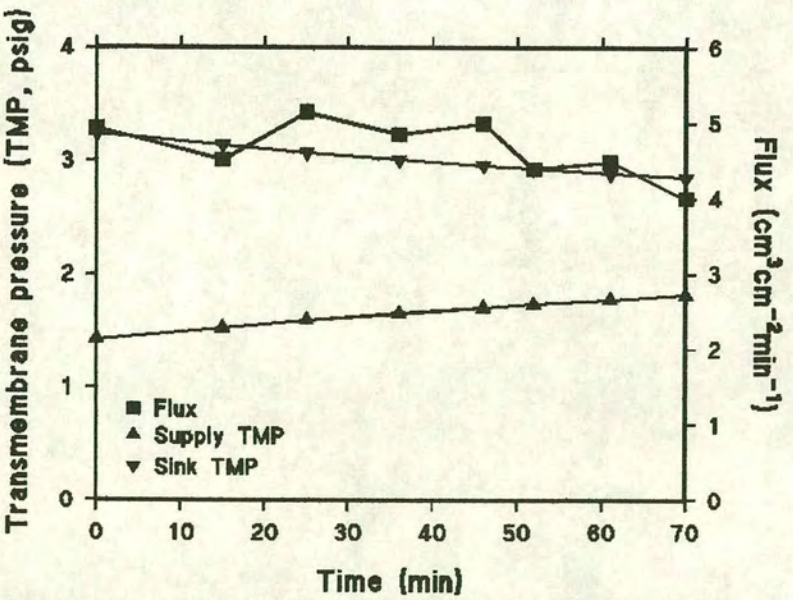

Test conditions:- small rig, 5 psig supply pressure, 0.1 μm supply and sink fibres (dead ended).

Figure 8.5:- Mixed fibre operation 100 kDa:100 kDa

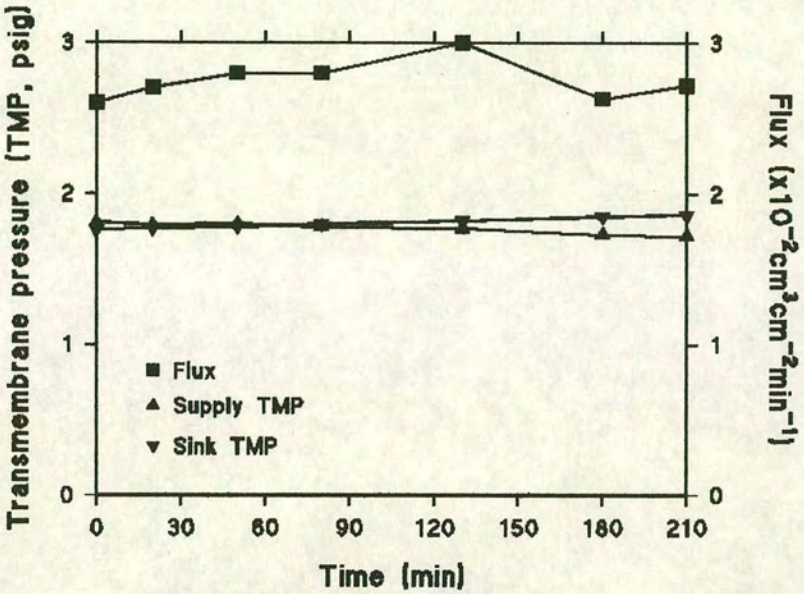

Test conditions:– small rig, 5 psig supply pressure, 100 kDa supply (crossflow) and sink fibres (dead ended).

Figure 8.6:- Mixed fibre operation 0.1 μm: 0.1 μm

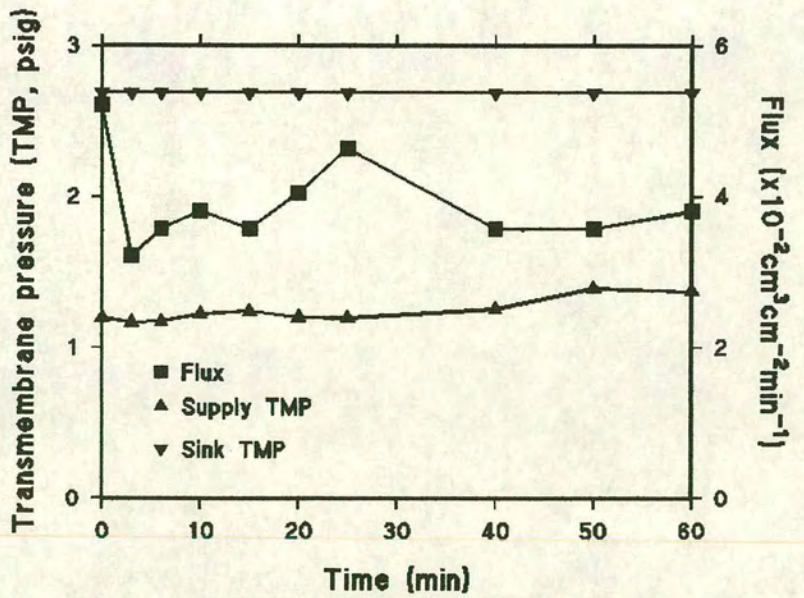

Test conditions:– small rig, 5 psig supply pressure, 0.1 μm supply (crossflow) and sink fibres (dead ended).

means that no significant reduction in flux was experienced throughout these experiments.

Results from rigs 5 and 6 (Figures 8.7 and 8.8)

Burns carried out these experiments to examine the effects of using fibres of different molecular weight cutoff for the supply and removal of the water passing through the test rig. The influence of the 100 kDa sink fibres on the transmembrane pressures of both sets of fibres is the most notable feature of these graphs. The transmembrane pressure of the sink fibres was approximately 0.5 psig lower than the gauge supply pressure, while that of the supply fibres was less than 0.3 psig in both cases. Little change in these values could be observed during the experimental period examined.

When the unit was operated with both sets of fibres dead ended (Figure 8.7), flux was shown to decline gradually to less than $1x10^{-2}$ $cm^3cm^{-2}min^{-1}$. When compared with the experiments where one type of fibre was used in the unit (Figure 8.3 and 8.4), the flux through the reactor unit appears to be limited by the gradual fouling of the 100 kDa sink fibre.

When the supply fibres were operated as a crossflow filter the flux (Figure 8.8), while appearing to be constant, was approximately 30% of the value observed for the experiment where 100 kDa fibres were used (Figure 8.5). It was because the pressure of the growth space (P2) often exceeds that of the outlet pressure of the supply fibre. Burns suggests that this condition would induce fluid to flow from the growth space into the downstream end of the supply fibre. This hypothesis is supported by theory and observations made with regard to Starling flow, where the pressure drop along the fibre enables fluid to flow out of the fibres at the feed end, and return to the fibres at the outlet of the reactor, see Chapter 4 for more information.

Conclusions

On re-examination of the results of Burns, the importance of fibre selection and the importance of the pressure profile within the reactor are upheld. The behaviour of the

Figure 8.7:- Mixed fibre,dead end operation,0.1 μm:100 kDa

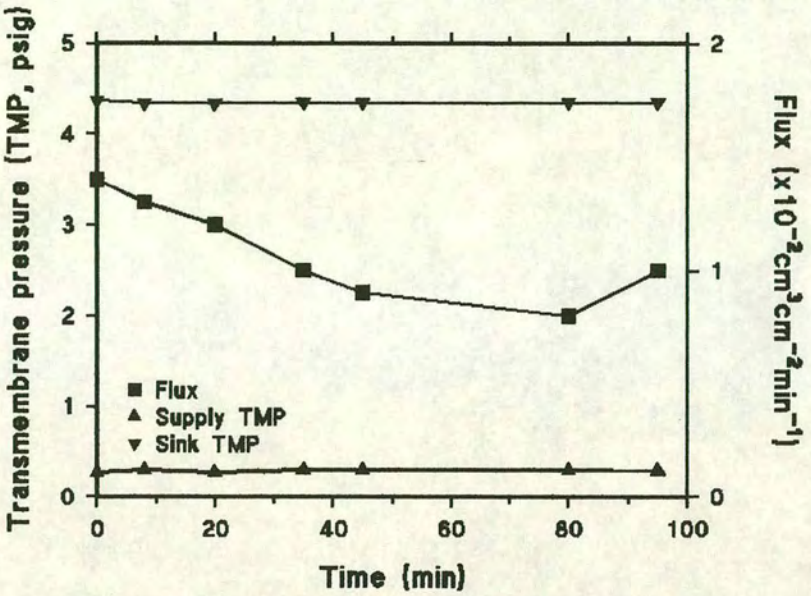

Test conditions:- small rig, 5 psig supply pressure,
0.1 μm supply and 100 kDa sink fibres (dead ended).

Figure 8.8:- Mixed fibre, mixed operation, 0.1 μm:100 kDa

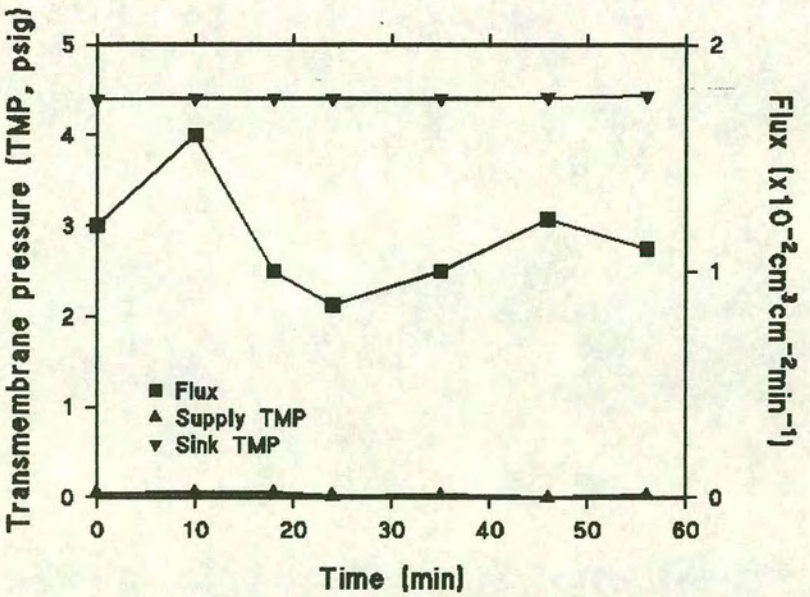

Test conditions:- small rig, 5 psig supply pressure,
0.1 μm supply (crossflow) and 100 kDa sink fibres (dead ended).

test medium, distilled water, is of particular interest. In the tests where the supply fibres were the same type as the sink fibres, the supply fibre tended to act as a pre-filtration step, reducing the fouling of the sink membranes. The influence of the test medium upon the behaviour of the bioreactor will be discussed in Section 8.4.

The re-examination of Burns' results by the author was intended to look for the influence of fouling upon the transmembrane pressures of the supply and sink fibres. Burns did not apply this approach during his initial investigations. The trends observed were that, on the fouling of the supply fibres, their transmembrane pressures were found to increase, while those of the sink fibres decreased. If the sink fibres were found to foul, the transmembrane pressure of the supply fibres would be expected to decrease, while those of the sink fibres increased, resulting in a reduction in flux. This theory will be applied to the later analysis of the full scale bioreactor runs.

8.2 Fluid Characteristics

In order to understand the transport characteristics of a number of different media through the membrane unit a number of different fluids were examined. These included the general RPMI 1640, with and without serum supplementation, and a dyed dextran solution developed in order to assess the general filtration behaviour of the hollow fibres.

8.2.1 Dyed dextran solutions.

Dextran is a polysaccharide consisting of glucose monomers which are linked to each other by α-1,6 linkages, although there are occasional α-1,2 , α-1,3 and α-1,4 linked side chains. Dyed dextran solutions were developed for testing the filtration characteristics of the fibres for several reasons:-

(1) A serum supplemented test solution was shown to be prone to contamination under the test conditions, requiring the sterilisation of the apparatus before use.

(2) Serum supplemented RPMI 1640 proved difficult to analyze directly at 280 nm using a spectrophotometer. The main reason for this difficulty was the presence of amino acids in the test mixture which also absorbed at 280 nm, e.g. tyrosine. Serum is also a multicomponent mixture, excluding the study of a species of known molecular weight.

(3) Dyed dextran solutions of known molecular weight could be prepared cheaply and in quantity, were easily assayed using a spectrophotometer.

A wide range of dyes have been developed for use in the dying of cotton. Cellulose, a major constituent of cotton, consists of long unbranched chains of predominantly ß-1,4 linked glucose units. As glucose is the basic monomeric unit for both cellulose and dextran, it was thought that these dyes could be used for modification of dextran.

Procion dyes, developed by I.C.I. for dying cotton, are synthesised by reacting a water soluble, acid-type dye with cyanuric chloride. The resulting dichlorotriazinyl amino compound constitutes the basis of all Procion dyes (Figure 8.9). These dyes are water soluble and anionic in nature, adsorbing to the cellulose when mixed with a neutral solution. In the presence of a cold, mild alkali, one of the two chlorine atoms attached to the triazinyl group reacts with one of the ionised hydroxyl groups of the monomeric glucose units. These dyes form the Procion MX family of dyes and are said to be 'cold reactive'.

The dyes used in this work, monochlorotriazinyl dyes, from the procion H and H-E families, are less reactive than the dichloro substituted dyes, requiring an additional period of heating to over 60°C for the reaction with the glucose monomer to occur.

The preparation of the dyed dextran solution has been outlined in Section 6.3.3 of the Materials and Methods chapter. The method consists of two main stages, first the salting-on of the dye using sodium chloride solution and then the heated stage of the reaction between the dye and the dextran in the presence of sodium carbonate.

Figure 8.9:- General formula for Procion MX dyes.

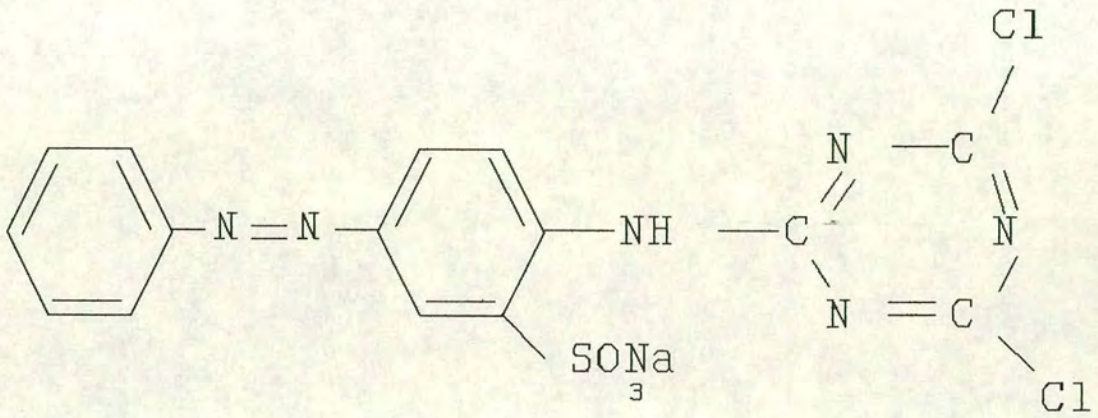

8.2.2 Spectrophotometric analysis of dyed dextrans.

A Philips SP5000 scanning spectrophotometer was used to determine the optimal reading wavelengths for the different dye and dyed dextran solutions prepared by the previously described method. The following solutions were diluted, as appropriate, for reading on the spectrophotometer:-

(1) Procion dye, unreacted in distilled water.

(2) Dextran solution in distilled water.

(3) Dyed dextran solution.

The spectrophotometer was set to a scan speed of 2 nm/s, covering the full range of the instrument, 190 to 850 nm, with the results presented in Table 8.3. A representative scan of the blue dyed dextran is presented in Figure 8.10.

Table 8.3:- Table of Absorption Peaks for Dextrans, Procion Dyes and Dyed Dextrans.

Test Material	Absorption Peaks (nm)
Procion Red Dye P-4BN	227 282 364-374 508-532
Procion Blue Dye SP-3R	204 222 252 576-628
Dextran solutions (all Molecular Weights)	272
Red Dyed Dextran (all Molecular Weights)	272 282 366 513-538
Blue Dyed Dextran (all Molecular Weights)	256 586-626

The cuvettes used during these experiments were not UV grade, explaining the initial high absorbance levels observed in the samples prior to 300 nm. The peaks observed in the visible range were found to be suitable for the analysis of the samples, therefore further analysis of the samples in the UV range was not required. The wavelengths selected for the red and blue dextrans were chosen as 525 and 590 nm respectively.

8.2.3 Dry weight analysis.

In order to calculate the yields obtained from the dyeing procedure, and the relationship between absorbance and dyed dextran concentration, dry weight experiments were carried out. Set volumes (100ml) of a known absorbance were measured into pre-weighed beakers. The beakers were then dried at 90°C until all of the residual liquid had evaporated. The beakers were reweighed and the differences in weight were used to calculate the yield and absorbance/concentration relationship.

Figure 8.10:- **Absorption scan of a 19kda dyed dextran.**

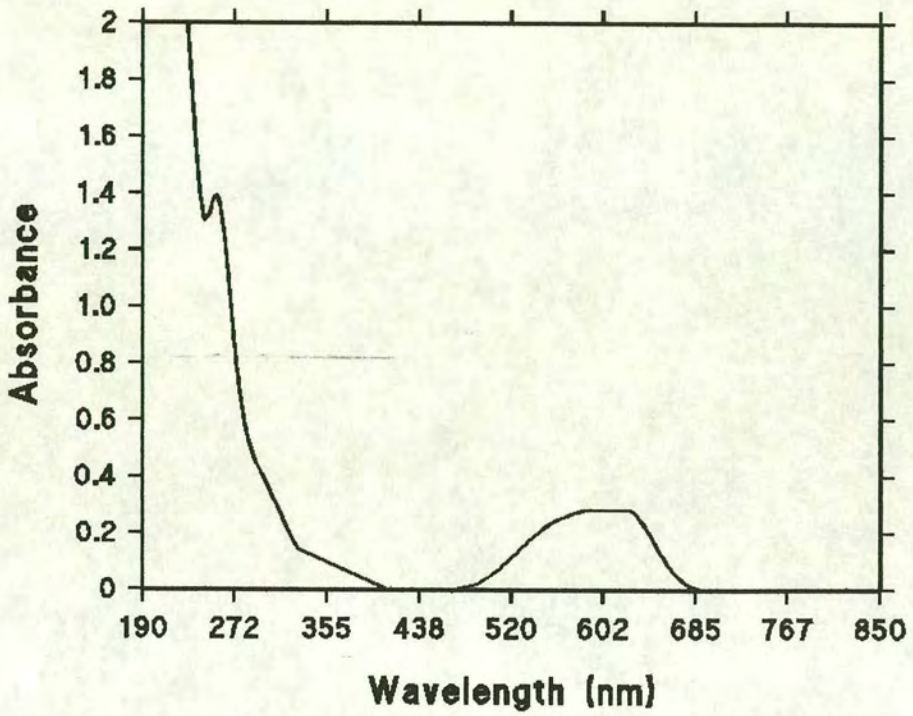

A plot of absorbance versus concentration for 19 kDa, blue dyed dextran is presented in Figure 8.11, with other correlations between absorbance, dry weight and yield for the different preparations of dyed dextran outlined in Table 8.4. All of the tested solutions returned a near linear correlation between absorbance and concentration.

The efficiency of the binding of the dye to the dextran was not examined. It can be seen from the **k** (gradient of the graph) values in Table 8.4 that there was a difference between the slopes of the dry weight calibration graphs (calculated using the method of least squares). Two explanations can be given for these results, either there was a different binding capacity for the dyes to the dextran molecules, reducing the

Table 8.4:- Correlations and recovery yields for Dyed Dextran solutions.

Dyed Dextran	**k** Where Conc. (g/l) = **k** * Absorbance (O.D.)	Correlation coefficient (r^2)	Percentage Recovery (Based on initial weight of dextran used)
Blue 19 kDa	2.88	0.99	69
Blue 87 kDa	5.26	0.99	48
Blue 162 kDa	0.13	0.99	65
Red 19 kDa	0.65	0.99	58
Red 162 kDa	2.07	0.99	73

absorbance of the sample, or more likely, the efficiency of binding varied in the preparation of the dye. In the latter case, a large proportion of undyed dextran in the sample would reduce the **k** value recorded from the calibration curve.

8.2.4 Viscometric analysis of the test solutions.

Dyed dextran solutions of known absorbance were compared with the viscosity of distilled water at room temperature using a U-tube viscometer (Technica, size A). The experimental apparatus measured the time taken for a known volume of test solution to pass between two points marked on the tube. By comparing the recorded time for the test solution against water, a direct measure of the solutions viscosity can be made, with the viscosity of distilled water being unitary (1 Centipoise or 10^{-3} Pa s).

For all of the test solutions used in this work the viscosity, at the concentrations used, varied by less than 10 % when compared to that of water. The results from the viscometric studies are presented in Table 8.5.

8.3 Small rig experiments using test solutions

This section describes the experiments carried out using the solutions characterised in the previous section.

8.3.1 Dyed dextran experiments

A limited series of dyed dextran experiments were carried out using the small rig designed by Burns (1991) and fibres with a pore size of 0.1 μm. Using a 19 kDa dyed dextran solution (1 gl^{-1}), the apparatus was operated in a similar fashion to that of the bioreactor, i.e. the upstream fibre as a crossflow filter and the downstream fibres as dead ended filters (with the flow from the outside of the lumen to the inside) under conditions similar to those found in the full scale device. This molecular weight of dyed dextran was used to simulate the behaviour of the bioreactor in the presence of a low molecular weight protein. Each of these experiments was carried out in duplicate, with the pooled results reported in the following sections. The conditions used were based on a supply fibre transmembrane pressure (TMP) of 1.2 psig, with a liquid flow rate of 12 ml min^{-1} and a sink fibre TMP of 0.8 psig. These values were selected from data obtained during the small rig bioreactor simulation.

Crossflow experiment

The conditions used in this experiment were that the supply fibre was maintained at a TMP of 1.2 psig and a liquid flow rate of 12 ml min^{-1}. The trends observed were similar to those reported in the distilled water tests carried out by Burns (1991), with a initial decline in flux to a steady state value of 2.4 $x10^{-2}$ $cm^3cm^{-2}min^{-1}$ (Figure 8.12). This was approximately half of the distilled water flux reported by Burns (1991) under similar operational conditions. The difference between the two values was related to the presence of dyed dextran in the test solution, and the resultant concentration polarisation of the fibres.

Figure 8.11:- Relationship between absorbance and dyed dextran (blue, 19 kDa)

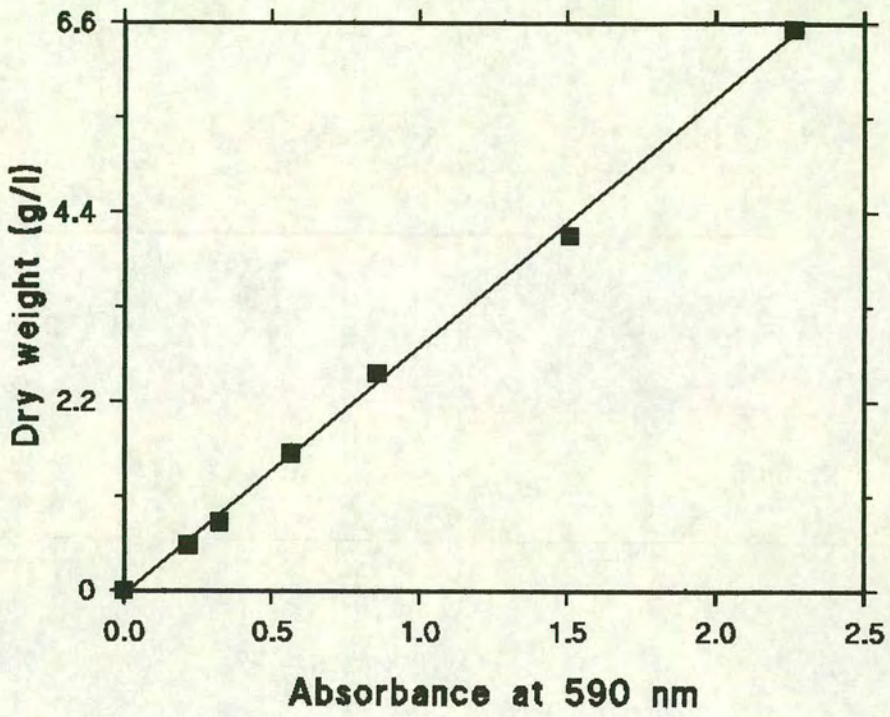

Table 8.5:- Viscosity of the different test solutions (based on 5 replicate tests per viscosity measurement).

Solution	Viscosity (μ_d/μ_w)
Distilled water	1.00 (σ=0.01)
Blue 19 kDa	1.10 (σ=0.02)
RPMI 1640	1.00 (σ=0.01)
RPMI 1640 with 5% Newborn calf serum	1.02 (σ=0.03)

The rejection ratios recorded during these experiments were found to rise over the first 16 h, reaching a steady value of about 0.27.

Dead end experiments

In these experiments the TMP of the two sink fibres was maintained at 0.8 psig. While the dead end experiments followed conventional filtration theory, with a volume related decline in flux from 1.3 to 0.3 $x10^{-2}$ $cm^3cm^{-2}min^{-1}$ (Figure 8.13), the rejection ratio at the end of the experiment was found to be lower than that of the crossflow filtration experiment, 0.1 versus 0.27. This may, in part, be explained by the differences in size between the dextran molecules and the pores, with the latter being significantly larger, and the different fouling mechanisms observed in the two modes of operation.

Small rig bioreactor simulation

Using one supply fibre and two sink fibres, the apparatus was operated in a similar manner to the previous experiments, with a supply and sink fibre TMP of 1.2 and 0.8 respectively. In Figure 8.15 it can be seen that flux decreased to a steady state of between 0.9 and $1x10^{-2}$ $cm^3cm^{-2}min^{-1}$ and a rejection ratio of 0.5 after 50 h of operation. The flux after 50 h was greater than that observed for dead end filtration after 24 h, 0.9 versus $0.3x10^{-2}$ $cm^3cm^{-2}min^{-1}$, suggesting that a lower rate of fouling had occurred on the downstream fibres. A comparison of the crossflow experiment and the bioreactor simulation experiment after 30 h suggests that fluxes were similar, indicating the greater influence of the supply fibres on the performance of the bioreactor simulation. This latter point was confirmed by the increased level of rejection observed after 50 h, suggesting that the flow of dextran through the apparatus was limited by the supply fibres rather than the sink fibres. This observation agrees with the reanalysis of the similar experiment in which distilled water was used.

Figure 8.12:- Dyed dextran (19 kDa) flux and rejection characteristics for a crossflow fibre.

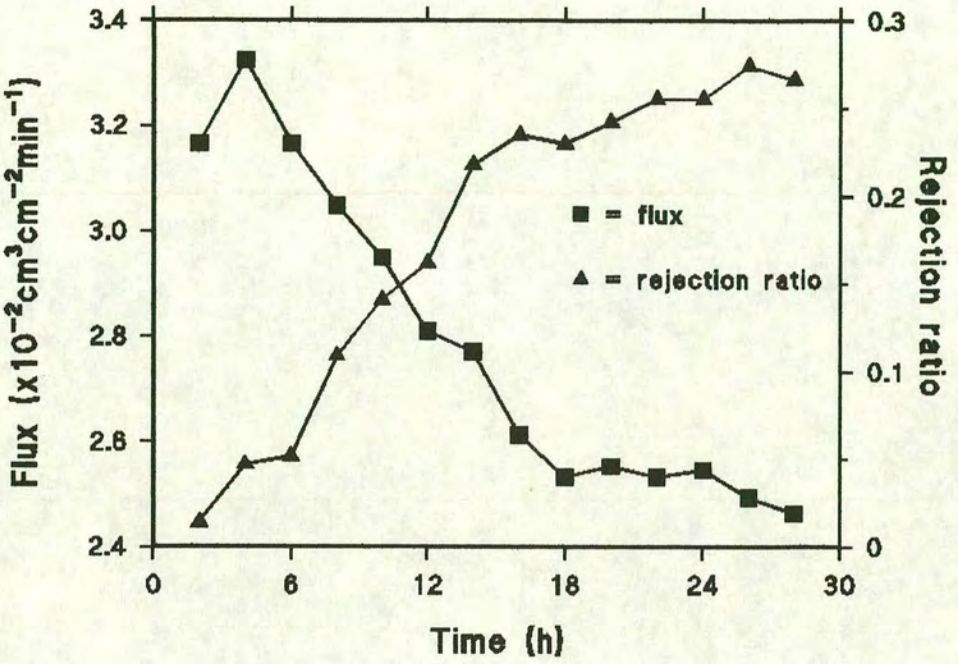

Figure 8.13:- Dyed dextran (19 kDa) flux and rejection characteristics for a dead ended fibre.

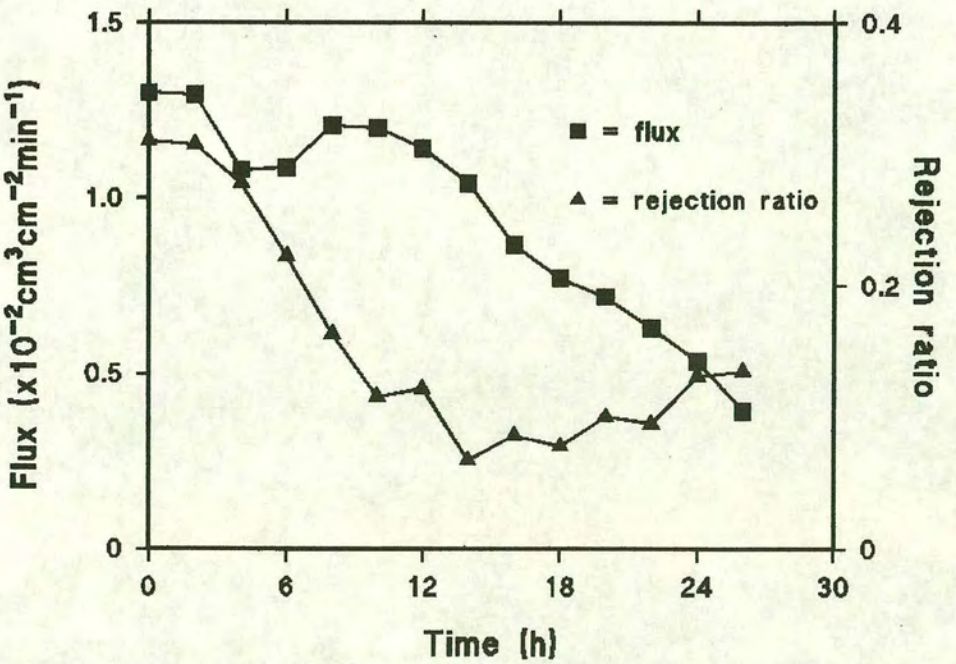

Figure 8.14:- **Dyed dextran (19 kDa) flux and rejection characteristics for a simulated bioreactor.**

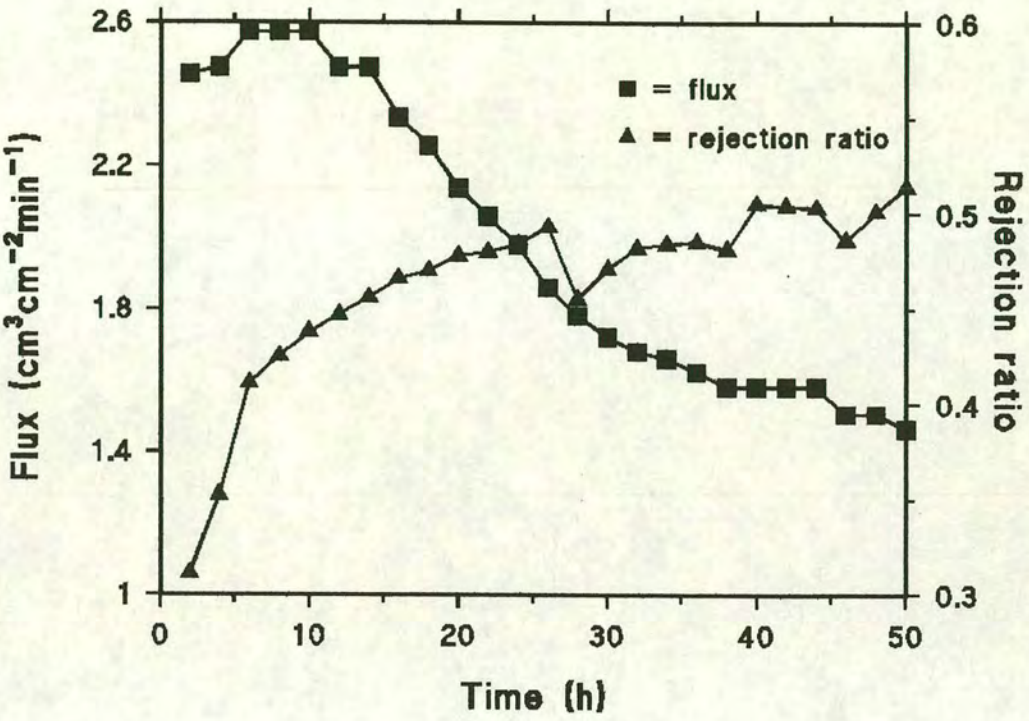

Summary

From these filtration experiments it would appear that the supply fibres were the key determinants of the flux and rejection characteristics of the bioreactor. The behaviour of the supply fibres agrees well with the basic theory discussed in Chapter 5. However, the combination of a surprisingly low rejection ratio and the flux decline observed in the dead ended fibre experiments would, at first, appear to contradict the described theory. It would be expected that, with a decrease in flux across the downstream fibres, the rejection ratios observed would also increase, however, this was not observed. One explanation for this result is that the small macromolecules (19 kDa) were not retained by the 0.1 μm diameter membrane pores. Whether this was due to the way in which the downstream fibres were operated, i.e. with the flow from the outside to the inside of the fibre, or some other factor could not be determined.

8.3.2 New born calf serum supplementation experiments

In this section a number of experiments (a minimum of 3) were carried out using the 'new style' design of bioreactor (0.1 μm supply: 0.1 μm sink fibres) and RPMI 1640, with and without 5% serum supplementation. These experiments were carried out during the sterility checking of the bioreactor circuit prior to the addition of cells to the bioreactor. The bioreactor circuit used during this experiment was operated under a recycling regime (Figure 6.6), with a liquid flow rate in the upstream fibres of 18 $l.h^{-1}$.

The main features of this experiment were to show the effects of serum addition upon the filtration rate through the bioreactor. The results of these experiments are summarised in Figure 8.15 where the transreactor pressures reported were calculated according to Equation 8.5.

$$\textit{Transreactor pressure } (TRP) = P1 - P3 \quad (8.5)$$

$$\textit{Where } P1 = \textit{average of upstream pressures,}$$
$$P3 = \textit{sink pressure}$$

The effects of increasing the transreactor pressure in the presence of unsupplemented RPMI 1640 leads to an increase in the flux across the bioreactor, as expected from standard filtration theory. A direct comparison of the serum supplemented and the serum free RPMI shows a reduction in flux to less than half of the value recorded with unsupplemented RPMI 1640, highlighting the fouling effects of serum in the feed medium.

These experiments confirmed that basic filtration theory applied to the bioreactor, with respect to increased flux on increasing the pressure differential across the bioreactor and the influence of protein in the fouling of the bioreactor.

Figure 8.15:- **Influence of transreactor pressure on the filtration rate for the bioreactor.**

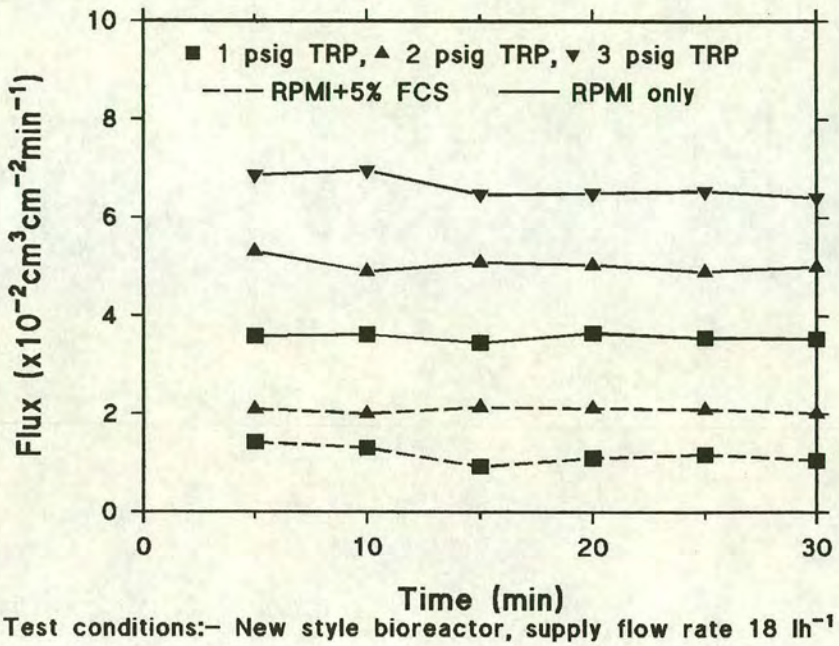

Test conditions:– New style bioreactor, supply flow rate 18 lh^{-1}

8.4 Summary

The re-evaluation of Burns' (1991) distilled water experiments and the extension of this work to include the use of dyed dextran solutions and new born calf supplemented medium allowed a preliminary prediction of the expected behaviour of the bioreactor to be made. As expected the test modules were found generally to comply with the basic filtration theory described in Chapter 5, with flux being a pressure driven process and the use of protein (or dyed dextran) supplemented feed stocks leading to flow limitations. The influence of protein supplementation was found to be greatest in the supply fibres which, while still freely allowing the passage of low molecular weight metabolites, restricted the passage of higher molecular weight moieties due to concentration polarisation and fouling at the membrane surface. Surprisingly the passage of macromolecules across the sink fibres, effectively operated as dead ended

filters, was less restrictive. This was thought to be related to a combination of the tortuous geometry of the pore, and its size in relation to the molecular weight of the dyed dextran used, resulting in the reduced the fouling of membrane.

Altshuler *et al.* (1986) have described varying degrees of rejection by single circuit hollow fibre bioreactors and the ways in which these affect cell growth and product collection. The first of these was that lower viable cell numbers were observed in the bioreactors with 10 and 50 kDa MWCO ($8x10^6$ viable cell ml^{-1} of growth space) than in the 100 kDa bioreactor ($12x10^6$ viable cells ml^{-1}). They attribute this difference in the cell numbers to a poor supply of essential growth factors to the biomass due to rejection by the 10 and 50 kDa pore sizes present in the other bioreactors. The second observation was that antibody (IgG of 156 kDa) was observed to cross from the growth space back into the feed stream in the 100 kDa MWCO hollow fibre unit. They also suggest that this leakage of IgG (156 kDa) into the feed vessel could be used as a means of product collection.

These observations would appear to support the findings of this work by considering the single circuit bioreactor to be a crossflow filter when the flow is from the fibre lumen to the growth space and as a dead end filter when the flow is from the growth space back into the fibre lumen.

The use of a 19 kDa dyed dextran to simulate protein behaviour within the bioreactor was justified given that low molecular weight species are present in the serum component of the medium, for example insulin (6 kDa) and transferrin (66 kDa). M^{c}Donogh *et al.* (1992) identify small macromolecules as being the determinants of filter performance by occluding pores during the initial stages of filtration. Where the use of dyed dextrans becomes invalid is the use of a pure mixture to mimic the behaviour of a complex mixture such as serum. The filtration behaviour of complex mixtures differs significantly from those of the individual components through the interactions between the species. For example Zhang (1993) describes the increased rejection of BSA in the presence of IgG, possibly due to aggregate formation between the BSA and IgG.

Under simulated operational conditions it was found that the transmembrane pressure of the supply fibres was the primary determinant of the flux across the bioreactor, despite a parity in pore sizes between the two circuits and a ratio of supply to sink fibres of 1:2. This suggests that the fouling of the supply fibres dictates the behaviour of the bioreactor.

By increasing or decreasing the pore size of either the upstream or downstream fibres, the pressure profiles and subsequently the flow regime within the bioreactor could be altered from radial to Starling flow. Flux was shown to be pressure related, with the main limitation to flow being the composite of concentration polarisation, fouling and the inherent resistance of the membrane. In a system containing two sets of fibres with different pore sizes, flow was shown to take the path of least resistance, travelling from a higher to a lower pressure. If these conditions were satisfied by the outlet of the supply fibres, then the flow would return to the supply fibres leading to the adoption of a Starling flow regime. Ideally the selection of fibres should favour the use of the lowest resistance filters on the sink circuit, leading to the major flow regime within the module being radial. This regime would tend to favour the collection of product from the waste stream, with the use of higher molecular weight cutoff membranes on the downstream circuit. A design in which the product was to be concentrated in the cellular growth space would have to rely upon membranes with smaller pore sizes e.g 30 kDa for the supply fibres and 100 kDa for the sink fibres.

The effects of fouling on cartridge bioreactors would be expected to be high, given that the cells continually produce macromolecules and the flow regime present in single fibre bioreactors would suggest that this would be a problem. The work of Piret and Cooney (1990) using flow reversal would appear to suggest that fouling is a problem, with their approach being analogous to backflushing. Using this approach extends the life of the bioreactor although it is reported to only delay the effects of fouling (personal communication, Robin Hood, FSM Technologies, Clydebank, Glasgow). Another aspect of the operation of the single fibre bioreactors that reduces the level of fouling is associated with the way in which the product is harvested. Antibody (or product) is usually harvested by venting the extracapillary space, with

the medium flow out of the growth space mediated by the flow from the hollow fibres. This again is analogous to backflushing, which would lead to the removal of foulant layers from the fibre bundle.

Implications for the full sized bioreactor

Several features influencing the behaviour of the full scale bioreactor were noted from these experiments. Under conditions where the test medium did not contain any protein supplement, the bioreactor was found to conform to standard filtration theory, with an increase in flux with increasing transmembrane pressure. When the test solution contained macromolecular species, flux was observed to drop to approximately one third of the distilled water flux, while the rejection of macromolecules by the supply (crossflow) fibres increased.

If the cells require the presence of a specific protein in the growth space for maximum viability, and the protein concerned never reaches the cells due to rejection by the supply membranes, this will obviously affect the productivity of the bioreactor.

Chapter 9

Growth and metabolism of ES4

9.0 Introduction

This chapter describes the batch growth characteristics of the murine hybridoma, ES4, cultured in two different recipes of RPMI 1640. By understanding the growth requirements and potential limitations associated with toxic metabolites, an indication of the environmental parameters important in the growth of this cell line could be made.

The first formulation, subsequently referred to as Searle's medium (based on Searle's modification of RPMI 1640), was a specially pre-formulated medium which contained 1 mM glutamine in its initial form and had been used by an on campus company (Bioscot Ltd) for the culture of ES4. The second formulation, shortened to Gibco medium, contained no glutamine in its initial form and was used in a series of medium modification experiments. The medium modification experiments were aimed at preventing the potentially toxic build up of ammonia in the culture medium through the partial replacement of the main source of ammonia, glutamine, by an intermediary of the TCA cycle, α-ketoglutaric acid.

Section 9.1 describes the batch growth characteristics of ES4 in the medium used for the bioreactor experiments, i.e. Searle's medium. Sections 9.2 describes the development of two protocols used for the determination of glutamine and α-ketoglutarate levels in the medium modification experiments. Section 9.3 describes foundation experiments carried out to assess the effects of glutamine replacement by α-ketoglutarate (abbreviated to α-kg for the remainder of the chapter) using Searle's medium. Section 9.4 describes experiments that were carried out using Gibco medium to assess the effects of α-kg in the absence of glutamine. A summary and discussion of the results described in this chapter is provided in Section 9.5.

The results from these experiments showed that the partial replacement of glutamine by α-kg had no appreciable effect on the growth and antibody production of the cells, while having a significant effect on the ammonia levels observed at the end of each batch growth period. The cells were unable to grow in the absence of glutamine, suggesting that while the α-kg was able to substitute for glutamine in some of the metabolic functions within the cell, it was not capable of fully replacing glutamine.

9.1 ES 4 batch growth characteristics in Searle's medium

This section summarises the growth curve data obtained using ES4, reporting the mean specific growth rates, substrate utilisation (e.g. glutamine and glucose), and metabolite production rates (e.g. antibody, ammonia and lactate) and their associated standard deviations (σ). The medium was prepared according to the protocol described in Chapter 6 (Section 6.1). The equations used for the calculation of the various rates based on those reported by Butler (1991).

9.1.1 Experimental method

Growth experiments were carried out using 80 cm^2 culture flasks containing 50 ml of 5% foetal calf serum supplemented Searle's medium containing a total of 3mM glutamine. Unless otherwise stated, all the various media used for this chapter were supplemented with 5% serum. The cells were inoculated at $1x10^5$ viable cells ml^{-1} of medium per test flask. The preculture, harvesting, sampling and assay protocols used during these experiments are described in Chapter 6. The results reported in Table 9.1 were based on a single experiment containing 5 replicate flasks (n = 5). The pooled values reported in Table 9.2 were based on 8 sets of experiments in which growth curves were examined, with a maximum of number (n) of 29 flasks. Figures 9.1 to 9.4 represent a typical set of results for a growth curve (based on one of the replicate experiments summarised in Table 9.1), with the reported mean values being based on the assessment of relative cell numbers or substrate/metabolite concentrations from three individual samples taken at each time point. The error bars reported in these, and subsequent figures, in this chapter represent the standard deviation of the mean.

Where the number of flasks from which the reported rate was based falls below n = 29, the particular assay had either not been available in a number of experiments, e.g. prior to the development of the glutamine assay, or was not carried out.

9.1.2 General growth characteristics

Typical growth and substrate/metabolite curves were observed for Searle's medium formulation. The viable cell number was observed to increase to a mean value of 5.8×10^5, with a standard deviation of 0.2×10^5 cells ml^{-1} (n=29). The non-viable population increased gradually with time during the observed period of growth, with a higher death rate observed at the end of the log phase of growth.

Substrate and metabolite levels were observed to be at their minimum (substrate) and maximum (metabolite) concentrations after the stationary phase of growth. Glucose and glutamine concentrations were routinely observed to fall from 12 and 3 mM to below 4 and 1 mM respectively. Lactate and ammonia concentrations were observed to increase to maximum values of 17 and 3.5 mM respectively. The production of antibody followed a similar profile to that of lactate and ammonia, with a mean value of 15 μgml^{-1} (σ=2.45 μgml^{-1}) observed at the end of the culture period (n = 29).

9.1.3 Specific growth rate

The specific growth rate (μ, h^{-1}) for each culture was calculated from the gradient of a plot of the natural logarithm of cell number against the time during which the cells were in the exponential phase of growth. Equation 9.1 describes the relationship between cell number, time and the specific growth rate with a full derivation given in Butler (1991).

$$\ln N = \ln N_0 + \mu t \qquad (9.1)$$

Where N = *final cell number,*
N_0 = *initial cell number,*
t = *time*

The cell specific growth rates calculated from these experiments were based on a minimum of three sample times per growth curve, with a majority of the rates based on four or more time points. The correlation coefficients for the calculated lines of best fit for these curves were usually significant at the 95% level, according to pre-tabulated significance levels, as reproduced in Clarke (1994). In cases where the calculated correlation coefficients fell below the 95% significance level, the sample rate was either too low to realise values of r above this level, or the duration of the exponential phase of growth was insufficient for this level of significance. However, all of the correlation coefficients were significant at the 90% level.

A comparison of the mean specific growth rate reported in Tables 9.1 for five flasks in one experiment (0.024 h^{-1}, σ=0.003) with that reported for the mean of the larger number of samples (0.023 h^{-1}, σ=0.003, n=29), Table 9.2, using Students' t-test, showed that there was not a significant difference between these two means at the 5% level. Students' t-test was used for the comparison of means throughout this chapter.

9.1.4 Specific metabolic rates

Specific substrate utilisation and metabolite production rates over a sustained period of exponential growth were calculated according to Equation 9.2 (Butler, 1991). Values are reported in millimoles (mmole) or μg 10^{-6} cells h^{-1} along with their standard deviations. Figures 9.2 to 9.4 show typical batch culture substrate, waste metabolite and antibody production profiles for ES4. Table 9.1 summarises the calculated rates for n=5 flasks, with the values for the larger sample size reported in Table 9.2.

$$K = \frac{\Delta C}{t} \cdot \frac{\ln N - \ln N_0}{N - N_0} \qquad (9.2)$$

Where ΔC = *Concentration change of moeity during time* (t)
N, N_0 = *cell concentrations*

Students' t-tests confirm that the values reported in Tables 9.1 and 9.2 do not differ significantly at the 5 % level, with the exception of K_{gln}.

Table 9.1:- Growth characteristics of ES4 cultured in RPMI 1640 (Searle's modification) based on a single experiment with 5 replicate flasks

Growth parameter	Mean	Sample size (n, flasks)	Standard deviation (σ)
Specific growth rate (μ , h^{-1})	0.023	5	0.002
Glucose utilisation rate (K_{glc}, mmole 10^{-6} cells h^{-1})	0.27	5	0.03
Glutamine utilisation rate (K_{gln}, mmole 10^{-6} cells h^{-1}	0.074	5	0.002
Ammonia production rate (K_{amm},mmole 10^{-6} cells h^{-1})	0.072	5	0.009
Lactate production rate (K_{lac},mmole 10^{-6} cells h^{-1})	0.34	5	0.14
Antibody production rate (K_{mab},μg 10^{-6} cells h^{-1})	0.40	5	0.07

Table 9.2:- Comparison of ES 4 growth characteristics from eight different culture experiments.

Growth parameter	Mean	Sample size (n, flasks)	Standard deviation (σ)
Specific growth rate (μ , h^{-1})	0.024	29	0.003
Glucose utilisation rate (K_{glc}, mmole 10^{-6} cells h^{-1})	0.27	29	0.04
Glutamine utilisation rate (K_{gln}, mmole 10^{-6} cells h^{-1}	0.082	15	0.007
Ammonia production rate (K_{amm},mmole 10^{-6} cells h^{-1})	0.080	29	0.009
Lactate production rate (K_{lac}, mmole 10^{-6} cells h^{-1})	0.34	15	0.1
Antibody production rate (K_{mab}, μg 10^{-6}cells h^{-1})	0.43	26	0.09

Figure 9.1:- Growth of ES4 in RPMI 1640 (Searle's modification)

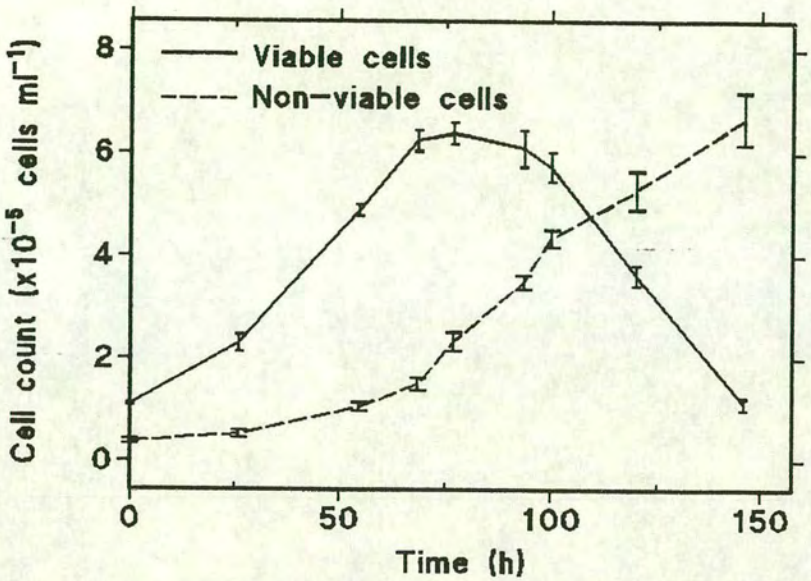

Figure 9.2:- Glucose and Lactate profiles for ES4

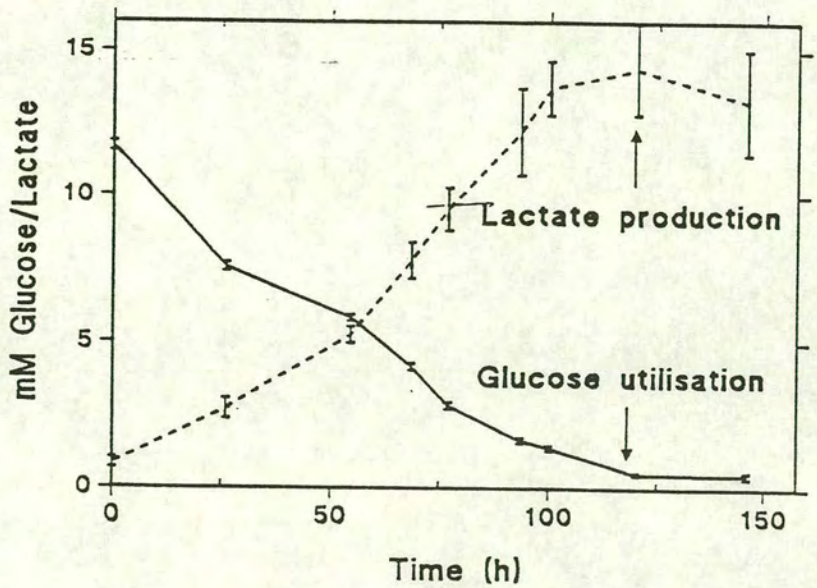

Figure 9.3:- Glutamine and ammonia profiles for ES4

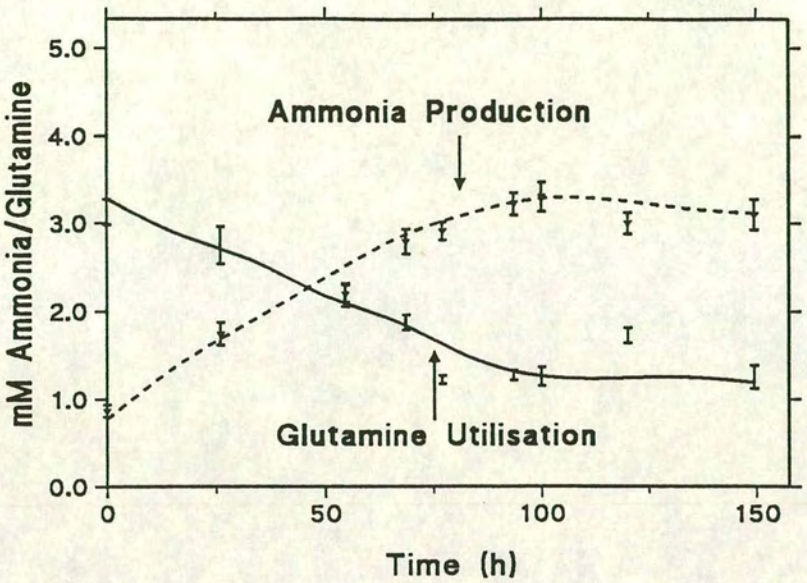

Figure 9.4:- Antibody profile for ES4

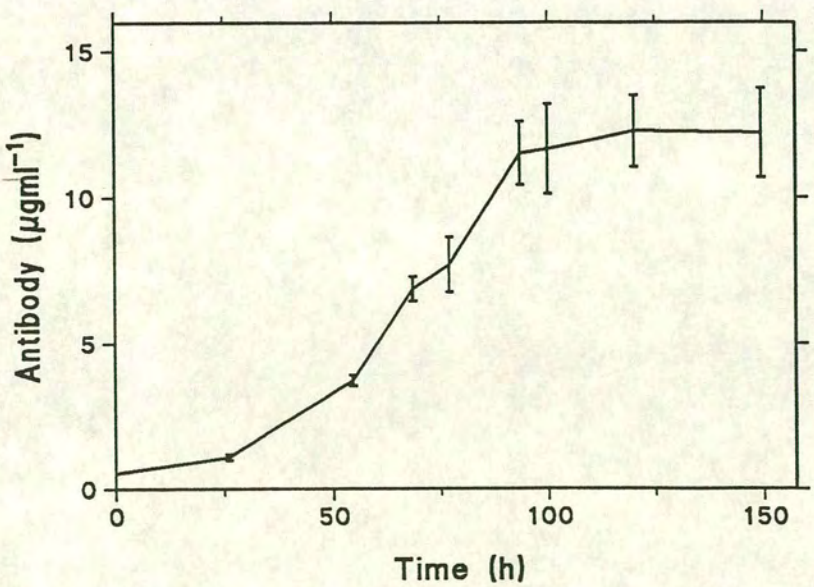

9.2 Developing assays for glutamine and α-ketoglutaric acid

In order to ascertain the glutamine utilisation rates and monitor their replacement by α-ketoglutaric acid, assays had to be developed for the determination of their levels in samples taken from the culture experiments. Both assays were based on the enzymatic modification of the test species, with the amination (addition of an NH_3 group) of α-kg and the deamination of glutamine. The utilisation rates for these species were calculated in a similar manner to that described in Section 9.1.4.

9.2.1 Glutamine assay

The protocol outlined in Section 6.2.4 is based on a two stage process for assessing glutamine levels in test samples. The first step involves the enzymatic degradation of L-glutamine to L-glutamate using glutaminase, according to the following reaction.

$$\text{glutamine} \xrightarrow{\text{Glutaminase}} \text{glutamate} + NH_4^+$$

This reaction leads to the liberation of 1 mole of ammonium ions per mole of glutamine. The concentration of liberated ammonium ions could then be determined using the ammonia assay protocol (Section 6.2.3). By comparing the relative concentrations of ammonium ions in the sample before and after glutaminase treatment an estimation of glutamine levels could be calculated.

The level of glutaminase used in this assay was similar to that reported by M^{c}Queen *et al.* (1990a) who used a similar method to determine glutamine levels in hybridoma culture. Sigma have also developed an assay which follows the first stage degradation of glutamine by glutaminase, by a second enzymatic degradation of glutamate, using L-Glutamic Dehydrogenase, to α-ketoglutarate.

Figure 9.5 shows the time related deamination of glutamine, carried out according to the protocol in Section 6.2.4 using known standards prepared in 5% foetal calf serum supplemented RPMI 1640 (Searle's modification). Each point represents the mean of

Figure 9.5:- Glutaminase reaction curves

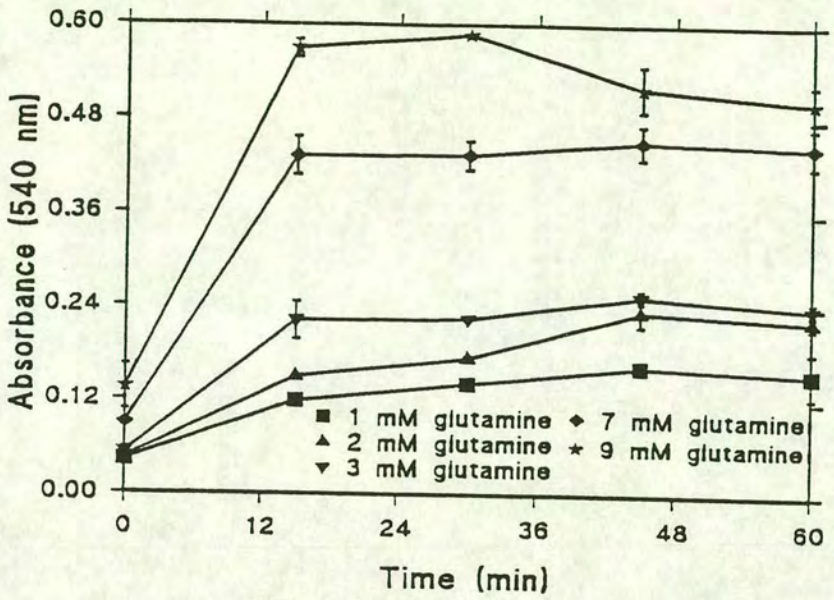

three individual samples with their standard deviation reported in Figure 9.5.

Figure 9.6 shows the relationship between glutamine degradation and ammonia production, the least squares line of best fit for the first 6 points was calculated to be $y = 0.91x + 0.70$, where x corresponds to the start concentration of glutamine and y corresponds to the concentration of liberated ammonia, with a correlation coefficient (r) of 0.996. This assay was observed to be inaccurate above sample concentrations of 6 mM, primarily due to the time for which the sample was incubated at 37°C with the enzyme. While extending the incubation time increased the level of deamination observed at higher glutamine concentrations, the intended use of the assay was to be below 4 mM for which a 30 min incubation time was sufficient.

Figure 9.6:- Glutamine standard curve

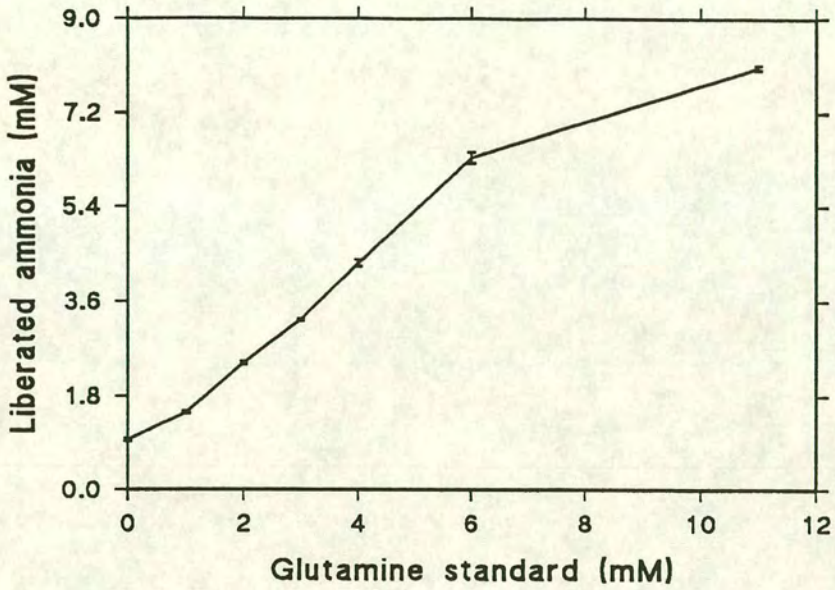

9.2.2 α-kg assay

This assay was modified from a quality control procedure used by Sigma to determine the activity of L-Glutamic Dehydrogenase (L-GLDH), a copy of which was kindly provided by Sigma Technical Services. The basis of the assay was as follows:-

$$\alpha\text{-kg} + \text{ß-NADH} + NH_4^+ \xrightarrow{\text{L-GLDH}} \text{L-glutamate} + \text{ß-NAD} + H_2O$$

This assay measures the conversion of ß-NADH to ß-NAD by monitoring a reduction in the absorbance of the assay solution at 340 nm. As the conversion of ß-NADH and α-kg are linked on a mole per mole basis, the measured reduction of ß-NADH to ß-NAD indirectly measures the level of α-kg in the test sample.

Several modifications were made to the Sigma protocol, replacing the Triethanolamine buffer by a phosphate buffer of the same concentration and pH. As the Sigma protocol

Figure 9.7:- Reaction curve for L-Glutamic dehydrogenase

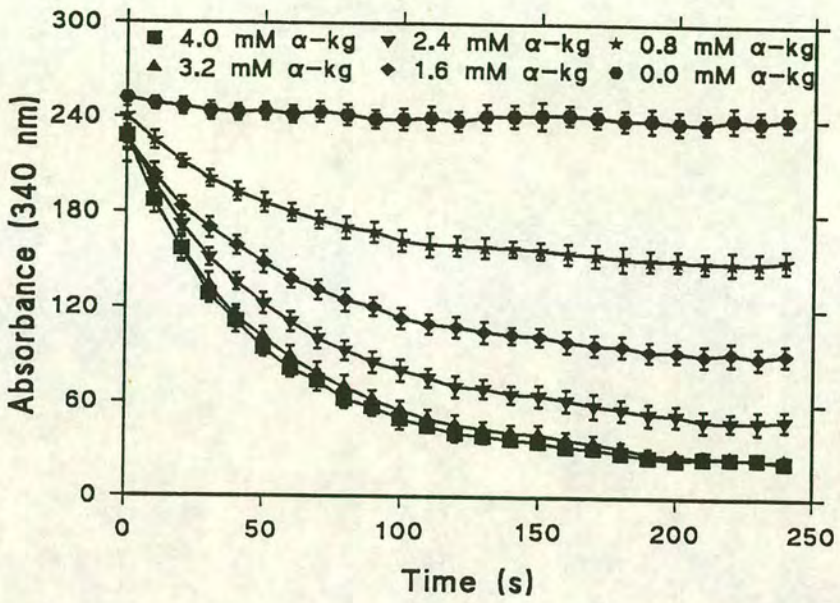

was designed to measure the activity of L-GLDH, the primary substrate (α-kg) was provided in excess. For this protocol the test levels of α-kg (i.e. samples and standards) were diluted so that the final α-kg concentration fell below 0.05 mM to ensure that this was the limiting substrate. The relative volumes of the enzyme mixture and sample used in the assay were also reduced to 0.301 (Modified) from 3.01 ml (Sigma) in order that a microplate reader (Dynatech MR5000) could be used. The use of the microplate reader led to a reduction in the quantities of chemicals required for the assay procedure, while increasing the number of samples that could be analyzed at any one time. As the microplate reader was computer interfaceable, the results from a single test could be stored on a PC and imported directly into a suitable spreadsheet package for analyses.

The L-GLDH reaction profile for a number of concentrations of α-kg and the associated calibration curve for these standards are reported in Figures 9.7 and 9.8.

Figure 9.8:- α-kg calibration curve

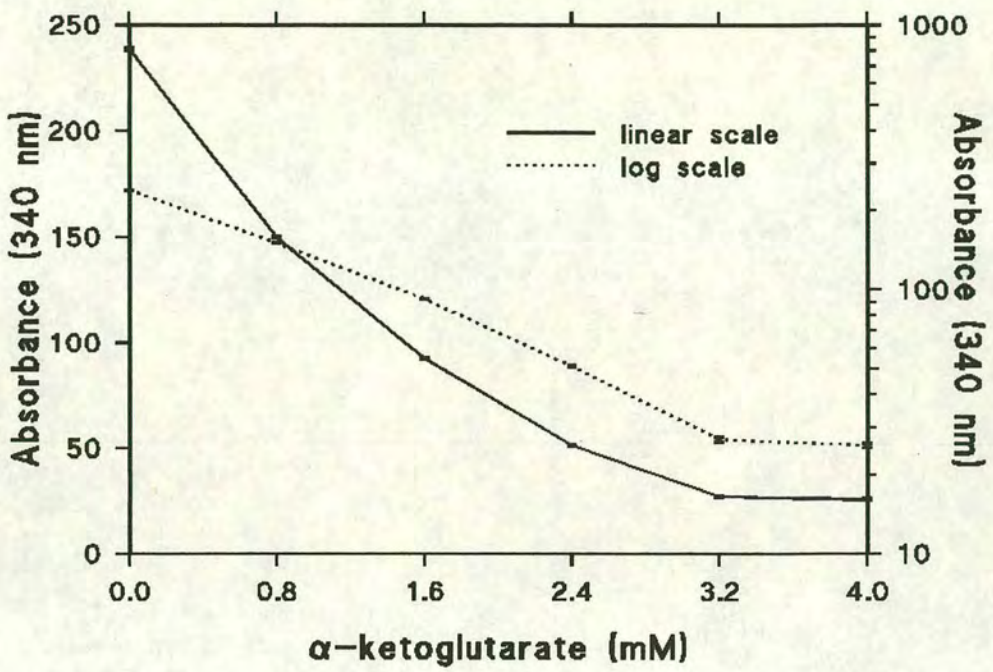

These curves were based on the mean of eight individual assays at each time point, and the concentration of α-kg. The α-kg was prepared in 5% serum supplemented RPMI 1640 (Gibco, glutamine free formulation), with the standard deviations reported for each sample point. The protocol used in these assays has already been reported in Chapter 6 (Section 6.2.5).

The line of best fit for the curves presented in Figure 9.8 was determined from a semi-log plot (dotted line) giving the following equation for the straight line fit, $\log(y) = -0.29x + 2.40$, $r = 0.997$, where y corresponds to the absorbance at 340 nm and x the concentration of α-kg. According to the calibration curve reported in Figure 9.8, this technique gives a linear relationship between absorbance (340 nm) and α-kg concentration up to 3.2 mM (sample concentration). Above 3.2 mM the curve was observed to plateau. Over the range of experimental values examined, i.e. 2 mM α-kg or lower, the linear relationship between absorbance and α-kg concentration was found to have a high correlation coefficient (above 0.975).

9.2.3 Conclusions

Two assays were developed using enzymes which either removed ammonia from glutamine (glutaminase) or added ammonia to α-kg (L-GLDH). In the glutamine assay the concentration of liberated ammonia was assessed using the protocol described in Chapter 6. From the calibration curves, based on known standards prepared in serum supplemented medium, a linear relationship was determined with a correlation coefficient which was significant at the 95% level.

The α-kg assay monitors the conversion of ß-NADH to ß-NAD, allowing an indirect measurement of α-kg levels to be made. A log-linear relationship was found to provide the best line of fit, with a correlation coefficient significant at the 95% level.

These assays were then used to determine the levels of these two species in a number of medium modification experiments investigating the partial or total replacement of glutamine by α-kg.

9.3 Initial glutamine replacement experiments

Ammonia from glutaminolysis and the decomposition of glutamine has been identified by several groups as a potentially toxic metabolite limiting the growth of hybridomas in batch culture (Section 3.2.4). Wilson (1992) carried out a range of experiments determining the sensitivity of ES4 cells to ammonia by the supplementation of medium with ammonium chloride prior to the start of the experiment, concluding that levels up to 3 mM had little effect on the cells. Between 3 and 3.4 mM, the growth rate of the cells was observed to decline, leading to the total inhibition of growth at 4 mM. Figure 9.3 shows that the levels of ammonia in batch culture can reach 3.5 mM, which would affect the growth of the cells.

It was originally envisaged that the hollow fibre bioreactor would require the recycling of medium throughout the bioreactor circuit, in order to fully utilise the nutrients in the RPMI 1640. Under these conditions inhibitory levels of ammonia in the bulk

Figure 9.9:- The primary role of glutamine in the cell

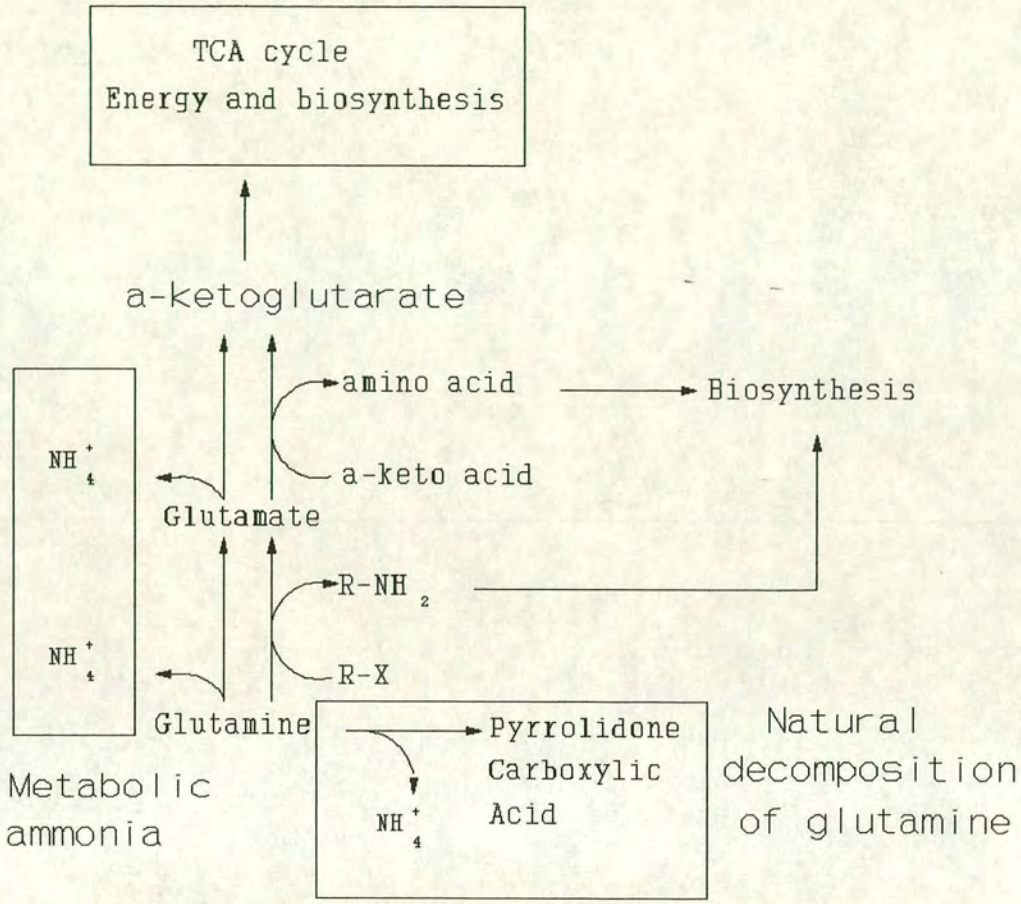

medium were predicted, affecting cell viability and growth within the bioreactor. As glutamine was identified as the principal source of metabolic ammonia, an alternative was sought that could partially or fully replace the cells' requirement for this glutamine. The sodium salt of α-ketoglutarate, referred to as **α-kg** in subsequent text and figures, was chosen. The rationale for this selection is discussed in the following paragraphs.

The role of glutamine in the cell

Based on the summary provided in Chapter 3 and illustrated in Figure 9.9, the fate of glutamine in the cells can be categorised as follows:-

(1) Biosynthesis, either directly as glutamine, or alternatively as an intermediate of glutaminolysis or the TCA cycle.

(2) As an energy source, primarily via the TCA cycle.

(3) Natural decomposition to a pyrrolidone form.

(4) Direct integration into proteins.

All of these pathways lead to the formation of metabolic ammonia. The liberation of ammonia from glutamine, via glutaminolysis, results in the formation of α-ketoglutarate, an intermediary of the TCA cycle. The direct addition of α-ketoglutarate to the medium was expected to allow either its direct integration into the TCA cycle, reducing the requirement for the breakdown of glutamine via glutaminolysis, or as a sink for ammonia via transamination reactions to form glutamate.

9.3.1 Glutamine replacement using Searles medium

The first series of experiments was carried out using Searle's medium supplemented with 5% foetal calf serum, glutamine and α-kg (Table 9.3). Each of the two sets of experiments was carried out using three 80 cm^2 flasks containing 50 ml of the appropriate test mixture. A minimum of two cell counts were taken per sample, at each time point, with the analyses of the various substrate and metabolite concentrations carried out in duplicate.

The mean cell and substrate/metabolite profiles, along with their associated standard deviations are reported in Figures 9.10 to 9.13, with the mean production and utilisation rates and their standard deviations summarised in Table 9.4. It should be noted that all of the flasks of medium used in this and subsequent sections were supplemented with 5% foetal calf serum.

Growth rates

The viable cell plots obtained as curves based on flasks 3 to 7 show similar profiles, with the main differences occurring in the duration of the lag period at the start of the culture period. Thereafter the observed growth rates (μ) for these conditions were observed to be similar, ranging from 0.024 to 0.027 h^{-1}. These values

Table 9.3:- Test conditions used in the replacement of glutamine.

Condition No.	RPMI 1640 + sodium pyruvate + Pen./ strep	Foetal calf serum (5% v/v)	Glutamine (mM)	α-keto-glutarate (mM)
1	+	-	1.0	0.0
2	+	+	1.0	0.0
3	+	+	1.0	2.0
4	+	+	1.5	1.5
5	+	+	2.0	1.0
6	+	+	2.5	0.5
7	+	+	3.0	0.0

did not differ significantly at the 5% level from the data presented in Table 9.2 when Students' t-test was applied. This suggests that the partial replacement of glutamine had little effect on the growth rate of the cells, when compared with the medium containing 3 mM glutamine. The maximum viable cell counts for these flasks also fell within the range reported in Section 9.1.2, i.e. 5.8×10^5 cells ml^{-1} ($\sigma = 0.22 \times 10^5$).

Growth was also observed for Condition 2 (1.0 mM glutamine+5% serum),however, the growth rate was shown to differ significantly from the mean growth rate reported in Table 9.2), with a lower maximum viable cell count of 4.5×10^5 cells ml^{-1}. This differs from the 2 mM α-kg supplemented flask which showed little difference from the growth rate reported in Table 9.2, suggesting that the presence of α-kg as a supplement to glutamine was beneficial to cell growth. No growth was observed under conditions where no serum supplementation was employed (i.e. Flask 1, Table 9.3).

Figure 9.10:- Growth profiles for initial glutamine replacement experiments

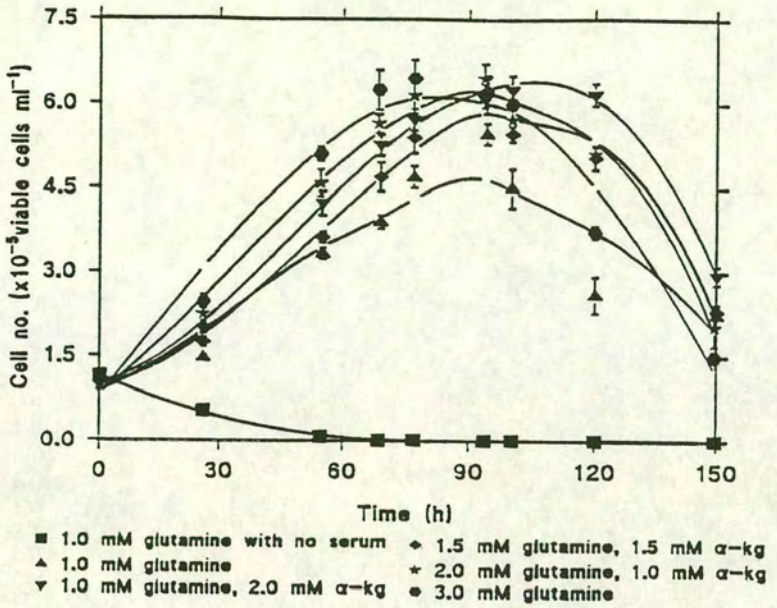

Figure 9.11:- Glucose profiles for initial glutamine replacement experiments

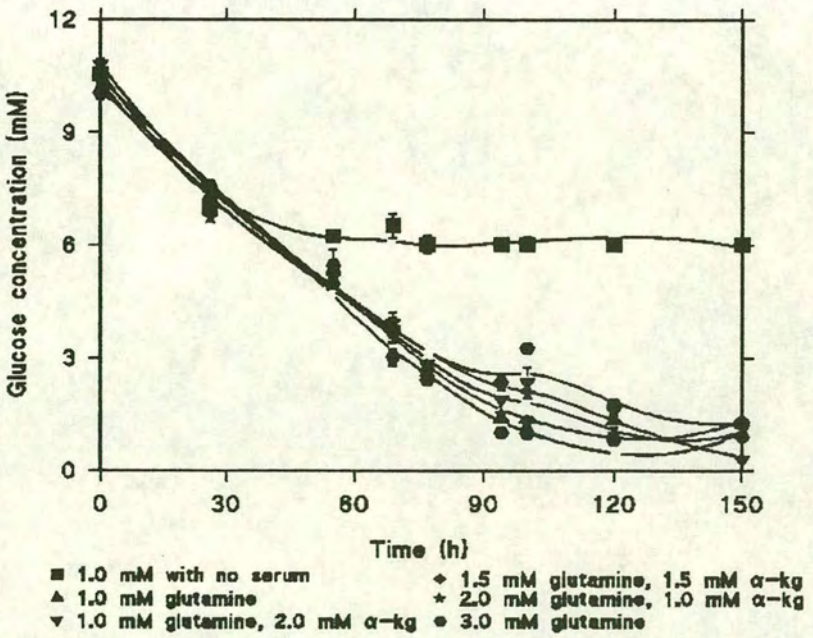

Figure 9.12:- Ammonia profiles for initial glutamine replacement experiments

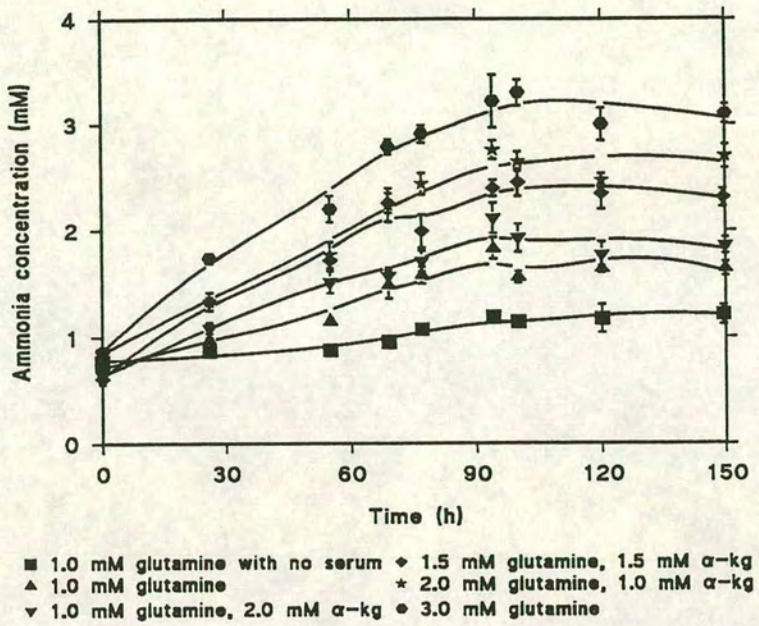

Figure 9.13:- Antibody profiles for initial glutamine replacement experiments

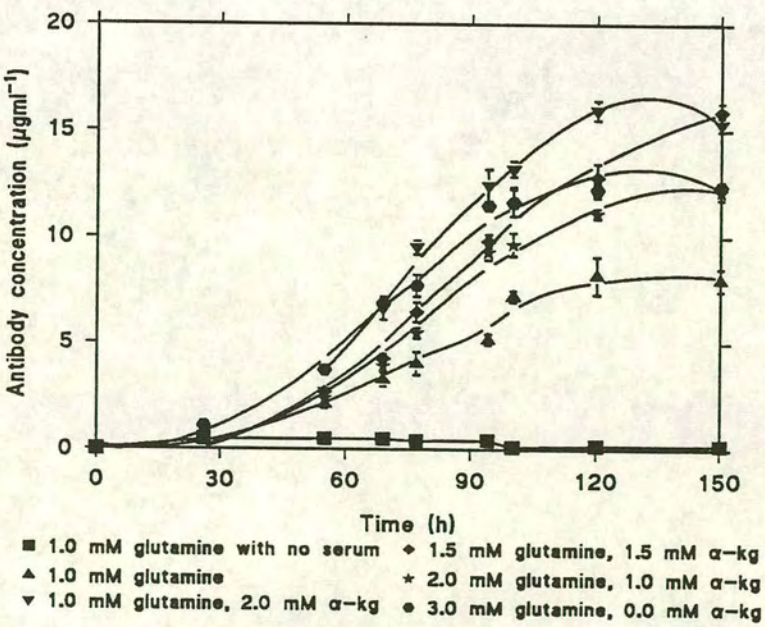

Table 9.4:- Calculated growth and metabolic rates for Figures 9.10 - 9.13 (n=6, 3 flasks per condition, 2 experiments)

Flask No.	μ	K_{glc}	K_{amm}	K_{mab}
1	-	+	+	+
2	0.019 σ=0.002	0.427 σ=0.032	0.046 σ=0.004	0.389 σ=0.083
3	0.024 σ=0.001	0.362 σ=0.023	0.052 σ=0.005	0.459 σ=0.069
4	0.024 σ=0.002	0.372 σ=0.031	0.079 σ=0.004	0.477 σ=0.053
5	0.026 σ=0.002	0.340 σ=0.023	0.072 σ=0.005	0.354 σ=0.042
6	0.027 σ=0.002	0.361 σ=0.019	0.085 σ=0.004	0.359 σ=0.051
7	0.027 σ=0.0013	0.359 σ=0.021	0.089 σ=0.003	0.452 σ=0.044

+ = observed utilisation/production of metabolite or substrate, no rate calculated. - = no growth observed. For the definition of, and units for, growth and metabolic rates, please refer to Table 9.2.

Glucose utilisation

The glucose utilisation profiles presented in Figure 9.11 were similar for Conditions 3 to 7, falling from an initial value of 11.6 mM to a minimum value of 1 mM, with the mean glucose utilisation rates presented in Table 9.4. The mean utilisation rate calculated for Condition 2 was significantly different from that reported in Table 9.2 with a higher glucose utilisation rate per 10^6 cells. There was also a 5 mM decrease observed in glucose concentration for the serum unsupplemented culture (Flask 1), despite a lack of observed cell growth.

Antibody production

The antibody levels observed at the end of the experiment for test Conditions 3 to 7 fell in the range of 12 to 16 μgml^{-1}. These levels were comparable to those observed for the standard conditions. The antibody production rates also complied with the standard conditions when compared by Students' t-test (Table 9.2).

The antibody production rate for test Condition 2 was also observed to be similar to those measured under standard conditions, although the final levels of antibody were lower than the other flasks, due to the lower growth rate and cell numbers present in the flask. While antibody was detected in the flasks for Condition 1, the levels produced were too low to determine any significant antibody production rate.

Ammonia production

Ammonia production was observed in all of the test flasks, with the highest ammonia concentrations observed for Condition 7 (3.0 mM glutamine supplemented). The ammonia production rates were, in general, observed to decrease with increasing α-kg concentration, with a significant difference observed between Conditions 2-4 and the value reported in Table 9.2.

Figure 9.14 compares the change in ammonia concentration (maximum - minimum value) for each set of flasks with the initial level of glutamine present in each set of flasks. A linear relationship was observed, with a least squares line of best fit of $y = 0.55x + 0.72$ and a correlation coefficient of 0.997, where y corresponds to the maximum ammonia differential and x corresponds to the initial level of glutamine.

9.3.2 Effects of conditioning the cells to α-kg supplemented medium

Three of the conditions (Conditions 3,4 and 7, Table 9.3) were selected for further tests which examined the effects of conditioning the cells to the new medium formulation and the possibility that the cells were glucose limited in the previous experiments. Cells were reconstituted from frozen and added to the appropriate medium. The cell numbers in each of the formulations were increased to a suitable levels for the inoculation of two 175 cm^2 culture flasks at a level of $1x10^5$ viable cells ml^{-1} of culture volume (100 ml). The cells were then cultured in a fed batch mode for a period of one month, replacing 75% of the volume with fresh medium whenever the cells reached $4x10^5$ viable cells ml^{-1}. Each of the three flasks containing

Figure 9.14:- Difference between maximum and minimum ammonia levels for each set of flasks versus initial glutamine:α-kg ratio.

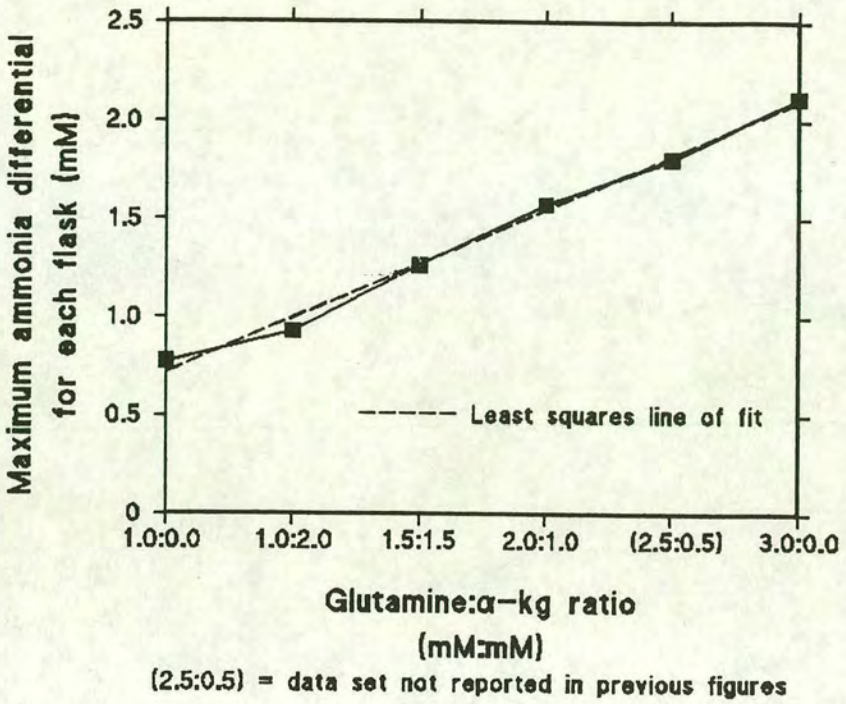

the different medium formulations was then used as seed flasks for duplicate 80 cm^2 culture flasks containing 50 ml of the different medium formulations. For example, cells precultured in Searle's modified medium containing 5% foetal calf serum and a 2 mM supplement of glutamine (Condition 7) were used to inoculate smaller duplicate flasks containing media from Conditions 3,5 and 7.

Glucose supplementation was also examined for these flasks with the addition of a further 4 mM glucose to a second set of flasks containing Condition 5 medium (giving an initial glucose concentration of 16 mM). These flasks were used to examine the effects of supplemental glucose in the absence of potentially inhibitory levels of ammonia.

Tables 9.5 to 9.7 report the calculated mean metabolic rates for the two flasks

corresponding to each medium condition. As these values were only based on n=2 flasks the standard deviations of the mean have not been reported, however, the differences between the recorded values never exceeded $\pm 5\%$ of the mean value. The values in bold text in Tables 9.5 to 9.7 were those that differed significantly from the values reported in Table 9.2.

Similar growth, metabolite and substrate curves were observed for this set of experiments when compared with those reported in Section 9.3.1. A majority of the rates calculated for these curves were similar to those reported in Section 9.3.1, supporting the conclusions given for that section. The lowest ammonia levels recorded at the end of the culture period were found in the α-kg supplemented flasks (Figures 9.15-9.17). Unlike the previously reported data the ammonia production rates for Condition 5 were significantly different from those reported in Table 9.4. The plot used in Figure 9.14 compared the initial theoretical levels of glutamine with the maximum ammonia differentials during the experiments. Figure 9.18 compares the mean level of glutamine utilised in each set of duplicate flasks (glutamine differential) with the maximum ammonia differentials for the flasks examined in this series of experiments. The least squares line of best fit for this data gave the following equation $y = 0.79x + 0.62$ and a correlation coefficient of 0.75, where x was the glutamine differential and y was the maximum ammonia differential.

The extension of the analyses to include lactate and glutamine led to further information on the metabolic profiles of the cells to be obtained. In all three of the preculture experiments the effects of higher levels of α-kg led to a reduction in glutamine utilisation and lactate production. The reduction in the glutamine utilisation rate may be explained by its partial replacement in the TCA cycle by the α-kg supplement, although the evidence for this was indirect as the levels of α-kg were not determined during these experiments. The suppression of lactate production by the cells was less easily explained, especially since the glucose utilisation rates did not differ significantly from the standard conditions reported in Table 9.2.

Table 9.5:- Cells precultured in glutamine rich medium (Condition 7, Table 9.3)

Flask conditions	μ	K_{glc}	K_{lac}	K_{gln}	K_{amm}	K_{mab}
1mM gln: 2mM α-kg (Condition 3)	0.022	0.357	**0.903**	**0.067**	**0.053**	0.411
2mM gln: 1mM α-kg (Condition 5)	0.021	0.304	1.083	**0.055**	**0.051**	0.431
2mM gln:1mM α-kg + glucose (Condition 5)	0.021	0.352	**1.247**	0.080	**0.071**	0.37
3 mM gln (Condition 7)	0.023	0.320	1.002	0.074	0.064	0.397

Table 9.6:- Cells precultured in α-kg rich medium (Condition 3, Table 9.2)

Flask conditions	μ	K_{glc}	K_{lac}	K_{gln}	K_{amm}	K_{mab}
1mM gln: 2mM α-kg (Condition 3)	0.019	0.360	**0.878**	**0.072**	**0.051**	0.468
2mM gln: 1mM α-kg (Condition 5)	0.021	0.310	1.116	**0.049**	**0.049**	0.429
2mM gln:1mM α-kg + glucose (Condition 5)	0.026	0.304	**1.285**	0.077	**0.079**	0.431
3mM gln (Condition 7)	0.020	0.324	1.100	0.064	0.060	0.417

Table 9.7:- Cells precultured in 2:1 mixture of glutamine and α-kg supplemented medium (Condition 5, Table 9.3)

Flask conditions	μ	K_{glc}	K_{lac}	K_{gln}	K_{amm}	K_{mab}
1mM gln: 2mM α-kg (Condition 3)	0.023	0.392	**0.869**	0.081	**0.073**	0.480
2mM gln: 1mM α-kg (Condition 5)	0.024	0.313	1.060	0.083	**0.055**	0.397
2mM gln:1mM α-kg + glucose (Condition 5)	0.025	**0.418**	**1.223**	0.074	0.095	0.327
3mM gln (Condition 7)	0.020	0.383	1.061	0.074	0.074	0.401

N.B. Rate units as per Table 9.1

Figure 9.17: Cells precultured in 2 mM α-kg:1 mM gln, ammonia/ glutamine.

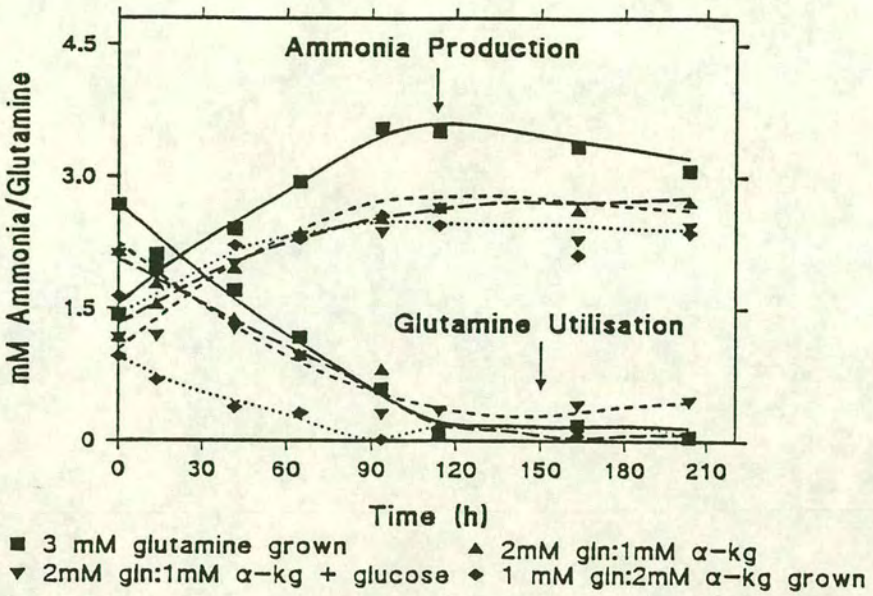

Figure 9.18: Plot of ammonia and glutamine differentials for Tables 9.5 to 9.7.

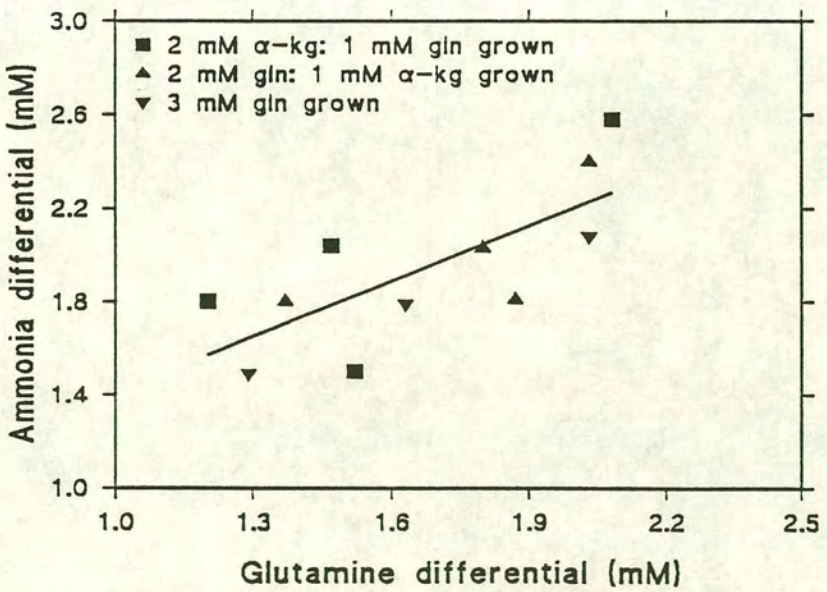

9.3.3 Conclusions from the Searle's medium modification experiments.

The following conclusions can be drawn from these sets of experiments:-

(1) A significant reduction in the final levels of ammonia was observed at the end of the culture period when supplemental glutamine was replaced with α-kg (Figure 9.12), with about 0.5 moles of ammonia liberated per mole of glutamine present in the initial medium (Figure 9.14).

(2) The partial replacement of glutamine had little effect on cell growth, glucose utilisation and antibody production rates (Tables 9.4-9.7).

(3) Ammonia production, glutamine utilisation and lactate production were reduced in the presence of higher levels of α-kg (Tables 9.5-9.7).

(4) Searles medium, containing 1 mM glutamine, supplemented with 5% serum, alone, led to a significant reduction in the calculated growth rate and maximum viable cell density achieved when compared with similar flasks which were further supplemented with α-kg. This suggests that α-kg was being used by the cells to counterbalance the reduced glutamine levels. The absence of foetal calf serum from these flasks resulted in no growth and cell death.

(5) Glucose supplementation experiments showed that the cells in the previous experiments were not glucose limited, with high levels of glucose recorded at the end of the growth period. The production of lactate was significantly increased in these flasks when compared with those conditions reported in Table 9.2.

9.4 Experiments using Gibco medium

While an overall reduction in the levels of ammonia present in the culture flasks was recorded in the previous set of experiments, no extension to the period of cell growth, as a result of these lower levels of ammonia, was observed. The reason for the populations' entry into the stationary and decline phases of growth was therefore

unlikely to be related to inhibitory ammonia levels. These experiments also indicated that α-kg was partially fulfilling the role of glutamine in cell metabolism. This evidence was indirect as the levels of α-kg were not directly monitored and Searles medium contained a small amount of glutamine, which may have been sufficient for the maintenance and growth of the cells. The use of α-kg by the cells had not been proven.

With these points in mind it was decided that a glutamine free formulation should be used (Gibco RPMI 1640), which would allow an examination of the cell's behaviour in glutamine free or glutamine limited culture. Unfortunately, differences between the formulation of the Searles modified medium and Gibcos' RPMI 1640 (primarily in glutamine and buffer levels) led to changes in the metabolic profiles of the cells, reducing the maximum viable population and consequently the amount of antibody produced by the cells. As the intended use of the glutamine free RPMI 1640 was to examine whether or not the cells could be grown with only α-kg and their utilisation of this substrate, rather than a direct comparison between the performance of the two media, the differences between the growth characteristics of the cells was accepted.

9.4.1 Initial experiments

Initial experiments were used to set up bench marks from which further experiments could be compared. This consisted of reconstituting six vials of cells from frozen with Gibco RPMI 1640 containing 2 mM glutamine, 1 mM α-kg:1 mM glutamine or 2 mM α-kg supplementation and the glucose supplemented versions of these media. All of these flasks were further supplemented with 5% foetal calf serum and these flasks were then used as inocula for the individual tests.

These starter cultures were used as inocula for 80 cm^2 flasks containing 50 ml of the respective medium formulation (i.e. 2 mM glutamine, a mixture of glutamine and α-kg and α-kg only). No growth was observed in the flasks supplemented with 2 mM α-kg, despite several attempt at using both fresh vials of frozen cells and the transferring viable cells from flasks containing a mixture of α-kg and glutamine. No

results are reported for the flasks containing no glutamine (i.e. medium containing α-kg only). Each of the experiments carried out using the other two medium formulations was based on six flasks (n=6), with the mean values for calculated metabolic rates and their associated standard deviations reported in Figures 9.19-9.21 and Table 9.8.

General characteristics

The medium formulations in which cell growth was detected show typical growth curves, with similar growth rates (Table 9.8). The maximum viable cell population observed at the end of the exponential period of growth was significantly higher for the cells grown in the α-kg:gln mixture. A significant difference was also observed for the rates at which glucose and glutamine were utilised and ammonia and lactate were produced by the cells, with these rates lower for the α-kg:gln grown cells.

Glucose levels were observed to fall from an initial value of approximately 13 mM to a minimum value of 2.67 mM for the glutamine grown cells. The lower rate of glucose utilisation by the cells grown in the α-kg:gln supplemented medium was evidenced by the higher levels of glucose present in the medium at the end of the growth period (4.3 mM). This was unusual considering the higher viable population obtained at the end of the exponential growth period. Lactate production followed a similar trend, with lower overall levels recorded for the cells with the lowest lactate production rate, that is cells grown in α-kg:gln.

The difference between the glutamine levels at the start and end of the experimental period was 0.81 mM and 0.5 mM for the 2 mM glutamine and the 1 mM α-kg: 1 mM gln supplemented cultures respectively. Values for the differences in ammonia at the start and finish of the experimental period for these two sets of flasks were 1.15 and 0.57 mM respectively. These results suggest that 1.4 millimoles of ammonia were liberated per millimole of glutamine in the 2.0 mM gln supplemented medium while 1.1 mM of ammonia were liberated per mM of glutamine for the α-kg:gln supplemented medium. These results, when combined with the significant differences in the rate at which glutamine was utilised by the cells in the two different media

Figure 9.19:- Growth curves for RPMI 1640 (Gibco) supplemented with glutamine (2 mM) and a 1 mM α-kg:1 mM glutamine mixture.

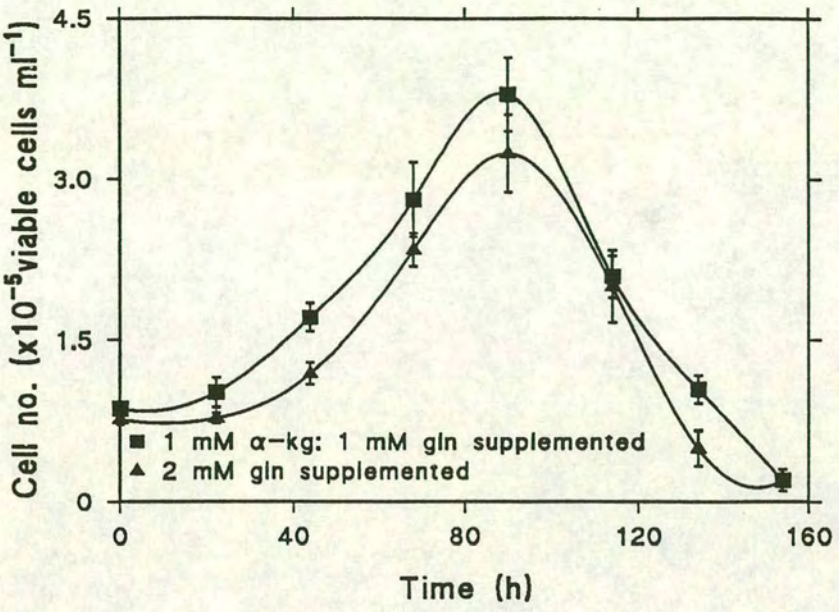

Figure 9.20:- Glucose and Lactate levels for Figure 9.19

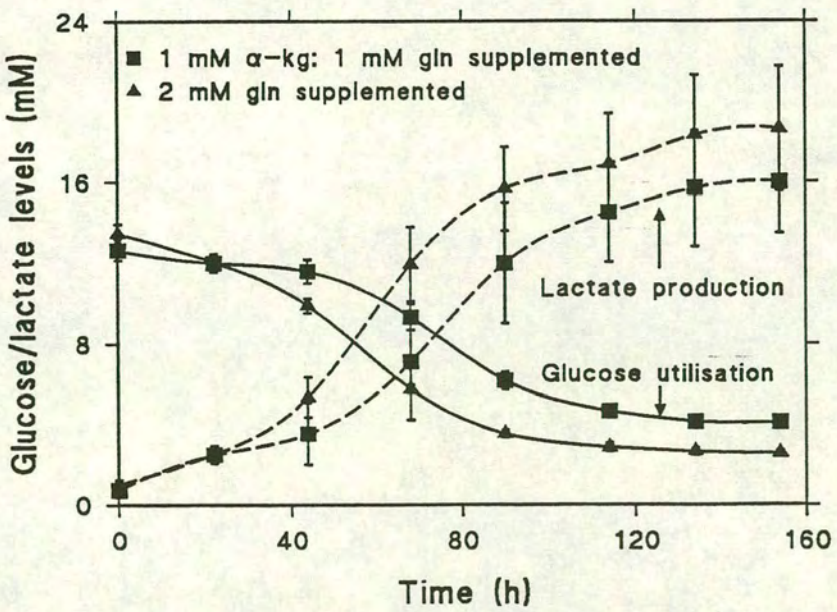

Figure 9.21:- **Glutamine, ammonia and α-kg levels for Figure 9.19**

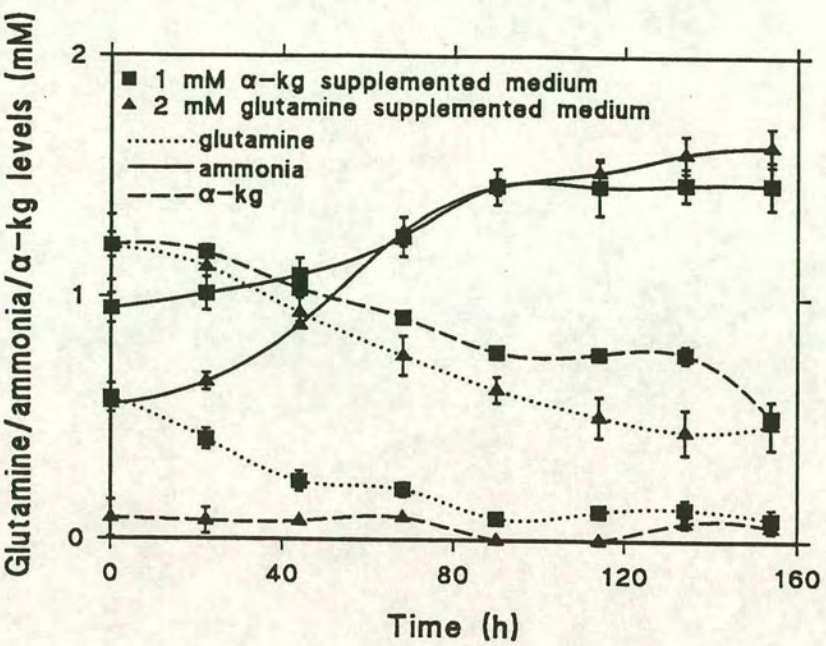

formulations, suggest that the pattern of glutamine metabolism had altered in the presence of α-kg.

The use of the α-kg assay, described in Section 9.2.2, showed that the cells were indeed utilising a proportion of the supplemental α-kg with a 0.44 mM decrease recorded for the 1 mM supplemented medium. Medium supplemented with 2 mM gln had a final antibody concentration of 8.01 (σ= 0.13) μgml^{-1} and 1 mM gln: 1 mM α-kg supplemented medium produced 8.17 (σ= 0.21) μgml^{-1}. These figures do not differ significantly from each other.

9.4.2 Conditioning experiments in Gibco RPMI 1640

In a similar approach to Section 9.3.2, cells were reconstituted from three vials and precultured in 3 mM glutamine,1 mM α-kg: 1 mM gln and 2 mM α-kg: 1 mM gln

Table 9.8:- Cells grown on 2 mM gln and 1 mM α-kg: 1mM gln supplemented Gibco RPMI 1640 (n=6 flasks per condition)

Growth parameter	Cells grown on 2mM Glutamine supplemented medium	Cells grown on 1mM glutamine: 1mM α-kg supplemented medium	Significant difference between means (using Students t-test)
μ	0.021 (σ=0.002)	0.022 (σ=0.001)	No
K_{glc}	0.62 (σ=0.02)	0.66 (σ=0.02)	Yes
K_{lac}	0.98 (σ=0.12)	1.31 (σ=0.09)	Yes
K_{gln}	0.053 (σ=0.004)	0.040 (σ=0.002)	Yes
K_{amm}	0.060 (σ=0.004)	0.028 (σ=0.004)	Yes
$K_{\alpha kg}$	-	0.024 (σ=0.001)	-
K_{mab}	0.33 (σ=0.08)	0.37 (σ=0.08)	No
Maximum cell count ($x10^5$ viable cells ml^{-1})	3.24 (σ=0.36)	3.79 (σ=0.34)	Yes

supplemented Gibco RPMI 1640 medium containing 5 % serum for a period of 1 month. At the end of this period these cells were used to inoculate replicate flasks containing fresh aliquots of the preculture medium so that the cells were only cultured in their preculture medium. Each condition was tested using six replicate flasks (n=6). The results from these experiments are summarised in Figures 9.22 to 9.27, with the further results summarised in Tables 9.9 to 9.11.

The results corresponding to 2 mM α-kg in Figures 9.22 to 9.27 were based on a series of flasks where viable cells precultured in a 2 mM α-kg: 1 mM glutamine

Figure 9.22:- Growth curves from preculture experiments in Gibco RPMI 1640

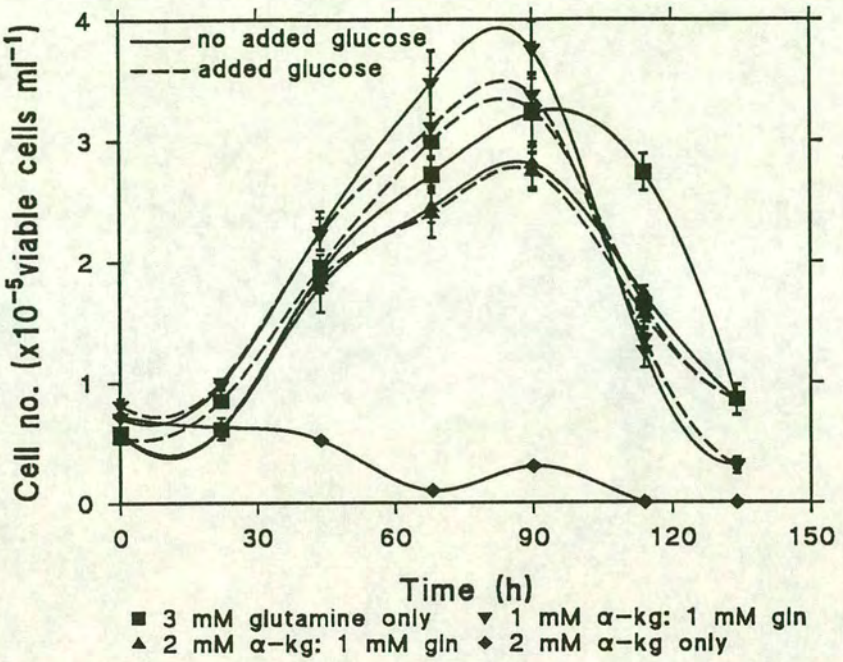

Figure 9.23:- Glucose levels for Figure 9.22

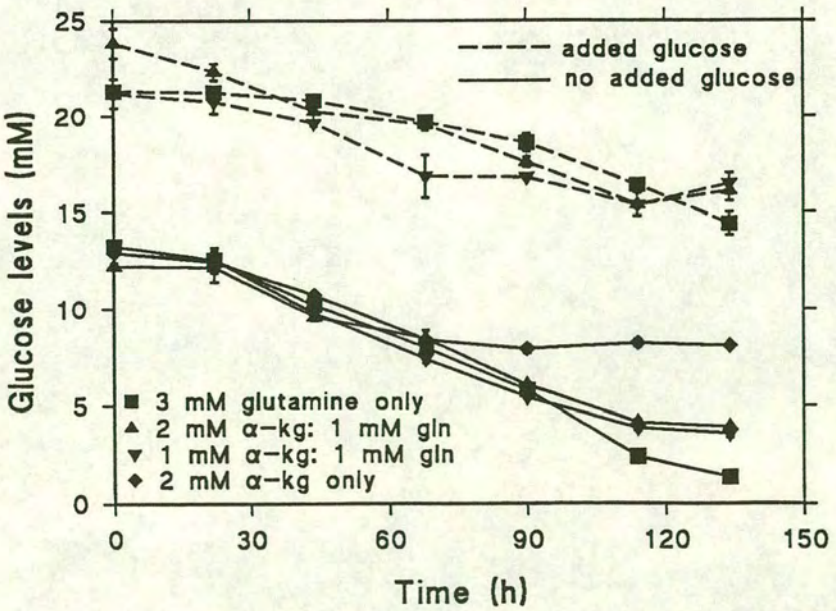

Figure 9.24:- Lactate levels for Figure 9.22

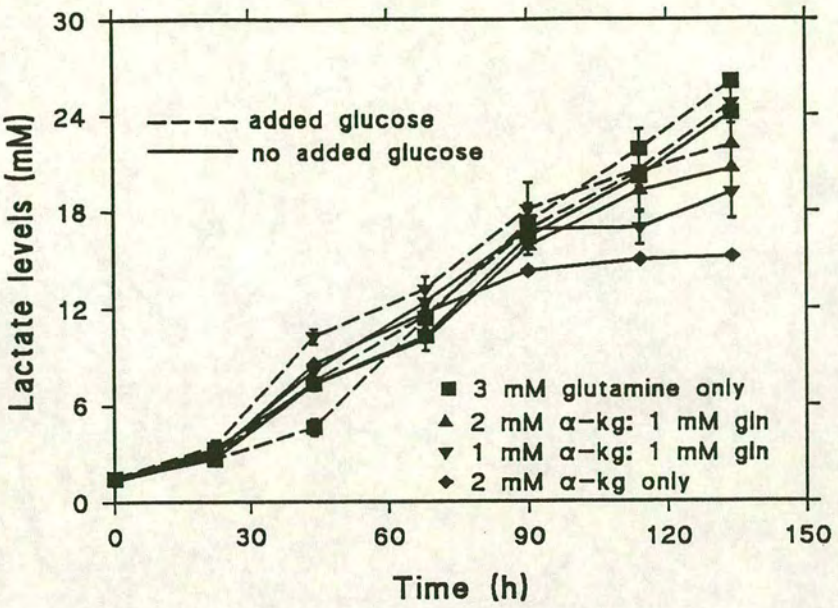

Figure 9.25:- α-kg levels for Figure 9.22

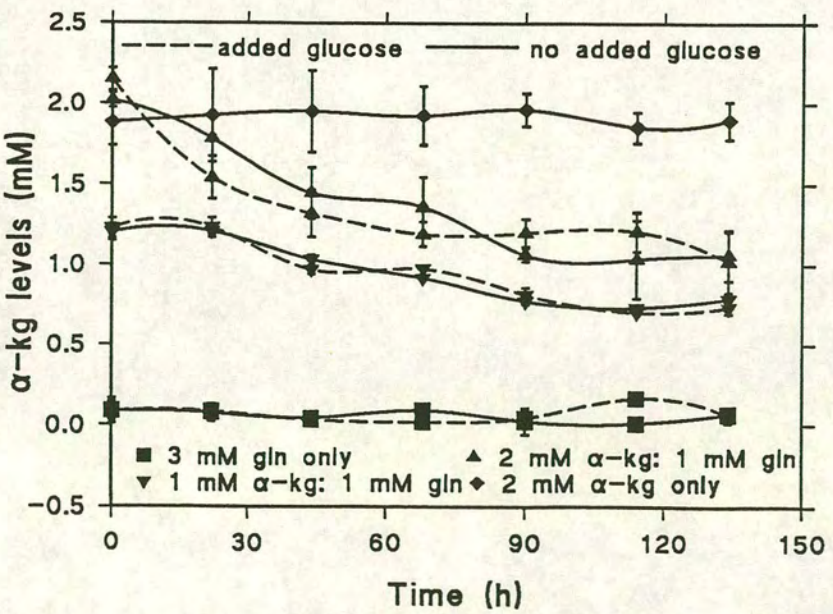

Figure 9.26:- Ammonia levels for Figure 9.22

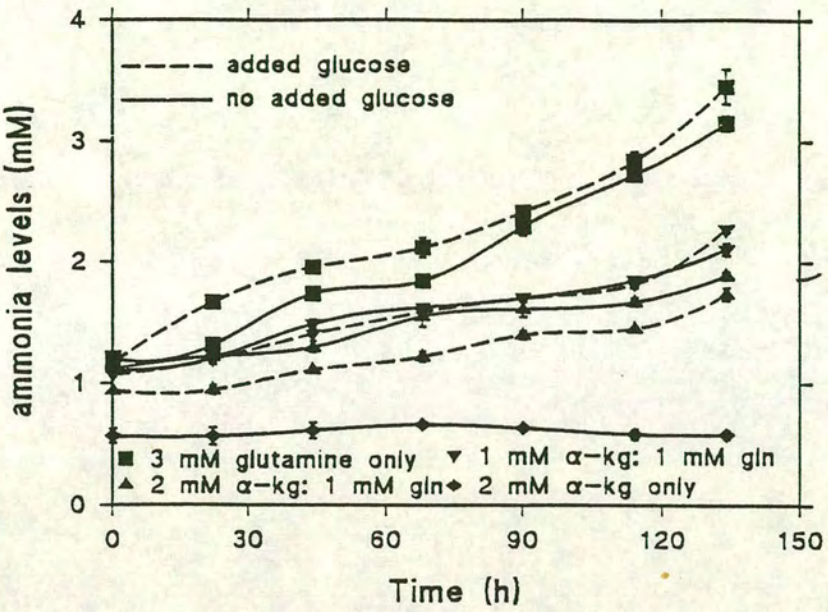

Figure 9.27:- Glutamine levels for Figure 9.22

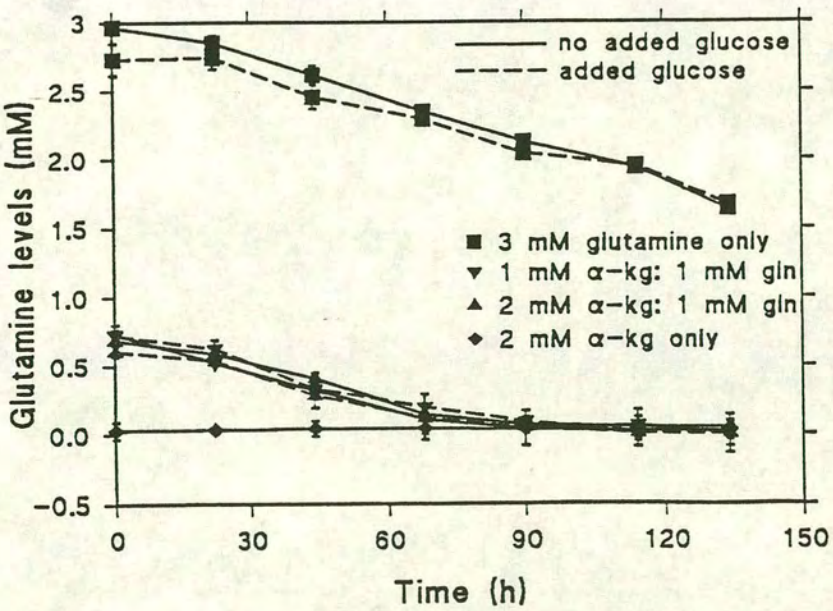

Table 9.9:- Cells grown and precultured on 3mM glutamine supplemented Gibco RPMI 1640 (n=6 flasks per condition)

Growth parameter	Cells grown on 3mM Glutamine supplemented medium	Cells grown on 3mM glutamine + glucose supplemented medium	Significant difference between means (using Students t-test)
μ	0.024 (σ=0.002)	0.025 (σ=0.001)	No
K_{glc}	0.76 (σ=0.04)	0.42 (σ=0.02)	Yes
K_{lac}	1.30 (σ=0.10)	1.36 (σ=0.08)	No
K_{gln}	0.073 (σ=0.005)	0.065 (σ=0.003)	Yes
K_{amm}	0.085 (σ=0.006)	0.088 (σ=0.005)	No
$K_{\alpha kg}$	-	-	-
K_{mab}	0.30 (σ=0.07)	0.32 (σ=0.06)	No
Maximum cell count ($x10^5$ viable cells ml^{-1})	3.23 (σ=0.33)	3.25 (σ=0.30)	No

mixture were used to inoculate medium containing α-kg supplementation only. The cells from the other flask were used due to the repeated failure of attempts to grow cells in the 2 mM α-kg supplemented medium.

Comparison of cells grown on different media

A comparison of the data presented in the second column of Tables 9.9 to 9.11 shows the following trends. In the presence of α-kg supplementation the mean calculated specific growth rates were significantly higher than the cells grown in medium containing only glutamine when compared using Students' t-test. No growth was

Table 9.10:- Cells grown and precultured on 1mM:1mM α-kg:glutamine supplemented Gibco RPMI 1640 (n=6 flasks per condition)

Growth parameter	Cells grown on 1mM:1mM gln:α-kg supplemented medium	Cells grown on 1mM:1mM gln:α-kg + glucose supplemented medium	Significant difference between means (using Students t-test)
μ	0.028 (σ=0.001)	0.024 (σ=0.002)	Yes
K_{glc}	0.73 (σ=0.01)	0.49 (σ=0.01)	Yes
K_{lac}	1.46 (σ=0.08)	1.50 (σ=0.09)	No
K_{gln}	0.053 (σ=0.004)	0.057 (σ=0.004)	Yes*
K_{amm}	0.042 (σ=0.002)	0.042 (σ=0.006)	No
$K_{\alpha kg}$	0.042 (σ=0.003)	0.026 (σ=0.003)	Yes
K_{mab}	0.34 (σ=0.04)	0.31 (σ=0.07)	No
Maximum cell count ($x10^5$ viable cells ml^{-1})	3.76 (σ=0.24)	3.37 (σ=0.43)	Yes

***Calculated difference only just significant at the 95% level, further tests required.**

observed in the 2 mM α-kg supplemented medium. The difference in growth rates between 1 mM and 2 mM α-kg supplemented medium was not statistically significant. The maximum viable cell count recorded for each of the set of flasks (Figure 9.18) was found to be significantly higher in the 1 mM α-kg:1 mM gln supplemented flasks than the other two flasks. The lowest maximum viable cell population, where cell growth was observed, was found in the 2 mM α-kg:1 mM gln supplemented medium.

As the growth rate and relative cell numbers were use to calculate the metabolic rates

Table 9.11:- Cells grown and precultured on 2mM:1mM α-kg:glutamine supplemented Gibco RPMI 1640 (n=6 flasks per condition)

Growth parameter	Cells grown on 1mM:2mM gln:α-kg supplemented medium	Cells grown on 1mM:2mM gln:α-kg + glucose supplemented medium	Significant difference between means (using Students t-test)
μ	0.029 (σ=0.001)	0.031 (σ=0.002)	Yes
K_{glc}	0.50 (σ=0.02)	0.58 (σ=0.02)	Yes
K_{lac}	1.15 (σ=0.01)	1.88 (σ=0.19)	Yes
K_{gln}	0.039 (σ=0.004)	0.052 (σ=0.004)	Yes
K_{amm}	0.039 (σ=0.002)	0.049 (σ=0.002)	Yes
$K_{\alpha kg}$	0.050 (σ=0.004)	0.077 (σ=0.005)	Yes
K_{mab}	0.32 (σ=0.07)	0.36 (σ=0.07)	No
Maximum cell count ($x10^5$ viable cells ml^{-1})	2.80 (σ=0.19)	2.75 (σ=0.16)	Yes

reported in Tables 9.9 to 9.11, the similar substrate/metabolite profiles reported in Figures 9.22-9.27 did not necessarily result in similar calculated rates (Equation 9.2).

For example, the levels of glucose reported for all of the medium formulations containing glutamine fell from an initial value of approximately 13 mM to a value of approximately 6 mM within the first 90 h, generating similar calculated gradients. The effects of converting these values from mMh^{-1} to mmole $x10^{-6}$ cells h^{-1} alters values that previously showed no statistical difference to a significantly lower glucose utilisation rate for the 2 mM α-kg: 1 mM gln grown cells when compared with the other media.

Significant differences were also observed for lactate production, with the highest rates recorded for 1 mM α-kg: 1 mM gln and the lowest values recorded for 2 mM α-kg: 1 mM gln supplemented medium. Glutamine utilisation rates were highest for the 3 mM gln grown cells and lowest for the 2 mM α-kg: 1 mM gln grown cells. The opposite and expected trend was observed for ammonia production. The differences between the calculated antibody production rates and the final antibody levels were not significant for the three medium formulations where cell growth occurred.

The substrate and metabolite profiles reported for this data suggest that glucose was non-limiting and that α-kg was utilised, confirming the previously reported results that the cells were indeed using α-kg. Glutamine levels were non-limiting for the cells growing in 3 mM glutamine supplemented medium, while the levels of glutamine in the 1 mM supplemented media reached zero. A comparison of glutamine and ammonia differentials for the different medium formulations gives the following millimole to millimole production levels:- 1.1 moles of ammonia liberated per mole of glutamine for the 3 mM gln supplemented medium and 1.2 moles per mole for the 1 mM gln supplemented medium. These values are in general agreement with those observed in the previous sections.

Effects of glucose supplementation

The addition of supplemental glucose to the three formulations containing glutamine had different effects on the metabolic characteristics of the cells.

In the presence of 3 mM glutamine a significant decrease in glucose and glutamine utilisation rates were observed, with no significant differences observed for any of the other growth parameters examined.

The addition of glucose to medium containing 1 mM α-kg: 1 mM gln significantly reduced the growth rate, glucose, glutamine and α-kg utilisation rates when compared with the medium containing lower levels of glucose. The maximum viable cell number was also reduced, while the cell associated production rates were unaffected.

A different pattern emerges for cells cultured in 2 mM α-kg : 1 mM gln, with an apparent increase in all of the observed growth parameters except the antibody production rate and the maximum viable cell count. Explanations and further analysis of these results will be given in Section 9.5.

Effects of conditioning.

A comparison of the data presented in Tables 9.8 and 9.10 for cells grown in 1 mM α-kg:1 mM gln suggests that a number of growth characteristics had changed over the 1 month conditioning period. A significant increase in the growth rate was observed in the cells which had been conditioned to this medium. The higher growth rate may explain the observed increase in all of the substrate utilisation and metabolite production rates.

9.4.3 Conclusions from Gibco RPMI 1640 experiments

Several general conclusions can be drawn from these results:-

(1) The levels of ammonia produced in α-kg supplemented culture are significantly reduced. The replacement of 1 mM glutamine with a similar amount of α-kg led to no significant deterioration in the growth rate, with a small, but significant increase in the viable cell population.

(2) While α-kg can be used by the cells in the partial replacement of glutamine, the use of high levels (i.e. 2 mM) in the presence of 1 mM glutamine leads to a reduction in cell growth and maximum cell numbers. In the absence of glutamine, the presence of α-kg does not support growth. Lower levels, when used in the presence of glutamine appear to be beneficial to the growth of the cells.

(3) Glucose supplementation affects the cells grown in the different medium formulations in different ways. In glutamine rich culture, the uptakes of both glutamine and glucose are reduced. The uptake of these two species in the 1 mM α-kg:1 mM gln medium was unaffected,

while that of α-kg was suppressed. The effects of glucose supplementation on 2 mM α-kg:1 mM gln supplemented medium led to enhancement of almost all of the uptake and production rates.

(4) A comparison between the 1 mM α-kg grown cells, before and after the preconditioning experiments, suggests that an increase in growth rate and the associated metabolic rates had occurred.

9.5 Summary and discussion of results

The general aims of this chapter were achieved with the growth characteristics of ES4 in batch culture determined and benchmark results used to investigate the partial replacement of glutamine with α-kg. Using the latter approach a reduction in the final levels of ammonia, a potentially toxic metabolite, present in the culture medium in both of the medium formulations examined was observed. The growth characteristics of the cells in these two formulations differed, with the primary differences between the two media associated with the presence of L-glutamine in the medium and the modifications made to the formulation of RPMI 1640 suggested by Searles. These modifications were not applied to the Gibco medium as its use was intended to examine the effects of a glutamine deficient medium, rather than a direct comparison with Searles medium.

When glutamine was absent from the medium formulation, it was found that α-kg could not support the growth of, or maintain, a viable cell population. However α-kg utilisation was shown to occur when it was used in the partial replacement of glutamine in the culture medium. The partial replacement of glutamine with α-kg led to a significant increase in the maximum viable population present in both the Searles and Gibco media when compared to medium supplemented with glutamine only.

The rate of utilisation of α-kg increased with its relative concentration, although these results were based on only two concentrations, with differing levels of glutamine supplementation. While a decrease in α-kg within the medium was taken to indicate its utilisation as a substitute for glutamine, this could only be confirmed by using

carbon labelled α-kg and an examination of its incorporation into other compounds.

The levels of ammonia present at the end of the culture period were shown to be related to the amount of glutamine used by the cells, with between 0.55 and 1.2 moles of ammonia produced per mole of glutamine used by the cells. The levels of ammonia observed at the end of batch culture in the Searle's and Gibco media did not reach inhibitory levels, suggesting that some other factor was responsible for the entry of cells into the exponential phase of growth.

Discussion

While these results have clearly shown that the partial replacement of glutamine with α-kg can lead to a reduction of metabolic ammonia and that α-kg is used by the cells, as evidenced by a reduction in the levels observed in the culture medium, the means by which α-kg fulfils this support function is more difficult to discern. The transport of α-kg into the cell is likely to be similar to that of glutamine and glucose, via the facilitated co-transport of sodium across the outer membrane. Once in the cell glutamine can be transported directly into the mitochondrion for further participation in the TCA cycle (Devlin, 1992). However, while a mechanism for the transport of α-kg, produced via the TCA cycle, has been identified for its passage out of the mitochondrion, a direct method for its passage into the mitochondrion has not. This would suggest that any influence that α-kg supplementation may have on the production of ammonia from glutaminolysis would be indirect.

In a discussion of the work by Street and Brindle (1991), who used ^{15}N-labelled glutamine to follow its passage during glutaminolysis, and Jenkins and co-workers (1992) who examined the relative activities of the enzymes involved in glutaminolysis, the production of ammonia from glutamine was identified as being related to its conversion to glutamate via glutaminase. The subsequent conversion of glutamate to α-kg was shown to have a negligible effect on the levels of metabolic ammonia with the transamination reaction between pyruvate and glutamate leading to the formation of α-kg and alanine. This reaction dominates over the direct formation of ammonia via the deamination of glutamate to α-kg catalysed by glutamate dehydrogenase. These

results strongly suggest that the ammonia levels observed in the experiments carried out for this work were derived from the initial deamination of glutamine to glutamate.

A strong correlation was observed between the initial levels of glutamine and the final levels of ammonia present in the medium for Section 9.3.1 with 0.55 moles of ammonia liberated per mole of glutamine present at the start of the experiment. As the level of glutamine utilisation was not monitored for these flasks, this value would be artificially low as glutamine was expected to be in excess for these flasks. The experiments carried out in Section 9.3.2 show that under the preculture conditions used for Section 9.3.1 glutamine was indeed in excess, however this was found not to be the case for α-kg supplemented preculture medium. Figure 9.18 shows a similar linear relationship between the utilisation of glutamine and the production of ammonia suggesting a higher value of 0.79 moles of ammonia liberated per mole of glutamine utilised. A similar dependency was also observed for subsequent experiments where Gibco medium was used, with between 1.0 and 1.2 moles of ammonia liberated per mole of utilised glutamine (based on values at the end of the exponential phase of growth). Glacken *et al.* (1986) controlled ammonia levels by decreasing the extracellular levels of glutamine through its pulsed addition to the culture medium. Dalili *et al.* (1990), while examining the effects of glutamine limitation on hybridoma cells, also observed lower levels of ammonia present at the end of the culture period when lower initial levels of glutamine were used. Whether the lower ammonia levels observed in this work were as a direct result of lowering the levels of glutamine in a similar manner to these two groups, or as a direct result of α-kg addition could not be readily determined.

The rationale for investigating the potential for reducing the levels of ammonia produced by the cell was based on the results of Wilson (1992) who found inhibitory levels at the end of the exponential growth phase. Subsequent experiments carried out by Wilson using the addition of supplemental ammonia at the start of batch culture experiments using ES4 appeared to support this hypothesis. However, the approach taken by Wilson of adding ammonia at the start of the experiment may have been flawed, given that the cells are never usually exposed to inhibitory levels of ammonia

until the end of exponential growth.

Dalili *et al.* (1990) found that entry of the cells into the stationary phase of growth was commensurate with glutamine exhaustion. The results from Section 9.3.2, comparing medium supplemented with 1 mM glutamine and 5% serum and a similar mixture with 1 mM α-kg added, show that while cell growth was limited by the initial glutamine levels in the first set of flasks, agreeing with Dalili *et al.*, the addition of α-kg allowed the cells to continue growing in the second set of flasks. This strongly suggests that α-kg supplementation was beneficial to continued cell growth. Indeed, it was observed that the cell numbers achieved in 1mM gln:1mM α-kg supplemented media were reproducibly higher in both Searles and Gibco media than those cultured with only glutamine supplementation.

The pattern of ammonia production and glutamine utilisation from this work would appear to suggest that while the yields were similar, the rates at which glutamine utilisation occurred were generally lower for the α-kg supplemented medium. Lactate and glucose yields tended to fall in the range of 1.7 to 2.3 moles of lactate per mole of glucose utilised, although the rates of lactate production were up to three times that of glucose utilisation during the exponential phase of growth. As lactate can be derived from both glucose and the TCA cycle, the exact effects of α-kg addition could only be examined through carbon labelling.

One of the primary roles of α-kg in the cytosol is to act as an acceptor molecule in the degradation of other amino acids by either accepting ammonia in the deamination of compounds such as lysine and alanine, forming glutamate, or the formation of an intermediate compound in the degradation pathway of the amino acid cysteine (Devlin, 1992). While the direct entry of α-kg into the mitochondrion may be in doubt, the passage of glutamate in and out of the mitochondrion is not.

The lack of cell growth in the absence of glutamine suggests that the cells were not capable of synthesizing their own glutamine from the trace amino acids and the supplemental α-kg, requiring a low level of supplemental glutamine. This agrees with

the work of Ardawi and Newsholme (1984) who describe an absolute requirement for glutamine by lymphocyte derived cells and Bell (1990) who identifies a 0.5 mM minimum requirement for the culture of a hybridoma cell line (PQXB1/2). Butler (1985) also observed that MDCK and BHK cells either did not grow, or grew poorly, in the presence of α-kg. Studies in which the gene encoding glutamine synthetase, an enzyme catalysing the conversion of glutamate to glutamine, in the presence of ammonia and ATP, has been transfected into cells which lack this enzyme have allowed the growth of these cells on glutamate rather than glutamine (Bell *et al.*, 1992). This enzyme has also been used as part of an expression system for heterologous proteins in NS0 and CHO cells (Hassell *et al.*, 1992; Gofton *et al.*, 1992). These results suggest that in order for α-kg supplementation to be successful, in the absence of glutamine, then the test cell line should have the natural, or transfected, ability to produce glutamine synthetase to supply the cell with the required level of glutamine.

Whether supplemental α-kg, in the presence of glutamine, affects glutaminolysis indirectly by increasing the mitochondrial levels of glutamate, the levels of other intermediaries of the TCA cycle which may control the rate of glutamine degradation, or that it has little effect on this pathway and supports cell growth through pathways related to the TCA cycle requires a more in depth investigation than that carried out in this chapter.

Chapter 10

Bioreactor culture experiments

10.0 Introduction

A number of operating problems were identified for hollow fibre bioreactors in the literature survey carried out for this work (Chapters 2-5), with the high density culture of cells requiring a non-limiting, low shear environment. These included the build up of potentially toxic metabolites (e.g. ammonia, Chapter 3) around the cells, mass transport difficulties associated with the supply of nutrients to tissue concentrations of biomass and the effects that membrane fouling had on the supply of nutrients and growth factors to the cells (Chapter 5).

The Edinburgh Dual Hollow Fibre Bioreactor was designed to overcome these limitations, with the modifications made to the prototype described in Chapter 6 and discussed in Chapter 7. As the bioreactor was developed, the mass transport characteristics of the hollow fibres were examined and the potential effects of fibre selection on its performance characterised (Chapter 8). Chapter 9 then described the growth characteristics of the test cell line (ES4) proposing a method by which ammonia levels could be reduced in the culture environment.

This chapter provides a further examination of these factors by reference to a number of culture experiments carried out by the author using the Edinburgh Dual Hollow Fibre Bioreactor. Results from seven bioreactor experiments, lasting for between 11 and 40 days, are described in this chapter (Section 10.1). Other experiments which were terminated due to contamination or failures in the manufacture of the bioreactor are mentioned briefly in Section 10.6.

The maximum viable cell number achieved using this design was 1.2×10^7 cells ml^{-1} of the growth space volume. However, in order to obtain this level of cell growth the general design of the bioreactor, the number of fibres in the growth space and the way

in which serum was added to the medium all had to be changed. Some of the problems with the operation and design of the bioreactor circuit have already been described in Chapter 7, for example the failure of the oxygen probes and pressure transducers. A further discussion of the effects that these failures had on the control of the flow regimes within the bioreactor and the analysis of metabolic data are described in Sections 10.3 to 10.7. Many of the difficulties experienced were found to be related to the failure in obtaining samples that were fully representative of the cellular growth space.

10.1 Overview of bioreactor experiments

This section provides an overview of the general operational features of each run (Table 10.2) and a number of comments based on the observations made during these experiments (Table 10.3). These tables should be read in conjunction with Sections 10.1.1 and 2 and Table 10.1 for a description of the terms used. Further information about each particular run will be provided in the later sections of this chapter (Section 10.2 onwards). Runs 1-3 were carried out in collaboration with Dr. J. Burns (1991). It should be noted that Burns was primarily responsible for the control software and electronics support, while the author constructed six out of the seven bioreactors and bioreactor circuits used in the reported experiments (Table 10.2). The author also prepared the cells and medium for each run and carried out all of the metabolic assays reported in these experiments. Runs 4-7 were carried out solely by the author.

10.1.1 Clarification of terminology

The terminology used in Table 10.2 and the rest of this chapter provides basic information on the bioreactor type, medium supply regime, inoculation level, final cell counts achieved and the duration of each experiment. The following paragraphs provide a description of these terms.

Bioreactor type

Table 10.1 summarises the general features of the four bioreactor designs used in this work. They are categorised as 'Old style'(described in Chapter 6), 'New style' in which the bucket style templates were used (Sections 7.4.1 and 7.4.2), 'high density' (Section 7.4.3) and 'Large scale' (Section 7.4.4). The numbers below each bioreactor design refer to the pore size of the membranes used in each experiment (100 = 100 kDa MWCO, 0.1 = 0.1 μm pore size) with the first and second figures referring to the supply and sink fibres respectively. Table 10.1 describes the number of fibres used in each design, their partition between supply (upstream) and sink (downstream) fibres, the total surface area associated with the cellular growth space, the fibre volume and liquid volume of the cellular growth space and the previously described packing ratio (P.R.) for each bioreactor.

Medium supply regime

This column of Table 10.2 describes the way in which the experiments were operated, based on the following categories:-

RECIRCULATED:- In these experiments the configuration of the apparatus used was that indicated in Figure 6.6, where spent medium was returned to the feed vessel.

SINGLE PASS:- The medium was not generally returned to the feed vessel in these experiments. The configuration of apparatus used was outlined in Figure 6.7. Recirculation of the waste stream was used to ensure that the feed vessel remained charged with medium overnight due to the limited size of the medium bottle.

NBC FEED:- In these experiments the feed vessel was supplemented with new born calf serum (NBC), with the percentage used expressed in terms of volume per volume of medium.

NBC DOSED:- Newborn calf serum was added to the cellular growth space (CGS) semi-continuously during the experiment, using the inoculation ports of the bioreactor. This involved the dosing of the CGS with 25 ml (small scale bioreactors) or 50 ml (large scale bioreactor) of serum every 2-3 days.

Table 10.1:- Bioreactor specifications

Type of Bioreactor	No. of fibres (Total: Supply: Sink)	Surface area of fibres (cm^2)	Fibre volume: liquid volume (cm^3:cm^3)	Packing Ratio
Old style	72:24:48	588	29.4:40	0.43
New style	72:24:48	679	34:45	0.43
High density	90:30:60	848	42.5:37	0.53
Large scale	306:106:200	2882	144:175	0.45

Inoculation level and final cell count

These values are presented as viable (abbreviated to **v.**) and non-viable (abbreviated to **n.v.**) cell counts, as determined by the Trypan Blue exclusion method (Section 6.1.2), with the values reported ml^{-1} of available liquid volume in the growth space, that is the total volume minus the volume taken up by the fibres. Where two values are reported, a second inoculum was used on the day specified. All inocula used had a population viability of greater than 95%, assessed using the Trypan Blue staining method (Section 6.1.2). The final cell counts reported in Table 10.2 were determined from the rinse samples taken after the shaking, drainage and rinsing of the cellular growth space at the end of the run. A modification of this protocol was used for Runs 4-7 (Section 10.6.2).

10.1.2 Overview of bioreactor experiments

Table 10.2 summarises the bioreactor experiments in which biomass was recovered from the growth space, with the final values recorded based on the drainage of the cellular growth space at the end of the experiment. A relatively low percentage viability of the cells recovered from the bioreactor (between 4 and 31%) was a common feature of these experiments. A number of reasons for the low viabilities can be given, including the poor supply of growth factors to the cells due to their rejection by the membranes, and the failure to maintain the cells within the fibre bundle.

Table 10.2:- Operational features of bioreactor runs

Run No.	Bioreactor type and supply:sink pore sizes	Medium supply regime	Inoculation level	Final cell count	Run time (days)
1	Old style 100:0.1	Recirculated, NBC feed 5%	$1.0x10^6$ **v.** (day 1) $1.0x10^6$ **v.** (day 11)	$2.0x10^6$ **n.v.**	11
2	Old style 0.1:0.1	Recirculated, NBC feed 5%	$0.5x10^6$ **v.**	$4.0x10^6$ **v.** $16.6x10^6$ **n.v.**	14
3	New style 0.1:0.1	Recirculated, NBC feed 5%	$0.6x10^6$ **v.**	$2.5x10^6$ **v.** $11.8x10^6$ **n.v.**	30
4	New style 0.1:0.1	Recirculated, NBC feed 3%	$31.0x10^6$ **v.**	$2.2x10^6$ **v.** $48.4x10^6$ **n.v.**	28
5	New style 0.1:0.1	Recirculated NBC dosed	$2.8x10^6$ **v.**	$4.9x10^6$ **v.** $17.0x10^6$ **n.v.**	23
6	High density 100:0.1	Single pass/ Recirculated, NBC dosed	$2.0x10^6$ **v.**	$12.0x10^6$ **v.** $26.3x10^6$ **n.v.**	18
7	Large scale 100:0.1	Single pass/ Recirculated, NBC dosed	$2.0x10^6$ **v.**	$2.4x10^6$ **v.** $46.8x10^6$ **n.v.**	40

An outline of the key observations and the developments applied to bioreactor design and operation for the cell culture experiments are described in Table 10.3. The viable population recorded within the bioreactor was improved for the smaller bioreactors (Runs 2 - 6, Table 10.2) by periodically dosing the growth space with newborn calf serum, negating the effects of fouling upon their supply, and by increasing the number of fibres within the growth space for retaining cells within the growth space.

An attempt was made to apply these developments to the design and operation of a prototype large scale bioreactor. Unfortunately, the construction difficulties encountered in this 'one-off' design led to the leakage and failed integrity of the growth space. However, a viable population was maintained within the growth space,

Table 10.3:- Observational comments from runs

Run No.	Comments
1	First uncontaminated run with no potting failures. A dual end supply regime was used on the supply circuit, resulting in a significant level of fouling. No viable cells were present at the end of the run.
2	In order to counteract the effects of fouling the supply fibres were operated as crossflow filters and their pore size increased to 0.1μm. This improved performance with the maintenance of a viable population in the growth space. Antibody accumulated in the supply circuit, despite the 0.1μm pore size of the fibres. Protein precipitates observed in the supply circuit were thought to originate via sparging.
3	First use of bucket templates, designed to reduce potting failures during construction. A switch from sparged to surface aeration was aimed at reducing precipitation. A viable population was maintained and antibody was still found to accumulate in the supply circuit.
4	Increasing the inoculation level had little effect on the number of viable cells within the bioreactor. Viable cells were found to be associated with the fibres after the dissection of the bioreactor at the end of the run. Antibody was again retained in the supply circuit despite a reduction in the level of serum addition. Bioreactor inverted to mix settled biomass.
5	It was thought that the cells might be growth factor limited due to the rejection of proteins by the supply fibres. The addition of serum directly to the growth space solved this problem increasing the viable population within the bioreactor. Antibody again accumulated in the supply circuit. Problems were encountered in manual control at low filtration rates. Effects of pressure profiles and nutrient/product distribution on metabolic rate calculations were identified.
6	The pore size of the supply fibres was changed to 100 kDa from 0.1μm to increase protein rejection by these fibres and alter the pressure profile within the bioreactor. Increasing the fibre packing ratio led to an increase in the viable population within the bioreactor.
7	Using the accumulated knowledge from the small bioreactors, e.g. serum dosing, fibre packing and the importance of pressure profiles, a scaled up version was designed and constructed. Unfortunately the 'O' ring seals used in this design failed, although a viable population was maintained within the bioreactor.

free from contamination with other organisms (as assessed by the sampling regime described in Section 6.1.7) for a period of 40 days.

10.2 Distribution of cells within the bioreactor

In the description of the bioreactor given at the start of Chapter 7, the intended position of the cells within the growth space was to be between the two sets of fibres, within the fibre bundle where nutrients were readily available. The importance of adequately supplying high cell numbers with nutrients has been described in Chapter 4, with the use of a perfused supply of medium to the cell mass being more advantageous than a diffusionally limited system. With these concepts in mind the following sections will discuss the relevance of these principles to this design of bioreactor.

10.2.1 Gravitational settling of cells

A common feature of all of the experimental runs described in this chapter was the settling of the cells on the bottom of the bioreactor tube. As the bioreactor was operated horizontally, or at a slight angle, this usually meant that the cells settled along the length of the tube. This had two effects, the first was that the cells were now in a poorly mixed zone where the supply of nutrients was diffusionally limited and secondly that the influence of this biomass on the calculation of metabolic rates was unknown.

Attempts were made to redistribute the settled biomass within the fibre bundle by inverting the bioreactor twice a day during its operation, this may also have improved mixing and therefore the nutrient supply to the settled biomass. A comparison between Runs 3 (no inversion) and 4 (inverted twice daily) shows little difference in the final level of viable biomass, although the fourth run did differ in that it had a higher level of inoculum than the previous run. The bioreactor reported by Cousins *et al.* (1992) employs continuous mechanical mixing to maintain the viability of the cell mass. One observed problem with the approach used for the Edinburgh Dual Hollow Fibre Bioreactor was that the settled biomass, on inversion of the bioreactor, travelled through the loosely packed fibres in the bundle to resettle on the bottom of the bioreactor tube rather than being retained in the fibre bundle.

As a result of growth space sampling problems (Section 10.7.4) the total and viable cell population in the growth space was not known until the end of the experiment. In order to examine the distribution of the cells within the growth space, the bioreactor at the end of the fourth run was dissected and the distribution of the cells between the fibre bundle and the settled biomass was determined.

It was concluded from the dissection experiment that most of the viable cell mass was to be found associated with the hollow fibres and that the settled biomass mainly consisted of dead cells. As the viable biomass was associated with the fibres, a bioreactor in which a higher number of fibres were present to retain the cells within the fibre bundle through either their direct attachment, or the build up of clumps of biomass between more closely spaced fibres was designed. The high density bioreactor (Section 7.3.3) showed a significant improvement in the viable population when compared to the bioreactors with a lower number of fibres when operated in a similar way (cf. runs 5 and 6, Table 10.2).

10.2.2 Bioreactor dissection experiment

In order to test the distribution of the cells on the fibres, the bioreactor used in this experiment was carefully dissected on the completion of the run. An overview of this experiment is given in Figure 10.1. Several questions were to be answered by this experiment, a list of which are given below:-

(1) Are a majority of the viable cells associated with the fibres?

(2) Is there a maldistribution of cells within the fibre bundle caused by the gravitational settling of cells, or alternatively, the distal accumulation of cells through the adoption of a Starling flow, rather than a radial flow regime?

(3) Are the viable cells preferentially adherent to the supply or sink fibres within the bioreactor?

Experimental method

The bioreactor was operated in one orientation for the final 6 days of Run 4. On completion, orientation marks were placed on the outside of the bioreactor, identifying its top and bottom during operation. The cellular growth space was then drained and rinsed, and the free cells counted.

The end caps were then removed from the bioreactor and orientation marks placed on the potting of the outer templates. The inner membrane module was then carefully removed from the polycarbonate shell, with slurry collected in a small tray containing 20 ml of fresh medium.

The bioreactor was then placed on an aluminium foil sheet, where the fibres were removed from the inner module using a scalpel. The fibres were then either sectioned into three equal lengths for the sectional analysis, designated proximal (at the supply end of the bioreactor), medial (the mid section) and distal (at the exit of the bioreactor), or alternatively separated into supply and sink fibres for the length analysis. The aluminium foil was rinsed with 20 ml of fresh medium on completion and any cells present counted. The whole procedure took less than 15 minutes, during which time very little drying of the fibre surfaces was observed.

Each group of fibres was then added to 10 ml of fresh medium in a 50 ml sample bottle and the contents mixed thoroughly. The supernatant was removed and stored, with the repetition of this procedure for another two aliquots of fresh medium. The volumes were combined and the viable, non-viable and total cell counts were measured for each of the samples and expressed as the number of cells cm^{-2} of fibre, based on the total surface area of the fibres measured in each test.

Results and conclusions

The results from these experiments are reported in Tables 10.4 to 10.6. The length of the fibres used in the sectional analysis was 5 cm each, giving a surface area of 3.142 cm^2 per fibre, and the total length of the fibres used in the length analysis was 15 cm, giving a per fibre surface area of 9.425 cm^2.

It was found that approximately one third of the cells were readily associated with the fibres, being retained on, or in the body of the fibre bundle after its removal from its polycarbonate shell. As the cells reported in Tables 10.5 and 10.6 were recovered from the fibres, it would suggest that they were fairly adherent to the fibres surface. It was also apparent from these two tables, that the cell mass associated with the fibres was of a significantly higher viability than the cells recovered from the initial draining of the cellular growth space, approximately 90% viable as compared with 23 % for the latter.

The distribution of the cells along the length of the bioreactor suggests that the number of bound cells decreases towards the distal end of the bioreactor, although the viability continues to remain high.

The distribution of the cells within the bioreactor suggests that the cells were fairly evenly dispersed across the fibres, although the fibres tested in the length analysis experiment showed a bias towards the upper part of the bioreactor (Table 10.6). The reason for this difference was not ascertained. Analysis of the sectional data showed an even distribution of cells between the upper and lower sectors.

Given these results it would seem that the flow regime within the bioreactor was conducive to the growth of cells throughout the fibre bundle. The higher proximal levels of cells may be in response to a better supply of medium, with this sector of the bioreactor having the highest pressure difference, and consequently flux of medium, between the inside and outside of the supply fibre.

Some simple calculations were carried out in order to examine the degree of cell distribution on the fibres, i.e. did they exist as a monolayer covering the full surface of the fibre, or the growth of cells in clumps in a similar fashion to that described by Cima *et al.*(1990). By assuming the cells to grow in a monolayer, with each 10 μm cell considered a cube with a similar length of side (i.e. 10 x 10 x 10 μm), it can be calculated that a maximum of $1x10^6$ cells could occupy 1 cm^2 of membrane (1 cm^2/ $(1x10^{-3})^2$ cm^2). Based on the calculated results in Tables 10.5 and 10.6, the actual

Figure 10.1:- Overview of bioreactor dissection experiment

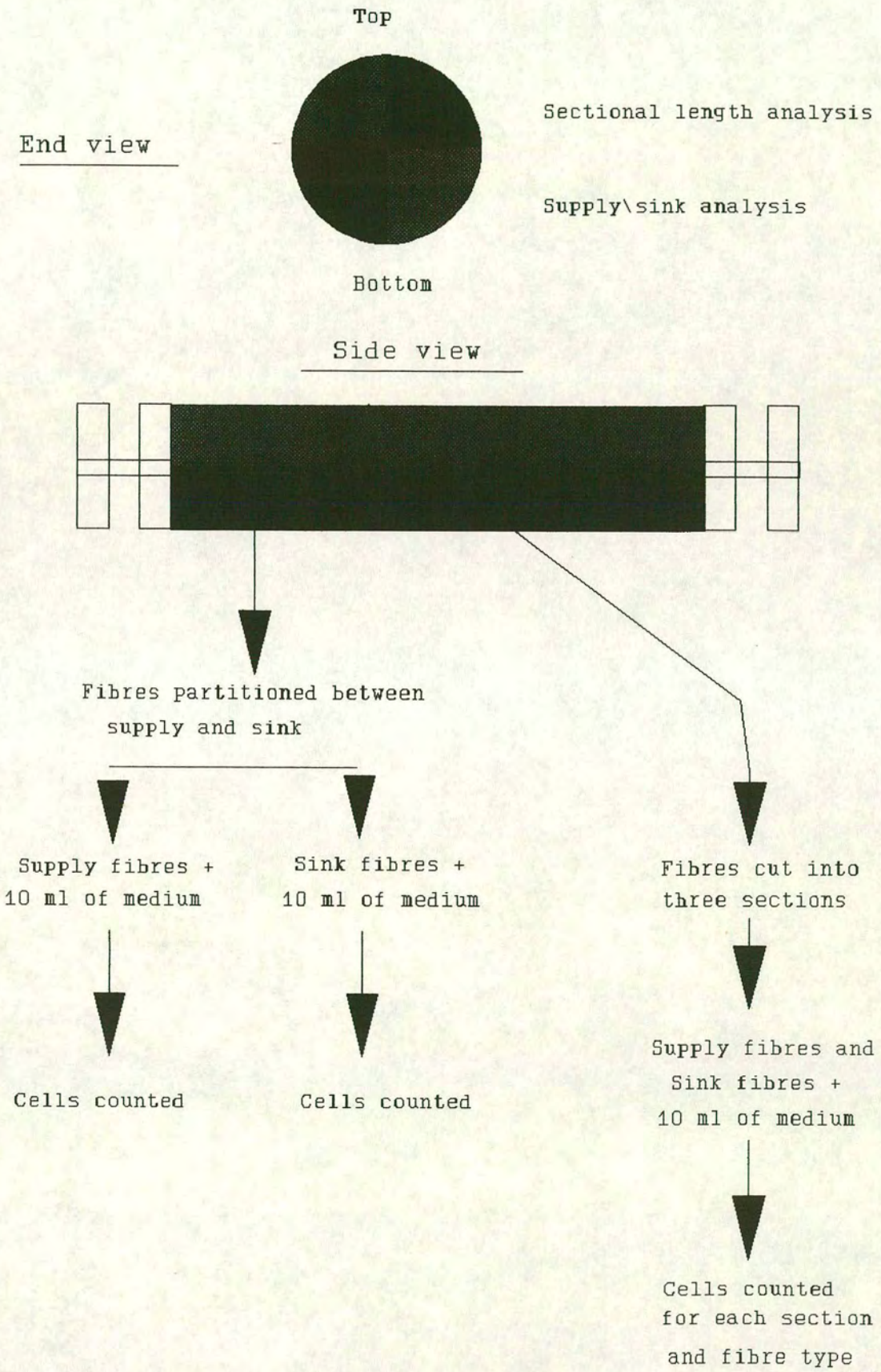

Table 10.4:- Combined washings and aluminium foil counts for dissection experiment.

Viable cell count ($x10^6$ cells ml^{-1})	Non-viable cell count ($x10^6$ cells ml^{-1})	Total cell count ($x10^6$ cells ml^{-1})	% viability of cell mass
2.22	48.32	50.54	4.39

Table 10.5:- Sectional analysis results for dissection experiment

Location in bioreactor	Sectional cell counts ($x10^6$ cells, where **v** = viable,**nv** = nonviable cells, **%** = percentage viable)		
	Proximal	Medial	Distal
Top quarter	**v** 3.44 **nv** 0.45 **%** 88.4	**v** 2.28 **nv** 0.63 **%** 78.3	**v** 2.46 **nv** 0.38 **%** 86.6
Bottom quarter	**v** 3.33 **nv** 0.21 **%** 94.1	**v** 2.23 **nv** 0.43 **%** 83.8	**v** 2.14 **nv** 0.33 **%** 86.6
Results expressed as total number cells per surface area of fibre ($x10^6$ cells cm^{-2})			
Top quarter	0.056	0.042	0.041
Bottom quarter	0.056	0.042	0.039

Table 10.6:- Length analysis results for the dissection experiment.

Location in bioreactor	Number of cells per fibre type ($x10^6$ cells, where **v** = viable,**nv** = nonviable cells, **%** = percentage viable)	
	Supply	Sink
Top quarter	**v** 1.32 **nv** 0.22 **%** 85.7	**v** 5.45 **nv** 0.33 **%** 94.3
Bottom quarter	**v** 0.29 **nv** 0.21 **%** 58.0	**v** 2.99 **nv** 0.32 **%** 90.3
Results expressed as total number cells per surface area of fibre ($x10^6$ cells cm^{-2})		
Top quarter	0.041	0.061
Bottom quarter	0.011	0.032

number of cells falls well below this value, ranging from 0.011 to 0.061 $x10^6$ cells cm^{-2}, suggesting that the continuous monolayer hypothesis does not apply.

Cima *et al.* (1990), in their model of the behaviour of the Tricentric bioreactor suggest that the cells may be associated with the pores. Fell and Kim (1990) have reported that approximately 5.5 % of the total surface area of a 100 kDa membrane was associated with pore openings. This value would appear to agree with the result calculated for this dissection experiment, assuming that 0.1 μm fibres would have a similar area associated with their pores. This data was not readily available, although it would suggest that the cells were either not very adherent to the surface of the polysulphone fibres, or alternatively, that the assumptions of Cima *et al.*, that cells were associated with the pores and not monolayers, were correct.

Further evidence supporting these observations can be derived from the way in which the cell counts at the end of each run were taken. Prior to the fourth run, and the subsequent dissection of the bioreactor, the bioreactor had been shaken vigorously before the drainage samples from the growth space were taken. In the fourth run the growth space was gently drained and rinsed with an equal volume of medium prior to the removal and analysis of the fibre bundle. This allowed a partial segregation between the settled biomass and that attached to the fibres. A modification of this protocol was used for Runs 5 and 6 with the drainage of the growth space followed by a rinse with an equal volume of medium, the bioreactor was then shaken vigorously with a second volume of medium, which was collected and the growth space rinsed with a third and final volume of medium. Table 10.7 shows the viability of the samples (assessed by Trypan blue staining) for all of the four samples. The results for the third run are shown for a comparison between the agitation of the module prior to sample collection and the drainage followed by agitation approach. A common feature of the samples assessed using this latter approach is that the percentage viability of the cell population in the samples taken before the agitation of the bioreactor is very low compared to those removed after agitation, and lower than those samples from the third run. This would suggest that the vigorous mixing of the bioreactor enabled the removal of the cells from the fibre bundle and that a majority

Table 10.7:- Recovery of cells from bioreactor at the end of the experiments.

Run no.	No. of cells in drain 1 ($x10^6$ cells)	% viable	No. of cell in rinse 1 ($x10^6$ cells)	% viable	No. of cells in rinse 2 ($x10^6$ cells)	% viable	No. of cells in rinse 3 ($x10^6$ cells)	% viable
3	**574.0**	**18.9**	**115.7**	**10.9**	**28.8**	**6.2**	-	-
4	227.4	4.4	-	-	**132.4**	**88.0**	-	-
5	503.5	2.7	212.8	17.3	**198.8**	**71.6**	**69.3**	**38.3**
6	686.2	2.3	269.0	23.6	**412.9**	**81.0**	**60.3**	**71.0**

(Figures in bold text relate to samples taken after the vigorous mixing of the bioreactor)

of these cells were viable. This data therefore supports the conclusions drawn from the dissection experiment.

The relationship between the viable biomass and their attachment to the fibres would explain the difficulties experienced in obtaining representative cell samples from the cellular growth space.

10.2.3 Increasing fibre packing

A comparison between the fifth and sixth runs (Table 10.2) shows that an increase in the viable cell population from $4.9x10^6$ to $12.0x10^6$ cells ml^{-1} occurred on increasing the fibre packing within the growth space. The increase in viable population between the fourth and fifth run was attributed to an improvement in the supply of serum related growth factors to the cells via the direct dosing of the cellular growth space (Section 10.5). By reapplying the calculations and assumptions used in the previous section to Runs 5 and 6 the following results were obtained (Table 10.8). These results assume that all of the viable cells collected in the washings after the termination of the experiments were fibre associated. While the number of fibre associated cells increases with attachment surface area it still does not approach the

Figure 10.2:- **Clumping of cells on fibres during Run 6**

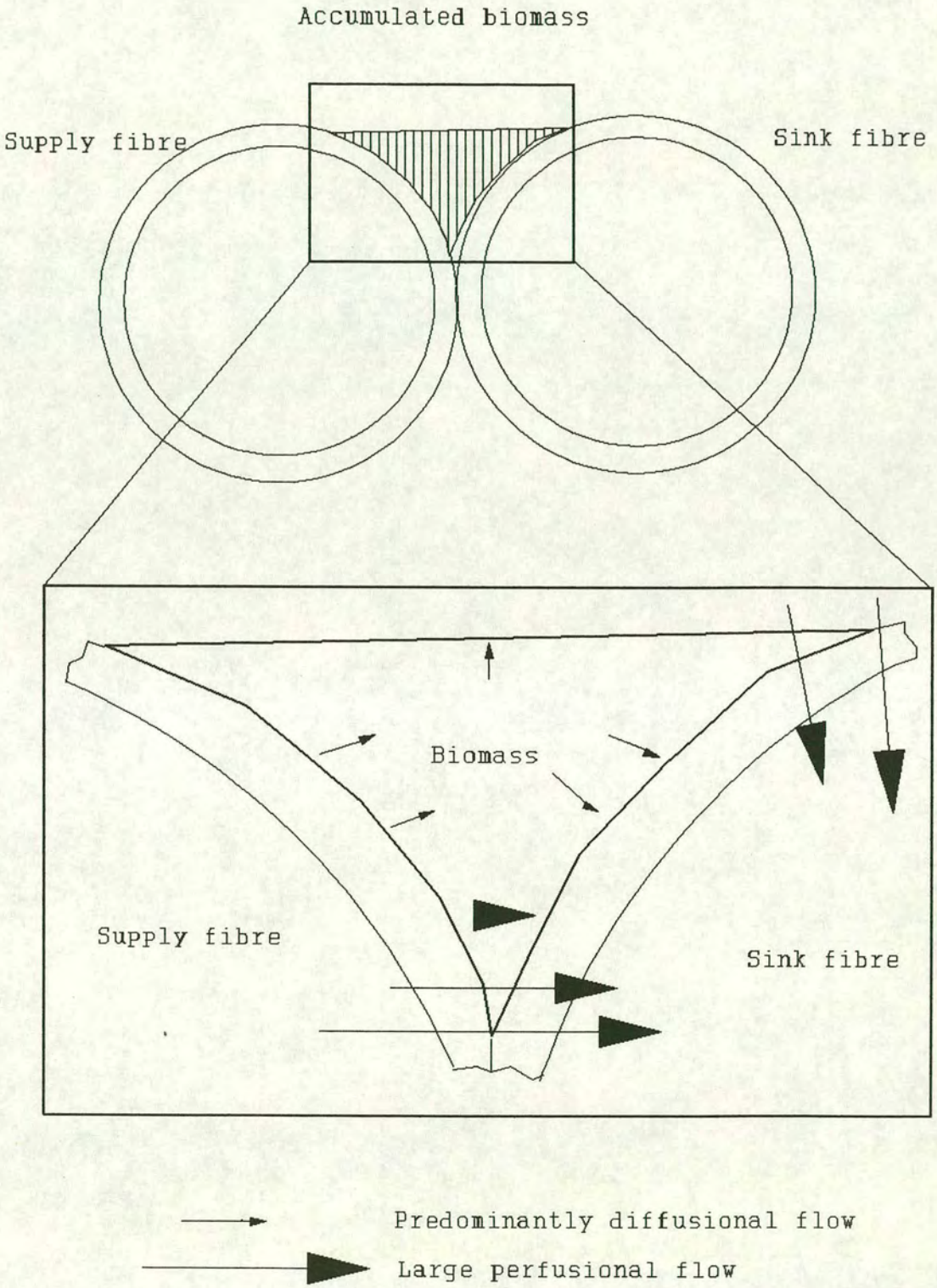

Table 10.8:- Calculated fibre related cell coverage

Run No.	Surface area of fibres (cm^2)	Total viable population in bioreactor ($x10^6$ cells)	Viable cells per unit surface area ($x10^6$ cells cm^{-2})
4	679	99.0	0.146
5	679	220.5	0.325
6	848	444.0	0.523

$1x10^6$ cells cm^{-2} calculated for a monolayer coverage of the fibre surface. It was observed during the sixth run that biomass was collecting between the adjacent touching fibres (Figure 10.2), this would decrease the total number of cells attaching directly to the fibres and it can therefore be concluded that the cell coverage calculated would be artificially high.

10.2.4 The effects of the cell mass on membrane fouling

While no direct experiments were carried out to assess the effects of cell related membrane fouling, the results which directly associate the viable biomass with the fibres would suggest that under high density cell culture the flows within the bioreactor may be affected by the uneven distribution of cells on the fibres. For example, in Run 6 (Figure 10.2) the accumulation of cells between the fibres could be expected to increase the resistance to flow across the membrane. The concept of the pressure driven flow regime present in the bioreactor has already been described at the start of Chapter 7, with the flow taking the path of least resistance, i.e. where the pressure drop across the membrane is the lowest. For an uneven distribution of biomass within the bioreactor it could be foreseen that the flow would preferentially cross the membrane at a point where the cell mass was negligible, in a similar manner ascribed to the initial permeability of membranes described by Grund *et al.* (1992), with the larger pores dictating flux until fouling reduced their effective pore size to match the majority of pores (Section 5.1.1). This would suggest a serious limitation to the performance of the bioreactor in the build up of biomass, with flow preferentially occurring where the cell mass was lowest, forcing areas of higher cell

density to rely on a more diffusionally limited flow regime.

Another interesting point related to the vigorous mixing of the bioreactor carried out in the latter set of experiments was the effect that the back flushing experiment had on the biomass attached to the fibres (Section 10.5.2). When the back flush experiment was carried out, its principal aim was to remove the protein related fouling of the membranes, however, it was also possible that some of the biomass attached to the fibres within the growth space may have also been removed, settling on the bottom of the bioreactor.

10.3 Influence of flow patterns on bioreactor performance.

The theory behind the operation of other types of hollow fibre bioreactors has been described in Chapter 5, with the effects of filtration, medium composition and pressure profiles identified as key operational parameters.

This section (Section 10.3) provides a theoretical discussion of how the pressure profile of the bioreactor affects the passage of a number of species which are present within the apparatus and the subsequent calculation of metabolic rates. This discussion describes the performance of the bioreactor from the view of three different classes of species present within the system, those that are freely distributed within the bioreactor circuit and are indirectly affected by filtration (Section 10.4), e.g. low M.W. compounds such as glucose, those which are partially rejected by the membranes (Section 10.5), for example proteins, and cells which are fully retained within the growth space (Section 10.6). In each of these sections results from the various bioreactor experiments are used to support these theories.

10.3.1 The distribution of species present in the bioreactor

Three different species can be identified as being directly or indirectly affected by the flow regimes present in the bioreactor:-

Freely distributed:- These include all low molecular weight (M.W.) compounds, e.g. glucose, ammonia, lactate and glutamine. These species are unaffected by the rejection characteristics of the fibres, however the calculation of cellular metabolic rates determined across the bioreactor can be affected by both the rate of flux and the flow regime present in the bioreactor.

Partially retained:- These include cell and serum related macromolecules such as serum albumin and antibody. In this case the effects of membrane polarisation and fouling can lead to a significant level of protein rejection by the fibres. The accumulation of antibody in the upstream circuit will be shown as one such example of this phenomenon. It will also be shown that the filtration rate and the flow regime within the growth space can influence the distribution of antibody in the bioreactor circuit.

Fully retained:- This primarily involves the cells contained within the bioreactors growth space which, by virtue of their size, are unable to cross either the upstream or sink membranes, assuming no leakage at the potting within the bioreactor. It can also be argued that any protein precipitates can be included in this category. This latter point primarily relates to the formation of aggregates due to sparging and the desiccation of wall bound aggregates.

10.3.2 Flow regimes dictated by bioreactor pressure profiles

Under ideal operating conditions the intended flow pattern within the bioreactor is from the supply fibres to the sink fibres, with the direction of flow mediated by a pressure gradient between the two sets of fibres. As a direct result of control problems (discussed in Section 10.6) there was no way of ensuring that the correct pressure profile was present within the bioreactor.

Given this background, and a difficulty in analysing the metabolic data associated with these experiments (Sections 10.4 and 10.5), alternative pressure profiles have to be considered, in a similar approach to that of Bruining (1989). Figures 10.3 and 10.4 show four different operational scenarios that could have occurred during the bioreactor runs, where P1 and P2 are the pre- and post-supply pressures, P3 is the CGS pressure and P4 is the pressure of the sink circuit. These conclusions could not be supported by comprehensive pressure data during the runs due to the repeated failure of the pressure transducers. A summary of the effects of these different conditions under the four predicted flow regimes are given in Tables 10.9 and 10.10. These conditions assume that the supply fibres were being operated as crossflow filters and that the degree of mixing within the growth space was not a limiting factor. Further description of each condition can be found in the following paragraphs and at the end of this chapter.

Condition 1

Under conditions where P1 and P2 are both significantly greater than P3, the flux across the bioreactor is high and the residence time of the medium in the CGS is low, leading to very small differences between the levels of metabolite in the supply and sink circuits. As a direct result the metabolic rates have to be calculated using the bulk levels monitored in the feed vessel. This method of calculation can only be carried out where the waste medium is continuously being recycled back into the medium reservoir so that a continuous monitoring of the bulk nutrients can be maintained.

The sensitivity of the metabolic data then becomes dependent upon the volume of the

feed vessel in relation to the filtration rate. For example, the decrease in bulk levels of metabolite in a 5 l vessel will be less than that of a 1 l vessel at the same utilisation and filtration rate, over a similar time period. This decrease can be directly related to the effects of dilution on the waste stream on its return to the feed vessel.

Under these conditions the cells may be liable to a phenomenon similar to 'wash out' in continuous culture, with the cells being washed off of the fibres and settling on the bottom of the bioreactor. This topic was discussed in Section 10.2.

Condition 2

As pressure P2 approaches P3, the reduction in the filtration rate across the bioreactor increases the residence time of medium in the CGS. As a direct consequence the differences in metabolite levels between the supply and sink circuits becomes greater. This difference can then be used to calculate the metabolic rates with greater accuracy by relating them directly to the filtration rate according to the calculation in Table 10.9.

Condition 3

Under conditions where the CGS pressure (P3) exceeds that of the post supply pressure (P2) the flow within the CGS would gradually shift from radial, i.e. from the supply to the sink fibres, to axial, where a proportion of the flow returns to the feed stream through the distal end of the supply fibres. The greater the difference between the two pressures, the greater the axial component of the flow.

The calculation of metabolic rates under these conditions becomes more difficult, depending on the degree of axial flow. During single pass operation the differences in metabolite concentration across the bioreactor will represent only the radial component of the flow within the bioreactor. The axial component will be represented by changes in the bulk concentration of nutrients in the medium reservoir, although this only likely to apply to freely dispersed moieties, e.g. glucose and ammonia. The sensitivity of the axial utilisation rates for the freely dispersed metabolites will be decreased by the effect that the dilution of the waste stream has on its re-entry to the

supply fibres. As a result of the two flow patterns present within the bioreactor, the best mode of operation for calculating metabolic rates for the freely dispersed metabolites is the monitoring of bulk concentrations in the feed vessel, with the recycle of the waste stream. Under these conditions the use of metabolite differentials between the supply and sink circuits for the calculation of metabolic rates would not give a true indication of the actual utilisation rates within the CGS.

Antibody production rates cannot be accurately determined due to the accumulation of antibody in the CGS, associated with the axial flow component. This calculation is further limited by the problems associated with getting representative samples from the CGS.

Condition 4

This condition approximates to a typical cartridge bioreactor where the axial component of the flow greatly exceeds that of any radial component. With fully developed Starling flow occurring within the growth space the metabolic rates for freely dispersed moieties would be dependent upon monitoring bulk concentrations in the medium supply vessel. The accumulation of antibody in the CGS would be expected with production rates usually assessed via the periodic sampling of the CGS, e.g. Piret and Cooney (1990).

10.3.3 Effects of fibre selection

One of the factors influencing the pressure profiles, and therefore the flow patterns within the bioreactor, was the selection of the pore size of the supply and sink fibres used in the construction of the bioreactor. For example, the flux associated with 100 kDa MWCO fibres was less than that of the fibres with a 0.1 μm pore size under similar test conditions (see Table 8.1), which implies that for a given flux, a greater transmembrane pressure is required for the 100 kDa MWCO fibres in order to generate a similar filtration rate. The construction of the 100:0.1 high density bioreactors used in Runs 6 and 7, gave the sink fibres a higher permeability than the supply fibres, resulting in a condition where P3 should never have exceeded P2. The

Table 10.9:- Summary of bioreactors' operational characteristics.

Condition	Bioreactors' pressure profile	Critical pressures	Filtration rate across bioreactor	Flow regime
1	P1,P2 > P3 > P4	P2 >> P3	High	Radial, from supply to sink circuit
2	P1,P2 > P3 > P4	P2 > P3	Medium	Radial, from supply to sink circuit
3	$\frac{(P1 + P2)}{2} > P3 > P4$	P1 > P3 ≥ P2	Low	Gradual shift from Radial to Axial as P3 approaches $\frac{(P1 + P2)}{2}$
4	$\frac{(P1 + P2)}{2} = P3 \approx P4$	P3 ≈ P4	Negligible	Fully developed Axial flow

Table 10.10:- Summary of metabolite profiles and rate calculations.

Condition	Dispersal of low M.W. metabolites	Dispersal of high M.W. moieties	Suggested mode of operation	Calculation of production and utilisation rates
1	Full	CGS, sink and accumulation in medium vessel	Recycle	Time related change in bulk medium components in the medium supply reservoir
2	Full	**Recycle:-** as condition 1 **Single pass:-** CGS and passage to waste stream	Recycle or single pass	As condition 1, or dependant on the difference in metabolite concentrations in the supply and sink circuits and the filtration rate e.g. $Flow \cdot \Delta Concentration_{metabolite}$
3	Full	Accumulation in CGS and sink	Recycle preferred, single pass ineffective	Combined medium reservoir based and transreactor utilisation rates. CGS accumulation of antibody leads to error in production rates.
4	Supply circuit and CGS only	Accumulation in CGS	Recycle	Changes in bulk medium reservoir concentrations. Poor antibody production rates due to CGS sampling errors.

Figure 10.3:- Bioreactor pressure profile - Conditions 1 and 2

Condition 1 :- P1 , P2 > P3 > P4 Filtration rate:- High
Critical pressures:- P2 >> P3

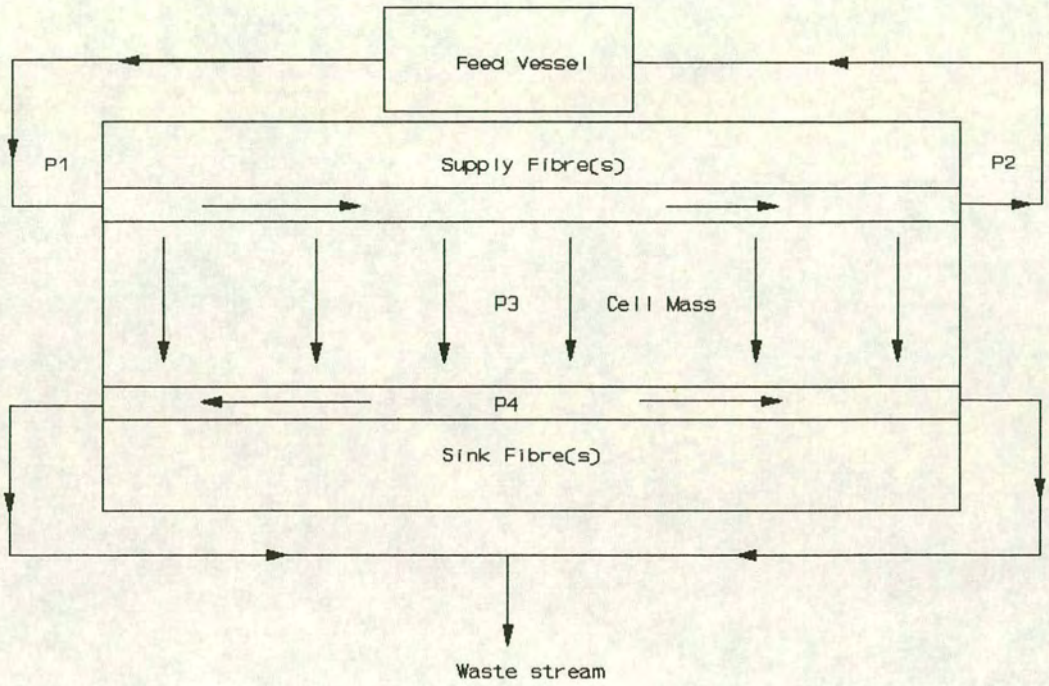

Condition 2:- P1 , P2 > P3 > P4 Filtration rate:- Medium
Critical pressures:- P2 > P3

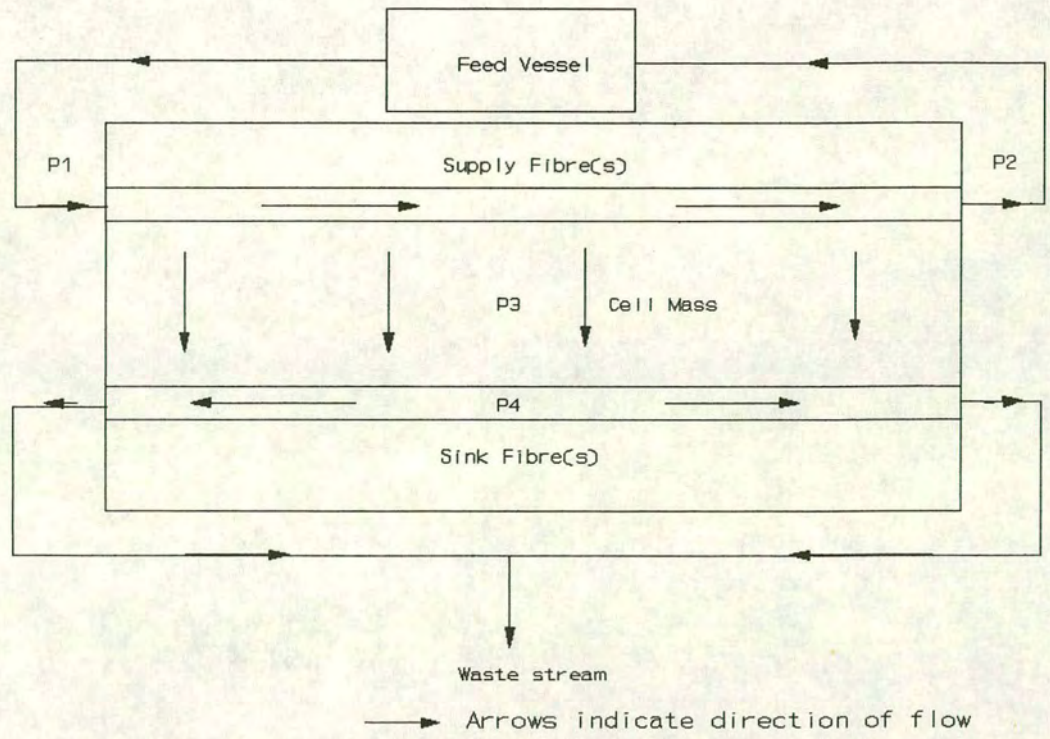

Figure 10.4:- Bioreactor pressure profile - Conditions 3 and 4

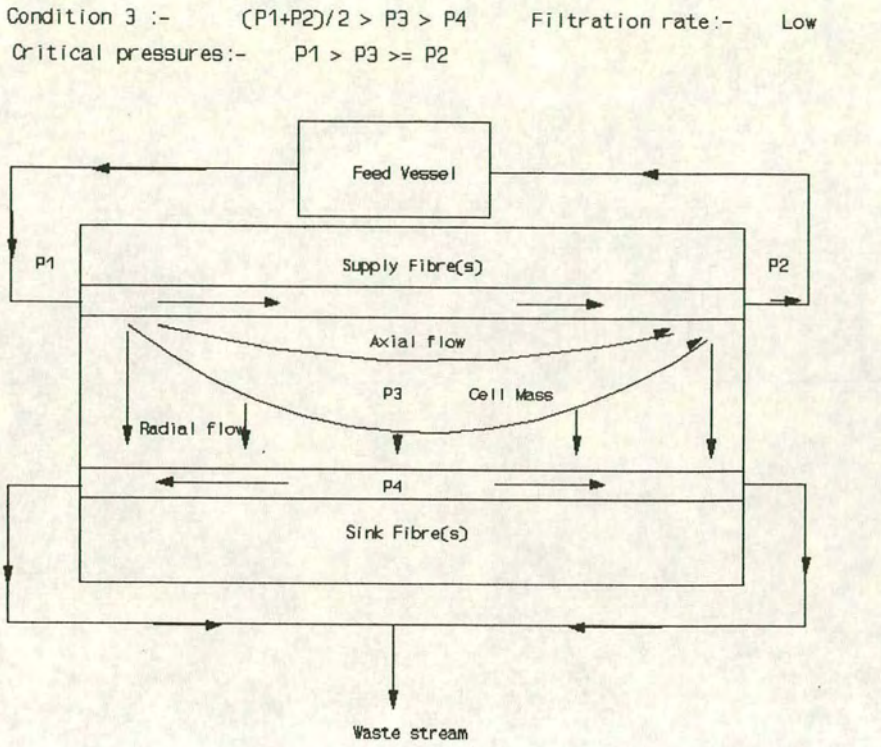

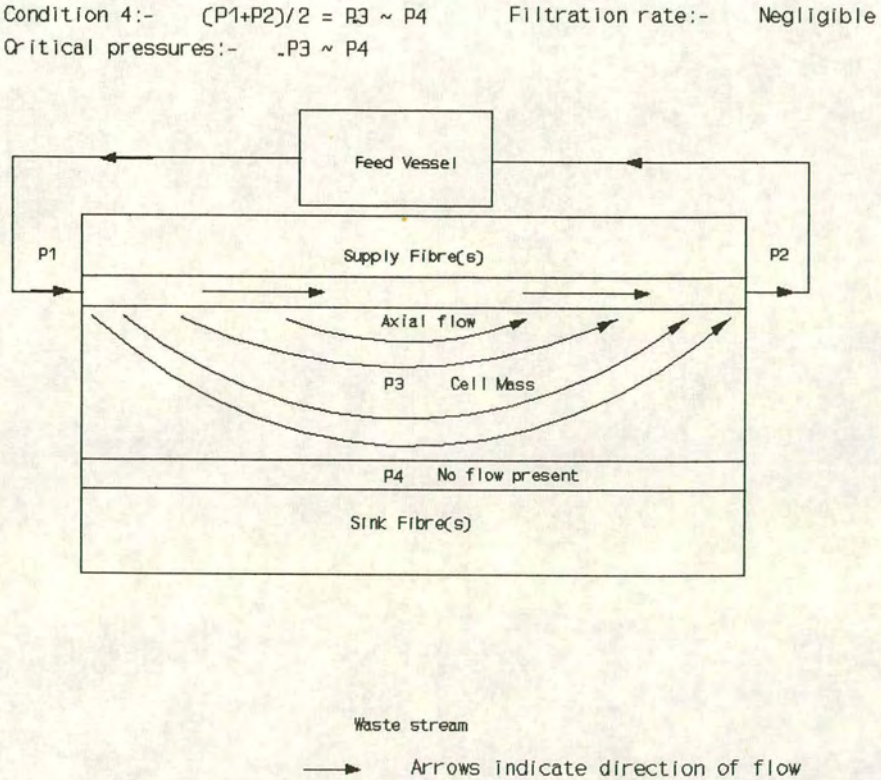

flow pattern within the bioreactor was therefore expected to be radial, with the potential for a higher degree of control over lower filtration rates, resulting in conditions 1 or 2 (Table 10.9).

10.4 Pressure profiles and low molecular weight species

Low molecular weight species such as glucose, glutamine and ammonia were fully dispersed throughout the bioreactor circuit, that is the pore size of the membranes, fouled or unfouled did not greatly impede their movement. The main limitation for these species was associated with the filtration rate and flow regimes present within the bioreactor. The following sections describe the influence of these factors on the calculation of metabolic rates determined from the bioreactor experiments.

There were two methods used to calculate the cellular metabolic rates for cells within the bioreactor. The first relied directly on the utilisation of nutrients by the cells and was calculated by multiplying the difference in the levels of metabolite between the supply and sink circuits by the filtration rate across the bioreactor. The second method, used under conditions where the difference between the two circuits was negligible, relied on the gradual change in bulk nutrient levels measured from the feed vessel. Of these two methods, the first method would appear to be the most sensitive, giving an indication of the actual metabolic rate at the time of sampling, assuming that the sink sample is fully representative of the utilisation by the cells, a topic that is discussed further in Section 10.6.

The second method would be expected to be less sensitive due to the effects of dilution. Under circumstances where there was a negligible difference between the supply and sink circuits, the effects that the waste stream had on the bulk concentrations in the feed vessel would be small over a short period of time. For example, at a filtration rate of 0.1 lh^{-1}, with a constant 1 mmole change in a key nutrient in the filtrate stream, and a feed vessel volume of 4 l it would take 40 h (4 l/ 0.1 lh^{-1}) for a similar change to occur in the feed vessel. For a 1 l feed vessel

it would only take 10 h. Given the longer time required for the determination of metabolic rates using this method, this approach would not be very sensitive to changes in metabolic rate.

10.4.1 Effects of higher filtration rates on metabolic results

For high filtration rates it can be assumed that the pressure profiles within the bioreactor comply with Condition 1 (Tables 10.9 and 10.10). Two features of the bioreactor circuit become important for accurate rate determination. The first is the residence time of the medium within the growth space, with shorter residence times resulting in a lower utilisation of nutrient per unit volume and therefore a smaller the measured difference between the supply and sink circuits. As explained in the previous section the volume of the feed vessel then becomes an important factor in determining the metabolic rates with a greater delay associated with larger vessels.

The range of filtration rates used for Runs 2-4, along with the sizes of the feed vessel are reported in Table 10.11, and the results from the assays for glucose, ammonia and oxygen are presented in Figures 10.5 - 10.9, where these results were available. The medium changes referred to on these graphs relate to either a small addition of medium to the feed vessel (to compensate for sampling losses) or larger replacements (e.g. greater than 25%) of the medium in the feed vessel to increase the levels of bulk nutrients in the supply circuit. The calculated metabolic rates and correlation coefficients (r) for each of these species, along with the sample size and the significance level for each value of r, are presented in Tables 10.12 - 10.14. The calculation of the metabolic rates for glucose and ammonia (mMh^{-1}) were based on the gradient of the line of best fit to the data plotted for each of the time periods.

The results from the second run show differences between the supply and sink levels of glucose and ammonia in samples taken at the same point in time. Levels of these metabolites in samples taken from the cellular growth space tended to be similar to those taken from the sink circuit. While the differences between the supply and sink

circuits could be quantified, the control method and the low sampling rate used during this experiment did not allow for an accurate measurement of the metabolic rates within the bioreactor to be made. Metabolic rates were calculated using the changes in the levels of nutrient in the feed vessel which, due to the low sample number used for each calculation, were also prone to inaccuracy, as evidenced by the low levels of significance ascribed to each.

The results from the third run show a less consistent pattern of differences between the supply and sink circuits. Two explanations can be given for this observation, the first is associated with possible sampling errors, with the immediate sampling of the sink circuit after a medium change leading to an artificially low value (Section 10.6.2). The second explanation is related to the higher filtration rates used during this run (0.18-0.24 lh^{-1}) which led to shorter residence time for the medium in the growth space, resulting in smaller changes in the level of metabolites across the bioreactor. This compares with the previous run where the filtration rates used were lower, allowing for larger changes in the level of nutrients between the supply and sink circuits. An increase in the sampling rate allowed for the calculation of metabolic rates based on changes in the feed levels of metabolite to be determined with a higher level of significance.

In the fourth run the higher sampling rates, a reduction in the feed vessel volume and the successful operation of the oxygen probes increased the pool of available data to be analysed. As the differences in metabolite levels across the bioreactor were not clear cut, the supply circuit levels were taken as being the best indicator for metabolic rate calculation. The higher sampling rate increased the number on which rate calculations were based, improving the level of their significance, and the size of the observed differences in the levels of metabolites in the feed vessel.

By monitoring the filtration rate and the differences in oxygen concentrations between the supply and sink circuits, a correlation between these two measurements was observed. Figure 10.9 shows this relationship and two calculated lines of best fit. It can be seen that as the filtration rate is increased the difference in the concentration

Table 10.11:- Filtration rates and feed vessel volumes for Runs 2-4

Run Number	Range of filtration rates (lh^{-1})	Feed vessel volume (l)
2	0.13-0.18	4
3	0.18-0.24	4
4	0.08-0.20	1.5

of oxygen between the supply and sink circuits decreased, suggesting that the product of filtration rate and concentration difference (Equation 6.6) indicates the level of oxygen utilisation. The slope of the line favours the hypothesis that as the filtration rate was increased to 0.22 lh^{-1}, the oxygen levels between the two circuits became immeasurable for the oxygen probes used in this work, indicating the transition between conditions 2 and 1 at around this point (Tables 10.9 and 10.10).

While the oxygen probe was responsive to the filtration rate, a comparison of the glucose and oxygen utilisation rates for this run suggests that the calculated oxygen values were wrong. It would be expected that the oxygen utilisation rate for the cells would exceed that of glucose by a factor of 12, assuming the complete oxidation of 1 mole of glucose requires 12 moles of oxygen. The most likely explanation for the apparently low oxygen utilisation rates lies in the low flow rates observed in the sink circuit, resulting from the flow regime adopted within the bioreactor. Under these conditions it would be expected that the degree of mixing at the probe surface would be too low to remove any liquid film effect, especially since the probe surface was not protruding directly into the medium flow. This would affect the rate of oxygen transport to the probe surface. Under these conditions the levels of oxygen observed in the sink circuit would not be expected to be representative of the levels in the bioreactor. This is further complicated by medium returning to the supply circuit, due to any Starling flow regime. As both of these values are required for the calculation of the oxygen utilisation rate, the value obtained would be in error. A further discussion of the errors associated with the oxygen readings will be carried out at the end of this chapter (Section 10.6).

Figure 10.5:- **Glucose and ammonia levels during Run 2**

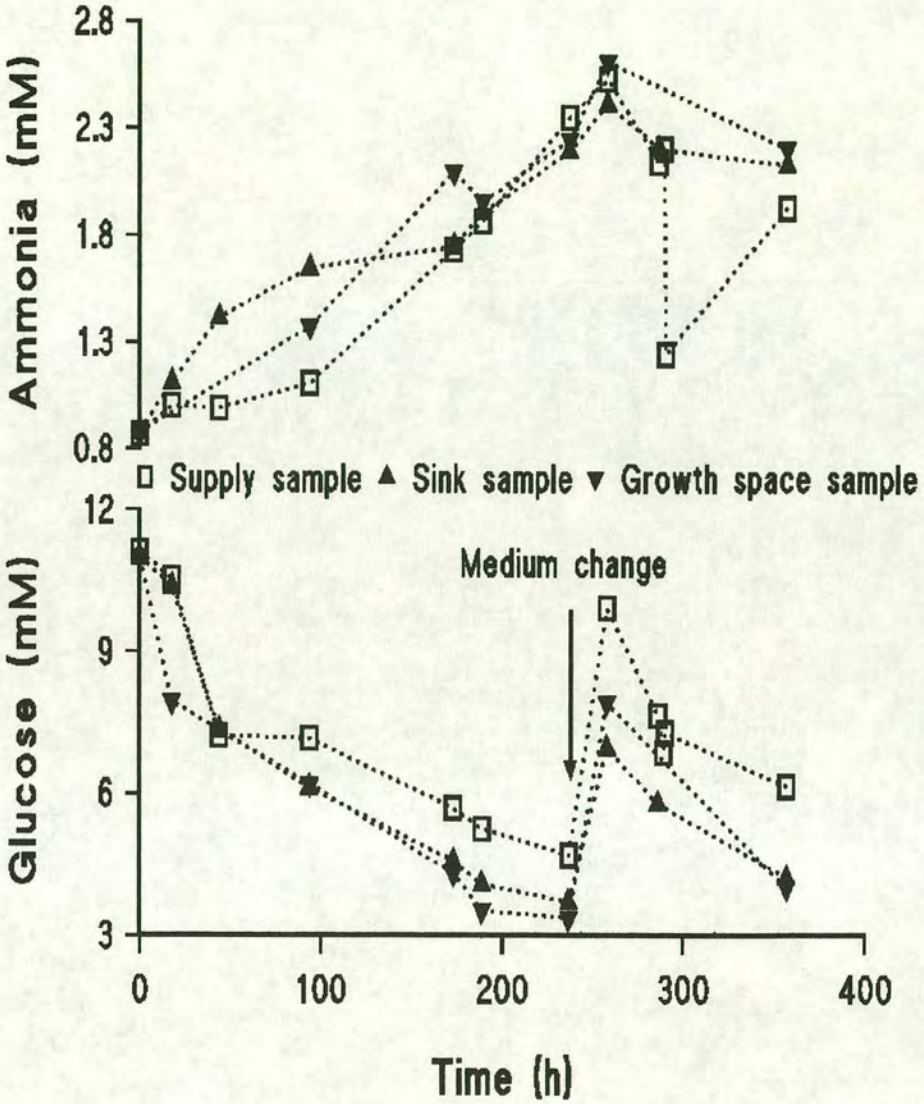

Table 10.12:- **Calculated metabolic rates for Run 2**

Run time (h)	Glucose utilisation rate			Ammonia production rate		
	$mmoleh^{-1}$	r	Sample size	$mmoleh^{-1}$	r	Sample size
18-237	0.016	0.90[a]	4	0.028	0.95[b]	4

[a] r fails to differ significantly from 0 (nonlinearity) at the 5% level in a two tail test.

[b] r differs significantly from 0 (nonlinearity) at the 5% level in a two tail test.

[c] r differs significantly from 0 (nonlinearity) at the 1% level in a two tail test.

[d] r differs significantly from 0 (nonlinearity) at 0.1% level in two tail test.

Figure 10.6:- **Glucose and ammonia levels for Run 3**

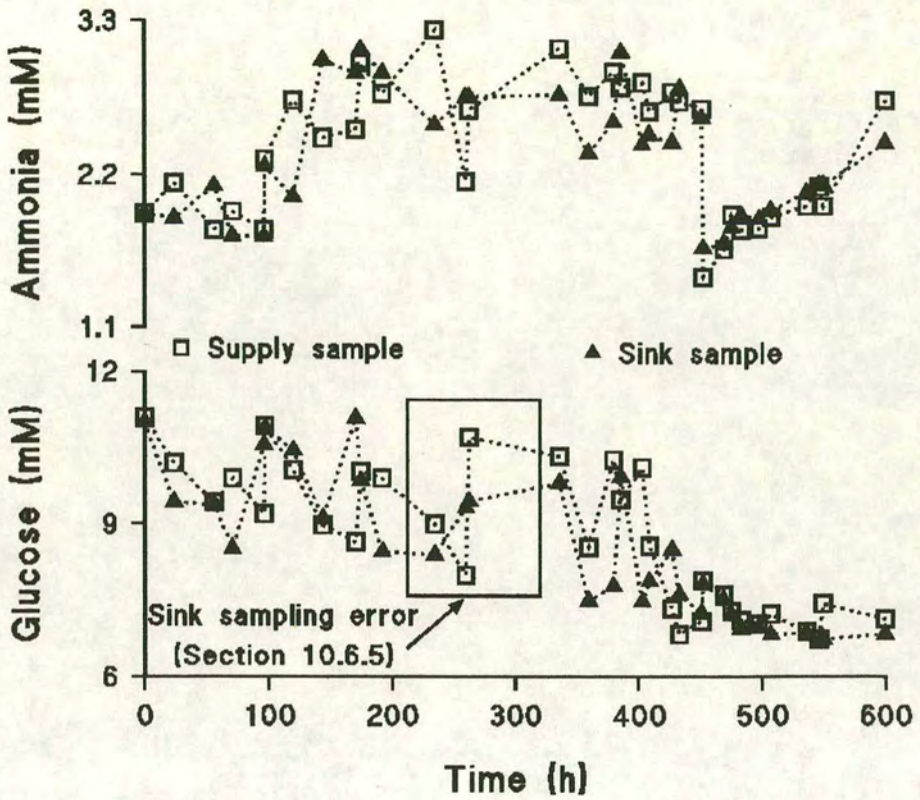

Table 10.13:- **Calculated metabolic rates for Run 3**

Run time (h)	Glucose utilisation rate			Ammonia production rate		
	$mmolh^{-1}$	r	Sample size (n)	$mmolh^{-1}$	r	Sample size (n)
97-171	0.128	0.97[b]	4	0.040	0.79[a]	4
175-260	0.096	0.96[b]	4	-	-	-
380-451	0.204	0.90[c]	7	-	-	-
452-497	-	-	-	0.032	0.96[d]	8

[a,b,c,d] **Notes as per Table 10.12.**

Figure 10.7:- **Glucose, ammonia and oxygen levels for Run 4**

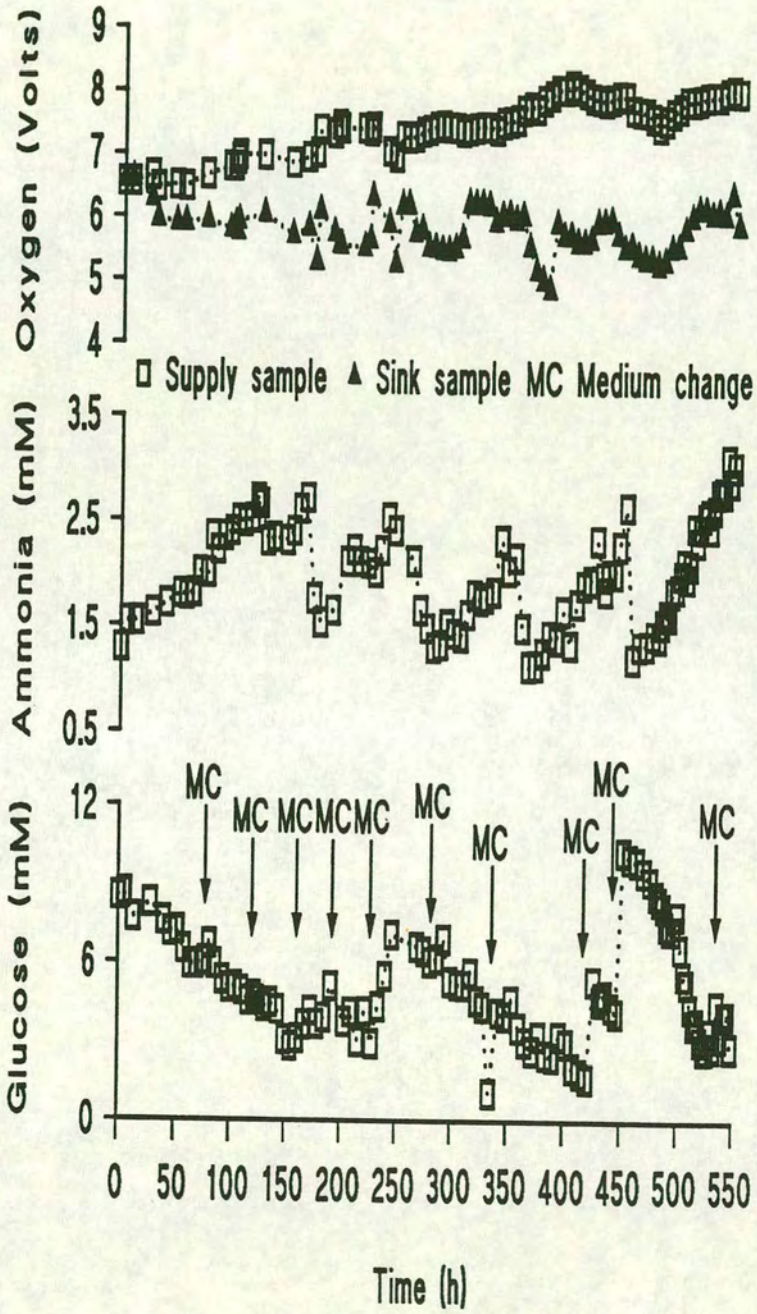

Figure 10.8:- **Oxygen utilisation rates during Run 4**

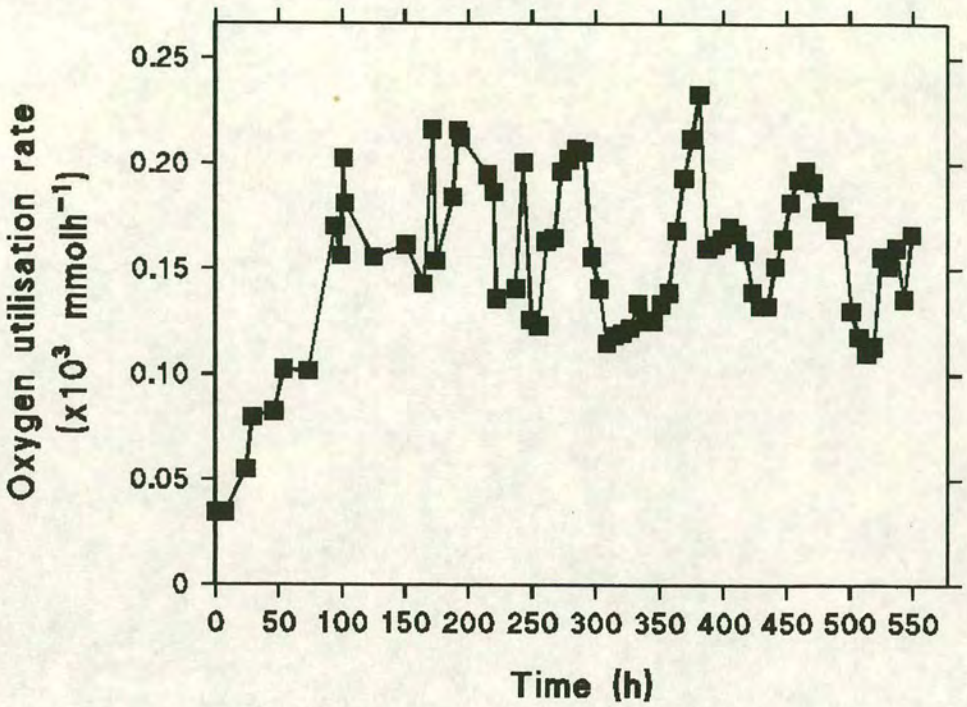

Table 10.14:- **Calculated metabolic rates for Run 4**

Run time	Glucose utilisation rate			Ammonia production rate		
(h)	$mmolh^{-1}$	r	Sample size(n)	$mmolh^{-1}$	r	Sample size(n)
13-52	0.091	0.99[c]	5	0.011	0.99[c]	5
52-86	0.070	0.87[b]	7	0.003	0.87[b]	7
81-131	0.090	0.95[d]	10	0.017	0.95[a]	10
137-173	-	-	-	0.017	0.86[b]	7
234-287	0.038	0.96[d]	7	0.018	0.82[b]	7
317-348	-	-	-	0.028	0.89[b]	6
354-420	0.132	0.96[d]	12	0.021	0.93[d]	12
426-452	0.078	0.90[c]	7	0.048	0.89[b]	7
460-499	0.109	0.97[d]	10	0.024	0.94[d]	10
506-530	0.273	0.96[c]	9	0.036	0.85[c]	9

[a,b,c,d] **Notes as per Table 10.12.**

Figure 10.9:- Relationship between the oxygen differential and the filtration rate during Run 4

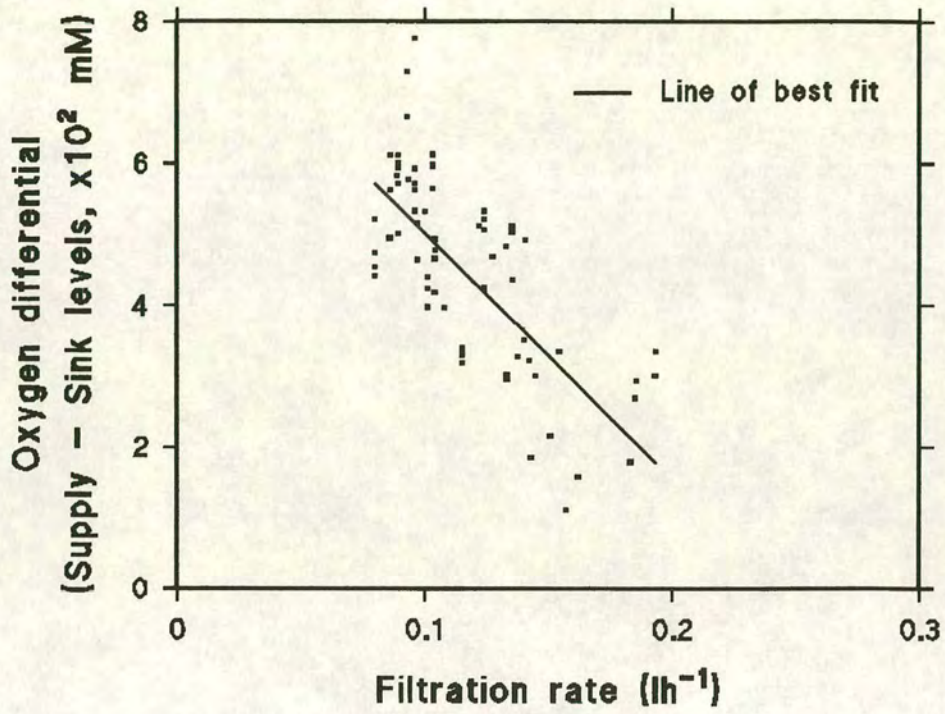

10.4.2 Effects of low filtration rates on metabolic results

The effects of lowering the filtration rate on bioreactor performance was examined in Run 5. The levels of glucose and oxygen in the supply and sink circuit are reported in Figure 10.10. No oxygen levels were monitored in the sink circuit between 160 and 306 h due to the failure and subsequent replacement of the cable connecting the oxygen probe to its signal amplifier. Ammonia levels were not adequately recorded during this experiment due to a miscalculation in the quantity of sample required for all of the assays. This situation occurred as a result of supplementary glucose assays being carried out at each time point in order to verify the low levels of glucose recorded in the sink circuit. The difficulties associated with the maintenance of filtration rates below 0.05 lh^{-1} are described further in Section 10.6, with the highly unstable filtration rates recorded during the run reported in Figure 10.24.

There was a marked difference between the levels of glucose in the supply and sink circuits during the run, with a slower decline in the levels of glucose recorded in the supply circuit when compared with the previous runs, despite the use of a 1.5 l feed vessel. Plots of the glucose and oxygen differentials across the bioreactor versus the filtration rate at each time point are presented in Figure 10.11. The results excluded from the calculated lines of fit (open symbols, Figure 10.11) were related to the start of the run, where the cell number within the bioreactor was not thought to have stabilised. Based on the apparent linear relationship between the filtration rate and the glucose differentials across the bioreactor it was thought that the use of the filtration related calculation of metabolic rates, outlined for condition 2 (Table 10.10) was valid, with the calculated metabolic rates reported for Run 4 in Figure 10.12. The use of this method of calculation was also preferable to using the feed levels of glucose due to the small changes observed in the bulk nutrients in the supply circuit, relative to the previous experiment (Run 4).

Extrapolation of the least squares line of best fit for the glucose data (Figure 10.11) would suggest that the use of this calculation method would not be valid above about 0.04 lh^{-1}, where the differences in the levels of glucose between the two circuits would be small, with the largest differences occurring as the filtration rate approached zero. A more likely scenario for higher filtration rates was that suggested in the previous section, with the difference between the two circuits approaching zero.

However, the lines of fit calculated for the differential oxygen levels in Run 5 (Figure 10.11) appear to increase with the filtration rate. The least squares line of fit suggests that at 0.04 lh^{-1} the difference between the supply and sink circuits is continuing to rise, unlike the results for Run 4, while a polynomial line of fit using these parameters suggests that the difference between the two circuits starts to decline after reaching a maximum value at 0.037 lh^{-1}. The calculated oxygen utilisation rates again fell below the value expected for the complete oxidation of glucose, suggesting there was once again a problem with the oxygen readings. Another possible explanation is that at the low filtration rates used in this run, the pressure profile in the bioreactor

Figure 10.10:- **Glucose and oxygen levels for Run 5**

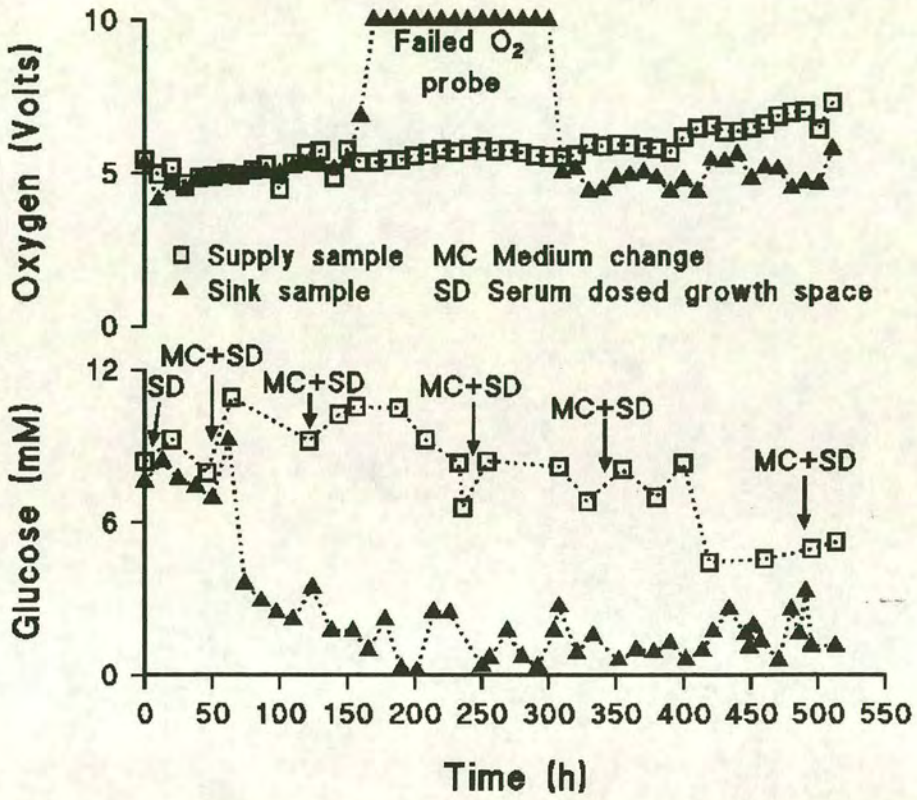

was favouring a Starling flow regime. The absence of an oxygen probe on the outlet of the bioreactors supply circuit meant that the degree of oxygen utilisation related to any Starling flow component could not be determined. Combining this flow profile with an increased liquid film effect on the sink probe, due to the lower filtration rates used, would be expected to increase the errors associated with the oxygen readings.

One of the effects associated with the use of this method of calculation has been highlighted in Figure 10.12, where 'peaks and pits' were noted where there were

Figure 10.11:- Relationship between oxygen and glucose differentials and the filtration rate during Run 5.

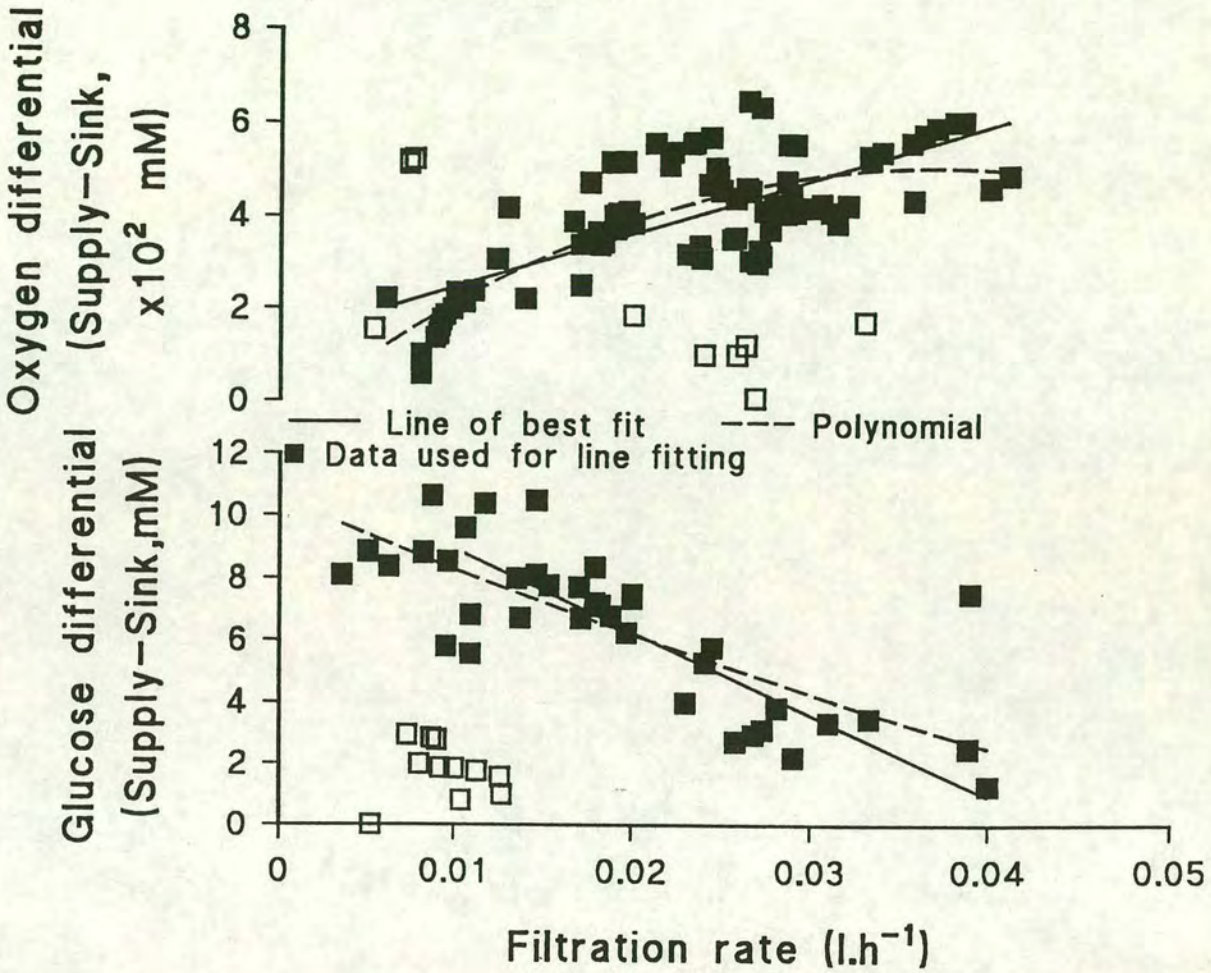

large changes in filtration rate. For example at 306 h on Figure 10.12 an increase in filtration rate was implemented from 0.003 to 0.039 lh^{-1}, with an associated change in the glucose utilisation rate from 0.08 to 0.15 $mmoleh^{-1}$. At 390 h the filtration rate was changed to 0.04 from 0.02 lh^{-1}, with related changes in glucose and oxygen utilisation rates from 0.14 $mmoleh^{-1}$ and $3.12x10^{-4}$ $mmoleh^{-1}$ to 0.32 and $23.41x10^{-4}$ $mmoleh^{-1}$ respectively. Over periods where no alterations in the filtration rate were made, e.g. 340-380 h (0.020, σ=0.005 lh^{-1}) and 450-480 h (0.027, σ=0.003), the calculated rates remained at a fairly constant level, 0.127 (σ= 0.003) $mmoleh^{-1}$, 0.053 $mmoleh^{-1}$ (σ= 0.007), suggesting that the 'peaks and pits' were associated with changes in the filtration rate.

A likely explanation for these observations lies in the sink circuit sampling problems

(Section 10.6) with the samples taken immediately after the change being representative of the previous filtration rate. This would result in the large differences between the supply and sink circuits observed at the low filtration rate being multiplied by the new higher rate resulting in a peak in the data. For the converse situation, from high to low filtration rates, the product of the flow and small difference between the two circuits would result in an artificially low metabolic rate, i.e. a pit. Under conditions where no changes in the filtration rate had occurred, the conditions would be constant within the bioreactor with sink samples being fully representative of the growth space levels of nutrient. A further comparison of the metabolic information derived from these experiments will be made in Section 10.6, with an emphasis placed on how representative the samples and calculated metabolic rates were in describing the performance of the bioreactor.

10.4.3 Effects of changing supply fibres

The bioreactor used for Run 6 differed from those used in Runs 2-5 in that the supply fibres had a molecular weight cutoff of 100 kDa. The reason for altering the pore size of the supply fibres was outlined in Table 10.3 and it will be discussed further in Section 10.5. Based on the observable differences between the supply and sink circuits in Run 5, the bioreactor was operated in a single pass mode (see Section 10.1.2) as the filtration related calculation of metabolic rates was thought to be applicable under the intended operational conditions, i.e. the use of changes of feed levels should not be needed for rate calculations. This decision was further influenced by the effects that the change in the MWCO of the supply fibres had on the performance of the bioreactor. This altered the pressure profile of the bioreactor so that the full length of the supply fibres was, in theory, maintained at a higher pressure than the cellular growth space, minimising the degree of back flow returning to the supply fibres (Section 10.3.3).

The filtration rates used in this run ranged from 0.005 to 0.08 $l.h^{-1}$, with the analysis of metabolite levels also extended to include lactate. The results from this experiment are presented in Figures 10.13 to 10.16.

Figure 10.12:- **Oxygen and glucose utilisation rates during Run 4.**

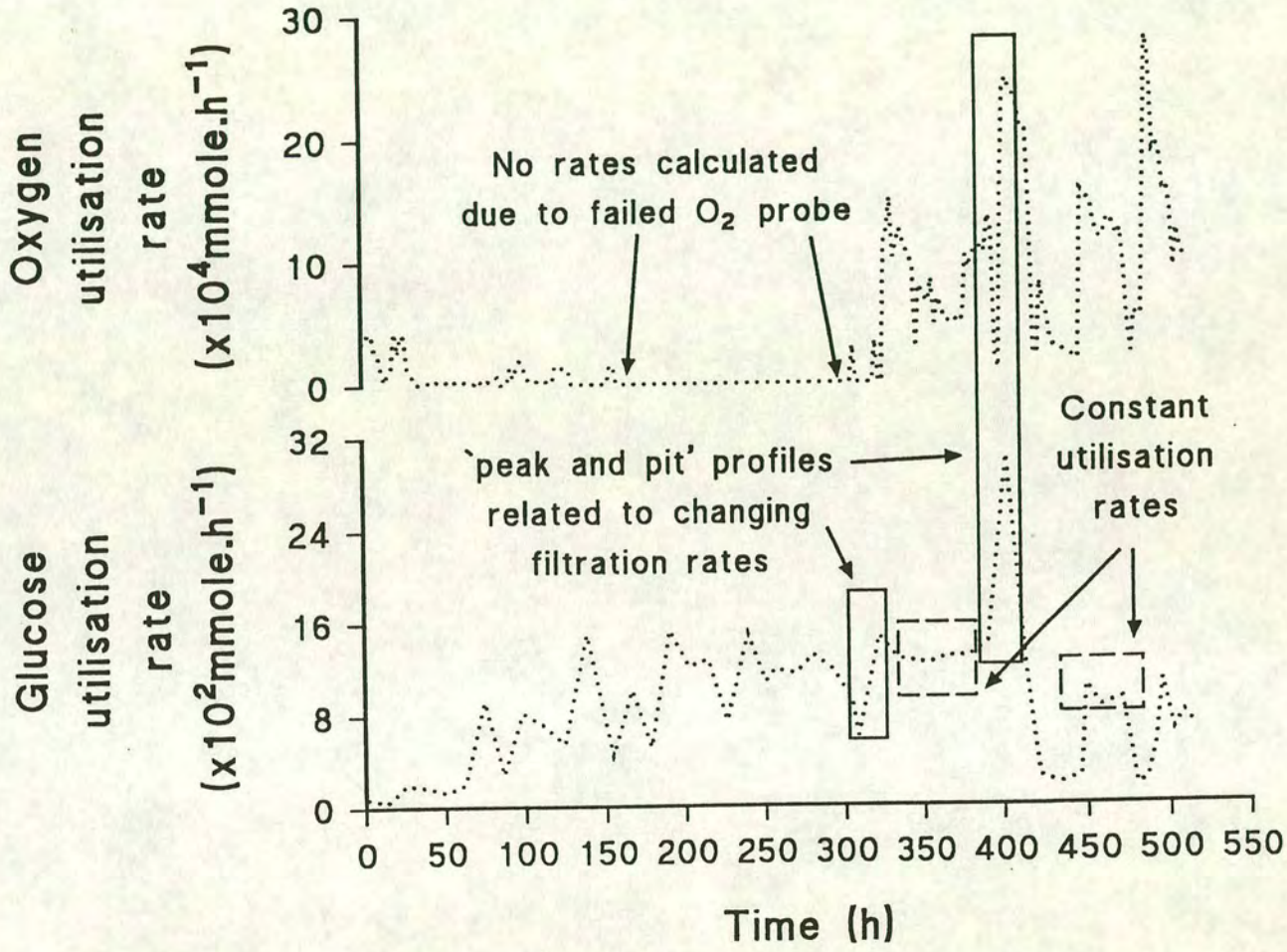

Examination of the nutrient profiles for the bioreactor circuits (Figures 10.13 and 10.14) showed two types of behaviour, where the differences in nutrient levels between the two circuits was either negligible or observably different. In order for the use of a filtration rate related calculation of metabolic rates to be justified, the relationship between nutrient differentials and the filtration rate had to be established. Plots of this data (Figures 10.15 and 10.16) showed no clear relationship between these two parameters, with the correlation coefficients for the least squares lines of

Figure 10.13:- Oxygen and glucose levels during Run 6

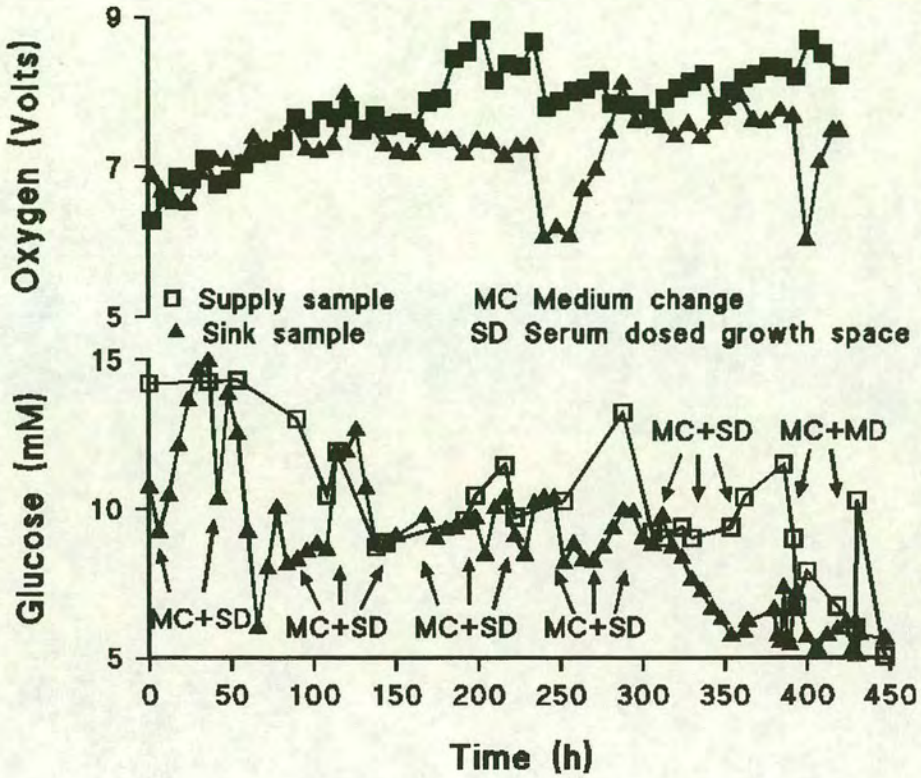

Figure 10.14:- Lactate and ammonia levels during Run 6

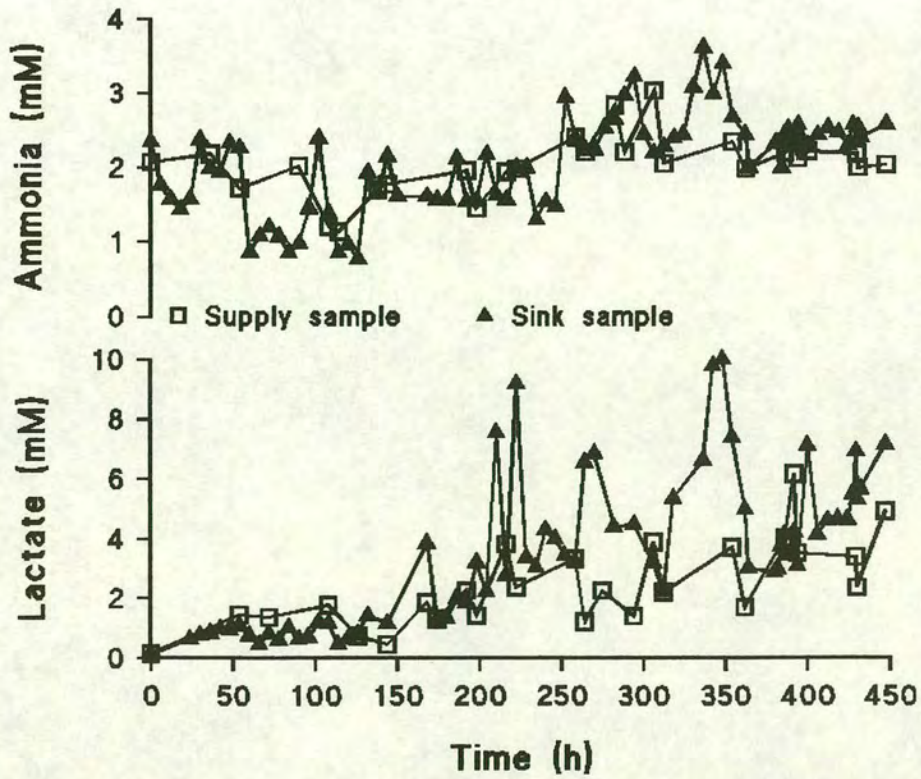

Figure 10.15:- Oxygen and glucose differentials versus filtration rate (Run 6)

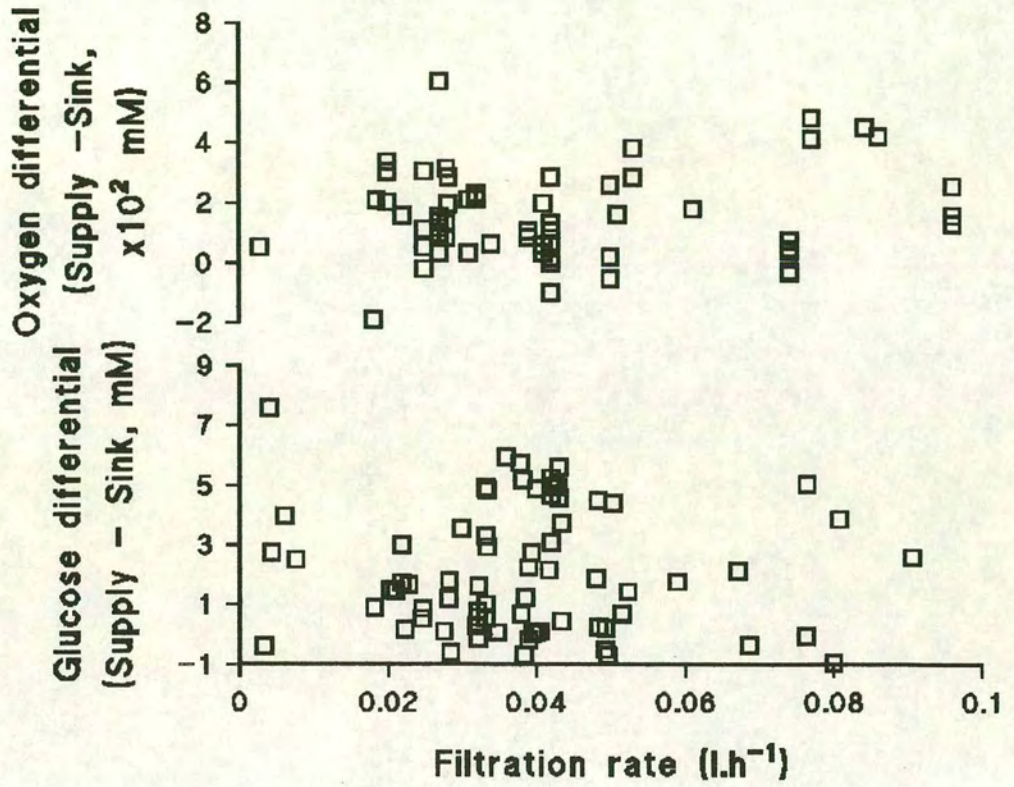

Figure 10.16:- Lactate and ammonia differentials versus filtration rate (Run 6)

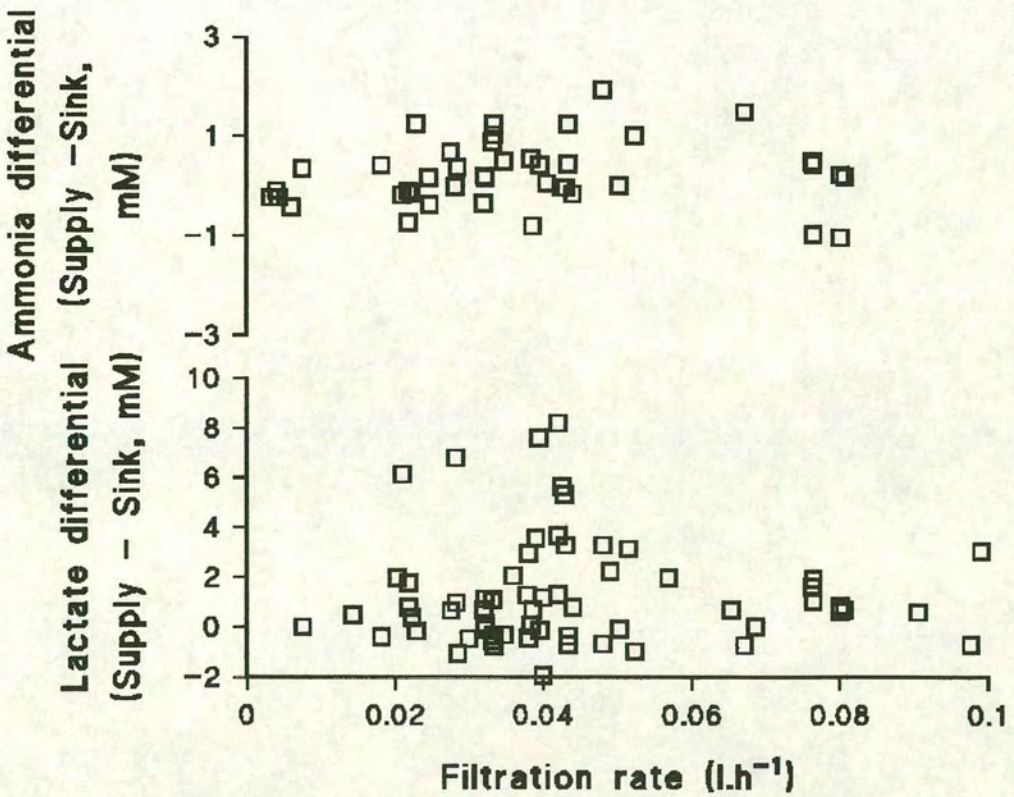

fit falling below 0.15. Polynomial lines of fit were also visually tested against this data, with no satisfactory solutions found. A number of reasons may be proposed for the failure of this data's filtration dependency, including the apparent consumption of ammonia and lactate, and the production of glucose. This suggests that the faults lay in sampling errors, i.e. that the sink samples were not fully representative of the growth space. The effects of flow regimes within the bioreactor on the metabolic data will be discussed in Section 10.6.

As the bioreactor was mainly operated in a single pass mode, the feed vessel could not be used as an indicator of the metabolic performance of the cells. The failure to find any relationship between the filtration rate and nutrient differentials across the bioreactor meant that any metabolic rates calculated using the filtration rate method were meaningless. The variability in this data meant that no useful conclusions could be drawn other than that the production of metabolites and the utilisation of nutrients was occurring.

10.5 Pressure profiles and protein components

The theory described in Chapter 5, relating to dead end and crossflow filtration, outlines the effects that proteins have on the flux and rejection of conventional hollow fibre cartridges. In this section the influence of partially retained species, primarily proteins, on bioreactor performance will be discussed. The only protein which was specifically tested for was the IgM produced by the ES 4 hybridoma. In this section the antibodies are used both as indicators of their own distribution within the bioreactor and as potential markers of the behaviour of the other serum related macromolecules present in the medium. Other indicators, such as flux and pressure profiles, were used as indirect evidence, where this information was available.

10.5.1 Effects of dead end filtration

The first experiment (Run 1) was carried out with a dual end supply regime, outlined in Figure 10.17. This entailed the supply of the serum supplemented medium to both ends of the supply fibres, effectively operating the supply fibres as dead end filters. It was found that the flux across the bioreactor rapidly declined to zero within the first two days of operation, despite attempts at increasing the liquid flow rates and transmembrane pressures. The pH of the growth space was observed to increase to 8.2, measured at the end of the experiment, from an initial value of between 7.2 and 7.4. The presence of phenol red within the medium allowed a visual estimation of the pH in different parts of the circuit to be made. The colour of the phenol red equating to a pH of 8.2 was observed to be present in all parts of the supply and sink circuit except the feed vessel from day 3 onwards, suggesting that there was no flow entering the supply fibres, or traversing the growth space to the downstream circuit. The feed vessel remained at a constant pH of 7.2.

The run was terminated on day 11 and the bioreactor module visually inspected and cleaned. A visual inspection of the ends of the bioreactor showed that the supply fibres were blocked. These blockages were removed using a syringe and it was concluded that they had developed as a result of protein rejection by the pores of the supply fibres. This was thought to be due to the macromolecular components present in new born calf serum most of which range from 6 (Insulin) to 440 kDa (fibronectin) in size (Jenkins ,1991, Macleod, 1991). The pore size of the supply fibres was 100 kDa which is larger than the most abundant species in the serum (BSA), which would imply that the rejection of the serum components by the membrane should be low. Amicon report a 30% rejection of BSA by cartridges containing similar 100 kDa cutoff fibres to those used in this study which supports this hypothesis. However, the Amicon experiments were carried out on single component mixtures, which tend to behave in a different way to multiple component mixtures, e.g. Amicon also report rejection levels of 30% and 50% for a 1% solution of bovine serum using a 0.1 μm pore sized fibre, operated as a crossflow filter at 1 and 5 psig transmembrane pressures respectively. Another possible contributory factor was related to the method

of sparging used in the feed vessel (Section 10.6.7) where, as a result of foaming and its subsequent breakdown, macromolecular aggregates were formed from the precipitates observed on the walls of the feed vessel. These aggregates would also aid in the fouling of the membranes producing the observed cake formation and the resultant decline in flux. Based on this data and as a direct result of the observed fouling of these membranes, the pore size of the supply fibres was increased to 0.1 μm for Runs 2 to 5 in order to minimise protein rejection.

Whether the cell death observed during this run was attributable to the mode of operation, or some other factor, such as the alkaline pH was not ascertained. Based on these result the supply fibres were operated as crossflow filters for the remaining runs.

10.5.2 Effects of crossflow filtration

The remaining filtration rate data for Runs 3, 4 and 6 are presented in Figure 10.18, with the data for Run 5 reported in Figure 10.22. In the runs where the supply fibres were operated as crossflow filters the flux never declined to zero, other than in those periods when control was poor (Section 10.6.3). This agrees with general filtration theory which predicts that the build up of foulant layers on the supply fibres would be reduced in the crossflow mode of operation (Section 5.1.3). The effects of membrane fouling were however, still observed, especially during periods where the operating conditions, i.e. pressure and liquid flow rate, remained unaltered. The effects of medium changes during these periods had no noticeable effect on the flux across the bioreactor, suggesting that the fouled layer was fairly stable.

Figure 10.17:- Bioreactor circuit used in Run 1

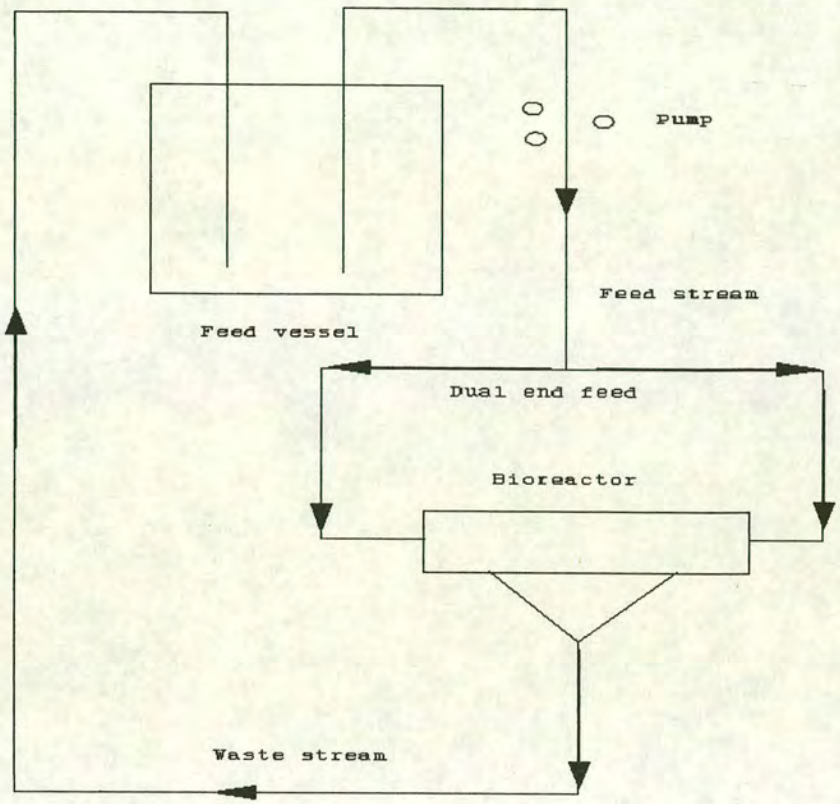

Back flushing is a commonly used technique for removing foulant layers from membrane surfaces by reversing the direction of flow across the membrane (Mulder, 1991 and Chapter 7). This technique was applied during Run 4, with the flow pattern in the bioreactor being reversed from the normal supply to sink circuit regime using a peristaltic pump and the residual medium present in the sink circuit. The pump on the supply circuit was switched off for the two minute period that the reverse flow regime was applied. A comparison of the filtration rates before and after the back flush showed an immediate increase of 0.02 lh^{-1} from the pre-back flushing level of 0.12 lh^{-1}. The filtration rate was then observed to continue declining for the remainder of the run. It was thought that the main fouling had occurred on the supply fibres, rather than the sink fibres, although the back flushing of the bioreactor would have removed fouling from both sets of fibres. The build up of cells on the fibres within the growth space could also be considered as a form of fouling. The effects of back flushing on the biomass within the CGS were discussed in Section 10.2.4.

Figure 10.18:- **Filtration rates for Runs 3,4 and 6**

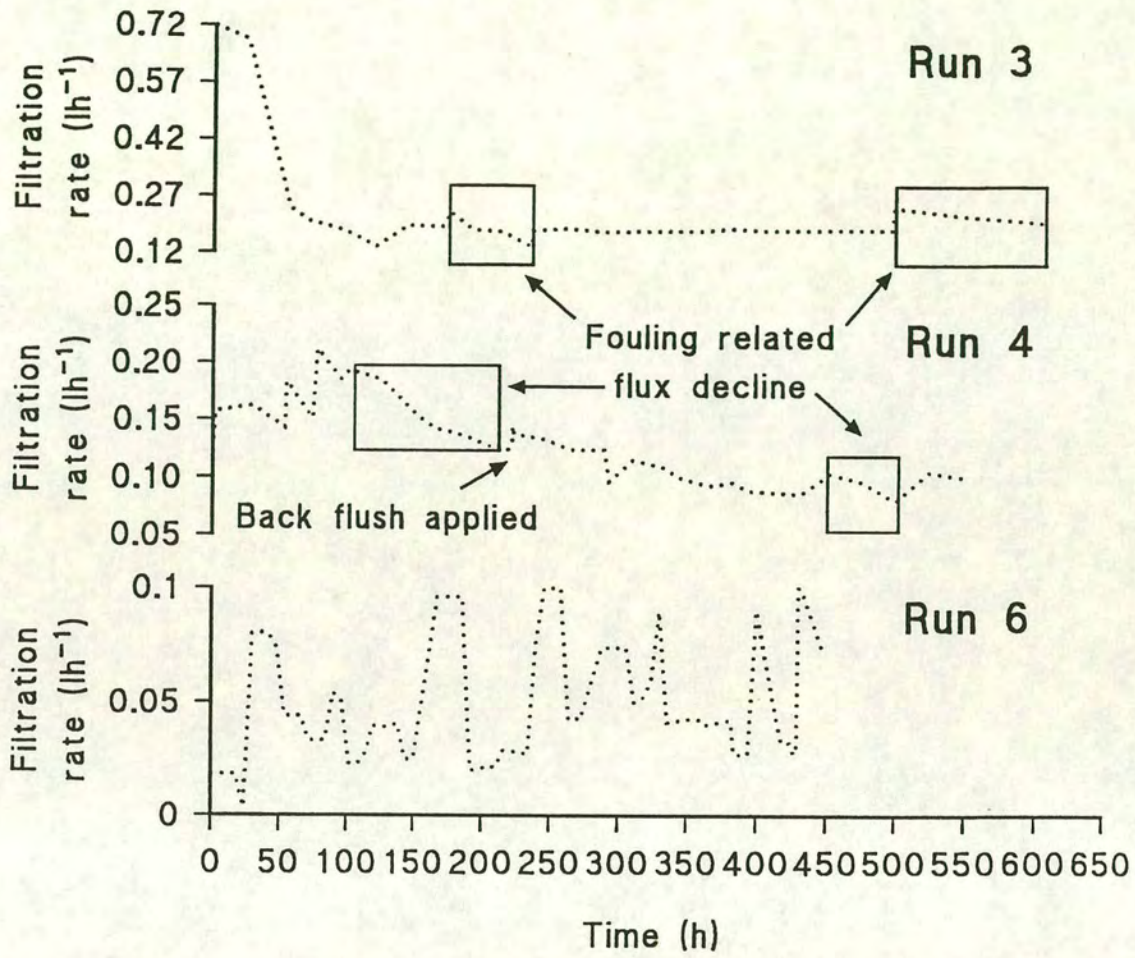

The filtration rates attained during Run 6 showed less fouling than the previous runs, with the oscillations in Figure 10.18 being associated with either intentional changes or a failure in the manual control of the bioreactors filtration rate. Whether this was due to the changes in filtration rate applied to the bioreactor during the experiment, as a result of the lower filtration rates used or as a result of the change in the method of serum addition, i.e. the direct dosing of the growth space, was not determined.

10.5.3 Macromolecular rejection within the bioreactor

The antibody levels in the supply and sink circuits during Runs 2 to 6 are reported in Figure 10.19. In the runs where recirculation of the waste stream occurred in combination with a high filtration rate (Runs 2-4), i.e. above 0.10 lh^{-1}, the antibody levels were observed to increase in the supply circuit, with low levels monitored in the sink circuit. The opposite was found to be true for lower filtration rates (Run 5), i.e. below 0.08 lh^{-1}, where the levels of antibody in the sink circuit were found to be higher, but the rate of accumulation in the feed vessel was lower due to the effects of dilution, the larger feed vessel volume and medium changes. In Run 6 the use of a single pass mode of operation meant that the only accumulation of antibody in the feed vessel was as a direct result of the periods where recirculation was used (Section 10.1.2). The levels of antibody in Run 6 were higher in the sink circuit, agreeing with the results from Run 5 where lower filtration rates were also used.

If antibody was freely dispersed throughout the bioreactor, i.e. its flow was not restricted by the membranes, then it would be expected that the supply and sink levels of antibody would be similar in the runs in which recirculation was used at a high filtration rate (Runs 2-4). However, antibody was found to be retained in the feed vessel suggesting that it was being rejected by the supply fibres. Amicon report a 70% rejection of Gamma Globulin Fraction II, which contains species ranging from 160 kDa to 900 kDa, for a 0.1μm hollow fibre cartridge operated as a crossflow filter, at a transmembrane pressure of 10 psi (0.7 bar). The rejection data reported by Amicon in this paragraph and the previous section, when combined with these results strongly suggest that the IgM was being rejected by the pores in the membrane and concentrated in the supply circuit, despite the pore size of the supply fibres (0.1μm).

The levels of antibody in the sink circuit also indicate that the antibody was able to cross these 0.1 μm pore sized fibres. This would appear to suggest that the fibres, which were operated as dead end filters, were not fouling to an extent that antibody was retained within the growth space. This agrees with the findings in Section 8.3, where dyed dextran rejection was found to be low for the simulated bioreactor.

Figure 10.19:- Antibody levels for Runs 2-6

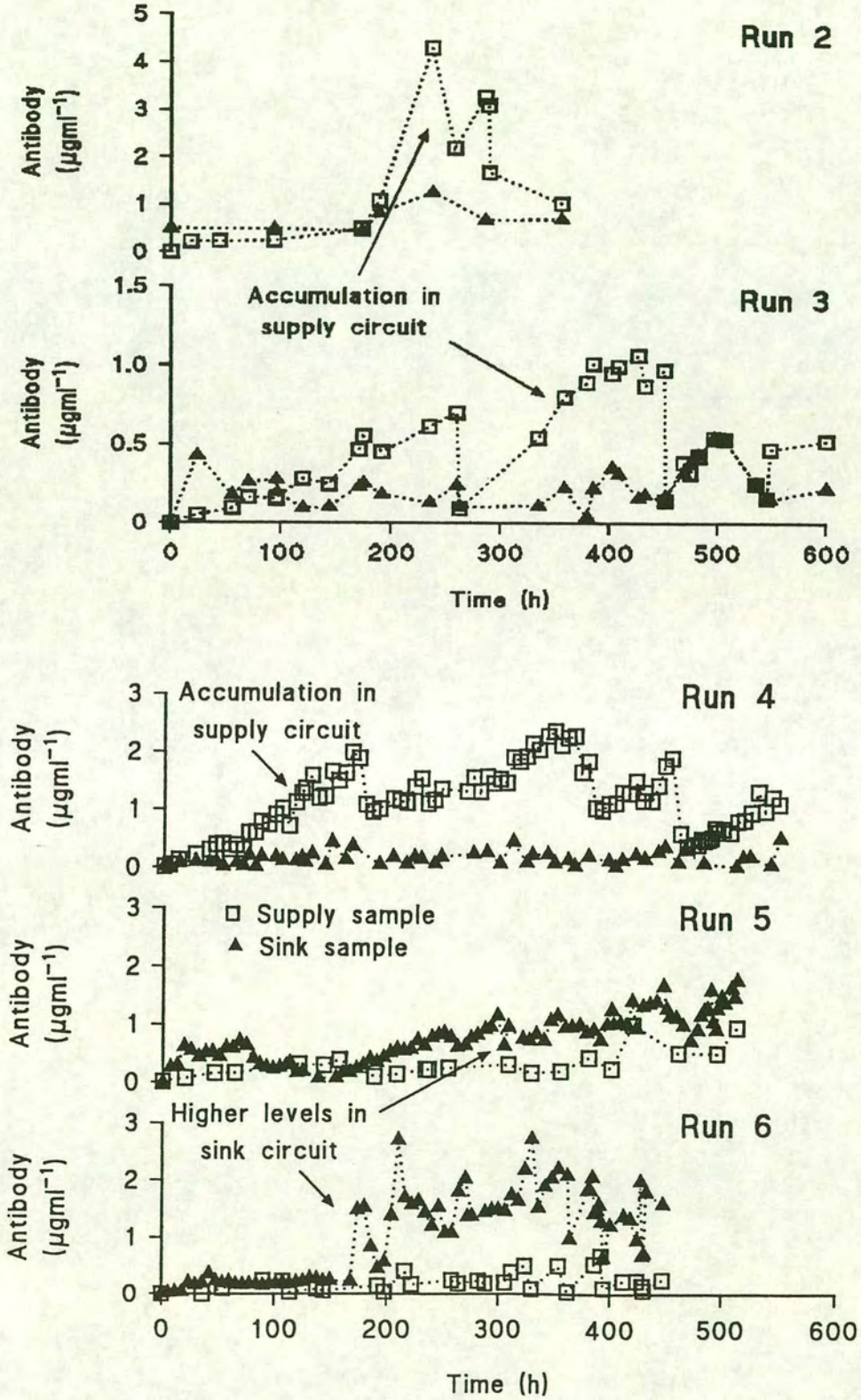

10.5.4 Antibody production rates

High filtration rates

The basis for the calculation of the antibody production rates for Runs 2 and 3 was similar to those described for the freely dispersed species, i.e. glucose and ammonia (Section 10.4.1), using the changes in the levels of antibody in the feed vessel over time (Table 10.15). However, unlike the freely dispersed species the accumulation of the antibody in the supply circuit suggested that the IgM was rejected by the supply fibres which, when associated with a reduction in the volume of the feed vessel, related to the greater volumes required for sampling, led to the concentration of antibody in the supply circuit. This was not a great problem where low sampling frequencies were used, for example Runs 2 and 3, but proved to be a fairly large source of error for Run 4 where a higher sampling frequency was employed.

Table 10.16 outlines a modified method for calculating the effective antibody production rate for Run 4, with the conversion factors used in these calculations presented in Table 10.17 and the summarised results for this run presented in Table 10.18. The conversion factor takes into account the volume of the vessel at the start and end of the sample period and measures the degree to which the antibody within the supply circuit has been concentrated. By correcting the gradient of the calculated line to take account of the concentration factor, the effective antibody production rate, based on the volume of the vessel at the start of the sample period, could be calculated.

Low filtration rates

The rationale behind using the product of the filtration rate and the difference between the supply and sink levels of freely dispersed nutrients at low filtration rates has already been described (Section 10.4.2). The rejection of antibody by the supply fibres (assuming 100% rejection) suggests that the product of the levels of antibody in the sink circuit and the filtration rate would give a good indication of the antibody production rate by the cells within the growth space. The differences in feed level concentrations of antibody over time were not high enough to warrant the use of these

Table 10.15:- Calculated antibody production rates for Runs 2 and 3

Run 2			
Run time (h)	Antibody production rate (mgh^{-1})	r	Sample size
18-173	0.08	0.994[c]	4
173-237	0.24*	0.905[c]	5
Run 3			
97-171	0.02	0.964[c]	4
175-260	0.02	0.995[c]	4
263-386	0.03	0.995[c]	4
380-451	0.04	0.548[a]	7
452-497	0.03	0.954[d]	8

[a,b,c,d] Notes as per Table 10.12

Table 10.16:- Corrected calculation for Run 4 antibody production rates

Step 1			
Time period	Calculated antibody production rate	Line of best fit from experimental data	Recalculated antibody concentrations at t=13,t=52 (mgl^{-1})
h	mgh^{-1} **(Form 1)**	$y = mx+c$	$C_{t=13}$, $C_{t=52}$
13-52	0.01	$y = 0.007x+0.026$	0.121, 0.408
Step 2			
Feed volumes	Conversion factor	New concentration	New production rate (mgh^{-1})
$V_{t=13h}$, $V_{t=52h}$ (l)	$C.F. = V_{t=52}/V_{t=13}$	$C_{corr} = C.F. * C_{t=52}$	$((C_{corr}-C_{t=13})/dt)* V$ = **Form 2**
1.0, 0.9	0.9/1.0 = **0.9**	0.9 * 0.408 = **0.330**	(0.330-0.121)/(52-13)*1.5 = **0.075**

Where V = original feed vessel volume

*** value high due to the effects of antibody accumulation in the supply circuit**

Table 10.17:- Conversion factors used in the calculation of production and utilisation rates (Table 10.16)

Period of run (h)	Conversion factor (C.F.)
13-52	0.90
52-86	0.82
81-131	0.75
137-173	0.83
234-287	0.88
317-348	0.85
354-420	0.80
426-452	0.80
460-499	0.88
506-530	0.80

Table 10.18:- Antibody production rates for Run 4

Run time (h)	Calculated production rate (mgh^{-1})	r	Sample size (n)	Corrected production rate (mgh^{-1})
13-52	0.01	0.985^{d}	5	0.01
52-86	0.02	0.905^{c}	7	0.02
81-131	0.02	0.866^{d}	10	0.01
137-173	0.03	0.894^{c}	7	0.02
234-287	0.01	0.854^{c}	7	0.01
317-348	0.02	0.943^{c}	6	0.01
354-420	0.02	0.975^{d}	12	0.01
426-452	0.04	0.922^{c}	7	0.02
460-499	0.01	0.927^{d}	10	0.01
506-530	0.04	0.938^{d}	9	0.02

^{a,b,c,d} Notes as per Table 10.12

values for the determination of production rates.

Figure 10.20 shows the antibody differentials versus filtration rate for Runs 5 and 6. While there may be a filtration related trend for antibody differentials in Run 5, the data for Run 6 was too scattered to find any meaningful relationship between these two parameters. This parallels the finding for the freely dispersed metabolites, i.e. a good agreement with the filtration rate for the Run 5 data and a poor agreement for the Run 6 data.

The calculated antibody production rates for Runs 5 and 6 are presented in Figure 10.21, although the validity of the applying the filtration rate dependent method for rate calculation below 0.04 lh^{-1} was again called into question. The 'peak and pit' profiles highlighted were also in evidence for Run 5 (Figure 10.21) where the filtration rate at 390 h was altered from 0.02 to 0.04 lh^{-1} with an immediate increase in the antibody production rate of 0.02 from 0.049 mgh^{-1}. This information, when combined with the plot of antibody differentials and the filtration rate for Run 5, suggests that at the lower filtration rate antibody had been accumulated in the cellular growth space, and was subsequently washed out at higher filtration rates. This resulted in an artificially high antibody production rate measurement. This enhanced production rate was short lived reverting to a more normal level shortly after the change in the filtration rate. The failure to find any such agreement for Run 6 affects the validity of this conclusion.

10.5.5 Influence of macromolecular rejection on bioreactor performance

The implications associated with the observed rejection data and its effects on the performance of the bioreactor were investigated in Runs 4 to 6. The first alteration in operation involved reducing the serum levels in the feed medium to 3 % from 5% (Run 4) with a view to reducing the levels of fouling on the supply fibres. A significant flux decline was still observed during period where no alterations in the operating conditions had occurred (Figure 10.18), suggesting that a reduction in serum levels had little effect on fouling.

Figure 10.20:- Antibody differentials versus filtration rate for Runs 5 and 6

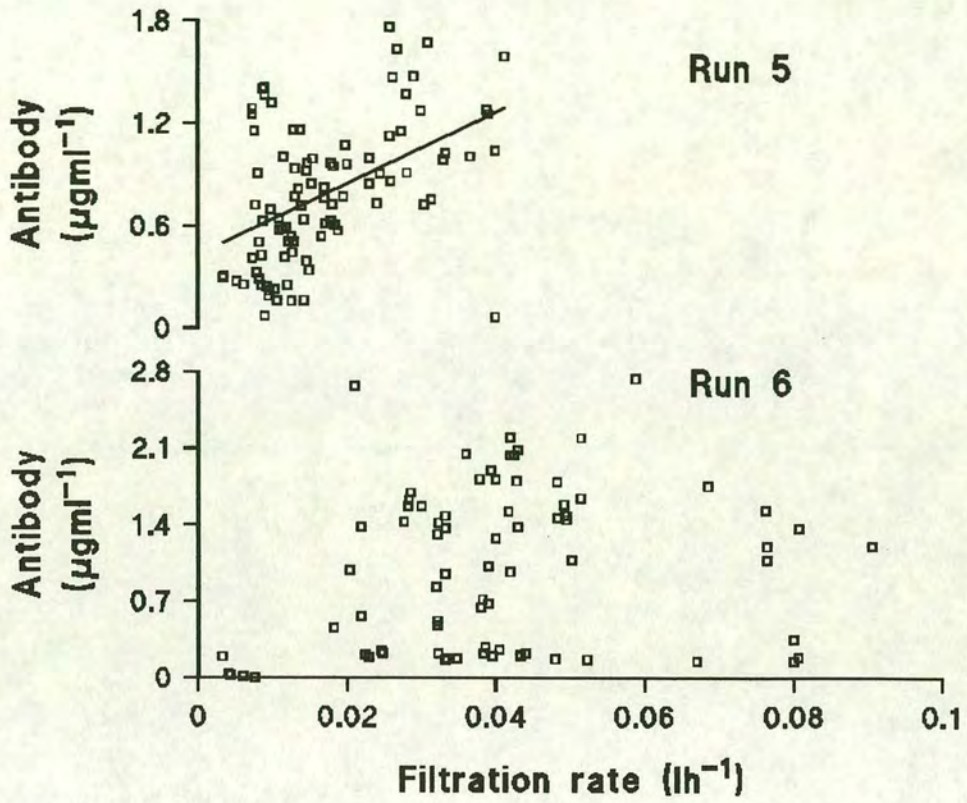

Based on the evidence that macromolecular species were being retained by the supply fibres, it was thought that the fouling of these fibres may have been excluding growth factors present in the serum from the cells within the growth space. Altshuler *et al.* (1986) suggested a similar hypothesis for the poor levels of cells observed in hollow fibre bioreactors with fibre MWCO of 10 and 50 kDa. With this hypothesis in mind serum addition was changed from the supplementation of the medium in the feed vessel to the direct dosing of the cellular growth space for Runs 5 and 6, in a similar approach to Rosenberg *et al.* (1991). The serum dosing regime used has already been described (Section 10.2.1) and annotated on the appropriate diagrams (Figures 10.11 and 10.14).

An increase in the viable cell population from an average value of 2.35×10^6 viable cells ml^{-1} of growth volume for Runs 3 and 4 (Table 10.2), where a serum supplemented feed was used, to 4.9×10^6 viable cells ml^{-1} (Run 5) for the serum dosed

Figure 10.21:- Antibody production rates for Runs 5 and 6

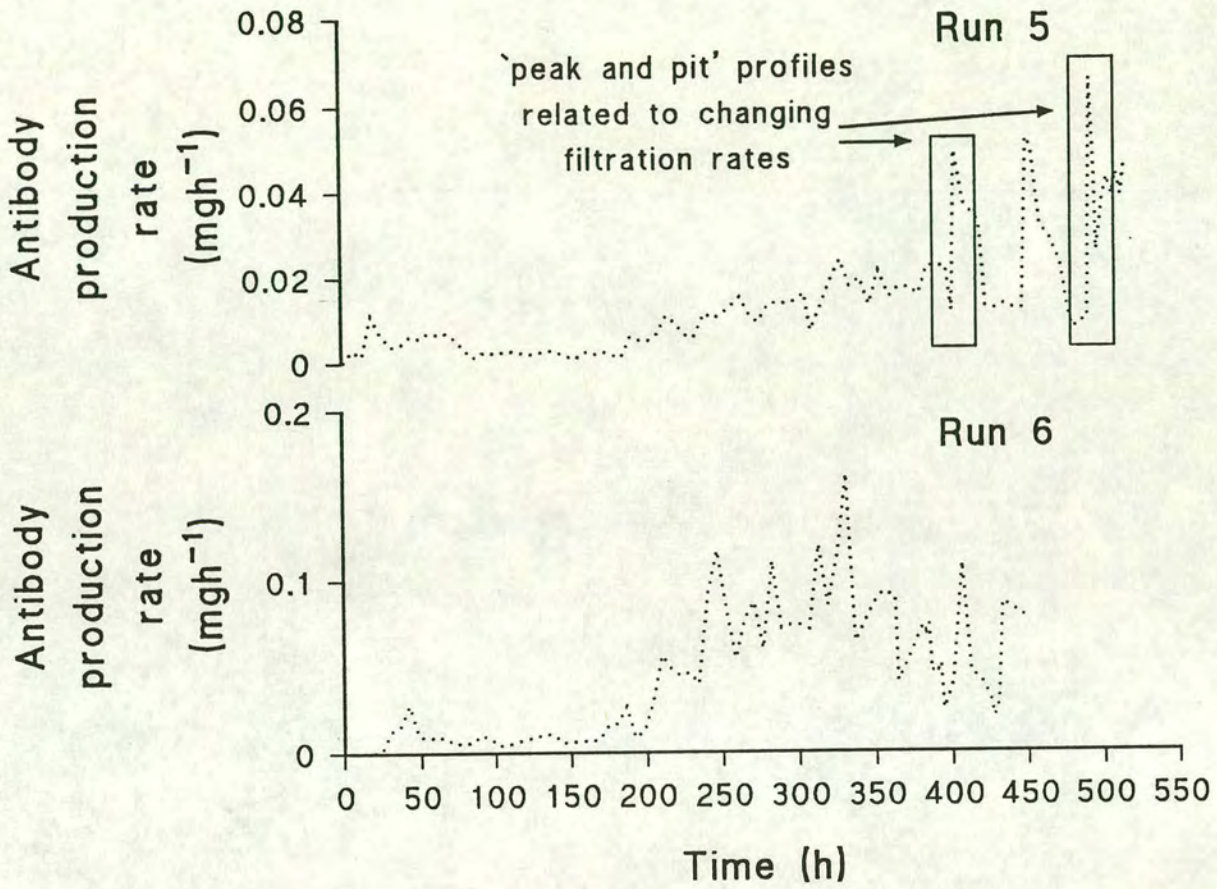

bioreactor was observed. These runs were carried out in the same design of bioreactor, that is the same pore sizes for the supply and sink fibres and the same fibre packing density. A further increase in the viable population was observed in Run 6 where a serum dosing regime was also used, although a direct comparison between this and the previous run may not be strictly valid due to the increased fibre packing ratio used in Run 6 (see Table 10.1, 'New style' versus 'High density' bioreactors). This suggests that the rejection of macromolecular species by the supply fibres has a direct effect on the biomass within the growth space, supporting the hypothesis

suggested in Section 8.3.

The accumulation of antibody, when used as an indicator of the fouling of the supply fibres, for Run 5 appears to suggest that the rejection of antibodies by the supply fibres still occurred when the waste medium was returned to the feed vessel. The accumulation of antibody in the supply circuit for Run 6 was expected, given the 100 kDa MWCO of the supply fibres.

10.5.6 Long term effects of operation on transmembrane pressures

The sterilisation protocol for the pressure transducers, described in Sections 7.2 and 10.6, enabled accurate measurement of the pressures to be obtained in the supply and sink circuits and the growth space during Run 6. The results for this experiment are presented in Figure 10.22, with the transmembrane pressures determined using the calculations described in Chapter 8 (Equations 8.1 to 8.5).

One of the reasons for the using 100 kDa pore sized supply fibres was that the intended pressure profile for the bioreactor should be conserved, i.e. the supply circuit pressure should always exceed that of the cellular growth space, which in turn should exceed that in the sink circuit. The only observed exception to this rule during Run 6 occurred during the first 30 h, where the post-supply pressures, the cellular growth space and sink circuit pressures were similar. This period coincides with the lowest filtration rates used during the experiment, with higher rates being used for the remainder of the experiment.

The general trends for Figure 10.22 suggest that the pressure drop along the supply fibres remained fairly constant at about 0.5 psig. The back pressure of the supply circuit was increased several times during the run at 45, 280, 330, 360 and 400 h. In each case an alteration in the cellular growth space pressure was observed, although in some instances during the run the pressure of the sink circuit was altered. The changes in the pressure of the cellular growth space were not as great as those of the supply fibres, which was not surprising given the greater pore size and number of sink

fibres. The pressure of the sink circuit was observed to decrease with time (Section 8.1.6) and was interpreted as an indication of the fouling within the bioreactor.

The results from the supply transmembrane pressures seem to suggest that little, or no fouling of the membranes within this circuit had occurred. Based on the discussion given in Section 8.1.6, the transmembrane pressure of the supply fibres would be expected to increase under fouling conditions. This does not appear to be the case, with the supply transmembrane pressure either remaining fairly constant (410 h onwards), or decreasing slightly during the run (340-360 h). These results would appear to suggest a negligible amount of fouling on the supply fibres. This seems quite likely, based on the presence of a low level of protein in the supply circuit, introduced through the periods of recirculation.

Based on the theory that two similar filtration rates should be produced by a similar transreactor pressure in an unfouled bioreactor, two periods were examined where the filtration rate was approximately 0.044 lh^{-1} (40-60 h and 336-382 h, Figure 10.20). The transmembrane pressure required to maintain this filtration rate in the latter period was significantly greater than that required for the earlier period, 2.2 psig versus 0.5 psig. While it may be suggested that a low level of fouling was observed on the supply fibres, the increased transmembrane pressure required to maintain a filtration rate of 0.044 lh^{-1} in the latter period of the run suggests that significant fouling within the bioreactor had indeed occurred.

With a low level of fouling, the sink transmembrane pressure should remain constant, with the difference between the two pressures attributable to the pressure drop across the membrane. If the sink fibres were fouled with either cells or proteins, the value for the sink transmembrane pressure would be expected to increase. The increased pressure drop would signify an increase in the resistance to flow across the membrane due to membrane fouling. Figure 10.22 suggests that as the run progresses, the downstream transmembrane pressure increases, suggesting that fouling had indeed occurred on these fibres.

Figure 10.22:- Bioreactor and transmembrane pressure profiles for Run 6

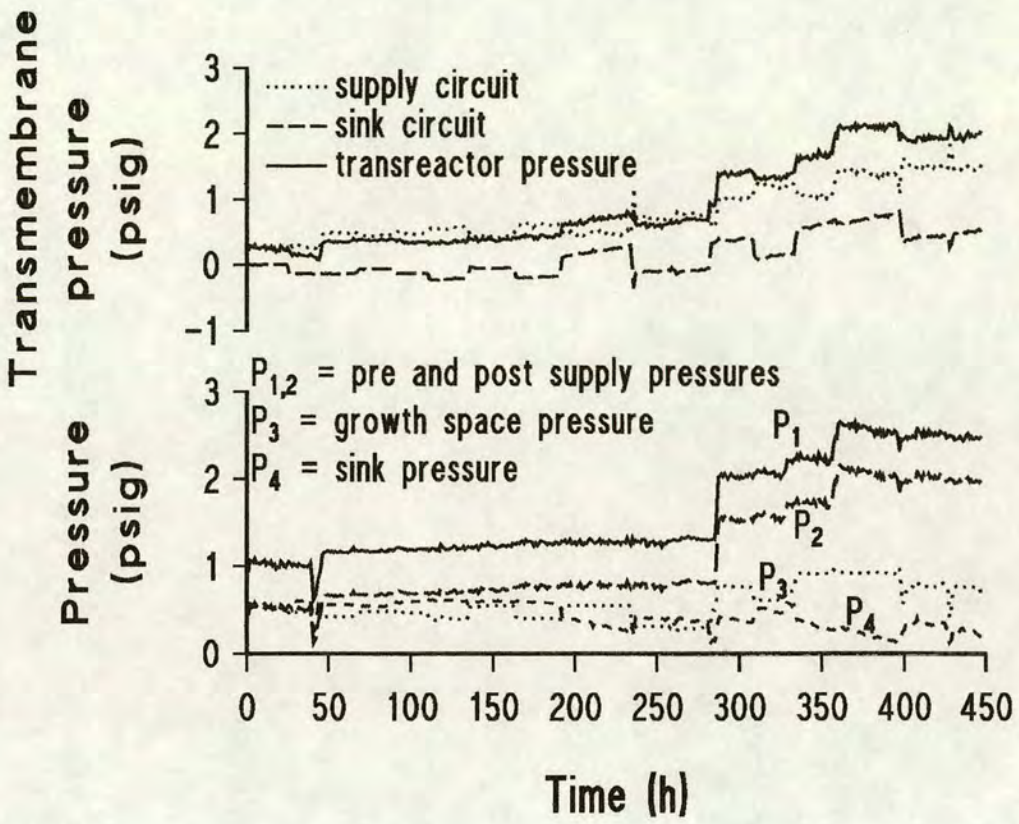

The continued presence of antibody in the sink circuit of the bioreactor would seem to contradict this observation, coupling the presence of antibody in this circuit with a low degree of fouling. The rejection of antibody by the sink fibres was not measured due to the unreliability of samples taken from the growth space. As a result, the passage of a low proportion of the antibody from the growth space may have still occurred, with a majority of the product being rejected by the membrane. This would satisfy the observed fouling of the sink membranes, while accounting for the presence of antibody in the sink circuit. It can be suggested that if some of the antibody was rejected by the sink fibres, the calculated production rates based on the product of the sink levels and filtration rate would be artificially low when compared with the actual production rate by the biomass. A comparison of the highest mean production rates calculated for this and the previous run would appear to support this theory, with a 140% increase in the viable cell number resulting in an 87% increase in antibody production rate. An antibody titre of 60 μgml^{-1} was determined for the growth space drain sample at the end of the run. It should be stressed that this comparison assumes

that the per cell antibody production rates were similar in Runs 5 and 6.

The final value calculated from the presented data constitutes the combination of the transmembrane pressures for the two fibre circuits, which is a summation of the supply and sink transmembrane pressures (Equation 8.5). In this instance the transreactor pressure could only be used to describe the total fouling of the bioreactor rather than aiding in the identification of the site of this fouling.

Combining the results of the three plots described in the upper graph of Figure 10.22, it can be seen that the predominant area of fouling was found to occur on the sink fibres, based on the rise in sink transmembrane pressure. The influence of the cell mass on the observed degree of fouling has already been discussed in Section 10.2.

10.6 Operational problems

In describing the factors influencing the performance of this type of bioreactor it is necessary to describe the effects that unreliable monitoring and control equipment, construction techniques, contamination and sampling methods had on experimental results.

10.6.1 Software problems

The maintenance of the idealised pressure profile within the bioreactor facilitating the desired radial flow regime required continuous and accurate monitoring and control of pressure. The software written by Burns (1991) for the continuous monitoring of pressures within the bioreactor circuit was developed in tandem with the bioreactor runs. Developmental failures of this program led to Runs 1 to 3 being carried out without control software. As the pressure profiles could not be monitored, other indicators had to be used for operating the bioreactor, for example increasing the flux across the unit by applying increased pressure to the supply circuit and monitoring it by measuring the volume entering the sink circuit. These methods are discussed in Section 10.6.3.

While this technique increased the flow into the sink circuit, there was reason to believe that not all of this flow was attributable to the passage of medium through the extracapillary space. The influence that the end regions of the bioreactor had on the flows within the bioreactor has already been discussed (Section 7.3.2). It was calculated that only 80% of the total flow entering the downstream circuit was attributable to the growth space, with the remainder associated with the end region. By covering the supply fibres in the end region with potting compound the leakage problem was solved.

A second undesirable flow regime can be identified as resulting from poor pressure control. If the desired pressure profile (Figure 7.1) within the bioreactor is not attained then the flow could be composed of two components, flow to the sink circuit and returning flow to the supply circuit in a situation analogous to 'Starling' flow. This flow pattern would be expected to lead to cell and product maldistribution in a similar manner to that described by Piret and Cooney (1990).

10.6.2 Pressure transducers

The calibration curves determined for the pressure transducers prior to the start of each run were found to be invalid after autoclaving, resulting in pressure control problems. The experiments in which more than one of these transducers failed (Runs 4 and 5) could not be accurately controlled and therefore no useful pressure records are available for these runs. The resolution of this problem, through the independent sterilisation of the pressure transducers has already been described (Section 7.2). Filtration rates were again used as the controlling parameter for the bioreactor.

10.6.3 Controlling the filtration rate

In the absence of reliable pressure transducers, altering the filtration rate became the primary means for controlling the bioreactor. Changing the pressure of the supply circuit by either the manual application of a backpressure to the outlet tubing of the supply circuit or changing the pump rate in the supply circuit were used to adjust the

filtration rate to the desired level. This altered the pressure profile within the bioreactor, with higher transreactor pressures giving higher filtration rates. Two methods were used for determining the filtration rate, the first involved the timed measurement of drops returning to the feed vessel from the sink circuit, with an approximate volume of 0.15 ml associated with each drop. The second method used a balance and the timed collection of medium in the waste medium vessel, equating 1 ml of medium to 1 g of weight on the balance, to measure the filtration rate. While increasing the supply pressure was a successful approach for high filtration rates, greater than 0.2 lh^{-1} (Figure 10.23, Run 3), difficulties were experienced in maintaining a constant filtration rate below this value, often resulting in episodes of no flux across the bioreactor, for example Figure 10.24 (Run 5). A marginal improvement in the level of control at lower filtration rates was developed by maintaining the supply circuit at a higher pressure (and therefore flux) and then increasing the back pressure on the sink circuit to reduce the flux to a lower value (330 h onwards). While this was an improvement over the previous method, control was again found to be difficult. The effects that this had on the pressure profiles within the bioreactor were discussed in Section 10.3 .

10.6.4 Sampling the cellular growth space

Sampling the cellular growth space via its access ports proved to be easy, however, obtaining a representative sample of the exact contents of the cellular growth space was difficult primarily due to the uneven distribution of cells. Cells were observed to settle to the bottom of the bioreactor during the culture experiments. Duplicate samples taken from the growth space towards the end of Run 2 (day 11) gave viable counts of $1x10^5$ and $1x10^6$ cells ml^{-1} of growth space volume, which represented between 3 and 5% of the total cell count for the samples. This compares with a final viable cell count of $4x10^6$ viable cells ml^{-1} of growth space volume, based on counts taken after the complete drainage and rinsing of the extracapillary space at the end of the experiment.

Figure 10.23:- Control of filtration rates above 0.2 lh^{-1} (Run 3)

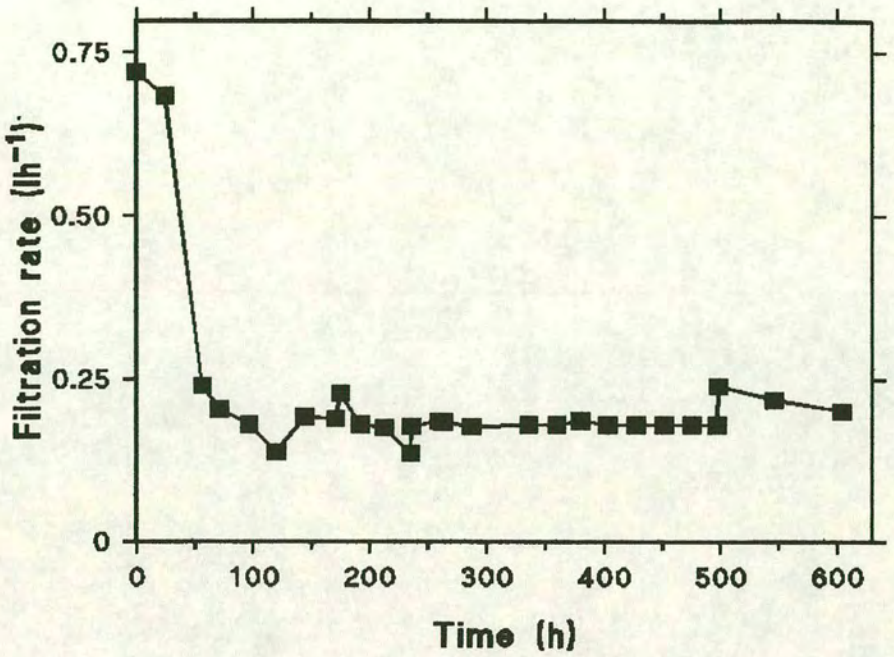

Figure 10.24:- Control of filtration rates below 0.05 lh^{-1} (Run 5)

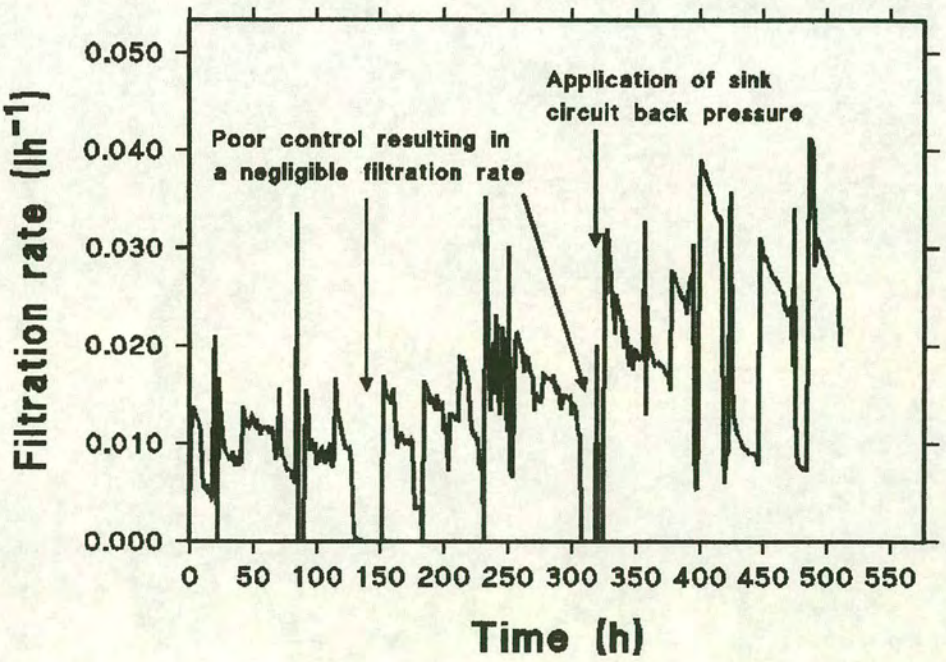

Numerous attempts were made to improve the accuracy of the cell counts obtained from this section of the bioreactor, for example agitating the bioreactor before sampling, with no successful resolution. The main value of these samples was found to be in ascertaining the presence of a viable cell population within the growth space. Section 10.2.2 provides a possible explanation as to why the samples from the extracapillary space were so unrepresentative, with a majority of the viable population found to be directly associated with the fibre bundle.

10.6.5 Sampling the supply and sink circuits

Problems were also encountered in obtaining representative samples from the supply and sink circuits. The first of these was related to the frequency of sampling in the supply circuits, which was initially low for Run 2 (1 sample every 18 to 24 h) increasing to samples taken every 6 h by Run 4. In these runs the measured changes in the bulk metabolite levels in the feed vessel were used for the calculation of metabolic rates. As the number of samples upon which these rates were based was initially low (n=3 to 5 samples per rate calculation) the significance of the calculated rates was affected by the low number of samples used. Correlation coefficients (r) determined from the lines of best fit for the data using the least squares method, tended to be of lower significance (95% or below) than those using higher sample numbers, where significance levels of 99.9% could be achieved. A comparison of Tables 10.11 to 10.13, which summarise the rates determined for Runs 2 to 4, show an increase in the levels of significance for r as the number of samples (n) used for the rate calculation is increased. Significance levels for r were determined according to pre-tabulated values reported in Clarke (1994).

Sampling the sink circuit just before and just after a change in filtration rate was found to be another source of error. This method was insensitive to the time needed for the growth space levels of nutrient to readjust to the new conditions and therefore little change in the level of the metabolites was observed between the pre- and post-change samples. For example, the two medium changes made in Run 3 at 250 and 380 h showed immediate increases in the supply levels of glucose of 4 and 2 mM

respectively (Figure 10.6). Pre and post-change samples for the sink circuit at these times showed immediate increases of 1 and 0.3 mM changes respectively. A further increase in these values was then observed to 2 and 4 mM respectively at the next sample point. The rate at which these samples become representative of the growth space after a condition change would be expected to be dependent upon the filtration rate across the bioreactor, with lower filtration rates increasing the delay required before representative samples could be obtained. While these samples are representative of the growth space levels of nutrient or metabolite entering the sink circuit, they would not indicate any portion of the nutrients or metabolites entering the supply circuit due to any 'Starling' flow component.

10.6.6 Contamination and construction failures

Bioreactor runs were terminated for one of two reasons, potting failure and leakage within the bioreactor or contamination (Table 10.19). In the early runs the problems associated with constructing a leak free bioreactor led to a number of experiments being stopped due to leakage from the silicone seals within the bioreactor (Section 7.3.1). Contamination was detected using peptone broth and the sampling approaches described in Sections 6.1.4 and 7.1.3. No further information obtained from these runs has been reported for the following reasons:-

(1) Metabolic information obtained from contaminated runs was deemed unreliable, because the influence of the contaminant upon the metabolic data could not be determined.

(2) Potting failures led to a progressive loss of cells from the CGS, while disrupting the desired flow of medium within the bioreactor (Figure 7.1). In one experiment, dated 2/11/90, cell growth was observed in the feed vessel, presumably due to the leakage of cells from the CGS.

These experiments were, however, useful, in enabling improvements in bioreactor design and operation to be made.

Table 10.19:- Contamination and construction failures

Run date	Reason for stopping
29/10/90	Potting failure in bioreactor
2/11/90	Potting failure
15/3/91	Contaminated with a Gram -ve bacillus, resulting from tubing failure.
20/3/91	Contaminated with a Gram -ve bacillus.
26/3/91	Contaminated with a mycelial fungus.
30/4/91	Contamination with mycelial fungus. Traced to a contaminated bottle of Newborn Calf Serum.
15/5/91	Yeast contamination and computer failure.
20/5/92	Contamination with a yeast-like organism
9/6/92	Contamination with yeast-like organism

Experiments carried out between March and May of 1991 were subject to a series of bacterial and fungal contaminations. These contaminations may have been attributable to one of two factors, a contaminated batch of medium, which contained a slow-growing fungal organism, and a period of rebuilding within the department which generated dust which, despite all precautions, may have been responsible for the failure of the remaining experiments.

The failure of the 'O' rings in Run 7 can also be included in this section. However, as a viable population was maintained within the growth space during this run, it has

also been included in Tables 10.2 and 10.3. Based on the design experience gained during the development of the smaller scale bioreactors, it could be foreseen that the problems associated with the large scale bioreactor could have been readily solved.

10.6.7 Aeration method

Two methods of aeration were used in the feed vessel of the supply circuit. The first involved the use of a sintered sparge which (Runs 1 and 2), due to the presence of serum proteins in the feed medium, caused foaming. Protein aggregates were observed to form in the supply circuit as a direct result of the resuspension of foam related deposits formed on the walls of the feed vessel. The denaturation of proteins and the subsequent formation of aggregates has been reported to affect not only the activity of the proteins (Thomas *et al.*, 1979) but also the degree of membrane fouling (Meireles *et al.*, 1991).

Based on these results the gassing method was changed from sparging to surface aeration of the feed vessel (Runs 4-7). This approach, while recognised as being a less efficient means of aeration due to a reduction in the total area available for gas exchange, solved the problems associated with aggregate/precipitate formation. In the experiments in which the oxygen probes were working and data was available, the oxygen differential between the supply and sink circuits never exceeded 30% of the 100% saturation value, i.e. the lowest value monitored was 70% of oxygen saturation, suggesting cells in the growth space were not oxygen limited. The accuracy of the data obtained from the oxygen probes was, however, suspect either due to the incomplete sampling of the of the bioreactor circuit, i.e. the two samples obtained did not measure the total oxygen utilisation within the circuit, or poor mixing was occurring within the growth space resulting in an unrepresentative sink sample.

10.7 Summary and conclusions

Through the progressive development in the design and operation of the Edinburgh dual hollow fibre bioreactor, the viable and total cell population within the bioreactor was increased to a final viability of $1.2x10^7$ cells ml^{-1} of bioreactor growth space volume. The difficulties observed in the interpretation of the results from these experiments made it clear that this design of bioreactor was a complicated system to analyze, which was not helped by the failure of pressure transducers, the control package, and a poor initial understanding of the effects of fouling within the bioreactor system. As a direct result many of the conclusions drawn from these experiments had to rely on fragmentary, indirect evidence to support the performance of the bioreactor.

The filtration characteristics described in Chapter 8 were shown to be applicable to the operation of the full sized bioreactor. A comparison of these two chapters shows that the following common features:-

(1) Transmembrane pressure profiles appear dictate the flow characteristics within the bioreactor, i.e. the degree of Starling or radial flow.

(2) Flux across the bioreactor could be controlled by the increasing the pressure of the supply fibres, with the selection of the pore size of the membranes in the supply and sink circuits important in determining the pressure required to mediate flux.

(3) The presence of protein within the feed stream led to a high degree of macromolecular rejection by the supply fibres. This was shown directly to influence the flux within the system.

(4) The fouling, and therefore the rejection characteristics, of the sink membranes were found to be similar in both the small rig and full scale bioreactor experiments, with free passage of dextran and antibody occurring across the sink circuit in both sets of experiments.

The failure of the pressure transducers severely limited the characterisation of this

designs performance, requiring the use of indirect evidence to piece together an overall picture. The control of the transmembrane pressures, and the resultant flow regimes, within the bioreactor were critical in both the dispersal of nutrients and macromolecular species between the two circuits and the accuracy of the metabolic rates calculated for the system. The 'poor' accuracy of the metabolic data determined for many of the earlier runs was due to a failure to appreciate the primary importance of the pressure profiles on the distribution of moieties throughout the bioreactor circuit. Initial calculations assumed that waste from the sink stream contained all of the metabolic byproducts from the bioreactors growth space.

Other limitations of this design of bioreactor were also highlighted during this work. The main factor affecting the productivity of the bioreactor, other than the flow regime, was thought to be associated with poor cell retention within the fibre bundle. While the cell line used was not anchorage dependent, its use highlighted the importance of either entrapping the cells within the fibre bundle, or providing an external source of mixing to mediate their passage through the fibre bundle. The increase observed in the viable cell population with an increase in the fibre packing ratio of the bioreactor was thought to be due to increased cell retention rather than any improvement in the nutrient supply to the cells.

The 'sloughing' of cells from the fibres within the bioreactor, when combined with the results from the dissection and draining experiments (Section 10.3) highlighted the poor adhesion of the cells to the fibres. This phenomenon had a marked effect on the viability of the biomass within the CGS. Cells retained within the fibre bundle were either directly attached to the fibres, or alternatively, closely associated with the fibres due to clumps trapped between the fibres, tended to have a high viability ($>$ 80 %) and be evenly distributed throughout the fibre bundle (see Section 10.3). Those cells that had sloughed off of the fibres and settled on the base of the tube had a significantly lower viability, approximately 5% . The disparity between the viabilities observed in these two areas was attributed to differences in nutrient supply between the fibre bundle, with a perfused supply of nutrients, and the bottom of the tube, which was reliant upon a more diffusionally limited supply regime.

The retention of growth factors by the supply fibres was also found to limit cell growth, a problem that was resolved by moving to the direct dosing of the bioreactors growth space. This improved the access of the cells to these key nutrients, increasing the viable population.

The similarities between the cell viabilities observed in the earlier successful runs (Runs 2-4) and the final run using the large scale bioreactor would appear to support the cell attachment theory, with approximately $2x10^6$ viable cells ml^{-1} of bioreactor volume. Whether the attachment phenomenon was directly related to the porosity of the membranes requires further investigation.

Methods for increasing the percentage viability of the biomass either involved improving nutrient dispersal within the bioreactor, or the redistribution of the biomass back into the fibre bundle. In this work the latter method was tried, inverting the bioreactor to move the biomass from the bottom of the tube back into the fibre bundle. A similar method of redistribution was used by Patankar and Oolman (1990a,b) and Piret and Cooney (1990). Another method involves the surface modification of the fibres to retain the cells within the fibre bundle (Tharakan and Chau,1986, Patankar and Oolman,1990a,b). Improving the mixing within the bioreactor has also been tried, by either periodically reversing the Starling flow regime (Piret and Cooney, 1990), or by the mechanical agitation of the bioreactor (Cousins *et al.*, 1992). Hirschel and Gruenberg (1987) counteracted the combined effects of fouling and nutrient and cell gradients upon bioreactor performance by using pressure cycling to provide improved mixing and periodic reversals in the direction of medium flow. This allowed cells numbers of up to $5x10^8$ cell ml^{-1} to be cultured in the ACUCYST system for up to 60 days.

The cell related fouling of fibres within the bioreactor was not found to limit its performance. However, the cell densities required to cause a high degree of fouling within the bioreactor may not have been achieved in these experiments.

Chapter 11

Conclusions and Future work

11.0 Overview

Hollow fibre bioreactors have the potential of providing a means by which tissue density concentrations of mammalian cells can be maintained in continuous culture. The advantages and disadvantages associated with these bioreactors, when compared with conventional culture techniques, e.g. airlift fermenters, were described in the introductory Chapters.

Mammalian cells were cultured in the Edinburgh Dual Hollow Fibre bioreactor for up to 40 days. The maximum viable population achieved was 1.2×10^7 cells ml^{-1} (Run 6) of the available growth space volume, which was approximately 30 % of the total biomass. While this was a 10 fold increase on the levels reported for the conventional culture of these cells (J.Wilson, 1992), the percentage viability of the biomass in the hollow fibre bioreactor was substantially lower. The maximum recorded antibody production rate recorded for Run 6 was 0.16 mgh^{-1}, although the problems encountered in obtaining representative samples from the bioreactor may have affected this value.

The difficulties observed in the operation of this prototype design were not fully resolved, with the current form being commercially non-viable. However, the factors limiting its performance were identified, including filtration related mass transfer limitations, and the poor control of pressures regimes within the bioreactor. By considering this type of hollow fibre device as both a filter, subject to concentration polarisation and fouling, and a bioreactor, requiring an adequate supply of the correct nutrients, the total and viable cell numbers achieved within this design were improved. Extending the use of this approach may, in the future, lead to a better understanding of these systems and result in further increases in the viable biomass within this style of bioreactor.

The following sections provide a brief summary of the results from this work, identifying the key limitations to the performance of this bioreactor (Section 11.1) and the areas in which future research would be beneficial (Section 11.2).

11.1 Summary of results

A number of factors were identified as being important in the culture of cells within this design of hollow fibre bioreactor:-

(1) The culture characteristics of the cells.
(2) The design of the bioreactor, ensuring a supply of nutrients for the maintenance and growth of a viable population throughout the bioreactor.
(3) A method of operating the bioreactor that ensures that this nutrient supply criterion could be attained.
(4) The effects of concentration polarisation and fouling on bioreactor performance.

11.1.1 Cell growth characteristics

Batch growth experiments were used to determine the initial nutrient requirements of the ES4 cell line (Chapter 9). The calculation of accurate metabolic rates in the bioreactor culture experiments was not possible due to the formation of unpredicted flow regimes and associated sampling difficulties.

The partial replacement of glutamine by α-ketoglutarate was found to reduce the build up of the potentially toxic waste metabolite, ammonia. The presence of glutamine in the culture medium was found to be essential for the growth of the cells in these experiments, with no growth observed in medium supplemented with α-ketoglutarate only.

The position of the cells within the bioreactor was found to affect the viable

population, with a higher percentage of viable cells (95%) found directly associated with the fibre bundle. The remaining 5% of the viable population was associated with the biomass which had settled on the bottom of the bioreactor. However, the maximum viable biomass obtained during these experiments only constituted 30% of the total population. The difference in the viable population at these two sites was thought to be due to the supply of fresh nutrients to, and the removal of waste metabolites from the biomass.

Increasing the number of fibres within the bioreactor led to an increase in the viable population. This was attributed to the increased retention of cells within the fibre bundle. If an anchorage dependant cell line had been used this may also have led to an increase in the number of viable, fibre related cells.

11.1.2 Bioreactor and equipment design

Burns' bioreactor design required considerable improvement before reproducible culture experiments could be carried out. This entailed altering the potting procedure and the method of inserting the bioreactor into the outer tube (Chapter 7). Using the previous construction method, the seals in more than 50% of the bioreactor constructs were found to leak, resulting in their disposal. The improvements made in this work led to a construction failure rate of less than 25% .

11.1.3 Bioreactor operation

The flow pattern within the bioreactor was intended to be radial, from the supply to the sink fibres. This flow regime required accurate monitoring and control of the pressures across the hollow fibre bioreactor. Unfortunately the reliability of the pressure transducers used during this work was found to decrease as a result of autoclaving. As a direct result the pressure profiles, and hence the adopted flow regime, could not be adequately controlled.

Under these poorly controlled conditions the pressure and flow regimes adopted within

the bioreactor were found to be dictated by the filtration characteristics of the hollow fibres. Under specified conditions (Section 10.3.2), the pressure profile across the bioreactor led to undesirable flow patterns tending towards Starling flow. This deviation from the intended radial flow regime was found to affect the distribution of both cell waste and nutrients between the supply and sink circuits, altering the method required for the calculation of metabolic rates for low molecular weight species (Section 10.4).

11.1.4 Effects of filtration

Concentration polarisation and fouling were found to influence the distribution of higher molecular weight species throughout the bioreactor circuit and the flux across the bioreactor. The theoretical performance of the bioreactor, with respect to the rejection and fouling of the fibres with high molecular weight species, was examined (Chapter 8), and found to lead to membrane fouling and a gradual decline in flux.

The effects of rejection (Section 10.5) and fouling were observed in the bioreactor culture experiments. Antibody was found to accumulate in the supply circuit in a number of experiments, with the application of a serum dosing regime for the supply of growth factors to the cells leading to a substantial increase in the viable population within the bioreactor.

11.1.5 Summary of key limiting factors.

The following key limitations were found to affect the performance and results obtained from the bioreactor used is this work, with some suggested solutions to these problems provided in the previous results chapters:-

(1) Poor cell retention within the nutrient rich hollow fibre bundle.

(2) Mass transfer limitations affecting the supply and removal of both high and low molecular weight species to and from the biomass.

(3) Poor control of the transreactor pressure profile, resulting in the

adoption of partial Starling flow regimes.

(4) Deviations from the intended flow regime resulting in errors in the calculation of accurate metabolic rates.

11.2 Future work

Based on the findings from these experiments, the author suggests that the following areas should be examined in order to improve the operation and design of hollow fibre bioreactors. This work should primarily concentrate on modelling the performance of the bioreactor using simulated protein solutions, it should then be extended to include characterising the growth of aerobic microorganisms within the bioreactor and finally extended to the growth of mammalian cells.

Cell free investigations

Using simulated protein/medium solutions to examine:-

- Filtration mediated effects on mass transfer within bioreactors, e.g. the fouling of hollow fibres by proteins and the associated effects on pressure profile and flux within the bioreactor.
- Improved control and optimisation of the Edinburgh design based on the simulated protein experiments and the related pressure data.
- Modelling of the bioreactor system with respect to both high and low molecular weight species.
- The use of imaging techniques, e.g. NMR imaging, to analyse flow patterns within the bioreactor under the different flow profiles described in Chapter 10.

Microorganism based work

- The attachment and retention of cells within the fibre bundle of the bioreactor, including the effects of increasing the fibre packing ratio.
- The distribution of nutrients and waste metabolites between the supply and sink circuits under the 4 conditions outlined in Chapter 10.
- Ann examination of the effects of biomass accumulation on filtration and the characteristics of the micro-environment of the formed biofilm.

Mammalian cell culture work

- The application of the results from the work described in the previous paragraphs to the culture of anchorage dependant and anchorage independent cell lines.
- An investigation into protein free culture and the methods by which proteinaceous growth factors, if required, can be distributed throughout the biomass with negligible effect on the fouling of the fibres.

While these areas for investigation look to characterise the performance of the Edinburgh Dual Hollow Fibre Bioreactor, the results could be usefully applied to a number of other areas where hollow fibre technology is employed, for example artificial livers.

REFERENCES

Abu-Reesh, I., Kargi, F. (1991) "Biological Responses of Hybridoma Cells to Hydrodynamic Shear in an Agitated Bioreactor"; *Enzyme Microb. Technol.* 13, p 913-919.

Adema, E., Sinskey, A.J. (1987) "An Analysis of Intra-Versus Extracapillary Growth in a Hollow Fiber Reactor"; *Biotechnology Progress* Vol 3 No.2, p 74-79.

Al-Rubeai, M., Emery, A.N. (1990) "Mechanisms and kinetics of monoclonal antibody synthesis and secretion in synchronous and asynchronous hybridoma cell cultures."; *Journal of Biotechnology* 16, p 67-86.

Avgerinos, G.C., Drapeau, D., Socolow, J.S., Mao, J., Hsiao, K., Broeze, R.J. (1990) "Spin Filter Perfusion System for High Density Cell Culture: Production of Recombinant Urinary Type Plasminogen Activator in CHO Cells"; *Bio/technology* 8, 54-57.

Belfort, G. (1989) "Membranes and Bioreactors: A Technical Challenge in Biotechnology"; *Biotechnology and Bioengineering* 33, p 1047-1066.

Belfort, G., Altshuler, G.A. (1986) *Chem. Ind.* 7, p 585.

Bell, S.L., Bushell, M.E., Scott, M.F., Wardell, J.N., Spier, R.E., Sanders, P.G. (1992) "Genetic Modification of Hybridoma Glutamine Metabolism: Physiological Consequences." p 180-182, IN: Spier, R.E., Griffiths, J.B., MacDonald, C. (1992) Animal Cell Technology: Developments, Processes and Products." Butterworth-Heinemann Ltd., Oxford, U.K.

Bleim, R. (1989) "A need for systematic investigations into the material properties of cultured animal cells."; *TIBTECH* 7, p 197-200.

Bleim, R.,Katinger, H. (1988a) "Scale-up engineering in animal cell technology: Part 1."; *TIBTECH* 6, p 190-195.

Bleim, R., Katinger, H. (1988b) "Scale-up engineering in animal cell technology: Part 2."; *TIBTECH* 6, p 224-230.

Boulton-Stone, J.M., Blake, J.R. (1993) "Gas Bubbles Bursting at a Free Surface." *Journal of Fluid Mechanics* 254, p 437-466.

Brotherton, J.D., Chau, P.C. (1990) "Modeling Analysis of an Intercalated-Spiral Alternate-Dead-Ended Hollow Fiber Bioreactor for Mammalian Cell Culture.";*Biotechnology and Bioengineering* 35, p 375-394.

Bruining, W.J. (1989) "A General Description of Flows and Pressures in Hollow Fiber Membrane Modules"; *Chemical Engineering Science* Vol 44 No. 6, p 1441-1447.

Burns, J. (1991) "Design, Construction, Modelling and Control of a Dual Hollow-Fibre Bioreactor for Hybridoma Cells." Ph.D. Thesis, Edinburgh University, U.K.

Butler, M. (1985) "Growth limitations in high density microcarrier cultures";; *Develop. biol. Standard.* 60, p269-280.

Butler, M. (Editor) (1991) "Mammalian Cell Biotechnology A Practical Approach", published by Oxford University Press, New York.

Catty,D. (Editor) (1988) "Antibodies Volume 1: a practical approach",published by IRL Press Ltd., England.

Catty,D. (Editor) (1989) "Antibodies Volume 2: a practical approach",published by IRL Press Ltd., England.

Cavegn, C., Blasey, H.D.., Payton,M.A., Allet, B., Li, J., Bernard, A.R. (1992) "Expression of Recombinant Proteins in High Density Insect Cell Cultures." p 569-578, IN: Spier, R.E., Griffiths, J.B., MacDonald, C. (1992) "Animal Cell Technology: Developments, Processes and Products." Butterworth-Heinemann Ltd., Oxford, U.K.

Cellpharm System 1 Brochure (1987), CD Medical.

Chandavarkar, A.S., Cooney, C.L. (1989) "Dynamics of Flux Decrease during Microfiltration Caused by Protein-Membrane Interactions."; *Abstracts of the American Chemical Society* 198, p 44.

Cherry, R.S., Papoutsakis, E.T. (1986) "Hydrodynamic Effects on Cells in Agitated Tissue- Culture Reactors." *Bioproc. Eng.* 1, p 29-41.

Cherry, R.S., Papoutsakis, E.T. (1988) "Physical Mechanisms of Cell-Damage in Microcarrier Cell-Culture Bioreactors." *Biotechnol. Bioeng.* 32, p 1001-1014.

Cherry, R.S., Papoutsakis, E.T. (1989) "Growth and Death Rates of Bovine Embryonic Kidney Cells in Turbulent Microcarrier Bioreactors" *Bioproc. Eng.* 4, p 81-89.

Chiou, T.W., Murakami, S., Wang, D.I.C., Wu, W.T. (1991) "A Fiber-Bed Bioreactor for Anchorage Dependent Animal-Cell Cultures 1. Bioreactor Design and Operation"; *Biotechnology and Bioengineering* 37, p755-761.

Cima, L.G., Blanch, H.W., Wilke, C.R. (1990) "A Theoretical and Experimantal Evaluation of a Novel Radial-flow Hollow Fiber Reactor for Mammalian Cell Culture"; *Bioprocess Engineering* 5, p19-30.

Clarke, G.M. (1994) "Statistics & experimental design- An introduction for Biologists and Biochemists"; Third edition, Edward Arnold, UK.

Coco-Martin, J.M., Oberink, J.W., van der Velden de Groot, T.A.M., Beuvery, E.C. (1992) "The potential of flow cytometric analysis for the characterization of hybridoma cells in suspension cultures."; *Cytotechnology* 8, 65-74.

Cousins, R.B., Gergen, R., Gerner, F.J. (1992) "A Dual Membrane Reactor For the Cultivation of Mammalian Cells." p 538-540, IN: Spier, R.E., Griffiths, J.B., MacDonald, C. (1992) "Animal Cell Technology: Developments, Processes and Processes." Butterworth-Heinemann Ltd., Oxford, U.K.

Croughan, M.S., Hamel, J., Wang, D.I.C. (1987) "Hydrodynamic Effects on Animal Cells Grown in Microcarrier Cultures." *Biotechnology and Bioengineering* 33, p 130-141.

Croughan, M.S., Wang, D.I.C. (1989) " Growth and death in overagitated microcarrier cell culture."; *Biotechnology and Bioengineering* 33, p 731-744.

Dalili, M., Ollis, D.F. (1990a) "A Flow Cytometric Analysis of Hybridoma Growth and Monoclonal Antibody Production."; *Biotechnology and Bioengineering* 36, p64-73.

Dalili, M., Sayles, G.D., Ollis, D.F. (1990b) "Glutamine-limited Batch Hybridoma Growth and Antibody Production: Experimentation and Model."; *Biotechnology and Bioengineering* 36, p74-82.

Dalili, M., Ollis,D.F. (1989) "Transient Kinetics of Hybridoma Growth and Monoclonal Antibody Production in Serum-Limited Cultures"; *Biotechnology and Bioengineering* 33, p984-990.

De la Broise, D., Noiseux, M., Massie, B., Lemieux,R. (1992) "Hybridoma Perfusion Systems: A Comparison Study"; *Biotechnology and Bioengineering* 40 p25-32.

Deutschmann, S.V., Valley, U., Jager, V., Wagner, R.;"Cell cycle analysis as a tool for control and regulation of mammalian cell cultures in bioreactors."; To be published in: Spier, R.E., Griffiths, J.B., and Berthold, W. (eds.), Proceedings of the 12th Meeting of ESACT (ESACT '93) 'Animal Cell Technology: Products for Today, Prospects for Tomorrow', Butterworth-Heinemann, Oxford, UK.

Dodge, T.C., Ji, G.Y., Hu, W.S. (1987) "Loss of viability in hybridoma culture - a kinetic study."; *Enzyme Microb. Technol.*, 9, p 607-611.

Dulbecco, R., Elkington, J. (1973) "Conditions limiting multiplication of fibroblastic and epithelium cells in dense cultures. *Nature* 246, p 197-199.

Duval,D., Demangel,C., Munier-Jolain, K., Miossec, S., Geahel, I. (1991) "Factors Controlling Cell Proliferation and Antibody Production in Mouse Hybridoma Cells: 1. Influence of the Amino Acid Supply"; *Biotechnology and Bioengineering* 38, p561-570.

Eagle, H., Barban, M., Levy, M., Schulze, H.O. (1958) *J. Biol. Chem.*, 233, 551.

Eason, G., Coles, C.W., Gettinby, G. (1992) "Mathematics and Statistics for the Bio-Sciences." Ellis Horwood Ltd., Chichester, U.K.

Enka data sheet (1987), sheet no. QC 58007 0387, Enka AG, Membrane Product Group, Postfach 20 09 16, Ohder Strasse 28, D-5600, Wuppertal 2, Germany.

Fell, C.J.D., Kim, K.J., Chen, V., Wiley, D.E., Fane, A.G. (1990) "Factors Determining Flux and Rejection of Ultrafiltration Membranes"; *Chem. Eng. Process* 27 p 165-173.

Fenge, C., Fraune, E. (1992) "Perfusion Cultivation Technique for Animal Cells"; *International Biotechnology Laboratory* May issue, p 20.

Goergen, J.L, Marc, A., Engasser, J.M. (1992) " Influence of medium composition on the death and lysis of hybridoma cells in continuous cultures."; p 122-124, IN: Spier, R.E., Griffiths, J.B., MacDonald, C. "Animal cell technology: developments, processes and products.", published by Butterworth-Heinemann Ltd, Oxford, UK.

Girardi, A.J., McMichael, H. Jr., Henle, W. (1956) "The Use of HeLa Cells in Suspension for the Quantitative Study of Virus Propagation"; *Virology* 2, p 532-544.

Glacken, M.W., Fleischaker, R.J., Sinskey, A.J. (1986) "Reduction of Waste Product Excretion via Nutrient Control: Possible Strategies for Maximizing Product and Cell Yields on Serum in Cultures of Mammalian Cells."; *Biotechnology and Bioengineering* 28, p 1376-1389.

Griffiths, J.B. (1990)"Advances in Animal Cell Immobilization Technology" Chapter 6, IN: Spier, R.E., Griffiths, J.B. (1990) "Animal Cell Biotechnology" Academic Press Limited, London, U.K., p149-166.

Grund, G., Robinson, C.W., Glick, B.R. (1992) " Protein Type Effects on Steady-State Crossflow Membrane Ultrafiltration Fluxes and Protein Transmission"; *Journal of Membrane Science* 70 p 177-192.

Handa, A., Emery, A.N., Spier, R.E. (1987) "On the Evaluation of Gas-Liquid Interfacial Effects on Hybridoma Viability in Bubble Column Bioreactors"; *Develop. biol. Standard* 66, p 241-253.

Handa-Corrigan, A., Emery, A.N., Spier, R.E. (1989) "Effect of gas-liquid interfaces on the growth of suspended mammalian cells; Mechanisms of cell damage by bubbles.";*Enzyme Microb. Technol.* 11, p 230-235.

Handa-Corrigan, A.(1991) "Bioreactors for Mammalian Cells" Chp 7, p 139-158 IN: Butler, M. (Editor) (1991) "Mammalian Cell Biotechnology A Practical Approach", Oxford University Press, Oxford, U.K.

Hamamoto, K., Ishimaru, K., Tokashiki, M. (1989) "Perfusion culture of hybridoma cells using a centrifuge to separate cells from culture mixture."; *J. Ferment. Bioengineering* 67, p 190-194.

Hammer, B.E., Heath, C.A., Mirer, S.D., Belfort, G. (1990) "Quantitative Flow Measurements in Bioreactors by Nuclear Magnetic Resonance Imaging."; *Biotechnology* 8, p 327-330.

Hassel, T., Brand, H., Renner, G., Westlake,A., Field, R.P. (1992) "Stability of Production of Recombinant Antibodies From Glutamine Synthetase Amplified CHO and NSO Cell Lines", p42-47, IN: Spier, R.E., Griffiths, J.B., MacDonald, C. "Animal Cell Technology: Developments, Processes and Products", Published by Butterworth-Heinemann Ltd., Oxford, U.K.

Hatanaka, M., Todaro, G.J., Gilden, R.V. (1970) *Int. J. Cancer*, 5, p 224-228.

Hayter, P., Kirkby, N., Spier, R.E. (1987) Unpublished data p 275 IN: McCullough, K.C., Spier, R.E. (1990) "Monoclonal Antibodies in Biotechnology: Theoretical and Practical Aspects." Cambridge University Press, Cambridge, U.K.

Hayter, P.M., Kirkby, N.F., Spier, R.E. (1992) "Relationship between hybridoma growth and monoclonal antibody production"; *Enzyme Microb. Technol.* 14, p 454-461.

Heath, C.A., Belfort, G., Hammer, B.E., Mirer, S.D., Pimbley, J.M. (1990) " Magnetic Resonance Imaging and Modeling of Flow in Hollow-Fiber Bioreactors"; *AlChE Journal* 36 No.4, p 547-558.

Heifetz, A.H., Braatz, J.A., Wolfe, R.A., Barry, R.M., Miller, D.A., Solomon, B.A. (1989) "Monoclonal antibody production in hollow fiber bioreactors using serum-free medium."; *Biotechniques* 7, p 192-199.

Himmelfarb, P., Thayer, P.S., Martin, H.E. (1969) "Spin filter culture: the propagation of mammalian cells in suspension." *Science* 164, p 555-557.

Hirschel, M.D., Gruenberg, M.L. (1987) "An automated hollow fiber system for the large scale manufacture of mammalian cell secreted product" p 115-144, IN: Lyderson, B.K. "Large Scale Cell Culture Technology" Hanser Publications, New York.

Hopkinson, J. (1985) "Hollow Fiber Cell Culture Systems For Economical Cell-Product Manufacturing"; *Bio/technology* 3, p 225-230.

Hulscher, M., Scheibler, U., Onken, U. (1992) "Selective Recycle of Viable Animal Cells by Coupling of Airlift Reactor and Cell Settler"; *Biotechnology and Bioengineering* 39, p442-446.

Jan, D.C.H., Emery, A.N., Al-Rubeai, M. (1992) "Optimization of Spin-Filter Performance in the Intensive Culture of Suspended Cells." p 448-451, IN: Spier, R.E., Griffiths, J.B., MacDonald, C. (1992) "Animal Cell Technology: Developments, Processes and Products." Butterworth-Heinemann Ltd., Oxford, U.K.

Jenkins, N. (1991) "Growth Factors." p 39-56, IN: Butler, M. (Editor) (1991) "Mammalian Cell Biotechnology A Practical Approach." Oxford University Press, Oxford, U.K.

Jo,E., Park, H., Park, J., Kim, K(1990) "Balanced Nutrient Fortification Enables High-Density Hybridoma Cell Culture in Batch Culture"; *Biotechnology and Bioengineering* 36, p717-722.

Jonsson, A., Tragardh, G. (1990) "Fundamental Principles of Ultrafiltration"; *Chem. Eng. Process.* 27, p 67-81.

Katinger, H., Scheirer, W. (1985) "Mass Cultivation and Production of Animal Cells"; IN: "Animal Cell Biotechnology" 1, Academic Press Inc., London, p167-193.

Kearns, K.J. (1990) "Integrated Design For Mammalian Cell Culture"; *Bio/technology* 8, p409-413.

Kelsey, L.J., Pillarella, M.R., Zydney, A.L. (1990) "Theoretical Analysis of Convective Flow Profiles in a Hollow-Fiber Membrane Bioreactor"; *Chemical Engineering Science* Vol 45 No.11, p 3211-3220.

Kilburn, D.G, Webb, F.C. (1968); " The cultivation of animal cells at controlled dissolved oxtgen partial pressure"; *Biotechnology and Bioengineering* 10, p801.

Knazek,R.A., Gullino,P.M., Kohler, P.O., Dedrich, R.L. (1972) "Cell Culture on Artificial Capillaries; An Approach to Tissue Growth in vitro"; *Science* 178, p 65-67.

Knazek, G., Pat, J. (1980) US Patent No. 4,206,015.

Knight, P. (1989) "Hollow Fiber Bioreactors For Mammalian Cell Culture." *Bio/technology* 7, p 459-461.

Knight, P. (1990) "Fermentor and Bioreactor Tables."; *Bio/technology* 8, p 415-418.

Kohler, G., Milstein, C. (1975) "Continuous cultures of fused cells secreting antibodies of predefined specificity."; *Nature* 256, p 495-497.

Kolmogorov, D.N. (1941) C.R. (Dokl.) Acad. Sci. U.S.S.R., N.S., 30, p 301.

Kunas, K.T., Papoutsakis, E.T. (1989) "Increasing Serum Concentrations Decrease Cell Death and Allow Growth of Hybridoma Cells at Higher Agitation Rates"; *Biotechnology Letters* 11, p 525-530.

Kunas, K.T., Papoutsakis, E.T. (1990) "Damage Mechanisms of Suspended Animal Cells in Agitated Bioreactors with and Without Bubble Entrainment"; *Biotechnology and Bioengineering* 36, p 476-483.

Leno, M., Merten, O.W., Moeurs, D., Keller, H., Cabanie, L., Hache, J. (1992) "Immunoglobulin Gene Expression During Hybridoma Batch and Semicontinuous Cultures." p 60-67. IN: Spier, R.E., Griffiths, J.B., MacDonald, C. (1992) "Animal Cell Technology: Developments, Processes and Products." Butterworth-Heinemann Ltd. Oxford, U.K.

Levesque, M.J., Sprague, E.A., Schwartz, C.J., Nerem, R.M. (1989) "The influence of shear stress on cultured vascular endothelial cells:The stress response of an anchorage-dependant mammalian cell."; *Biotechnol. Prog.* 5, p 1-8.

Long, W.J., Palombo, A., Schofield, T.L., Emini, E.A. (1988) "Effects of Culture Media on Murine Hybridomas: Definition of Optimal Conditions for Hybridoma Viability, Cellular Proliferation, and Antibody Production."; *Hybridoma* 7, p 69-77.

Low, K., Harbour,C. (1985a) "Growth Kinetics of Hybridoma Cells: (1) The Effects of Varying Foetal Calf Serum Levels"; *Develop. biol. Standard.* 60, p17-24.

Low, K., Harbour,C. (1985b) "Growth Kinetics of Hybridoma Cells: (2) The Effects of Varying Energy Source Concentrations"; *Develop. biol. Standard.* 60, p73-79.

Luan, Y.T., Mutharasan, R., Magee, W.E. (1987a) "Factors Governing Lactic Acid Formation in Long Term Cultivation of Hybridoma Cells."; *Biotechnology Letters* 9, p 751-756.

Luan, Y.T., Mutharasan, R., Magee, W.E. (1987b) "Strategies to Extend Longevity of Hybridomas in Culture and Promote Yield of Monoclonal Antibodies."; *Biotechnology Letters* 9, p 691-696.

MacDonald, C. (1991) "Genetic Engineering of Animal Cells" Chp 4 p 57-84, IN: Butler, M. (Editor) (1991) "Mammalian Cell Biotechnology A Practical Approach." Oxford University Press, Oxford, U.K.

Mancuso, A., Sharfstein, S.T., Tucker, S.N., Clark, D.S., Blanch, H.W (1994) "Examination of Primary Metabolic Pathways in a Murine Hybridoma with Carbon-13 Nuclear Magnetic Resonance Spectroscopy." *Biotechnology and Bioengineering* 44, p563-585.

McCullough, K.C., Spier, R.E. (1990) "Monoclonal antibodies in biotechnology: theoretical and practical aspects"; Cambridge University Press, Cambridge, UK.

McDonogh, R.M., Bauser, H., Stroh, N., Chmiel, H. (1992) "Separation Efficiency of Membranes in Biotechnology; An Experimental and Mathematical Study of Flux Control"; *Chemical Engineering Science* Vol 47 No.1, p 271-279.

MacLeod, A.J. (1991) "Serum and its Fractionation." p 27-38, IN: Butler, M. (Editor) (1991) "Mammalian Cell Biotechnology A Practical Approach." Oxford University Press, Oxford, U.K.

M^{c}Limans, W.F., Blumenson, L.E., Repasky, E., Ito, M. (1981) "Ammonia Loading in Cell Culture Systems."; *Cell Biology International Reports* 5, p 653-660.

McQueen, A., Meilhoc, E., Bailey, J.E. (1987) *Biotechnology Letters* 9 p 831-836.

M^{c}Queen, A.,Bailey, J.E. (1990a) "Effect of Ammonium Ion and Extracellular pH on Hybridoma Cell Metabolism and Antibody Production."; *Biotechnology and Bioengineering* 35, p 1067-1077.

McQueen, A., Bailey, J.E. (1990b) "Mathematical Modeling of the Effects of Ammonium Ion on the Intracellular pH of Hybridoma Cells." *Biotechnology and Bioengineering* 35, p 897-906.

Meireles, M., Aimar, P., Sanchez, V.(1991);"Albumin denaturation during ultrafiltration: Effects of operating conditions and consequences on membrane fouling"; *Biotechnology and Bioengineering* 38, p528.

Merten, O.W., Reiter, S., Himmler, G., Scheirer, W., Katinger, H. (1985) "Production Kinetics of Monoclonal Antibodies." *Develop. biol. Standard.* 60, p 219-227.

Merten, O.W. (1987) "Concentrating mammalian cells. I. large-scale animal cell culture."; *TIBTECH* 5, p 230-237.

Michaels, J.D., Petersen, J.F., McIntyre, L.V., Papoutsakis, E.T. (1991) "Protection Mechanisms of Freely Suspended Animal Cells (CRL 8018) from Fluid-Mechanical Injury. Viscometric and Bioreactor Studies Using Serum, Pluronic F68 and Polyethylene Glycol"; *Biotechnology and Bioengineering* 38, p 169-180.

Mijnbeek, G. (1991) "Shear Stress Effects on Cultured Animal Cells"; *Biotechknowledge* 1, p 3-7.

Miller, W.M., Wilke, C.R., Blanch, H.W. (1987) "Effects of Dissolved Oxygen Concentration on Hybridoma Growth and Metabolism in Continuous Culture."; *J. Cellular Physiology* 132, p 524-530.

Miller,W.M., Wilke, C.R., Blanch, H.W. (1988) "Transient responses of hybridoma metabolism to changes in the oxygen supply rate in continuous culture"; *Bioprocess Engineering* 3, p 103-111.

Miller,W.M., Wilke, C.R., Blanch,H.W. (1989) "Transient Responses of Hybridoma Cells to Nutrient Additions in Continuous Culture: I. Glucose Pulse and Step Changes"; *Biotechnology and Bioengineering* 33, p477-486.

Miller, W.M., Wilke, C.R., Blanch, H.W. (1989) "The transient Responses of Hybridoma cells to Nutrient Additions in Continuous Culture;II. Glutamine Pulse and Step Changes"; *Biotechnology and Bioengineering* 33, p487-499.

Modha, K., Whiteside, J.P., Spier, R.E. (1992) "Dissociation of M.A.B. Production from cell division using D.N.A. Biosynthesis Inhibitors." p 81-98, IN: Spier, R.E., Griffiths, J.B., MacDonald, C. (1992)" Animal Cell Technology: Developments, Processes and Products." Butterworth-HeinemannLtd, Oxford, U.K.

Mulder, M. (1991) "Basic Principles of Membrane Technology." Kluwer Academic Publishers, Netherlands.

Murkes, J., Carlsson, C.G. (1990) "Crossflow Filtration Theory and Practice." Published by Wiley, New York, USA.

Neil, G.A., Urnovitz, H.B. (1988) "Recent improvements in the production of antibody-secreting hybridoma cells."; *TIBTECH* 6, p 209-213.

New Brunswick Scientific (1994) Advertising Bulletin.

Nilsson, K. (1987) "Methods for immobilizing animal cells."; *TIBTECH*. 5, p 73-78.

Oh, D.J., Chang, H.N. (1992) "High Density Culture of Hybridoma Cells in a Dual Hollow Fiber Bioreactor"; *Biotechnology Techniques* Vol 6 No.1, p 77-88.

Ozturk, S.S., Palsson,B.O. (1991) "Physiological Changes During the Adaptation of Hybridoma Cells to Low Serum and Serum-free Media"; *Biotechnology and Bioengineering* 37, p 35-46.

Patankar, D., Oolman, T, (1990a) "Wall-Growth Hollow-Fiber Reactor for Tissue Culture:I. Preliminary Experiments."; *Biotechnology and Bioengineering* 36, p 97-103.

Patankar,D., Oolman, T. (1990b) Wall-Growth Hollow-Fiber Reactor for Tissue Culture:II. A Theoretical Model."; *Biotechnology and Bioengineering* 36, p 104-108.

Paul, W.E. (Editor) (1989) "The Immune System: An Introduction" Chp 1 IN: "Fundamental Immunology."; 2nd Edition, Raven Press Ltd., New York.

Perry, R.H., Green, D. (1985) "Perry's Chemical Engineering Handbook" 6th Edition, McGraw Hill Book Company, U.S.A.

Piret, J.M., Cooney, C.L. (1990) "Mammalian Cell and protein Distributions in Ultrafiltration Hollow Fiber Bioreactors"; *Biotechnology and Bioengineering* 36, p 902-910.

Probstein, R.F., Leung, W., Alliance, Y. (1979) "Determination of Diffusivity and Gel Concentration in Macromolecular Solutions by Ultrafiltration." *The Journal of Physical Chemistry* 83 p 1228-1232.

Ramirez, O.T., Mutharasan, R. (1990) "Cell Cycle and Growth Phase Dependent Variations in Size Distribution, Antibody Productivity, and Oxygen Demand in Hybridoma Cultures"; *Biotechnology and Bioengineering* 36, p839-848.

Ray, N.G., Karkare, S.B., Runstadler, P.W. (1989) "Cultivation of hybridoma cells in continuous cultures: kinetics of growth and product formation.";*Biotechnology and Bioengineering* 33, p 724-730.

Rietzer, L.J., Wice, B.M., Kennell, D. (1979) *J. Biol. Chem.* 254, 2669.

Renner, E.D., Plagemann,P.G.W., Bernlohr, R.W. (1972) *J. Biol. Chem.* 247 p 5765-5776.

Reuveny, S., Velez, D., Miller, L., Macmillan, J.D. (1986a) "Comparison of cell propagation methods for their effect on monoclonal antibody yield in fermentors."; *J. Immunol. Methods* 86, p 61-69.

Reuveny, S., Velez, D., Macmillan, J.D., Miller, L. (1986b) " Factors affecting cell growth and monoclonal antibody production in stirred reactors."; *J. Immunol. Methods* 86, p 53-59.

Rosenberg, J., Sorenson, J., Veeramallu, U., Gebhard, T. (1991) "Use of Hollow Fibre Technology for Large-Scale Production of Retroviruses and Retroviral Antigens." *International Biotechnology Laboratory* February 1991.

Sambanis, A., Stephanopoulos, G., Sinskey, A.J., Lodish, H.F. (1990) "Use of Regulated Secretion in Protein Production from Animal Cells: An Evaluation with the AtT-20 Model Cell Line."; *Biotechnology and Bioengineering* 35, p 771-780.

Sanders, P.G. (1990) "Protein Production by Genetically Engineered Mammalian Cell Lines." Chp 2, p 16-52 IN: Spier, R.E., Griffiths, J.B. (1990) "Animal Cell Biotechnology." Academic Press Limited, London, U.K.

Schumpp, B., Schlaeger, E. (1992) "Growth Study of Lactate and Ammonia Double-resistant Clones of HL-60 Cells", p183-185 IN: Spier, R.E., Griffiths, J.B., MacDonald,C. "Animal Cell Technology: Developments, Processes and Processes", Published by Butterworth-Heinemann Ltd, Oxford, U.K.

Shen, J.S., Probstein, R.F. (1977) "On the Prediction of Limiting Flux in the Laminar Ultrafiltration of Macromolecular Species"; *Ind. End. Chem., Fundam.* 16, p 459-465.

Sianno, S.A., Mutharasan, R. (1991) "NADH Fluoresence and Oxygen Uptake Responses of Hybridoma Cultures to Substrate Pulse and Step Changes"; *Biotechnology and Bioengineering* 37, p 141-159.

Seaver, S., Rudolph, J.L., Ducibella, T., Gabriels, J.E. (1984) "Hybridoma cell metabolism/antibody secretion in culture."; Biotechnology '84 USA, p 325-345, Online Publications, Pinner, UK.

Serotec's Harvest Mouse (1993) Serotec Ltd., 22, Bankside, Station Approach, Kidlington, Oxford, OX5 1JE.

Setec Brochure (1990), PO Box 20000, Livermore, California, CA94550.

Shacter, E. (1989) " Serum-free meia for bulk culture of hybridoma cells and the preparation of monoclonal antibodies."; *TIBTECH.* 7, p 248-253.

Spier, R.E. (1990) "Contemporary Issues in Animal Cell Biotechnology", Ch 1, p 1-13 IN: Spier, R.E., Griffiths, J.B. (1990) "Animal Cell Biotechnology" Academic Press Limited, London, U.K.

Spier, R.E., Whiteside, J.P. (1990) "The Oxygenation of Animal Cell Cultures by Bubbles." Chp 5, p 133-148, IN: Spier, R.E., Griffiths, J.B. (1990) "Animal Cell Biotechnology." Academic Press Limited, London, U.K.

Spier, R.E., Whiteside, J.P. (1976)," The production of foot and mouth disease virus from BHK 21 C13 cells grown on the surface of glass spheres"; *Biotechnology and Bioengineering* 8, p649.

Stanbury, P.F., Whitaker,A. (1984) "Principles of Fermentation Technology." Pergamon Press plc, Oxford, U.K.

Stoker, M.G.P. (1973) "Role of Diffusion Boundary Layer in Contact Inhibition of Growth." *Nature* 246, p 200-203.

Teillaud, J., Fourcade, A., Huppert, J., Fridman, W.H., Tapiero, H. (1989) "Effect of Doxorubicin on Mouse Hybridoma B Cells: Stimulation of Immunoglobulin Synthesis and Secretion." *Cancer Research* 49, p 5123-5129.

Tharakan, J.P.,Chau, P.C. (1986) "A Radial Flow Hollow Fiber Bioreactor for the Large-Scale Culture of Mammalian Cells."; *Biotechnology and Bioengineering* 18, p 329-342.

Thomas, C.R., Nienow, A.W., Dunnill, P. (1979) "Action of Shear on Enzymes: Studies with Alcohol Dehydrogenase"; *Biotechnology and Bioengineering*, 21, p2263.

Thomson, K., Wilson, J.S. (1993) "A Compact Gravitational Settling Device for Cell Retention." p 227, IN: Spier, R.E., Griffiths, J.B., Berthold, W. (Editors), Proceedings of the 12th Meeting of ESACT (ESACT '93) "Animal Cell Technology: Products for Today, Prospects for Tommorrow", Butterworth-Heinemann, Oxford, U.K.

Thompson, K.M., Melamed, M.D., Eagle, K., Gorick, B.D., Gibson, T., Holburn, A.M., Hughes-Jones, N.C. (1986) "Production of human monoclonal IgG and IgM antibodies with anti-D (rhesus) specificity using heterohybridomas."; *Immunology* 58, p 157-160.

Tramper, J., Smit, D., Straatman, J., Vlak, J.M. (1988) *Bioprocess Eng.* 3, p 37-41.

Van Wezel, A.L., van der Velden-de Groot, C.A.M., de Haan, H.H., Van den Heuvel, N., Schasfoort,R. (1985) "Large Scale Animal Cell Cultivation for Production of Cellular Biologicals"; *Develop. biol. Standard.*, 60, p229-236.

Veeramullu, U., Sorenson, J., Gebhard, T., Rosenberg, J. (1991) "Production of a Recombinant Protein Using a CHO Cell Line"; *International Biotechnology Laboratory* May issue, p 14.

Velez, D., Reuveny, S., Miller, L., Macmillan, J.D. (1986) " Kinetics of monoclonal antibody production in low serum growth medium."; *J. Immunol. Methods* 86, p 45-52.

Velez, D., Miller, L., Macmillan, J.D. (1989) "Use of Tangenital Flow Filtration in Perfusion Propagation of Hybridoma Cells for Production of Monoclonal Antibodies." *Biotechnology and Bioengineering* 33, p 938-940.

Wagner, R., Lehmann, J. (1988) " The growth and productivity of recombinant animal cells in a bubble-free aeration system."; *TIBTECH*. 6, p 101-104.

Wei, J., Russ, M.B. (1977) "Convection and Diffusion in Tissues and Tissue Cultures"; *J. theor. Biol.* 66, p 775-787.

Wijmans, J.G., Nakao, S., van der Berg, J.W.A., Troelstra, F.R., Smolders, C.A. (1985) "Hydrodynamic Resistance of Concentration Polarization Boundary Layers in Ultrafiltration." *Journal of Membrane Science* 22, p 117-135.

Wilson, J.S. (1992) "Process Intensification of Hybridoma Cell Fermentation." Ph.D. Thesis. Edinburgh University, U.K.

Wohlpart, D., Kirwan, D., Gainer, J. (1990) "Effects of Cell Density and Glucose and Glutamine Levels on the Respiration Rates of Hybridoma Cells"; *Biotechnology and Bioengineering* 36, p630-635.

Zhang, S., Handa-Corrigan, A., Spier, R.E. (1993) "A comparison of Oxygenation Methods for High-Density Perfusion Cultures of Animal Cells", *Biotechnology and Bioengineering* 41, p685-692.

Zhang,S.,Handa-Corrigan,A.,Spier, R.E.(1992a)"Oxygen Transfer Properties of Bubbles in Animal Cell Culture Media.";*Biotechnology and Bioengineering*40,p252.

Zhang,S.,Handa-Corrigan, A.,Spier, R.E. (1992b) "Foaming and Media Surfactant Effects on the Cultivation of Animal Cells."; *J. Biotechnology* 25, p289-306.

Zhang, W. (1993), PhD. Thesis, "A Study on The Affinity Cross-Flow Filtration Process", ISBN 90-9006329-3

Zhang, Z., Al-Rubeai, M., Thomas, C.R. (1993) "Estimation of disruption of animal cells by turbulent capillary flow" *Biotechnology and Bioengineering* 42, p987-993.

REFERENCES

Abu-Reesh, I., Kargi, F. (1991) "Biological Responses of Hybridoma Cells to Hydrodynamic Shear in an Agitated Bioreactor"; *Enzyme Microb. Technol.* 13, p 913-919.

Adema, E., Sinskey, A.J. (1987) "An Analysis of Intra-Versus Extracapillary Growth in a Hollow Fiber Reactor"; *Biotechnology Progress* Vol 3 No.2, p 74-79.

Al-Rubeai, M., Emery, A.N. (1990) "Mechanisms and kinetics of monoclonal antibody synthesis and secretion in synchronous and asynchronous hybridoma cell cultures."; *Journal of Biotechnology* 16, p 67-86.

Avgerinos, G.C., Drapeau, D., Socolow, J.S., Mao, J., Hsiao, K., Broeze, R.J. (1990) "Spin Filter Perfusion System for High Density Cell Culture: Production of Recombinant Urinary Type Plasminogen Activator in CHO Cells"; *Bio/technology* 8, 54-57.

Belfort, G. (1989) "Membranes and Bioreactors: A Technical Challenge in Biotechnology"; *Biotechnology and Bioengineering* 33, p 1047-1066.

Belfort, G., Altshuler, G.A. (1986) *Chem. Ind.* 7, p 585.

Bell, S.L., Bushell, M.E., Scott, M.F., Wardell, J.N., Spier, R.E., Sanders, P.G. (1992) "Genetic Modification of Hybridoma Glutamine Metabolism: Physiological Consequences." p 180-182, IN: Spier, R.E., Griffiths, J.B., MacDonald, C. (1992) Animal Cell Technology: Developments, Processes and Products." Butterworth-Heinemann Ltd., Oxford, U.K.

Bleim, R. (1989) "A need for systematic investigations into the material properties of cultured animal cells."; *TIBTECH* 7, p 197-200.

Bleim, R.,Katinger, H. (1988a) "Scale-up engineering in animal cell technology: Part 1."; *TIBTECH* 6, p 190-195.

Bleim, R., Katinger, H. (1988b) "Scale-up engineering in animal cell technology: Part 2."; *TIBTECH* 6, p 224-230.

Boulton-Stone, J.M., Blake, J.R. (1993) "Gas Bubbles Bursting at a Free Surface." *Journal of Fluid Mechanics* 254, p 437-466.

Brotherton, J.D., Chau, P.C. (1990) "Modeling Analysis of an Intercalated-Spiral Alternate-Dead-Ended Hollow Fiber Bioreactor for Mammalian Cell Culture.";*Biotechnology and Bioengineering* 35, p 375-394.

Bruining, W.J. (1989) "A General Description of Flows and Pressures in Hollow Fiber Membrane Modules"; *Chemical Engineering Science* Vol 44 No. 6, p 1441-1447.

Burns, J. (1991) "Design, Construction, Modelling and Control of a Dual Hollow-Fibre Bioreactor for Hybridoma Cells." Ph.D. Thesis, Edinburgh University, U.K.

Butler, M. (1985) "Growth limitations in high density microcarrier cultures";; *Develop. biol. Standard.* 60, p269-280.

Butler, M. (Editor) (1991) "Mammalian Cell Biotechnology A Practical Approach", published by Oxford University Press, New York.

Catty,D. (Editor) (1988) "Antibodies Volume 1: a practical approach",published by IRL Press Ltd., England.

Catty,D. (Editor) (1989) "Antibodies Volume 2: a practical approach",published by IRL Press Ltd., England.

Cavegn, C., Blasey, H.D.., Payton,M.A., Allet, B., Li, J., Bernard, A.R. (1992) "Expression of Recombinant Proteins in High Density Insect Cell Cultures." p 569-578, IN: Spier, R.E., Griffiths, J.B., MacDonald, C. (1992) "Animal Cell Technology: Developments, Processes and Products." Butterworth-Heinemann Ltd., Oxford, U.K.

Cellpharm System 1 Brochure (1987), CD Medical.

Chandavarkar, A.S., Cooney, C.L. (1989) "Dynamics of Flux Decrease during Microfiltration Caused by Protein-Membrane Interactions."; *Abstracts of the American Chemical Society* 198, p 44.

Cherry, R.S., Papoutsakis, E.T. (1986) "Hydrodynamic Effects on Cells in Agitated Tissue- Culture Reactors." *Bioproc. Eng.* 1, p 29-41.

Cherry, R.S., Papoutsakis, E.T. (1988) "Physical Mechanisms of Cell-Damage in Microcarrier Cell-Culture Bioreactors." *Biotechnol. Bioeng.* 32, p 1001-1014.

Cherry, R.S., Papoutsakis, E.T. (1989) "Growth and Death Rates of Bovine Embryonic Kidney Cells in Turbulent Microcarrier Bioreactors" *Bioproc. Eng.* 4, p 81-89.

Chiou, T.W., Murakami, S., Wang, D.I.C., Wu, W.T. (1991) "A Fiber-Bed Bioreactor for Anchorage Dependent Animal-Cell Cultures 1. Bioreactor Design and Operation"; *Biotechnology and Bioengineering* 37, p755-761.

Cima, L.G., Blanch, H.W., Wilke, C.R. (1990) "A Theoretical and Experimantal Evaluation of a Novel Radial-flow Hollow Fiber Reactor for Mammalian Cell Culture"; *Bioprocess Engineering* 5, p19-30.

Clarke, G.M. (1994) "Statistics & experimental design- An introduction for Biologists and Biochemists"; Third edition, Edward Arnold, UK.

Coco-Martin, J.M., Oberink, J.W., van der Velden de Groot, T.A.M., Beuvery, E.C. (1992) "The potential of flow cytometric analysis for the characterization of hybridoma cells in suspension cultures."; *Cytotechnology* 8, 65-74.

Cousins, R.B., Gergen, R., Gerner, F.J. (1992) "A Dual Membrane Reactor For the Cultivation of Mammalian Cells." p 538-540, IN: Spier, R.E., Griffiths, J.B., MacDonald, C. (1992) "Animal Cell Technology: Developments, Processes and Processes." Butterworth-Heinemann Ltd., Oxford, U.K.

Croughan, M.S., Hamel, J., Wang, D.I.C. (1987) "Hydrodynamic Effects on Animal Cells Grown in Microcarrier Cultures." *Biotechnology and Bioengineering* 33, p 130-141.

Croughan, M.S., Wang, D.I.C. (1989) " Growth and death in overagitated microcarrier cell culture."; *Biotechnology and Bioengineering* 33, p 731-744.

Dalili, M., Ollis, D.F. (1990a) "A Flow Cytometric Analysis of Hybridoma Growth and Monoclonal Antibody Production."; *Biotechnology and Bioengineering* 36, p64-73.

Dalili, M., Sayles, G.D., Ollis, D.F. (1990b) "Glutamine-limited Batch Hybridoma Growth and Antibody Production: Experimentation and Model."; *Biotechnology and Bioengineering* 36, p74-82.

Dalili, M., Ollis,D.F. (1989) "Transient Kinetics of Hybridoma Growth and Monoclonal Antibody Production in Serum-Limited Cultures"; *Biotechnology and Bioengineering* 33, p984-990.

De la Broise, D., Noiseux, M., Massie, B., Lemieux,R. (1992) "Hybridoma Perfusion Systems: A Comparison Study"; *Biotechnology and Bioengineering* 40 p25-32.

Deutschmann, S.V., Valley, U., Jager, V., Wagner, R.;"Cell cycle analysis as a tool for control and regulation of mammalian cell cultures in bioreactors."; To be published in: Spier, R.E., Griffiths, J.B., and Berthold, W. (eds.), Proceedings of the 12th Meeting of ESACT (ESACT '93) 'Animal Cell Technology: Products for Today, Prospects for Tomorrow', Butterworth-Heinemann, Oxford, UK.

Dodge, T.C., Ji, G.Y., Hu, W.S. (1987) "Loss of viability in hybridoma culture - a kinetic study."; *Enzyme Microb. Technol.*, 9, p 607-611.

Dulbecco, R., Elkington, J. (1973) "Conditions limiting multiplication of fibroblastic and epithelium cells in dense cultures. *Nature* 246, p 197-199.

Duval,D., Demangel,C., Munier-Jolain, K., Miossec, S., Geahel, I. (1991) "Factors Controlling Cell Proliferation and Antibody Production in Mouse Hybridoma Cells: 1. Influence of the Amino Acid Supply"; *Biotechnology and Bioengineering* 38, p561-570.

Eagle, H., Barban, M., Levy, M., Schulze, H.O. (1958) *J. Biol. Chem.*, 233, 551.

Eason, G., Coles, C.W., Gettinby, G. (1992) "Mathematics and Statistics for the Bio-Sciences." Ellis Horwood Ltd., Chichester, U.K.

Enka data sheet (1987), sheet no. QC 58007 0387, Enka AG, Membrane Product Group, Postfach 20 09 16, Ohder Strasse 28, D-5600, Wuppertal 2, Germany.

Fell, C.J.D., Kim, K.J., Chen, V., Wiley, D.E., Fane, A.G. (1990) "Factors Determining Flux and Rejection of Ultrafiltration Membranes"; *Chem. Eng. Process* 27 p 165-173.

Fenge, C., Fraune, E. (1992) "Perfusion Cultivation Technique for Animal Cells"; *International Biotechnology Laboratory* May issue, p 20.

Goergen, J.L, Marc, A., Engasser, J.M. (1992) " Influence of medium composition on the death and lysis of hybridoma cells in continuous cultures."; p 122-124, IN: Spier, R.E., Griffiths, J.B., MacDonald, C. "Animal cell technology: developments, processes and products.", published by Butterworth-Heinemann Ltd, Oxford, UK.

Girardi, A.J., McMichael, H. Jr., Henle, W. (1956) "The Use of HeLa Cells in Suspension for the Quantitative Study of Virus Propagation"; *Virology* 2, p 532-544.

Glacken, M.W., Fleischaker, R.J., Sinskey, A.J. (1986) "Reduction of Waste Product Excretion via Nutrient Control: Possible Strategies for Maximizing Product and Cell Yields on Serum in Cultures of Mammalian Cells."; *Biotechnology and Bioengineering* 28, p 1376-1389.

Griffiths, J.B. (1990)"Advances in Animal Cell Immobilization Technology" Chapter 6, IN: Spier, R.E., Griffiths, J.B. (1990) "Animal Cell Biotechnology" Academic Press Limited, London, U.K., p149-166.

Grund, G., Robinson, C.W., Glick, B.R. (1992) " Protein Type Effects on Steady-State Crossflow Membrane Ultrafiltration Fluxes and Protein Transmission"; *Journal of Membrane Science* 70 p 177-192.

Handa, A., Emery, A.N., Spier, R.E. (1987) "On the Evaluation of Gas-Liquid Interfacial Effects on Hybridoma Viability in Bubble Column Bioreactors"; *Develop. biol. Standard* 66, p 241-253.

Handa-Corrigan, A., Emery, A.N., Spier, R.E. (1989) "Effect of gas-liquid interfaces on the growth of suspended mammalian cells; Mechanisms of cell damage by bubbles.";*Enzyme Microb. Technol.* 11, p 230-235.

Handa-Corrigan, A.(1991) "Bioreactors for Mammalian Cells" Chp 7, p 139-158 IN: Butler, M. (Editor) (1991) "Mammalian Cell Biotechnology A Practical Approach", Oxford University Press, Oxford, U.K.

Hamamoto, K., Ishimaru, K., Tokashiki, M. (1989) "Perfusion culture of hybridoma cells using a centrifuge to separate cells from culture mixture."; *J. Ferment. Bioengineering* 67, p 190-194.

Hammer, B.E., Heath, C.A., Mirer, S.D., Belfort, G. (1990) "Quantitative Flow Measurements in Bioreactors by Nuclear Magnetic Resonance Imaging."; *Biotechnology* 8, p 327-330.

Hassel, T., Brand, H., Renner, G., Westlake,A., Field, R.P. (1992) "Stability of Production of Recombinant Antibodies From Glutamine Synthetase Amplified CHO and NSO Cell Lines", p42-47, IN: Spier, R.E., Griffiths, J.B., MacDonald, C. "Animal Cell Technology: Developments, Processes and Products", Published by Butterworth-Heinemann Ltd., Oxford, U.K.

Hatanaka, M., Todaro, G.J., Gilden, R.V. (1970) *Int. J. Cancer*, 5, p 224-228.

Hayter, P., Kirkby, N., Spier, R.E. (1987) Unpublished data p 275 IN: McCullough, K.C., Spier, R.E. (1990) "Monoclonal Antibodies in Biotechnology: Theoretical and Practical Aspects." Cambridge University Press, Cambridge, U.K.

Hayter, P.M., Kirkby, N.F., Spier, R.E. (1992) "Relationship between hybridoma growth and monoclonal antibody production"; *Enzyme Microb. Technol.* 14, p 454-461.

Heath, C.A., Belfort, G., Hammer, B.E., Mirer, S.D., Pimbley, J.M. (1990) " Magnetic Resonance Imaging and Modeling of Flow in Hollow-Fiber Bioreactors"; *AlChE Journal* 36 No.4, p 547-558.

Heifetz, A.H., Braatz, J.A., Wolfe, R.A., Barry, R.M., Miller, D.A., Solomon, B.A. (1989) "Monoclonal antibody production in hollow fiber bioreactors using serum-free medium."; *Biotechniques* 7, p 192-199.

Himmelfarb, P., Thayer, P.S., Martin, H.E. (1969) "Spin filter culture: the propagation of mammalian cells in suspension." *Science* 164, p 555-557.

Hirschel, M.D., Gruenberg, M.L. (1987) "An automated hollow fiber system for the large scale manufacture of mammalian cell secreted product" p 115-144, IN: Lyderson, B.K. "Large Scale Cell Culture Technology" Hanser Publications, New York.

Hopkinson, J. (1985) "Hollow Fiber Cell Culture Systems For Economical Cell-Product Manufacturing"; *Bio/technology* 3, p 225-230.

Hulscher, M., Scheibler, U., Onken, U. (1992) "Selective Recycle of Viable Animal Cells by Coupling of Airlift Reactor and Cell Settler"; *Biotechnology and Bioengineering* 39, p442-446.

Jan, D.C.H., Emery, A.N., Al-Rubeai, M. (1992) "Optimization of Spin-Filter Performance in the Intensive Culture of Suspended Cells." p 448-451, IN: Spier, R.E., Griffiths, J.B., MacDonald, C. (1992) "Animal Cell Technology: Developments, Processes and Products." Butterworth-Heinemann Ltd., Oxford, U.K.

Jenkins, N. (1991) "Growth Factors." p 39-56, IN: Butler, M. (Editor) (1991) "Mammalian Cell Biotechnology A Practical Approach." Oxford University Press, Oxford, U.K.

Jo,E., Park, H., Park, J., Kim, K(1990) "Balanced Nutrient Fortification Enables High-Density Hybridoma Cell Culture in Batch Culture"; *Biotechnology and Bioengineering* 36, p717-722.

Jonsson, A., Tragardh, G. (1990) "Fundamental Principles of Ultrafiltration"; *Chem. Eng. Process.* 27, p 67-81.

Katinger, H., Scheirer, W. (1985) "Mass Cultivation and Production of Animal Cells"; IN: "Animal Cell Biotechnology" 1, Academic Press Inc., London, p167-193.

Kearns, K.J. (1990) "Integrated Design For Mammalian Cell Culture"; *Bio/technology* 8, p409-413.

Kelsey, L.J., Pillarella, M.R., Zydney, A.L. (1990) "Theoretical Analysis of Convective Flow Profiles in a Hollow-Fiber Membrane Bioreactor"; *Chemical Engineering Science* Vol 45 No.11, p 3211-3220.

Kilburn, D.G, Webb, F.C. (1968); " The cultivation of animal cells at controlled dissolved oxtgen partial pressure"; *Biotechnology and Bioengineering* 10, p801.

Knazek,R.A., Gullino,P.M., Kohler, P.O., Dedrich, R.L. (1972) "Cell Culture on Artificial Capillaries; An Approach to Tissue Growth in vitro"; *Science* 178, p 65-67.

Knazek, G., Pat, J. (1980) US Patent No. 4,206,015.

Knight, P. (1989) "Hollow Fiber Bioreactors For Mammalian Cell Culture." *Bio/technology* 7, p 459-461.

Knight, P. (1990) "Fermentor and Bioreactor Tables."; *Bio/technology* 8, p 415-418.

Kohler, G., Milstein, C. (1975) "Continuous cultures of fused cells secreting antibodies of predefined specificity."; *Nature* 256, p 495-497.

Kolmogorov, D.N. (1941) C.R. (Dokl.) Acad. Sci. U.S.S.R., N.S., 30, p 301.

Kunas, K.T., Papoutsakis, E.T. (1989) "Increasing Serum Concentrations Decrease Cell Death and Allow Growth of Hybridoma Cells at Higher Agitation Rates"; *Biotechnology Letters* 11, p 525-530.

Kunas, K.T., Papoutsakis, E.T. (1990) "Damage Mechanisms of Suspended Animal Cells in Agitated Bioreactors with and Without Bubble Entrainment"; *Biotechnology and Bioengineering* 36, p 476-483.

Leno, M., Merten, O.W., Moeurs, D., Keller, H., Cabanie, L., Hache, J. (1992) "Immunoglobulin Gene Expression During Hybridoma Batch and Semicontinuous Cultures." p 60-67. IN: Spier, R.E., Griffiths, J.B., MacDonald, C. (1992) "Animal Cell Technology: Developments, Processes and Products." Butterworth-Heinemann Ltd. Oxford, U.K.

Levesque, M.J., Sprague, E.A., Schwartz, C.J., Nerem, R.M. (1989) "The influence of shear stress on cultured vascular endothelial cells:The stress response of an anchorage-dependant mammalian cell."; *Biotechnol. Prog.* 5, p 1-8.

Long, W.J., Palombo, A., Schofield, T.L., Emini, E.A. (1988) "Effects of Culture Media on Murine Hybridomas: Definition of Optimal Conditions for Hybridoma Viability, Cellular Proliferation, and Antibody Production."; *Hybridoma* 7, p 69-77.

Low, K., Harbour,C. (1985a) "Growth Kinetics of Hybridoma Cells: (1) The Effects of Varying Foetal Calf Serum Levels"; *Develop. biol. Standard.* 60, p17-24.

Low, K., Harbour,C. (1985b) "Growth Kinetics of Hybridoma Cells: (2) The Effects of Varying Energy Source Concentrations"; *Develop. biol. Standard.* 60, p73-79.

Luan, Y.T., Mutharasan, R., Magee, W.E. (1987a) "Factors Governing Lactic Acid Formation in Long Term Cultivation of Hybridoma Cells."; *Biotechnology Letters* 9, p 751-756.

Luan, Y.T., Mutharasan, R., Magee, W.E. (1987b) "Strategies to Extend Longevity of Hybridomas in Culture and Promote Yield of Monoclonal Antibodies."; *Biotechnology Letters* 9, p 691-696.

MacDonald, C. (1991) "Genetic Engineering of Animal Cells" Chp 4 p 57-84, IN: Butler, M. (Editor) (1991) "Mammalian Cell Biotechnology A Practical Approach." Oxford University Press, Oxford, U.K.

Mancuso, A., Sharfstein, S.T., Tucker, S.N., Clark, D.S., Blanch, H.W (1994) "Examination of Primary Metabolic Pathways in a Murine Hybridoma with Carbon-13 Nuclear Magnetic Resonance Spectroscopy." *Biotechnology and Bioengineering* 44, p563-585.

McCullough, K.C., Spier, R.E. (1990) "Monoclonal antibodies in biotechnology: theoretical and practical aspects"; Cambridge University Press, Cambridge, UK.

McDonogh, R.M., Bauser, H., Stroh, N., Chmiel, H. (1992) "Separation Efficiency of Membranes in Biotechnology; An Experimental and Mathematical Study of Flux Control"; *Chemical Engineering Science* Vol 47 No.1, p 271-279.

MacLeod, A.J. (1991) "Serum and its Fractionation." p 27-38, IN: Butler, M. (Editor) (1991) "Mammalian Cell Biotechnology A Practical Approach." Oxford University Press, Oxford, U.K.

M^{c}Limans, W.F., Blumenson, L.E., Repasky, E., Ito, M. (1981) "Ammonia Loading in Cell Culture Systems."; *Cell Biology International Reports* 5, p 653-660.

McQueen, A., Meilhoc, E., Bailey, J.E. (1987) *Biotechnology Letters* 9 p 831-836.

M^{c}Queen, A.,Bailey, J.E. (1990a) "Effect of Ammonium Ion and Extracellular pH on Hybridoma Cell Metabolism and Antibody Production."; *Biotechnology and Bioengineering* 35, p 1067-1077.

McQueen, A., Bailey, J.E. (1990b) "Mathematical Modeling of the Effects of Ammonium Ion on the Intracellular pH of Hybridoma Cells." *Biotechnology and Bioengineering* 35, p 897-906.

Meireles, M., Aimar, P., Sanchez, V.(1991);"Albumin denaturation during ultrafiltration: Effects of operating conditions and consequences on membrane fouling"; *Biotechnology and Bioengineering* 38, p528.

Merten, O.W., Reiter, S., Himmler, G., Scheirer, W., Katinger, H. (1985) "Production Kinetics of Monoclonal Antibodies." *Develop. biol. Standard.* 60, p 219-227.

Merten, O.W. (1987) "Concentrating mammalian cells. I. large-scale animal cell culture."; *TIBTECH* 5, p 230-237.

Michaels, J.D., Petersen, J.F., McIntyre, L.V., Papoutsakis, E.T. (1991) "Protection Mechanisms of Freely Suspended Animal Cells (CRL 8018) from Fluid-Mechanical Injury. Viscometric and Bioreactor Studies Using Serum, Pluronic F68 and Polyethylene Glycol"; *Biotechnology and Bioengineering* 38, p 169-180.

Mijnbeek, G. (1991) "Shear Stress Effects on Cultured Animal Cells"; *Biotechknowledge* 1, p 3-7.

Miller, W.M., Wilke, C.R., Blanch, H.W. (1987) "Effects of Dissolved Oxygen Concentration on Hybridoma Growth and Metabolism in Continuous Culture."; *J. Cellular Physiology* 132, p 524-530.

Miller,W.M., Wilke, C.R., Blanch, H.W. (1988) "Transient responses of hybridoma metabolism to changes in the oxygen supply rate in continuous culture"; *Bioprocess Engineering* 3, p 103-111.

Miller,W.M., Wilke, C.R., Blanch,H.W. (1989) "Transient Responses of Hybridoma Cells to Nutrient Additions in Continuous Culture: I. Glucose Pulse and Step Changes"; *Biotechnology and Bioengineering* 33, p477-486.

Miller, W.M., Wilke, C.R., Blanch, H.W. (1989) "The transient Responses of Hybridoma cells to Nutrient Additions in Continuous Culture;II. Glutamine Pulse and Step Changes"; *Biotechnology and Bioengineering* 33, p487-499.

Modha, K., Whiteside, J.P., Spier, R.E. (1992) "Dissociation of M.A.B. Production from cell division using D.N.A. Biosynthesis Inhibitors." p 81-98, IN: Spier, R.E., Griffiths, J.B., MacDonald, C. (1992)" Animal Cell Technology: Developments, Processes and Products." Butterworth-HeinemannLtd, Oxford, U.K.

Mulder, M. (1991) "Basic Principles of Membrane Technology." Kluwer Academic Publishers, Netherlands.

Murkes, J., Carlsson, C.G. (1990) "Crossflow Filtration Theory and Practice." Published by Wiley, New York, USA.

Neil, G.A., Urnovitz, H.B. (1988) "Recent improvements in the production of antibody-secreting hybridoma cells."; *TIBTECH* 6, p 209-213.

New Brunswick Scientific (1994) Advertising Bulletin.

Nilsson, K. (1987) "Methods for immobilizing animal cells."; *TIBTECH*. 5, p 73-78.

Oh, D.J., Chang, H.N. (1992) "High Density Culture of Hybridoma Cells in a Dual Hollow Fiber Bioreactor"; *Biotechnology Techniques* Vol 6 No.1, p 77-88.

Ozturk, S.S., Palsson,B.O. (1991) "Physiological Changes During the Adaptation of Hybridoma Cells to Low Serum and Serum-free Media"; *Biotechnology and Bioengineering* 37, p 35-46.

Patankar, D., Oolman, T, (1990a) "Wall-Growth Hollow-Fiber Reactor for Tissue Culture:I. Preliminary Experiments."; *Biotechnology and Bioengineering* 36, p 97-103.

Patankar,D., Oolman, T. (1990b) Wall-Growth Hollow-Fiber Reactor for Tissue Culture:II. A Theoretical Model."; *Biotechnology and Bioengineering* 36, p 104-108.

Paul, W.E. (Editor) (1989) "The Immune System: An Introduction" Chp 1 IN: "Fundamental Immunology."; 2nd Edition, Raven Press Ltd., New York.

Perry, R.H., Green, D. (1985) "Perry's Chemical Engineering Handbook" 6th Edition, McGraw Hill Book Company, U.S.A.

Piret, J.M., Cooney, C.L. (1990) "Mammalian Cell and protein Distributions in Ultrafiltration Hollow Fiber Bioreactors"; *Biotechnology and Bioengineering* 36, p 902-910.

Probstein, R.F., Leung, W., Alliance, Y. (1979) "Determination of Diffusivity and Gel Concentration in Macromolecular Solutions by Ultrafiltration." *The Journal of Physical Chemistry* 83 p 1228-1232.

Ramirez, O.T., Mutharasan, R. (1990) "Cell Cycle and Growth Phase Dependent Variations in Size Distribution, Antibody Productivity, and Oxygen Demand in Hybridoma Cultures"; *Biotechnology and Bioengineering* 36, p839-848.

Ray, N.G., Karkare, S.B., Runstadler, P.W. (1989) "Cultivation of hybridoma cells in continuous cultures: kinetics of growth and product formation.";*Biotechnology and Bioengineering* 33, p 724-730.

Rietzer, L.J., Wice, B.M., Kennell, D. (1979) *J. Biol. Chem.* 254, 2669.

Renner, E.D., Plagemann,P.G.W., Bernlohr, R.W. (1972) *J. Biol. Chem.* 247 p 5765-5776.

Reuveny, S., Velez, D., Miller, L., Macmillan, J.D. (1986a) "Comparison of cell propagation methods for their effect on monoclonal antibody yield in fermentors."; *J. Immunol. Methods* 86, p 61-69.

Reuveny, S., Velez, D., Macmillan, J.D., Miller, L. (1986b) " Factors affecting cell growth and monoclonal antibody production in stirred reactors."; *J. Immunol. Methods* 86, p 53-59.

Rosenberg, J., Sorenson, J., Veeramallu, U., Gebhard, T. (1991) "Use of Hollow Fibre Technology for Large-Scale Production of Retroviruses and Retroviral Antigens." *International Biotechnology Laboratory* February 1991.

Sambanis, A., Stephanopoulos, G., Sinskey, A.J., Lodish, H.F. (1990) "Use of Regulated Secretion in Protein Production from Animal Cells: An Evaluation with the AtT-20 Model Cell Line."; *Biotechnology and Bioengineering* 35, p 771-780.

Sanders, P.G. (1990) "Protein Production by Genetically Engineered Mammalian Cell Lines." Chp 2, p 16-52 IN: Spier, R.E., Griffiths, J.B. (1990) "Animal Cell Biotechnology." Academic Press Limited, London, U.K.

Schumpp, B., Schlaeger, E. (1992) "Growth Study of Lactate and Ammonia Double-resistant Clones of HL-60 Cells", p183-185 IN: Spier, R.E., Griffiths, J.B., MacDonald,C. "Animal Cell Technology: Developments, Processes and Processes", Published by Butterworth-Heinemann Ltd, Oxford, U.K.

Shen, J.S., Probstein, R.F. (1977) "On the Prediction of Limiting Flux in the Laminar Ultrafiltration of Macromolecular Species"; *Ind. End. Chem., Fundam.* 16, p 459-465.

Sianno, S.A., Mutharasan, R. (1991) "NADH Fluoresence and Oxygen Uptake Responses of Hybridoma Cultures to Substrate Pulse and Step Changes"; *Biotechnology and Bioengineering* 37, p 141-159.

Seaver, S., Rudolph, J.L., Ducibella, T., Gabriels, J.E. (1984) "Hybridoma cell metabolism/antibody secretion in culture."; Biotechnology '84 USA, p 325-345, Online Publications, Pinner, UK.

Serotec's Harvest Mouse (1993) Serotec Ltd., 22, Bankside, Station Approach, Kidlington, Oxford, OX5 1JE.

Setec Brochure (1990), PO Box 20000, Livermore, California, CA94550.

Shacter, E. (1989) " Serum-free meia for bulk culture of hybridoma cells and the preparation of monoclonal antibodies."; *TIBTECH.* 7, p 248-253.

Spier, R.E. (1990) "Contemporary Issues in Animal Cell Biotechnology", Ch 1, p 1-13 IN: Spier, R.E., Griffiths, J.B. (1990) "Animal Cell Biotechnology" Academic Press Limited, London, U.K.

Spier, R.E., Whiteside, J.P. (1990) "The Oxygenation of Animal Cell Cultures by Bubbles." Chp 5, p 133-148, IN: Spier, R.E., Griffiths, J.B. (1990) "Animal Cell Biotechnology." Academic Press Limited, London, U.K.

Spier, R.E., Whiteside, J.P. (1976)," The production of foot and mouth disease virus from BHK 21 C13 cells grown on the surface of glass spheres"; *Biotechnology and Bioengineering* 8, p649.

Stanbury, P.F., Whitaker,A. (1984) "Principles of Fermentation Technology." Pergamon Press plc, Oxford, U.K.

Stoker, M.G.P. (1973) "Role of Diffusion Boundary Layer in Contact Inhibition of Growth." *Nature* 246, p 200-203.

Teillaud, J., Fourcade, A., Huppert, J., Fridman, W.H., Tapiero, H. (1989) "Effect of Doxorubicin on Mouse Hybridoma B Cells: Stimulation of Immunoglobulin Synthesis and Secretion." *Cancer Research* 49, p 5123-5129.

Tharakan, J.P.,Chau, P.C. (1986) "A Radial Flow Hollow Fiber Bioreactor for the Large-Scale Culture of Mammalian Cells."; *Biotechnology and Bioengineering* 18, p 329-342.

Thomas, C.R., Nienow, A.W., Dunnill, P. (1979) "Action of Shear on Enzymes: Studies with Alcohol Dehydrogenase"; *Biotechnology and Bioengineering*, 21, p2263.

Thomson, K., Wilson, J.S. (1993) "A Compact Gravitational Settling Device for Cell Retention." p 227, IN: Spier, R.E., Griffiths, J.B., Berthold, W. (Editors), Proceedings of the 12th Meeting of ESACT (ESACT '93) "Animal Cell Technology: Products for Today, Prospects for Tommorrow", Butterworth-Heinemann, Oxford, U.K.

Thompson, K.M., Melamed, M.D., Eagle, K., Gorick, B.D., Gibson, T., Holburn, A.M., Hughes-Jones, N.C. (1986) "Production of human monoclonal IgG and IgM antibodies with anti-D (rhesus) specificity using heterohybridomas."; *Immunology* 58, p 157-160.

Tramper, J., Smit, D., Straatman, J., Vlak, J.M. (1988) *Bioprocess Eng.* 3, p 37-41.

Van Wezel, A.L., van der Velden-de Groot, C.A.M., de Haan, H.H., Van den Heuvel, N., Schasfoort,R. (1985) "Large Scale Animal Cell Cultivation for Production of Cellular Biologicals"; *Develop. biol. Standard.*, 60, p229-236.

Veeramullu, U., Sorenson, J., Gebhard, T., Rosenberg, J. (1991) "Production of a Recombinant Protein Using a CHO Cell Line"; *International Biotechnology Laboratory* May issue, p 14.

Velez, D., Reuveny, S., Miller, L., Macmillan, J.D. (1986) " Kinetics of monoclonal antibody production in low serum growth medium."; *J. Immunol. Methods* 86, p 45-52.

Velez, D., Miller, L., Macmillan, J.D. (1989) "Use of Tangenital Flow Filtration in Perfusion Propagation of Hybridoma Cells for Production of Monoclonal Antibodies." *Biotechnology and Bioengineering* 33, p 938-940.

Wagner, R., Lehmann, J. (1988) " The growth and productivity of recombinant animal cells in a bubble-free aeration system."; *TIBTECH*. 6, p 101-104.

Wei, J., Russ, M.B. (1977) "Convection and Diffusion in Tissues and Tissue Cultures"; *J. theor. Biol.* 66, p 775-787.

Wijmans, J.G., Nakao, S., van der Berg, J.W.A., Troelstra, F.R., Smolders, C.A. (1985) "Hydrodynamic Resistance of Concentration Polarization Boundary Layers in Ultrafiltration." *Journal of Membrane Science* 22, p 117-135.

Wilson, J.S. (1992) "Process Intensification of Hybridoma Cell Fermentation." Ph.D. Thesis. Edinburgh University, U.K.

Wohlpart, D., Kirwan, D., Gainer, J. (1990) "Effects of Cell Density and Glucose and Glutamine Levels on the Respiration Rates of Hybridoma Cells"; *Biotechnology and Bioengineering* 36, p630-635.

Zhang, S., Handa-Corrigan, A., Spier, R.E. (1993) "A comparison of Oxygenation Methods for High-Density Perfusion Cultures of Animal Cells", *Biotechnology and Bioengineering* 41, p685-692.

Zhang,S.,Handa-Corrigan,A.,Spier, R.E.(1992a)"Oxygen Transfer Properties of Bubbles in Animal Cell Culture Media.";*Biotechnology and Bioengineering*40,p252.

Zhang,S.,Handa-Corrigan, A.,Spier, R.E. (1992b) "Foaming and Media Surfactant Effects on the Cultivation of Animal Cells."; *J. Biotechnology* 25, p289-306.

Zhang, W. (1993), PhD. Thesis, "A Study on The Affinity Cross-Flow Filtration Process", ISBN 90-9006329-3

Zhang, Z., Al-Rubeai, M., Thomas, C.R. (1993) "Estimation of disruption of animal cells by turbulent capillary flow" *Biotechnology and Bioengineering* 42, p987-993.